

Characterisation of the MID1/ α 4 multiprotein complex

INAUGURAL DISSERTATION

to obtain
doctor rerum naturalium (Dr. rer. nat.)

submitted to the Department of Biology, Chemistry and Pharmacy
of Freie Universität Berlin

by
Beatriz Aranda Orgillés
Born on 07 November 1976 in Zaragoza, Spain

Berlin, April 2006

1. Reviewer: Professor Dr. Susann Schweiger
2. Reviewer: Professor Dr. Volker A. Erdmann

Date of defence:

To Dirk, Gabriel, M^a Jesús and Ana

Table of Contents

| | |
|--|-----------|
| TABLE OF CONTENTS..... | 1 |
| 1 INTRODUCTION..... | 4 |
| 1.1 VENTRAL MIDLINE DEVELOPMENT | 4 |
| 1.1.1 Craniofacial development | 7 |
| 1.1.2 Heart development | 8 |
| 1.1.3 Ephrins as NCC pathfinders | 9 |
| 1.1.4 Midline development and disease | 10 |
| 1.2 X-LINKED OPITZ BBB/G SYNDROME (OS) AND MID1 | 11 |
| 1.2.1 The RBCC protein MID1..... | 12 |
| 1.2.2 The MID1 function | 15 |
| 1.2.3 Regulation of MID1 function..... | 16 |
| 1.3 MTOR PATHWAY | 17 |
| 1.4 AIM OF THE STUDY | 19 |
| 2 MATERIALS AND METHODS..... | 20 |
| 2.1 MATERIALS | 20 |
| 2.1.1 General reagents | 20 |
| 2.1.2 Enzymes | 22 |
| 2.1.3 Kits | 22 |
| 2.1.4 Instruments and Disposables | 22 |
| 2.1.5 Antibodies..... | 23 |
| 2.1.6 Vectors..... | 24 |
| 2.1.7 Buffers and Media | 24 |
| 2.1.8 Cell lines..... | 26 |
| 2.1.9 Bioinformatic tools and Databases | 26 |
| 2.1.10 Patients..... | 27 |
| 2.2 NUCLEIC ACID METHODS | 27 |
| 2.2.1 Polymerase chain reaction (PCR)..... | 27 |
| 2.2.2 Agarose gel electrophoresis | 28 |
| 2.2.3 RNA preparation and cDNA synthesis | 28 |
| 2.2.4 Phenol:Chloroform extraction | 29 |
| 2.2.5 EtOH precipitation of nucleic acids..... | 29 |
| 2.2.6 Cloning..... | 29 |
| 2.2.6.1 Cloning of pEGFP constructs and mutagenesis | 29 |
| 2.2.6.2 Preparation of the pCMVTag2C and pBMT116 constructs..... | 31 |
| 2.2.6.3 α 4/44aa peptide clones..... | 31 |
| 2.2.7 Plasmid DNA isolation and transformation..... | 32 |
| 2.2.7.1 Plasmid DNA isolation..... | 32 |
| 2.2.7.2 Chemical transformation | 33 |
| 2.2.7.3 Electroporation | 33 |
| 2.2.8 Transfection..... | 33 |
| 2.2.8.1 siRNA transfection | 33 |
| 2.2.8.2 Polyfect transfection of plasmid DNA | 33 |
| 2.2.8.3 Lipofectamine transfection of plasmid DNA | 34 |
| 2.2.9 Sequencing | 34 |
| 2.3 PROTEIN METHODS | 35 |

| | | |
|----------|--|-----------|
| 2.3.1 | <i>Bradford assay</i> | 35 |
| 2.3.2 | <i>SDS-PAGE Gel</i> | 35 |
| 2.3.3 | <i>Western blot</i> | 36 |
| 2.3.4 | <i>Silver staining</i> | 37 |
| 2.3.5 | <i>Coomassie/Colloidal coomassie staining</i> | 37 |
| 2.3.6 | <i>Immunofluorescence</i> | 37 |
| 2.3.7 | <i>Microtubule assembly experiment</i> | 38 |
| 2.3.8 | <i>Immunoprecipitation</i> | 38 |
| 2.3.9 | <i>Yeast two-hybrid experiments</i> | 39 |
| 2.3.9.1 | <i>Yeast-transformation</i> | 39 |
| 2.3.9.2 | <i>β-Galactosidase activity</i> | 40 |
| 2.3.10 | <i>Cell culturing and trypsinisation</i> | 41 |
| 2.4 | PREPARATION OF THE 44AA PEPTIDES | 41 |
| 2.4.1 | <i>Growth of E.Coli cultures</i> | 41 |
| 2.4.2 | <i>Preparation of cleared E.Coli lysates</i> | 42 |
| 2.4.3 | <i>Purification of 6xHis tagged proteins from E.Coli</i> | 42 |
| 2.4.4 | <i>Thrombin digestion</i> | 42 |
| 2.5 | CHROMATOGRAPHY COLUMN AND MASS SPECTROMETRY | 43 |
| 2.6 | SUCROSE GRADIENTS | 44 |
| 2.6.1 | <i>Discontinuous gradients</i> | 44 |
| 2.6.2 | <i>Linear sucrose gradient</i> | 44 |
| 2.7 | RNA-PROTEIN BINDING EXPERIMENTS | 45 |
| 2.7.1 | <i>Homopolymer binding assay</i> | 45 |
| 2.7.2 | <i>Ephrin mRNAs-MID1 binding experiments</i> | 45 |
| 2.7.2.1 | <i>Amplification of G-quartets and EFNB1 mRNA</i> | 45 |
| 2.7.2.2 | <i>In vitro transcription of biotinylated RNA</i> | 47 |
| 2.7.2.3 | <i>Biotinylation Efficiency Dot Blot</i> | 47 |
| 2.7.2.4 | <i>RNA-PROTEIN Binding Assay</i> | 47 |
| 2.7.3 | <i>Bioinformatics</i> | 48 |
| 3 | RESULTS | 49 |
| 3.1 | CHARACTERISATION OF THE BBOXES OF MID1 | 49 |
| 3.1.1 | <i>Mutations in Bbox1 disrupt MID1-α4 interaction</i> | 49 |
| 3.1.2 | <i>Analysis of the structure of the Bbox2 domain</i> | 52 |
| 3.1.3 | <i>C195F, mutated MID1 form found in an OS patient, disrupts MID1-α4 interaction</i> | 53 |
| 3.1.4 | <i>Bbox2 mutants do not interact with α4 in vivo</i> | 55 |
| 3.1.5 | <i>Bbox2 mutants interact with α4 in vitro</i> | 59 |
| 3.2 | CHARACTERISATION OF THE MID1 MULTIPROTEIN COMPLEX | 62 |
| 3.2.1 | <i>44aa peptide of α4 production in the PET32a vector system</i> | 62 |
| 3.2.2 | <i>α4-peptide production in the PinPoint vector system</i> | 65 |
| 3.2.3 | <i>Affinity chromatography column</i> | 67 |
| 3.2.4 | <i>Confirmation of novel MID1 interaction partners</i> | 71 |
| 3.2.5 | <i>The MID1 protein complex is found in purified microtubules</i> | 71 |
| 3.2.6 | <i>The MID1 complex associates with both ribosomal subunits</i> | 72 |
| 3.2.7 | <i>MID1 associates with intact ribosomes</i> | 73 |
| 3.2.8 | <i>MID1 forms part of a ribonucleoprotein complex</i> | 74 |
| 3.2.9 | <i>Characterisation of the association of MID1-FLAG with ribosomes</i> | 76 |
| 3.2.9.1 | <i>Salt and detergent treatments</i> | 76 |
| 3.2.9.2 | <i>EDTA treatment</i> | 77 |

| | | |
|-----------|--|------------|
| 3.2.9.3 | Puromycin and cycloheximide treatments | 78 |
| 3.2.10 | <i>Endogenous MID1 and other components of the complex associate with ribosomes</i> | 79 |
| 3.2.11 | <i>MID1 associates with polyribosomes</i> | 80 |
| 3.2.12 | <i>MID1 associates with homoribopolymers</i> | 81 |
| 3.2.13 | <i>Characterisation of the Poly-rG-MID1 binding</i> | 82 |
| 3.2.14 | <i>MID1 complex binds ephrin mRNA via G-quartet structures</i> | 84 |
| 3.2.15 | <i>Binding of the G-quartets to the MID1 Complex</i> | 86 |
| 3.2.16 | <i>MID1 complex associates with EFNBI mRNA</i> | 87 |
| 4 | DISCUSSION | 89 |
| 4.1 | A NOVEL PATHOMECHANISM FOR OS CAUSED BY MUTATIONS IN THE BBOXES DOMAINS OF MID1 | 89 |
| 4.2 | THE MID1 MULTIPROTEIN COMPLEX | 93 |
| 4.2.1 | <i>MID1 forms part of a ribonucleoprotein complex</i> | 93 |
| 4.2.2 | <i>The components of the MID1 complex associate with microtubules</i> | 94 |
| 4.2.3 | <i>The MID1 complex and its role in translation at the microtubules</i> | 95 |
| 4.2.4 | <i>The MID1 complex and translational repression</i> | 96 |
| 4.2.5 | <i>MID1 complex and development of the ventral midline development: implications in cell migration</i> | 98 |
| 4.2.6 | <i>The MID1 complex components and their involvement in cell migration, polarisation and adhesion</i> | 99 |
| 4.2.7 | <i>EphB and ephrin-B mRNAs can be integrated in the MID1 complex</i> | 101 |
| 5 | CONCLUSIONS AND OUTLOOK | 103 |
| 6 | SUMMARY | 105 |
| 7 | SUMARIO | 107 |
| 8 | ZUSAMMENFASSUNG | 109 |
| 9 | REFERENCES | 111 |
| 10 | ABBREVIATIONS | 126 |
| 11 | CURRICULUM VITAE | 129 |
| 12 | PUBLICATIONS | 130 |
| 13 | ACKNOWLEDGEMENTS | 131 |

1 Introduction

Opitz BBB/G syndrome (OS, MIM 300000 and MIM 145410) is a congenital disorder characterised by malformations of the ventral midline. BBB syndrome and G syndrome (Borden, 2000; Opitz, 1969b; Opitz, 1969a), formerly described as two different disorders, were merged into Opitz BBB/G syndrome subsequent to description of patients with a mixture of symptoms (Cordero and Holmes, 1978). The two cardinal phenotypic manifestations of OS are hypertelorism/telecanthus (abnormally widely spaced/increased innercanthal distance) and hypospadias (urethral cleft in male patients). However, they are often found to have in addition other typical features such as cleft lip and/or palate, laryngotracheoesophageal (LTE) anomalies, congenital heart defects, imperforate anus, agenesis of the corpus callosum, ear abnormalities, and mental retardation (Cox et al., 2000; De Falco et al., 2003; So et al., 2005).

OS is genetically heterogeneous with an autosomal and an X-linked locus. The two forms are clinically indistinguishable (Robin et al., 1996). In 1997, Quaderi et al identified by positional cloning the MID1 gene in Xp22.3; MID1 harbours mutations in about 68% of patients with X-linked OS. In contrast, while the autosomal locus has been mapped by linkage analysis to chromosome 22, the responsible gene remains unknown (Robin et al., 1995).

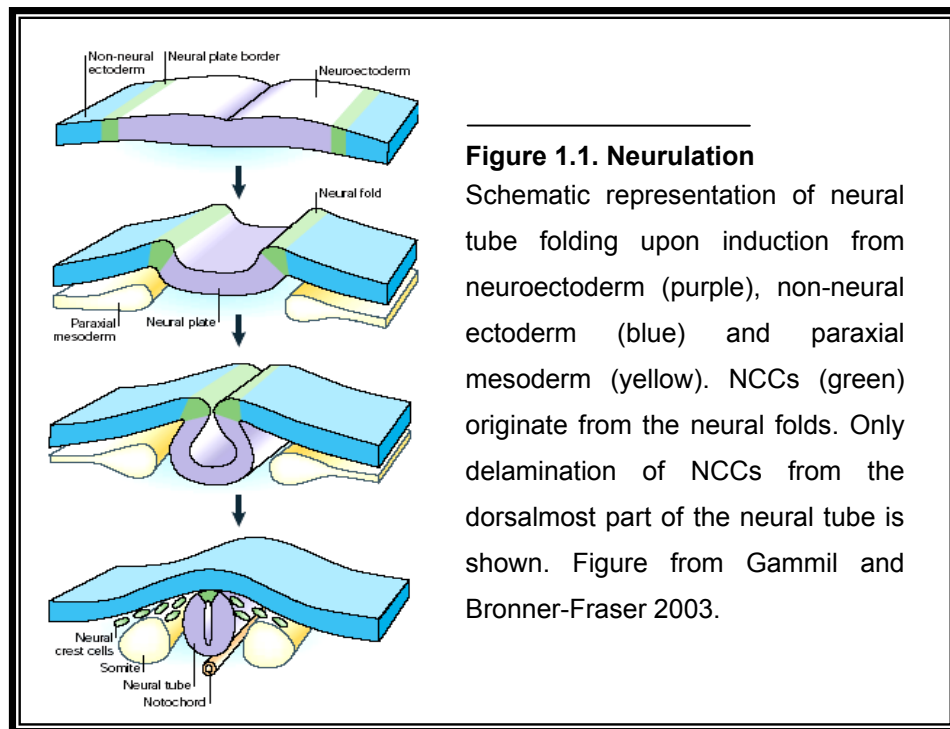
1.1 Ventral midline development

The development of the ventral midline of the human body is a highly complicated multistep process during embryogenesis which involves formation, development, and correct positioning of structures in the midline of the body (e.g. heart, oesophagus, trachea or craniofacial structures). Many of the molecular mechanisms involved in the development of the ventral midline are unidentified. However, neural crest cell (NCC) migration and epithelial-mesenchymal transition (EMT) are thought to be fundamental processes during these stages of embryonic development (Schweiger and Schneider, 2003).

Due to their importance during embryogenesis, NCCs have been considered the fourth germ layer, in addition to the three traditional germ layers, ectoderm, mesoderm and endoderm (Hall, 2000). Moreover, some scientists consider that migrating embryonic NCCs are the best evolutionary acquisition from vertebrates (Thorogood, 1989).

NCCs derive from the ectoderm and originate during neurulation at the dorsal most region of the neural tube between the neural and non-neural ectoderm (Figure 1.1; Gilbert, 2003). NCCs delaminate from the neural folds and migrate to different places, where they generate a prodigious variety of cells, such as neurons, pigment, smooth muscle, connective tissue, or bone, among others. Although the mechanisms involved in NCC formation and migration are highly conserved among vertebrates, the precise moment in which NCCs start their journey differs between species. For instance, in mammals NCCs are induced and

migrate concomitantly with neural plate folding. In contrast, in frogs and birds NCCs start migrating only after neural tube closure (Jones and Trainor, 2005).



NCCs are classified into four subpopulations that give rise to specific cell and tissue types (Gilbert, 2003; Jones and Trainor, 2005):

- **Trunk NCCs** differentiate into neurons of the glia and peripheral nervous system, part of the enteric nervous system, and melanocytes.
- **Cranial NCCs** give rise to cartilage, bone, cranial neurons, glia, and connective tissue of the face and, in addition, they produce pigment cells, and sensory and parasympathetic ganglia.
- **Cardiac NCCs** participate in the formation of the heart and, additionally, generate pigment, skeletal, and neuronal cells
- **Vagal NCCs** form nearly the entire gut, and the majority of neurons and glia of the enteric system.

Each population occupies a different region along the anterior-posterior axis of the neural tube, from which they migrate along unique pathways, that are defined by a Homeobox gene (Hox) gradient (Le Douarin et al., 2004; Lumsden et al., 1991; Selleck and Bronner-Fraser, 1995; Trainor and Krumlauf, 2001).

As previously mentioned, NCCs undergo different processes common to all kinds of NCCs and to all species. After induction of neural plate folding, some previously indistinguishable neuroepithelial cells are induced by signals coming from the presumptive epidermis and neural tube (Mancilla and Mayor, 1996; Selleck and Bronner-Fraser, 1995).

Induced cells then enter into EMT to finally delaminate and migrate (Duband et al., 1995; Knecht and Bronner-Fraser, 2002; Thiery, 2003). During all of these processes, contact-mediated interactions between neural and non-neural tissue take place. All these events take place under a very complex temporospatial collaboration of many different morphogens, such as Wnt, transforming growth factor β family (TGF β) (including bone morphogenic protein, BMP), Hedgehog (HH) family, fibroblast growth factor (FGF) family, Notch, and even retinoic acid and its receptors play a role here (extensively reviewed in Gammill and Bronner-Fraser, 2003; Jones and Trainor, 2005; Knecht and Bronner-Fraser, 2002). All of these pathways participate repeatedly during the life of NCCs; NCC fate is not a sequence of events, but a combination of events and intercalation of pathways functioning concomitantly.

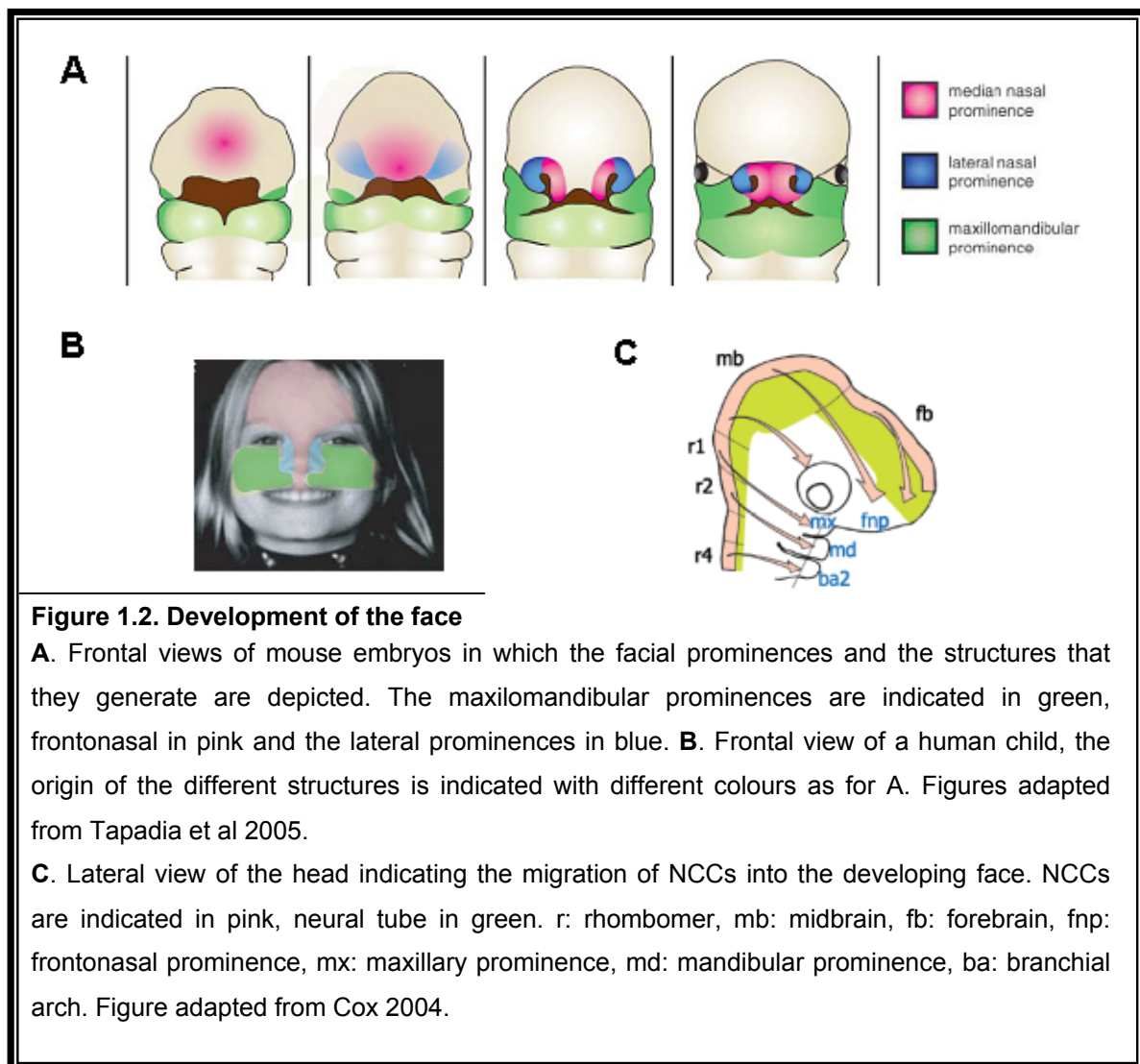
Nevertheless, BMP, Wnt, and FGF signalling by activating transcription factors such as Slug or FoxD3 seem to control the early steps in the induction of NCCs (Barenbaum and Bronner-Fraser, 2005; Huang and Saint-Jeannet, 2004; Nieto et al., 1994). Slug is one of the best-characterised NCC induction markers; it belongs to the Snail/Slug family, and is closely related to Snail. Slug and Snail are both expressed in NCCs in a vertebrate-specific manner (Barrallo-Gimeno and Nieto, 2005; Locascio et al., 2002; Nieto et al., 1994).

After induction, NCCs undergo EMT, process during which epithelial cells lose their polarity and adhesion properties by down-regulation of cell adhesion molecules such as E-cadherin (Pla et al., 2001), transform into mesenchymal cells, and acquire migratory properties. During EMT, an important reorganization of cytoskeletal structures and increase in expression of mesenchymal genes take place (Hay, 2005; Savagner, 2001). Important key players in EMT include again Snail/Slug.

Premigratory NCCs also respond to signals coming from the neural plate and non-neural ectoderm that assure their survival. Induction of Foxd3, Sox9 and Sox10, Zic genes, Pax genes, Notch, Delta, Msx genes, Rhob and Twist is important here (Gammill and Bronner-Fraser, 2003; Jones and Trainor, 2005; Steventon et al., 2005). Adjacent territories also have a strong influence on the delamination of NCCs. Thus, although other pathways like Wnt and FGF also participate (Morales et al., 2005), correct balance between BMP and its antagonist Noggin has been shown to be decisive for correct delamination (Sela-Donenfeld and Kalcheim, 1999).

1.1.1 Craniofacial development

Craniofacial development is one of the most complicated processes during development, which involves the formation of a large number of different tissues and the correct emplacement of the structures of the skull and face (Cohen, 2002; Wilkie and Morriss-Kay, 2001). It begins with the formation of five paired prefacial structures known as branchial or pharyngeal arches, at the ventral surface of the embryo. Next, invading NCCs (Figure 1.2C) in combination with mesodermal cells form the facial prominences (maxilomandibular, lateral and frontonasal), which grow, fuse and expand into more mature craniofacial structures, including the skull (Figure 1.2A). From the first pair of pharyngeal arches emerge the maxillomandibular prominences (Figure 1.2A,B, in green), which give rise to the lateral middle and lower face, the sides of the lips and the lower jaw (only the mandibular prominence) (Cox, 2004; Tapadia et al., 2005). The frontonasal process (Figure 1.2A,B, in pink) contributes to the forehead, the



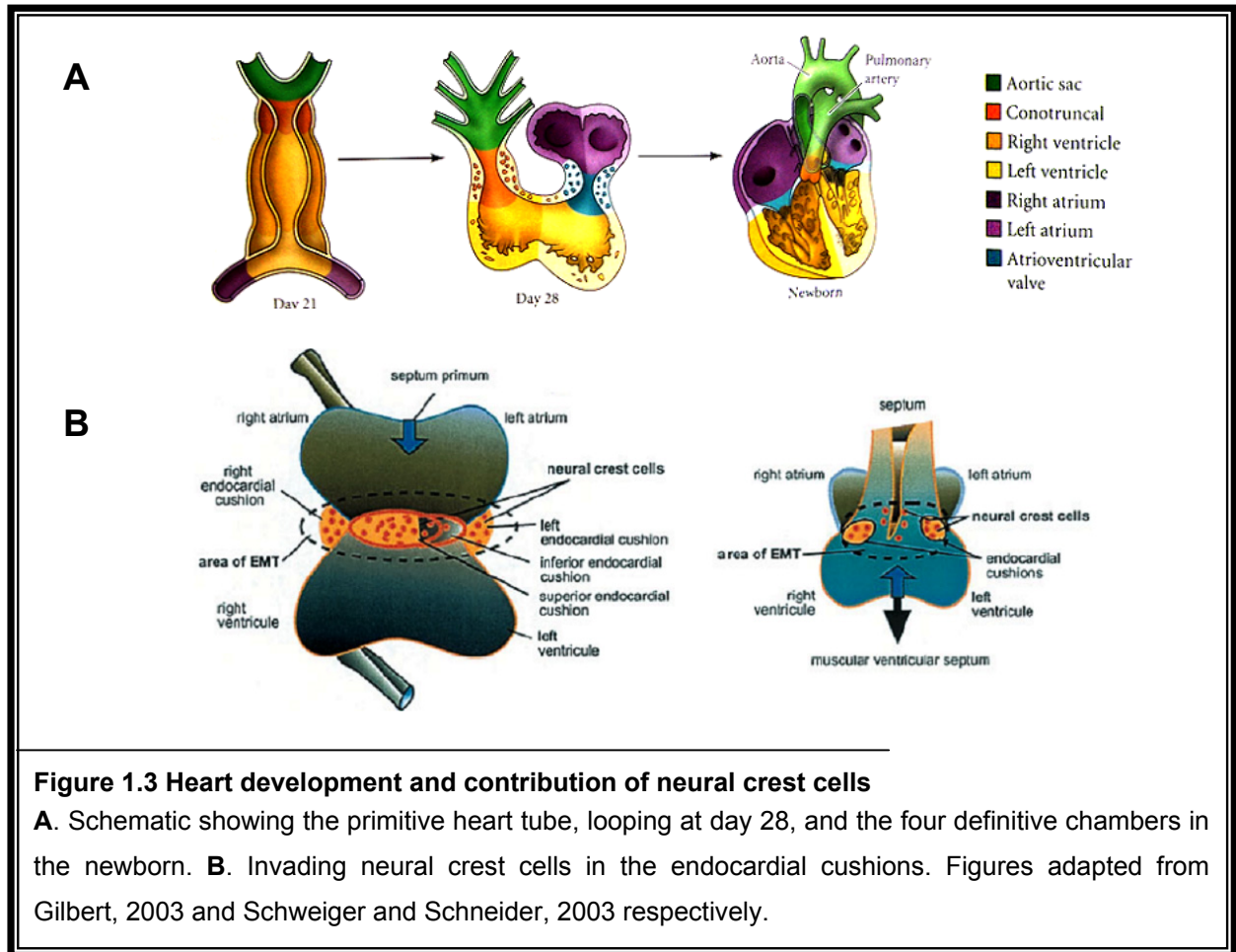
middle of the nose, and, in combination with the maxillary process, to the formation of the midlip and primary palate. Defective coordination of growth and fusion (governed by NCC invasion, EMT and programmed cell death (PCD)) of the prominences can result in cleft lip and palate (Cox, 2004; Kang and Svoboda, 2005; Kang and Massague, 2004; Schweiger and Schneider, 2003). The lateral prominences (Figure 1.2B, in blue) give rise to the lateral nasal structures.

Invading NCCs arising from different areas along the anterior-posterior neural axis (Figure 1.2C, Kontges and Lumsden, 1996) play an important role during craniofacial development. Positional identity along the anterior-posterior axis is obtained through a Hox gene gradient that defines each rhombomer (the parts into which the hindbrain is divided) (Krumlauf, 1993; Santagati and Rijli, 2003). A complex and cautiously regulated coordination of signalling pathways coming from both epithelia and NCCs are of high importance for a successful completion of craniofacial structures (Helms et al., 2005; Noden and Trainor, 2005; Tapadia et al., 2005).

1.1.2 Heart development

At embryonic day 21, the heart is a single chambered tube formed by fusion of two simple epithelial tubes (Figure 1.3A). By day 28, cardiac looping occurs and the presumptive atria are placed anterior to the presumptive ventricles. Upon myocardial signals, cells from the adjacent endocardium detach and form the endocardial cushions, which divide the primitive tube into the atrioventricular channels. Concomitantly, the primitive atrium becomes divided by two septa that grow towards the endocardial cushion. Up to the eighth week of gestation, there is a continuous process of looping and remodelling until the septa close to form the four definitive chambers of the heart, at which point the circulatory and pulmonary systems become independent, with the pulmonary artery connected to the right ventricle and the aorta to the left ventricle (Figure 1.3A, Gilbert, 2003; Schweiger and Schneider, 2003).

Cardiac NCCs, generated from the first to third somites, give rise to the smooth muscle of the aortic arches. In addition, they migrate through the third and more caudal branchial arches and invade the aortopulmonary septum and endocardial cushions collaborating to achieve correct aortopulmonary segmentation (Kirby et al., 1983; Waldo et al., 1998). Similarly to craniofacial development, induced cells producing the endocardial cushion (see above) undergo EMT (Runyan and Markwald, 1983), probably in parallel to PCD (Figure 1.3B, Keyes and Sanders, 2002). NCC invaded regions are commonly affected in patients with complex congenital disorders, such as OS.



1.1.3 Ephrins as NCC pathfinders

NCCs migrate in well-separated streams during development until they reach their site of differentiation. In addition to the earlier mentioned Hox genes, ephrin receptors (Eph receptors) and ephrins have been shown to be essential in delineating migratory routes of NCCs. Obstruction of single Eph receptors can cause a mixture of different streams, with severe developmental consequences (Helbling et al., 1998; Robinson et al., 1997; Smith et al., 1997).

Eph receptors, the largest family of membrane-bound receptor tyrosine kinases, interact with ephrin ligands, which are also membrane-bound proteins. Two classes of Eph receptors, A and B, have been described, distinguished by their predominant binding affinity to ephrin-A ligands (anchored to the membrane through glycosylphosphatidylinositol anchor, GPI anchor) or to ephrin-B ligands (transmembrane), respectively. On the cellular level, the interaction of Eph receptors with their ligands principally influences cytoskeletal organization and cell adhesion, and, consequently, cell migration (Pasquale, 2005). Furthermore, many developmental processes, such as morphogenesis, tissue border formation, vascularization, axon guidance or synaptic plasticity, mainly depend on correct Eph receptor-ephrin signalling (Davy and Soriano, 2005; Holder and Klein, 1999; Murai and Pasquale, 2004; Palmer and

Klein, 2003). Since both Eph receptors and ephrins are membrane-bound proteins, cell-to-cell contact is required for them to interact. They interact in a “kiss and tell” fashion, thereby inducing forward and reverse signals that result in attraction and adhesion or repulsion of participating cells (Gauthier and Robbins, 2003; Kullander and Klein, 2002). For instance, ephrin-B1 can either attract or repel EphB-expressing NCCs (Santiago and Erickson, 2002) and, in this way, the flow of NCC streams is regulated.

Eph receptors and ephrins are powerful patterning molecules. Interestingly, ephrin defects have more drastic effects in some cells than in others. Differential expression of ephrin genes in cells that should be the same makes them behave differently, and in the absence of ephrin expression, all the cells remain the same and their functions can be accomplished by redundant molecules (Compagni et al., 2003; Davy et al., 2004). A clear example is craniofrontonasal syndrome, where the loss of expression of ephrin-B1 (*EFNB1*), leads specifically to defects of the ventral midline, while other structures, where *EFNB1* differential expression is probably not needed, remain unaffected (Twigg et al., 2004; Wieland et al., 2004).

1.1.4 Midline development and disease

The development of the craniofacial structures is a very complicated process that is found altered in a multitude of congenital disorders (Wilkie and Morriss-Kay, 2001). Additionally, there is a high incidence (1 in 700 to 1 in 1000) of non-syndromic cleft lip and palate that involves a complex inheritance pattern (Prescott et al., 2001; Schutte and Murray, 1999). Interestingly, OS is one of the few known causes of monogenic cleft lip and palate.

Mutations of diverse genes participating in the establishment of the ventral midline result in overlapping phenotypes, demonstrating the complexity of this process and the concomitant participation of many pathways. An extensively studied example is holoprosencephaly (HPE) (Roessler and Muenke, 2001), which is characterised by defective forebrain development normally accompanied by cleft lip, cyclopia and overlying proboscis. Alterations in several members of the Sonic Hedgehog (Shh) pathway have been shown to cause HPE (Roessler and Muenke, 2003). In addition, mutations in *GLI3*, a target gene of Shh signalling, cause Greig syndrome (OMIM 175700), which is characterised by hypertelorism and polydactyly.

It has been suggested that defects in NCC migration and epithelial EMT lead to malformations in the ventral midline (Schweiger and Schneider, 2003). DiGeorge Syndrome (DGS; OMIM 188400), also referred as to del22q11, is characterised by aortic arch defects, contruncal heart defects, and pharyngeal and craniofacial anomalies, all structures derived from of NCCs. Since loss of *Tbx1* expression in mouse has been shown to generate a phenotype resembling DGS, *TBX1* has been proposed to be the key gene in DGS (Jerome and Papaioannou, 2001; Merscher et al., 2001). Loss of *Tbx1* expression has also been

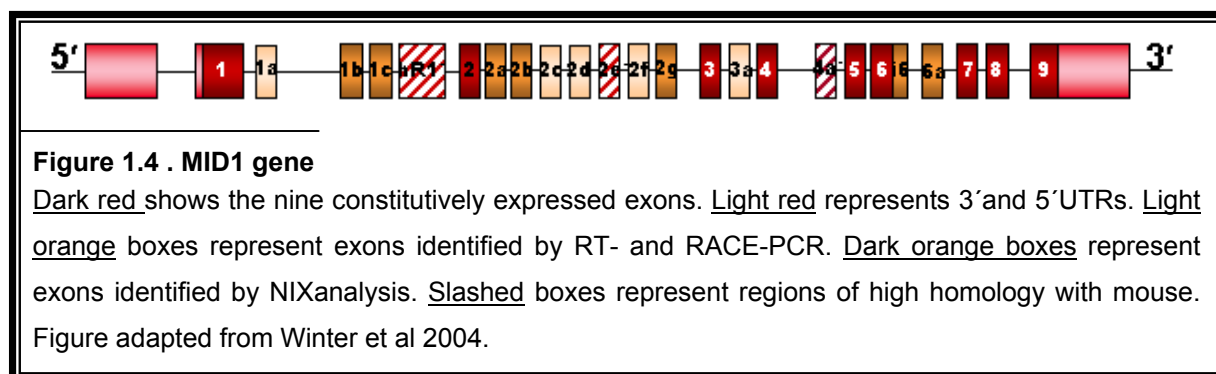
shown to severely affect neural crest and cranial nerve migratory pathways (Moraes et al., 2005; Vitelli et al., 2002)

Mowat-Wilson syndrome (OMIM 235730) is an autosomal dominant complex disorder caused by mutations in the *ZFHX1B* gene. The phenotype of Mowat-Wilson patients is characterised by craniofacial malformations, Hirschsprung disease, mental retardation, congenital heart disease, hypospadias and agenesis of the corpus callosum; all features are suggestive of a neurocristopathy affecting cranial, cardiac and vagal NCCs (Mowat et al., 2003).

In the previously mentioned craniofrontonasal syndrome (OMIM 304110), which is characterised by hypertelorism and broad nasal bridge, mutations in the *EFNB1* gene also result in improper NCC migration (Twigg et al., 2004; Wieland et al., 2004). Moreover, defective NCC migration and EMT have also been proposed to be involved in the pathogenesis of OS (Cox, 2004; Richman et al., 2002; Short and Cox, 2006).

1.2 X-linked Opitz BBB/G syndrome (OS) and MID1

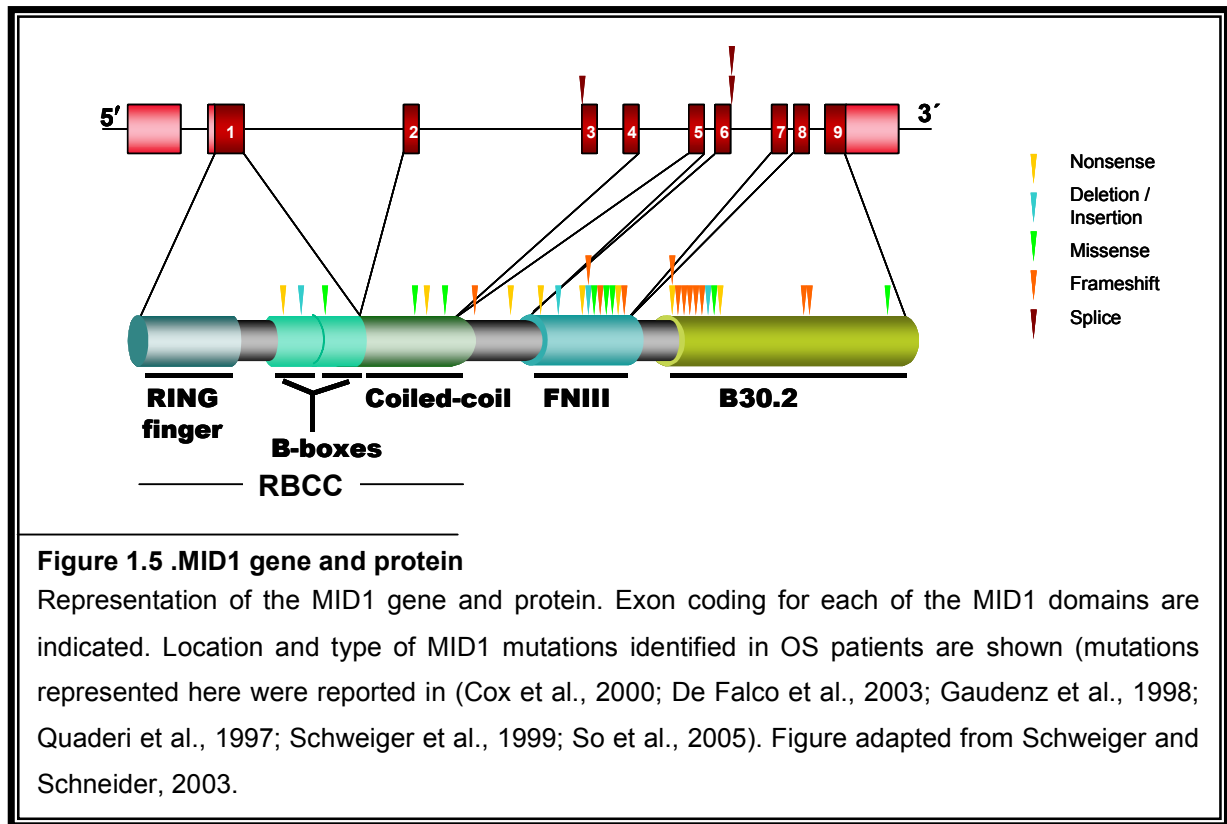
MID1 covers a genomic region of about 300 kb, from which nine exons are constitutively expressed to give an open reading frame (ORF) of approximately 2 kb (Figure 1.4). While the existence of 3' and 5' UTR alternative *MID1* transcripts has been known for some time (Landry and Mager, 2002; Winter et al., 2004), 14 novel alternative exons were recently identified in the human *MID1* gene (Figure 1.4, Landry and Mager, 2002; Winter et al., 2004).



Most of the mutations identified in OS patients are located at the 3' end of the ORF, hence affecting the C-terminus of MID1. With the detection of MID1 in 68% of X-linked OS patients, the majority of the identified mutations are nonsense and frameshift mutations. However, missense mutations, in-frame deletions and in-frame insertions have also been found (Figure 1.5, Schweiger and Schneider, 2003).

The ubiquitously expressed *MID1*-gene encodes a 667 amino acid phosphoprotein, MID1 (Figure 1.5), with a molecular weight of approximately 72 kDa. MID1, also known as TRIM18, belongs to the RBCC protein family, characterised by an N-terminal tripartite motif

(TRIM) and an RFP-like domain at the C-terminus. The RBCC domain comprises a RING finger, two Bboxes and a coiled-coil domain (Schweiger and Schneider, 2003).



1.2.1 The RBCC protein MID1

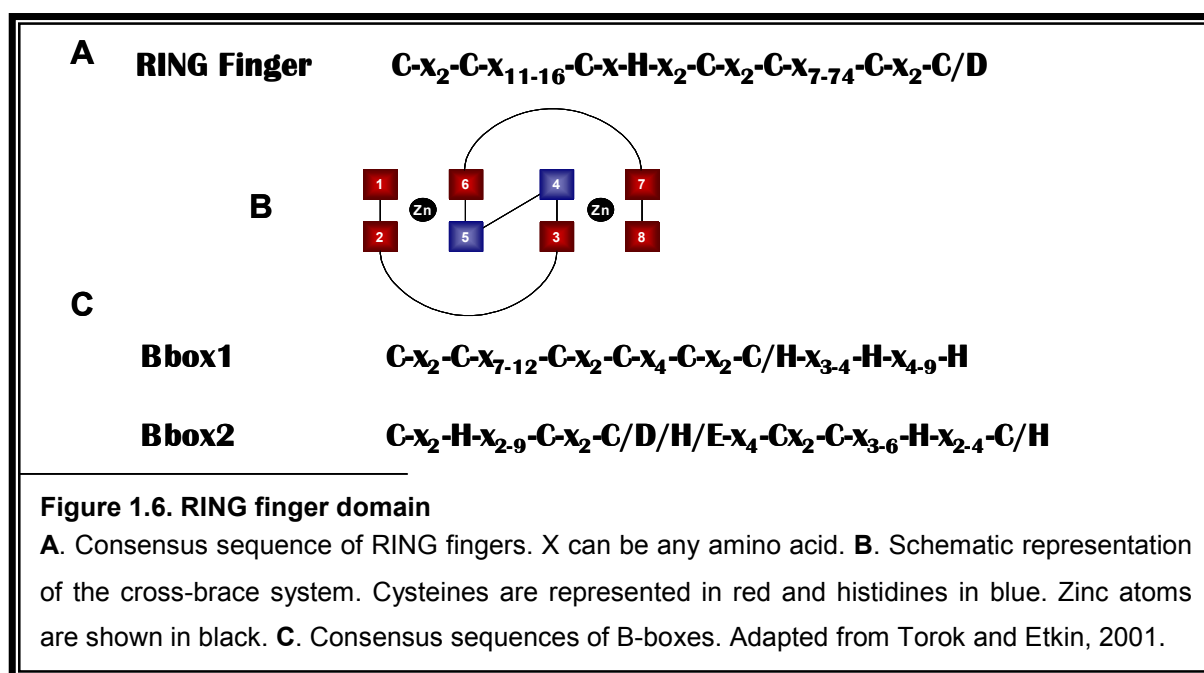
The first RBCC domain was identified in *Xenopus* nuclear factor 7 (XNF7), a protein that participates in the dorso-ventral patterning of *Xenopus* during development (El-Hodiri et al., 1997). The list of identified RBCC proteins has since then grown rapidly and today encompasses 68 members (Nisole et al., 2005; Reymond et al., 2001).

RBCC proteins participate in various important cellular processes such as development, cell growth, and proliferation. In addition, some of them have antiviral properties by targeting retroviruses (Nisole et al., 2005). However, they are recently gaining attention due to the increasing number of proteins in this family involved in human disease. Well-studied examples include the proto-oncogenic proteins RFP (ret finger protein) (Hasegawa et al., 1996), PML (promyelocytic leukaemia) and TIF1- α , which gain oncogenic properties when fused to RET, retionic acid receptor alpha (RAR α), or Braf (Borden et al., 1995a; Grignani et al., 1994; Jensen et al., 2001; Klugbauer and Rabes, 1999; Le Douarin et al., 1995). PYRIN/MARESNOSTRIN, which is mutated in familial Mediterranean fever (FMF) (consortium, 1997), MUL, mutated in Mulibrey nanism (Avela et al., 2000), and MID1, mutated in OS, are some examples of RBCC proteins involved in monogenic disorders.

So far, the only more general function of RBCC proteins that could be defined is ubiquitin ligase activity mediated by the RING finger domain (Meroni and Diez-Roux, 2005). Additionally, some members of this family have been shown to orchestrate the formation of large macromolecular complexes (Borden, 1998; Saurin et al., 1996; Torok and Etkin, 2001).

The RING finger domain of MID1 contains a cysteine rich metal binding domain corresponding to the RING finger consensus sequence (Figure 1.6A). This motif binds two zinc atoms through eight potential metal ligands to form a unique “cross brace” motif (Figure 1.6B, Borden, 2000).

Two Bboxes follow the RING domain in MID1 after a linker of forty-five amino acids, in agreement with the conserved relative position of different domains inside the RBCC motif. Bboxes, like RING fingers, are cysteine- and histidine-rich zinc binding motifs. On account of slightly differing consensus sequences, two different types of Bboxes have been described, Bbox type 1 (Bbox1) and Bbox type 2 (Bbox2) (Figure 1.6C, Torok and Etkin, 2001). The



RBCC motif contains one or two Bboxes; when both are present, as in MID1, Bbox1 always precedes Bbox2, but if only one is present, it is always Bbox2 (Reymond et al., 2001). Bboxes and Bboxes2 include seven potential metal binding ligands, while Bboxes1 include eight potential metal binding ligands. ¹H NMR studies performed on XNF7 Bbox have shown that they bind a single zinc atom in a tetrahedral disposition (Borden et al., 1995b). Curiously, Bboxes only exist in the RBCC protein family, suggesting that they fulfil an essential function of RBCC proteins. Thus far, however, no specific function apart from the mediation protein-protein interactions has been identified (Reymond et al., 2001).

Slightly overlapping and C-terminally situated to Bbox2 is the coil-coiled domain of MID1. Coiled-coil domains are bundles of α -helices, twisted around one another into a super coil or

super helix, which participate in protein-protein interactions and, particularly, in dimerisation processes (Burkhard et al., 2001). Many RBCC proteins homo- and/or heterodimerise through the coiled-coil domain, (e.g. MID1, MID2, RFP, TIF) (Reymond et al., 2001). For MID1, apart from forming homodimers, it can also heterodimerise with MID2, a well-known homologue with the same subcellular localisation (Cainarca et al., 1999). Despite having different expression patterns during development, MID1 and MID2 have 89% amino acid identity and perform overlapping functions (Granata et al., 2005; Short et al., 2002)

As mentioned previously, members of the RBCC protein family have been shown to participate in the formation of macromolecular complexes. PML is one of the most well-studied members; it forms parts of a multiprotein complex called PML nuclear bodies. The RING finger and Bboxes have been found to be necessary for nuclear bodies formation (Jensen et al., 2001). The RFP protein and TIF1- α , two other members of the family, have also been shown to associate with PML nuclear bodies and, additionally, the RFP protein has also been shown to be involved in the formation of homomultiprotein complexes through its Bboxes and coiled-coil domain (Cao et al., 1997).

In the case of MID1, Cainarca et al demonstrated in 1999 that MID1 is part of a large macromolecular complex. Interestingly, mutations in the coiled-coil domain do not disrupt the complex, but produce even larger aggregates. However, most of the interaction partners of the complex remain unknown, and no other members apart from MID1 itself, MID2, $\alpha 4$ (Liu et al., 2001; Trockenbacher et al., 2001), and Mig12 (Berti et al., 2004) have been identified.

An RFP-like domain, also known B30.2 domain, is located at the very C-terminal end of MID1. We have shown previously that MID1 interacts with microtubules through its C-terminal end, as evidenced by the detachment of MID1 from microtubules and subsequent formation of cytosolic aggregates when this domain is mutated (Schweiger et al., 1999). B30.2 domains are present in three different families of proteins: RBCC proteins, BTNs-receptor glycoproteins of the immunoglobulin superfamily and stonutoxin (STNX)- protein secreted with the venom expectorated by *Synanceia horrida* (Henry et al., 1998). As yet, attempts at elucidating a common function for B30.2 domains have been unsuccessful. However, it has been suggested that these domains, as in MID1, fulfil important roles in providing the correct subcellular location of RBCC proteins (Reymond et al., 2001).

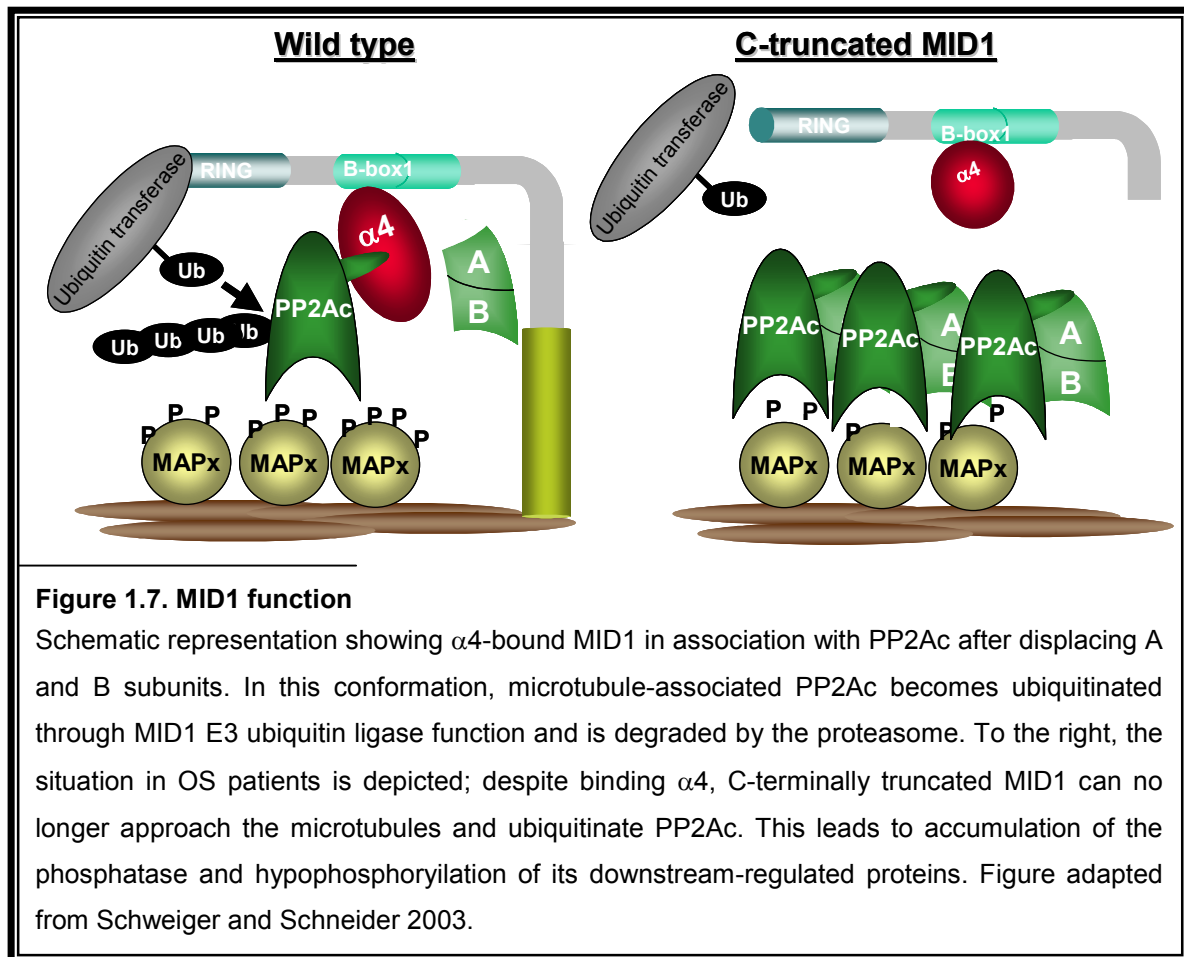
Between the RBCC motif and the B30.2 domain, an FNIII domain has been defined in the MID1 protein (Cox et al., 2000). FNIII domains are found in a huge variety of proteins such as proteins of the extracellular matrix, cell adhesion molecules, enzymes, or muscle proteins. In spite of being highly conserved domains, there is no common function attributable to all proteins in which the domain is found. FNIII domains have a β -sandwich fold closely related to the immunoglobulin fold, and contain several highly conserved prolines. Varying numbers of repeats of the motif are usually found in the different protein families. Last year, it was

proposed that the FNIII domain acts as an elbow linking the various functional sites of the MID1, and anchors the protein to the cytoplasmic region where it is needed, namely at the microtubules (Mnayer et al., 2005). However, these observations require further experimental proof.

1.2.2 The MID1 function

Apart from a microtubule stabilizing role (Schweiger et al., 1999), we could show previously that MID1 interacts with the $\alpha 4$ protein through its Bbox1 and that mutations in the coiled-coil domain or the C-terminus do not affect this interaction (Liu et al., 2001; Trockenbacher et al., 2001). $\alpha 4$, encoded by the *IGBP1* gene, binds and negatively regulates the catalytic subunit of phosphatase 2A (PP2Ac) (Figure 1.7, Chen et al., 1998; Murata et al., 1997). This mechanism was first observed in yeast, where TAP42 (yeast homologue of $\alpha 4$) regulates PP2Ac upon Target Of Rapamycin (TOR) signalling (see section 1.3, Nanahoshi et al., 1999; Raught et al., 2001). $\alpha 4$ is a cytosolic protein with a diffuse distribution, but in association with MID1, it is recruited to microtubules. Reciprocally, an excess of $\alpha 4$ can detach MID1 from microtubules and bring it to the cytosol, indicating that both proteins interact and collaborate in determining their subcellular localisation. The interaction between MID1 and $\alpha 4$ leads to a spatial proximity of the ubiquitin ligase activity of MID1, mediated by its RING-finger domain, and microtubule-associated PP2Ac, which results in a ubiquitin-specific modification and degradation of the phosphatase (Figure 1.7). C-terminally mutated MID1 can no longer bind the microtubules and, therefore, the interaction of the MID1- $\alpha 4$ complex with the pool of microtubule-associated PP2Ac can not take place. As a result, PP2Ac can not be degraded and accumulates at the microtubules, resulting in the hypophosphorylation of downstream regulated microtubule-associated proteins (MAPs) (Schweiger and Schneider, 2003; Trockenbacher et al., 2001).

Interestingly, the phosphorylation status of MAPs targeted by PP2A has been shown to be involved in a variety of developmental disorders, such as Miller-Dieker syndrome, X-linked double cortex syndrome (Avila et al., 1994; Gong et al., 2000). In addition, a similar pathomechanism has been observed in Alzheimer's disease (Trojanowski and Lee, 1995), where hyperphosphorylation of Tau protein is involved (Lim and Lu, 2005).



1.2.3 Regulation of MID1 function

Although MID1 is ubiquitously expressed, OS phenotype specifically affects the ventral midline, suggesting that MID1 function is carefully regulated in a tissue-dependent manner (Schweiger and Schneider, 2003). Moreover, a wide phenotypic variability among OS patients has been described (Cox et al., 2000; So et al., 2005) pointing at modifying factors that participate to regulate MID1 function. Three different mechanisms have been proposed for the regulation of MID1 function:

A - Splicing mechanisms. *MID1* produces a multitude of alternatively spliced transcripts that are differentially expressed in diverse tissues (Winter et al., 2004). The splice variants lead to loss-of-function through several mechanisms conserved in human, mouse and fugu. Some transcripts produce C-terminally truncated MID1 that binds more strongly to $\alpha 4$ and have a dominant negative effect over MID1. Others contain premature stop codons that, in contrast to the previously described transcripts, lead to non-sense mediated decay (NMD). Interestingly, a splice variant lacking the Bbox2 domain has been shown to bind with higher affinity to $\alpha 4$, hinting at an important role of this domain in regulating the interaction of MID1 with the PP2A complex.

B - Protein interaction. MID1 is a member of a multiprotein complex. Thus, the regulation of other members of the complex implies the regulation of MID1. Recently, it has been shown that $\alpha 4$ is expressed during development in tissues affected by OS, suggesting that the tissue-specific expression of $\alpha 4$ could contribute to regulate MID1 function (Everett and Brautigan, 2002). Similar observations have been made for Mig12 (Berti et al., 2004).

It is also known that MID2 is functionally equivalent to MID1. It has been proposed that in some tissues, MID2 substitutes for MID1 to a greater extent than in others and, consequently, only those tissues with less MID2 activity would suffer from MID1 loss (Buchner et al., 1999; Granata et al., 2005; Short et al., 2002).

C - Phosphorylation status. Having been shown to be a phosphoprotein, it has been proposed that MID1 phosphorylation status (or other post-transcriptional modifications) regulates its association with, and subsequent stabilization of, microtubules. In 2001, Liu et al showed that MAP kinase activity is required to maintain MID1 association to microtubules. Unfortunately, most of the mechanisms underlying MID1 posttranslational modification and regulation remain unknown.

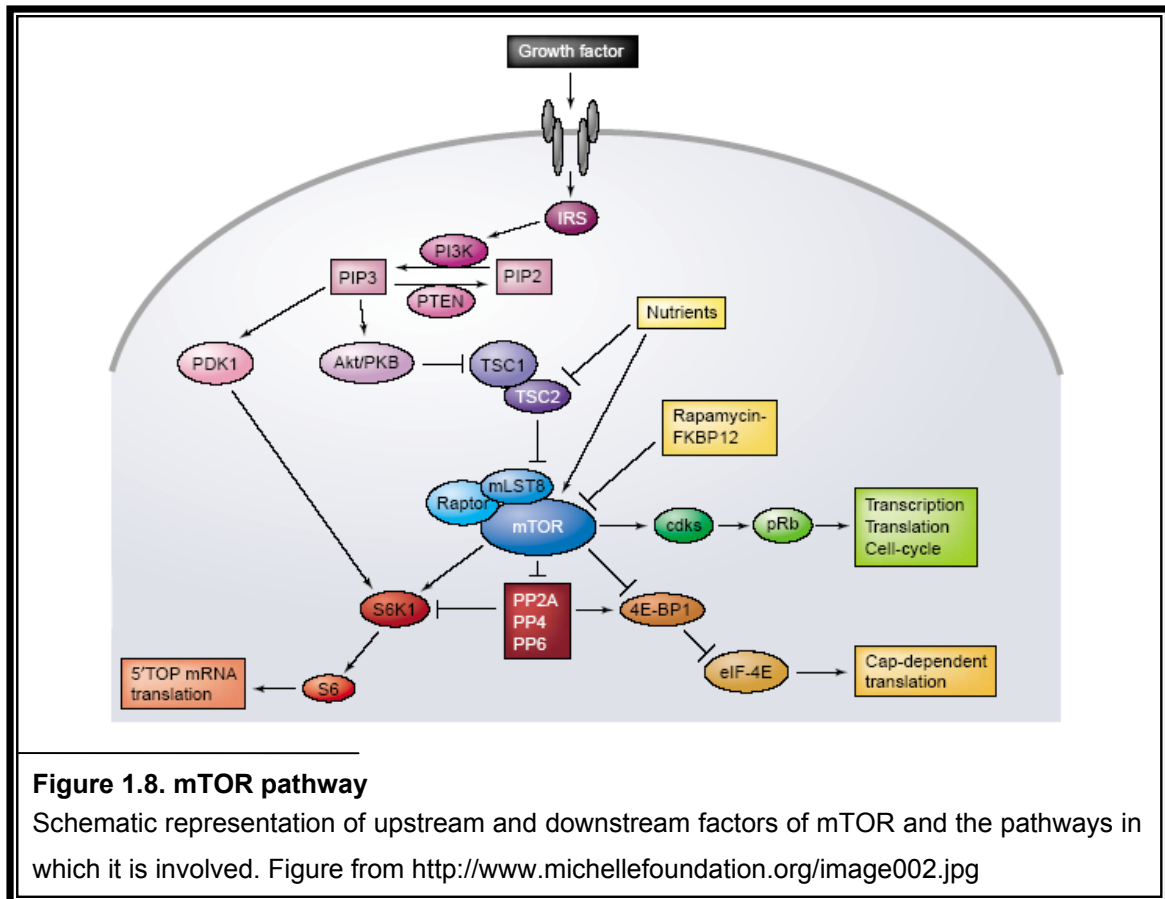
1.3 mTOR pathway

In 1991, a screening of mutations conferring resistance to rapamycin in *S.cerevisiae* led to identify TOR1, TOR2 (Target of Rapamycin) and FPR1 kinases (Heitman et al., 1991). Rapamycin, a potent cell proliferation and growth blocker, and immunosuppressant, forms a complex with FKBP12 (FK506-binding protein of 12kDa; coded by FPR1) that binds and inhibits TOR. This mode of action is well-conserved from yeast to mammals. TOR is an evolutionary conserved serine/threonine kinase, member of the phosphatidylinositol kinase-related protein kinase complex (PIKK). While the majority of lower eukaryotes have two Tor proteins, in higher eukaryotes only one orthologue is found (Jacinto and Hall, 2003).

mTOR, the mammalian TOR orthologue, is a large protein that forms large macromolecular complexes through its multiple protein-protein binding domains. So far, only three interaction partners of mTOR have been identified, RAPTOR (regulatory associated protein of TOR), G β L (G-protein β -subunit-like protein) and RICTOR (rapamycin-insensitive companion of TOR) (Hara et al., 2002; Kim et al., 2002; Kim et al., 2003; Sarbassov et al., 2004). The RICTOR complex, like the Tor2 complex in yeast, specifically regulates the cytoskeleton, independent of rapamycin-sensitive pathways (Jacinto et al., 2004).

As a key regulator of cell proliferation and growth, mTOR senses and integrates nutrients and growth factor signals to regulate protein translation and ribosome biogenesis (reviewed in Fingar and Blenis, 2004). Although the best-characterised downstream targets of mTOR are S6K1 and 4E-BP1 (Figure 1.8, Gingras et al., 2001), other upstream and downstream factors of mTOR have been extensively studied and reviewed (Hay and

Sonenberg, 2004). A complex pattern of signals regulates mTOR (Figure 1.8), probably because protein synthesis requires large amounts of energy, and the cell has to make sure that the conditions are adequate to proceed. mTOR activation is controlled by levels of nutrients (branched amino acids and energy) and growth factors, which activate PI3K signalling and regulate mTOR through a sequential pathway known as PI3K/Akt/TSC/Rheb pathway. Interestingly, PI3K can phosphorylate 4E-BP1 and S6K1 and, thus, control cell proliferation independently from mTOR (reviewed in Fingar and Blenis, 2004).



Activated mTOR, forming a complex with RAPTOR and G β L, and in collaboration with the PIK3 pathway, phosphorylates S6K at several residues. Once phosphorylated, S6K phosphorylates the 40S ribosomal protein S6 (rpS6). This mechanism was formerly believed to regulate 5'TOP mRNA translation, but recently, this has been shown to be unlikely (Tang et al., 2001a). However, it is clear that mTOR is involved in the induction of 5'TOP marked mRNA translation (Pende et al., 2004), and since many of these RNAs encode ribosomal proteins and elongation factors, the translational capacity of the cell as a total increases.

4E-BP1, the second well-known target of mTOR, is a repressor of the translation initiation factor eIF4E. When activated, eIF4E recognizes the cap structure (m7GpppN) at the 5' end of some mRNAs and initiates cap dependent translation by interacting with eIF4G, a scaffolding protein that recruits the translation machinery to the 5' end of mRNA (Gingras et al.,

2001). Under mTOR activation and PIK3 signalling, 4E-BP1 is phosphorylated and disassembles from eIF4E, thereby allowing the initiation of cap-dependent translation.

In addition, TOR regulates phosphatase activity by promoting the binding of TAP42 (type 2A associated protein) to the catalytic subunit of PP2A and to SIT4 (type 2A related phosphatase) in a rapamycin-sensitive manner. This results in the inhibition of PP2A activity (Di Como and Arndt, 1996; Jiang and Broach, 1999). In mammals, a similar mechanism mediated by the TAP42 homologue $\alpha 4$ has been proposed (Chen et al., 1998; Schweiger and Schneider, 2003). Although it has been shown that mTOR regulates phosphatase activity and that $\alpha 4$ negatively regulates PP2A activity, the contribution of rapamycin to the $\alpha 4$ -PP2A complex remains controversial (Dennis et al., 1999; Peterson et al., 1999).

1.4 Aim of the study

Upon binding the linker protein $\alpha 4$, the microtubule-associated RBCC protein MID1 targets the microtubule-associated PP2Ac towards ubiquitin specific modification and degradation. In OS patients, which are characterised by ventral midline malformations, MID1 harbours mutations in the C-terminal end, resulting in the loss of microtubule-association and formation of cytoplasmic clumps in the cell. Despite preserving its association with $\alpha 4$, C-terminally mutated MID1 can not approach the vicinity of PP2Ac and therefore, the ubiquitination and degradation of microtubule-associated PP2Ac becomes disrupted, leading to hypophosphorylation of its downstream targets. Recently, several OS patients have been found to hold mutations in the Bboxes in the N-terminal end of MID1. Although Bboxes are known to participate in protein-protein interactions, no common functional roles could be attributed to them thus far. For the MID1 protein, it has been shown that the first of the two Bboxes interacts with $\alpha 4$, and a regulatory role of this interaction has been suggested for the second Bbox. Consequently, any disruption of these domains interfering with $\alpha 4$ -binding would be expected to lead to accumulation of PP2Ac, thus causing OS. During this thesis, a detailed study of the influence of Bbox mutations on the MID1- $\alpha 4$ and MID1-microtubules interactions by immunofluorescence, immunoprecipitation and yeast two-hybrid experiments was performed to further analyse the functions of the two Bboxes and thus, pave the way for a novel pathomechanism responsible for OS.

Not only the Bboxes, but also, similar to other RBCC proteins, several other domains of MID1 have been proposed to participate in protein-protein interactions, thus forming a multiprotein complex consisting of as-yet-unknown protein components. Proteins belonging to the MID1 complex are potentially important players in the development of the ventral midline and the pathogenesis of OS. Consequently, another main focus of this study was to use affinity chromatography and mass spectrometry to biochemically purify the MID1 complex and identify associated proteins. Subsequently, the MID1 complex should be characterised.

2 Materials and Methods

2.1 Materials

2.1.1 General reagents

| Reagent | Manufacturer |
|---|---------------|
| β -mercaptoethanol | Merck |
| Acetic acid 100% | Merck |
| Acetone | Merck |
| Agarose | Invitrogen |
| Amino acids | Sigma |
| Ammonium persulfate | BioRad |
| Ampicillin | Sigma |
| Aqua ad inectabilia | Baxter |
| BACTO-Yeast extract | BDSciences |
| BACTO-Agar | Difco |
| BACTO-Tryptone | Difco |
| Biotin | Sigma |
| Biotin-16-UTP | Roche |
| Boric acid | Merck |
| Bovine Serum Albumin | Serva / Sigma |
| Bradford reagent | Sigma |
| Bromphenolblue | Serva |
| Chloramphenicol | Fluka |
| Chloroform | Merck |
| Complete/Complete mini protease inhibitors | Roche |
| Coomassie G250/Coomassie R250 | Serva |
| DABCO (1,4-diazobicyclo-2,2,2-octane) | Sigma |
| DAPI (4,6-diamino-2-phenylindole-2HCl·H ₂ O) | Serva |
| d-Biotine | Sigma |
| Deoxycholic acid sodium salt (DOC) | Fluka |
| Diethylpyrocarbonat | Sigma |
| DMEM (Dulbecco's Modified Eagle Medium) | Cambrex |
| DMSO | Sigma |
| dNTPs | Fermentas |
| DTT | Promega |
| EDTA | Merck |
| EGTA | Merck |
| Ethanol | Merck |
| Ethidium bromide | Serva |
| Fetal calf serum (FCS) | Biochrom |
| Ficoll | Pharmacia |
| Fixing solution | Agfa |
| Formaldehyde | Merck |
| Glucose monohydrate/Sucrose | Merck |
| Glutamine | Cambrex |
| Glycerol | merck |

| | |
|---|----------------------------|
| Glycin | Merck |
| Glycogen | Roche |
| GTP | Sigma |
| H ₃ PO ₄ | Merck |
| Heparin | Sigma |
| HCl | Merck |
| Imidazole | Fluka |
| Immersion oil immersol 518F | Zeiss |
| IPTG | Fermentas |
| Isopropanol | Merck |
| K ₂ PO ₄ | Merck |
| Kanamycin | Sigma |
| KCl | Sigma |
| LiAc | Sigma |
| LiCl | Sigma |
| Lipofectamine 2000 transfection reagent | Invitrogen |
| Lysozyme | Boehringer-Ingelheim |
| M280 streptavidine coated magnetic beads | DYNAL |
| Methanol | Merck |
| MgCl ₂ | Merck/ PerkinElmer |
| MgSO ₄ | Merck |
| Milk powder | Nutricia-Zoetermeer |
| Mineral oil | Sigma |
| Na ₂ HPO ₄ | Merck |
| NaAc/NaCl/NaOH | Merck |
| NaHPO ₄ | Merck |
| NBT/BCIP | Roche |
| Ni-NTA agarose | Qiagen |
| NP40 | Fluka |
| Oligofectamine | Invitrogen |
| OPTIMEM | GIBCO |
| Paraformaldehyde | Sigma |
| pdN ₆ | Pharmacia |
| PEG | Sigma |
| Penicillin/streptomycin | Cambrex |
| Phenol | Roth |
| PIPES | Sigma |
| Polyfect | Qiagen |
| Polyhomoribopolymers agarose (poly-rG, poly-rU, poly-rC, poly-rA) | Sigma |
| Prime RNAase inhibitor | Eppendorf |
| Protein agarose A/G | Roche |
| RNA guard | Amersham Pharmacia biotech |
| RNA loading dye | Fermentas |
| Rothiphorese gel 30 | Roth |
| Roty-Nylon Plus membrane | Roth |
| SDS (sodium dodecylsulfate) | BioRad/ Serva |
| siRNA oligos | Qiagen/Dharmacon |
| Streptavidine-AP | Roche |
| Taxol (Paclitaxel) | Sigma |

| | |
|-----------------------------------|--------------|
| Taxol (Paclitaxel) | Sigma |
| TEMED | GIBCO BRL |
| Trichloro acetic acid (TCA) | Sigma |
| Tris-(hydroxymethyl)-aminomethane | Merck |
| Triton X-100 | Serva |
| Trizol | Merck |
| Tween20 | Sigma |
| Urea | Merck/BioRad |
| Vivaspin 500 | Vivascience |
| X-Gal | Appligene |
| Xylencianolblue | Sigma |
| Yeast base without amino acids | Difco |
| Zeocin | Invitrogen |

Table 2.1. General reagents

2.1.2 Enzymes

| Enzyme | Concentration | Manufacturer |
|--------------------------------------|------------------|---------------------------------|
| Cloned Pfu DNA polymerase | 2,5 U/ μ l | Stratagene |
| DNAse I | 1 U/ μ l | Promega |
| Proteinase K | 10 mg/ml | Roche |
| Restriction endonucleases | 10-20 U/ μ l | New England biolabs / Fermentas |
| RNAse A | 10 mg/ml | Roche |
| Superscript II reverse transcriptase | 200 U/ μ l | Invitrogen |
| T4 DNA ligase | 400 U/ μ l | Promega |
| Tag DNA polymerase | 5 U/ μ l | House made |
| Thrombin, restriction grade | 1,58 U/ μ l | Novagen |

Table 2.2. Enzymes

2.1.3 Kits

| Kit | Manufacturer |
|--|--------------|
| Advantage 2 PCR Kit | Clontech |
| Endofree Plasmid Maxi Kit | Qiagen |
| Profound Pull-Down Biotinylated Protein: Protein Interaction Kit | Pierce |
| Qiaprep Spin Miniprep Kit | Qiagen |
| Qiaquick Gel Extraction Kit | Qiagen |
| Quick Change Directed Mutagenesis Kit | Stratagene |
| RiboMAX Large Scale RNA Production System-T7 | Promega |
| RNeasy Mini Kit | Qiagen |
| Termination Ready Reaction Mix | PerkinElmer |

Table 2.3. Kits

2.1.4 Instruments and Disposables

| Instrument/disposable | Manufacturer |
|----------------------------------|---------------------|
| 0,025 μ m filters | Millipore |
| Centrifuge Rotanta 46R/Rotina 4R | Hettich zentrifugen |
| Centriplus/Centricon | Millipore |
| Concentrator 5301 | Eppendorf |

| | |
|--|------------------------|
| Cover slips | Menzel Glaser |
| Electrophoresis power supply 2 | House made |
| Extra thick blot paper | BioRad |
| Filter paper | Schleicher and schuell |
| Fixogum | Marabu |
| Gene Pulser cuvettes/ Gene pulser I-Pulser chamber | BioRad |
| Handee Mini Spin Columns | Pierce |
| Horizontal gel apparatus Horizon® 11.14 and 20.25 | Life technologies |
| Hypercassete | Amersham biosciences |
| Inverted microscope Elipse TS100 | Nikon |
| L8-70M ultracentrifuge | Beckmann |
| Microscope slides | Roth |
| Phase lock gel light | Eppendorf |
| pH-meter | Knick |
| Photometer Ultrospec II | LKB biochrom |
| Pipett boy | Integra biosciences |
| Pipettes | Gilson |
| Potter | B. Braun Melsungen |
| Power Pac 300 electrophoresis power supply | BioRad |
| PVDF membrane | Roche |
| QIAshredder | Qiagen |
| RNA tips | Biozym |
| Rnase ZapWipes | Ambion |
| Rotors TLA120.1, TLS-55, SW40 | Beckmann |
| Single use filter unit Minisart | Sartorius |
| Slide-A-Lyzer mini dialysis unit | Pierce |
| Sonicator, SONOPLUS Homogenisator HD2070 | Bandolin electronics |
| Sorvall RC-5B refrigerated superspeed centrifuge | Sorvall |
| Steril plastic disposables for cell culture | TRP |
| Table centrifuge 5415C | Eppendorf |
| TL100 ultracentrifuge | Beckmann |
| UV stratalinker 1800 | Stratagene |
| UV trasiluminator | UVPinc |
| UVette | Eppendorf |

Table 2.4. Instruments and disposables

Note: Instruments and disposables not included in table 4 are indicated in the corresponding sections. All reusable lab ware was autoclaved before use.

2.1.5 Antibodies

| Antibody | WB | IF | IP | Animal | Purchased from |
|-----------------------|--------|--------|--------|--------|--|
| Anti-α4 | 1:200 | | | Rabbit | Self-produced (Trockenbacher et al., 2001) |
| Anti-MID1 | 1:1000 | | | Rabbit | Self-produced (Winter et al., 2004) |
| Anti-Actin | 1:500 | | | Rabbit | Sigma |
| Anti-Tubulin MCA 77s | 1:1000 | 1:3000 | | Rat | Serotec |
| Anti-Tubulin MCA 78s | 1:1000 | 1:3000 | | Rat | Serotec |
| Anti-c-myc monoclonal | 1:500 | 1:500 | | Mouse | Clontech |
| Anti-c-myc polyclonal | 1:500 | 1:800 | 1,5 µg | Rabbit | Santa Cruz |

| | | | | |
|-----------------------------|---------|--------|---------------|--|
| Anti-V5 | 1:3000 | 1:800 | Mouse | Invitrogen |
| Anti-FLAG-polyclonal | 1:400 | | 1,6 µg Rabbit | Sigma |
| Anti-FLAG-monoclonal | 1:1000 | 1:500 | Mouse | Stratagene |
| Anti-Nucleophosmin | 1:1000 | | Mouse | Zymed |
| Anti-EF-1α | 1:1000 | | Mouse | Upstate |
| Anti-Lamin A+C | 1:350 | | Mouse | Chemicon |
| Anti-Annexin II | 1:1000 | | Mouse | BD-transduccion laboratories |
| Anti-Hsp90 | 1:2000 | | Rat | Stressgene |
| Anti-Hcs70 | 1:10000 | | Rat | Stressgene |
| Anti-RACK1 | 1:2500 | | Mouse-IgM | BD-transduccion laboratories |
| Anti-HuR | 1:1000 | | Mouse | Santa Cruz |
| Anti-GFP | 1:500 | | Mouse | Roche |
| Ribosomal antibodies | 1:1000 | | rabbit | Gift from J. Stahl (Lutsch et al., 1990) |
| Anti-Rabbit HRP | 1:2000 | | Donkey | Amersham |
| Anti-Rabbit HRP non-reduced | 1:25000 | | mouse | Sigma |
| Anti-Mouse HRP | 1.5000 | | Goat | Dianova |
| Anti-Mouse IgM -HRP | 1:2500 | | Donkey | Dianova |
| Anti-Rat HRP | 1:1000 | | Rabbit | Serotec |
| Anti-Rat HRP | 1:1000 | | Goat | Santa Cruz |
| Anti-Rabbit Cy3 | | 1:1000 | Goat | Dianova |
| Anti-Mouse Cy3 | | 1:1000 | Donkey | Dianova |
| Anti-Rat Cy3 | | 1:1000 | Donkey | Dianova |
| Anti-Rabbit FITC | | 1:250 | Goat | Dianova |
| Anti-Mouse FITC | | 1:1000 | Goat | Dianova |
| Normal mouse IgG | | | | Santa Cruz |

Table 2.5. Primary and secondary antibodies

2.1.6 Vectors

| Vector | Host | Tag | Resistance/Selection | Use | Manufacturer |
|---------------|---------------------|---------------------------|----------------------|--------------------|--------------|
| pCMV Tag 2A-C | Mammalian | Flag | Kanamycin | IF, IP | Stratagene |
| pCMV Tag 3A-C | Mammalian | Myc | Kanamycin | IF, IP | Stratagene |
| pBUD CE4 | Mammalian | Myc / V5 | Zeocin | IF, IP | Invitrogen |
| pEGFP | Mammalian | GFP | Kanamycin | IF | Clontech |
| PinPoint Xa | <i>E. coli</i> | Biotin/HIS (incorporated) | Ampicillin | Protein expression | Promega |
| pET-32a | <i>E.coli</i> | His-tag, S-Tag, Trx-tag | Ampicillin | Protein expression | Novagen |
| pBMT116a | <i>E.coli</i> | | Ampicillin/ | Yeast two- | Clontech |
| | <i>/S.cerevisae</i> | | Tryptophane | hybrid | |
| PGAD1o | <i>E.coli</i> | | Ampicillin/ | Yeast two- | Clontech |
| | <i>/S.cerevisae</i> | | Leucine | hybrid | |

Table 2.6. Vectors

2.1.7 Buffers and Media

| Buffer/Media | Composition |
|------------------|---|
| APS 10% | 10% w/v APS in water, aliquoted and stored at -20°C |
| Annealing buffer | 100 mM KAc, 30mM Hepes-KOH pH 7,4, 2 mM MgAc ₂ |

| | |
|---------------------------------|--|
| Blocking buffer | 5% milk powder in PBST |
| Blotting buffer 1 x | 5x blotting buffer: MeOH: bidest H ₂ O 1:1:3 |
| Blotting buffer 5 x | 29,11g Tris; 14,65g Glycin; 18,75ml SDS in 1l bidest water |
| Colloidal coomassie staining | 1g CBB G-250 in 100 ml bidest H ₂ O; 100 g (NH ₄) ₂ SO ₄ and 20 g H ₃ PO ₄ (85%) in 800 ml bidest H ₂ O. Mix both solutions and adjust the volume to 1 l bidest H ₂ O. |
| Coomassie | 1 g Coomassie blue R250, 500 ml H ₂ O, 100 ml HAc, and 400 ml methanol. Mix and filter through a filter paper |
| Destaining Coomassie | 500ml H ₂ O, 100ml HAc, and 400 ml methanol. |
| DPEC H ₂ O | 0,1% DEPC was overnight stirred in water and afterwards autoclaved. |
| Dropout solution 10x | 200 mg/l L-Adenine Hemisulfat salt, L-Arginine HCl; L-Histidine HCl Monohydrate, L-Methionine, L-Tryptophane, L-Uracil; 300 mg/l L-Isoleucine, L-Lysine HCl, L-Tyrosine; 500 mg/l L-Phenylalanine; 1000 mg/l L-Leucine; 1500 mg/l L-Valine; 2000 mg/l L-Threonine; in 1l Bidest; autoclave |
| -TL/-HTL Dropout solution | Dropout solution without leucine and threonine/ and histidine |
| Elution buffer (HIS) | 50 mM NaH ₂ PO ₄ ; 300 mM NaCl; 250 mM imidazole. Adjust to pH 8,0 using NaOH |
| Ethidium bromide | 10 mg/ml EtBr in bidest H ₂ O |
| Hepes Sucrose (HS) buffer | 4 mM Hepes, 0,32 M sucrose in bidest H ₂ O, filter sterilized, stored at -20°C. |
| HSNM buffer | 4 mM buffer, 0,32 M Sucrose, 100 mM NaCl, 5 mM MgCl ₂ in DEPC-H ₂ O |
| IP1 buffer | 150 mM NaCl; 10 mM Tris pH 7,5; 1% NP40; autoclaved |
| IPTG | 100 mM in bidest, filter sterilized and stored at -20°C |
| Laemmli buffer | 25 mM TRIS p.a, 190 mM Glycin, 0,1% SDS in bidest H ₂ O |
| LB (Luria Bertani) medium | 15 g Agar; 10g Tryptone; 5g yeast extract in 1l bidest water; autoclaved |
| DNA-Loading buffer (LX, LB) | 15% Ficoll, 0,25% Bromphenolblue or Xylenecyanol in bidest H ₂ O |
| Lysis buffer (QIAexpressionist) | 50 mM NaH ₂ PO ₄ ; 300 mM NaCl; 10 mM imidazole adjust to pH 8,0 using NaOH |
| Magic mix 2x | 48% Urea (BioRad), 15mM Tris-HCl pH 7,5, 8,7% Glycerin, 1%SDS, 0,004% Bromphenolblue, 143 mM β-mercaptoethanol (add fresh) |
| Microtubule assembly buffer | 0,1 M PIPES ph 6,8; 1 mM MgSO ₄ ; 2 mM EGTA; 2 mM DTT; 0,1 mM GTP |
| MOPS 10 x | 0,4 M MOPS; 0,1 M NaAc; 10 mM EDTA pH 7,0 |
| Mounting medium | 90% glycerol; 0,1 M Tris-HCl pH 8,0; 2,3 % DABCO |
| Paraformaldehyde | 3,7% formaldehyde in 1,2 PEM Buffer |
| Paraformaldehyde 3,7% | In 1,2 x PEM. Dissolve at 60°C. Store at -20°C |
| PBS 1 x | 137 mM NaCl; 2,7 mM KCl; 10,1 mM Na ₂ HPO ₄ ; 1,8 mM KH ₂ PO ₄ |
| PBST | 1 x PBS; 1:1000 Tween 20 |
| PEM 10X | 1 M PIPES, 0,5 M EGTA, 0,02 M MgCl ₂ in bidest H ₂ O, adjust pH 7 with 10N NaOH and autoclave |
| RNA loading buffer | 1 µl MOPS, 5 µl loading dye, 1,5 µl 37% formaldehyde, 10 µl DEPC.water |
| SDS-PAGE buffer 5x | 15% β-Mercaptoethanol, 15% SDS, 1,5% Bromphenolblue, 50%glycerol |
| Separating gel buffer | 1,5 M Tris-HCl, 0,4 % SDS pH 8,8 |
| SSC 10x | 3M NaCl, 0,3M Na-citrate in bidest H ₂ O, adjust pH 7 with 1M HCl, filter |
| Stacking gel buffer | 0,5 M Tris-HCl, 0,4 % SDS pH 8,8 |
| Sucrose cushion | 0,2 g sucrose; were dissolved by shaking at 37°C in 280 µl MT buffer, afterwards 4µl dGTP (100 mM) and 1µ taxol (5 mg/ml) were added |

| | |
|-----------------------------------|--|
| TAE buffer 50 x | 50 mM EDTA, 5,71% v/v acetic acid, 2M Tris-HCl |
| TBS | 10 mM Tris-HCl (pH 8,0); 150 mM NaCl |
| TBST buffer | 10 mM Tris-HCl (pH 8,0); 150 mM NaCl; 0,05% tween 20 |
| TE | 10 mM Tris-HCl pH 7,5; 1 mM EDTA |
| TES | 10 mM Tris-HCl pH 7,5; 5 mM EDTA; 0,2 % SDS |
| TKM buffer | 20 mM Tris, 100 mM KCl, 5 mM MgCl ₂ in DEPC-H ₂ O |
| Wash buffer (QIAexpressionist) | 50 mM NaH ₂ PO ₄ ; 300 mM NaCl; 20 mM imidazole adjust to pH 8,0 using NaOH |
| Washing buffer for column | HS buffer with 250 mM NaCl, 0.5% Tween |
| YPD buffer | 20 g/L BACTO-tryptone, 10 g/L yeast extract, 20 g/L Bacto-Agar (only for plates) |
| Z-buffer | 1,61 g/L Na ₂ HPO ₄ *7H ₂ O, 5,5 g/L NaH ₂ PO ₄ *H ₂ O, 0,75 g/L KCl, 0,246 g/L MgSO ₄ *7H ₂ O, pH 7,0 |

Table 2.7. Buffers and media

2.1.8 Cell lines

| Cell line | Description | Medium |
|---------------------------|--|--|
| HeLa (Henrietta Lacks) | Human epithelial cells from cervical carcinoma | DMEM, 10% FCS, 2mM L-glutamine, 100 µg/ml streptomycin, 100 units/l penicillin |
| COS-7 | Transformed African Green Monkey Kidney Fibroblast Cells | |
| 855/02 | Human fibroblasts from OS patient | |
| 756/01 | Human fibroblast (man) | |
| 18/98 | Embryonic human fibroblasts | |

Table 2.8. Cell lines

2.1.9 Bioinformatic tools and Databases

The bioinformatic databases and tools used during this thesis are indicated in Table 2.9 including their online resource:

| Tool name | Type | URL/Programm |
|--|---|---|
| BLAST at NCBI | Blast | http://www.ncbi.nlm.nih.gov/BLAST/ |
| ENSEMBL | Sequence retrieval and analysis | http://www.ensembl.org |
| ExPaSy | Proteomics Server | http://www.expasy.org/ |
| GCG package | DNA sequences analysis | http://www.accelrys.com/products/gcg_wisconsin_package |
| STADEN package | DNA sequences analysis | http://www.hgmp.mrc.ac.uk/Registered/Option/staden.html |
| GenBank | Genome database | http://www.ncbi.nlm.nih.gov/Genbank/ |
| Online Mendelian Inheritance in Man (OMIM) | Database of human genes and genetic disorders | http://www.ncbi.nlm.nih.gov/Omim |
| Primer3 | Primer design | http://frodo.wi.mit.edu/cgi |
| PubMed | Medline biomedical articles | http://www.pubmed.org |
| RZPD (Resource zentrum Primary Database) | Clone collections | http://www.rzpd.de |
| STADEN package | DNA sequences analysis | Version 1999.0 |

| | | |
|---------------------------------|-----------------------|---|
| Swiss-Prot | Protein knowledgebase | http://www.expasy.org/sprot/ |
| UCSC Human Genome Working Draft | Genome Browser | http://genome.ucsc.edu/ |

Table 2.9. Bioinformatic tools and databases

2.1.10 Patients

The first patient was born to consanguineous parents and presented with hypertelorism, broad nasal bridge, strabismus, cleft lip and palate, hypospadias and small ears with a right pre-auricular pit. He was found to have a de novo 388G>A mutation in MID1, predicting an A130T change in the Bbox1 domain.

The second patient had hypertelorism, down-slanting palpebral fissures, broad nasal bridge, posteriorly rotated ears, cleft lip and palate, and hypospadias. He was found to harbour a de novo 433T>A MID1 mutation, predicting a C145S change in the Bbox1 domain.

2.2 Nucleic acid methods

2.2.1 Polymerase chain reaction (PCR)

PCR was used for the amplification of DNA fragments of known sequence using either genomic DNA or cDNA as template. If not otherwise stated, each PCR reaction was prepared as follows:

| Component | Amount |
|--|--------------|
| DNA/cDNA | 100 ng /3 µl |
| PCR buffer, | 5 µl |
| MgCl ₂ (25 mM) | x µl |
| dNTP mix (each dNTP 2,5 mM) | 2µl |
| Forward + reverse primer (each 10 pmol/µl) | 2µl |
| Taq polymerase | <u>1µl</u> |
| Aqua ad inectabilia. | 50 µl |

Table 2.10 Components of PCR reactions

The following thermal profile was used for the amplification:

| Step | Temperature | Time | Cycles |
|----------------------|-----------------|---|--------|
| Initial denaturation | 95°C | 4 min | 1x |
| Denaturation | 95°C | 30 sec | 29x |
| Annealing | Primer specific | 30 sec | |
| Elongation | 68°C/72°C | 1 min/kb amplified DNA 2 min/kb for Pfu polymerase | |
| Final elongation | 68°C/72°C | 10 min | 1x |
| Storage | 4°C | Infinite | |

Table 2.11. Thermal cycle reactions for PCR reactions

The amount of MgCl₂, Taq polymerase used and annealing temperature are indicated for each pair of primers in the corresponding sections.

Touchdown PCR was performed for fragments with sequences difficult for simple amplification.

| Step | Temperature | Time | Cycles |
|----------------------|----------------------------------|------------------------|--------|
| Initial denaturation | 95°C | 4 min | 1x |
| Denaturation | 95°C | 30 sec | 10x |
| Annealing | (T _A +10°C)-1°C cycle | 30 sec | |
| Elongation | 68°C/72°C | 1 min/kb amplified DNA | |
| Denaturation | 95°C | 30 sec | |
| Annealing | Primer specific (table) | 30 sec | 29x |
| Elongation | 68°C/72°C | 1 min/kb amplified DNA | |
| Final elongation | 68°C/72°C | 10 min | 1x |
| Storage | 4°C | infinite | |

Table 2.12. Touch down PCR thermal cycle

PCR reactions were carried out in a PTC200 Peltier Thermal cycler (Biozym).

All PCR products were evaluated by DNA electrophoresis. When required, PCR products were purified either directly with the QIAquick PCR purification kit, or run on an agarose gel and subsequently extracted with the Gel Extraction Kit. DNA was eluted with 30-50 µl EB buffer (Qiagen) diluted 1:10 in bidest water.

2.2.2 Agarose gel electrophoresis

1% - 2% w/v ultrapure agarose gels in TAE buffer were used to separate RNA or DNA samples. 0,5 µg/µl EtBr was added to the gels to visualise DNA or RNA via UV light. 1 µl of loading buffer* was added per each 9 µl of DNA solution before loading the samples on the gel. Samples were run at 80-150 V in an electrophoretic chamber for 30-60 min depending on the fragment size. Different DNA/RNA molecular weight markers were used according to the size of the analysed products. Fragments were visualised, and pictures were taken, with the E.A.S.Y Win32 gel documentation system (Herolab). The following DNA/RNA ladders were used, the sizes of the fragments characterised is indicated:

| DNA/RNA ladders | Fragment size | Manufacturer |
|---------------------------------|---------------|---------------|
| Hyperladder I | 300 - 7000 bp | Bioline |
| Hyperladder V /100bp DNA Ladder | 50 –500bp | Bioline/GIBCO |
| 0,24-9,5 KB RNA Ladder | all | Invitrogen |

Table 2.13. Nucleic acids ladders

*Note: LX was used for DNA fragments bigger than 1 kb and LB for fragments shorter than 1 kb. RNA samples were run in RNA loading buffer and heated for 10 min at 70°C prior to loading. 1 µl of RNA ladder was treated in the same way.

2.2.3 RNA preparation and cDNA synthesis

RNA was prepared with the RNeasy kit according to manufacturer's instructions. For subsequent removal of contaminant DNA in the sample, 1 µg of RNA was digested with 1 µl

DNAse I in 2 μ l DNAse buffer and bidest H₂O up to 20 μ l. The reaction took place for 30 min at 37°C. For purification, samples were subjected to phenol:chloroform extraction and EtOH precipitation. RNA samples were kept at –20°C.

For cDNA synthesis, 2 μ g of RNA were mixed with 2 μ l dNTPs (2,5 mM each), 6 μ l pd(N)₆ (100 ng/ μ l) and DEPC-H₂O up to 31 μ l of total volume. The reaction was incubated for 5 min at 70°C and quickly chilled on ice. Next, 10 μ l of 5x 1st strand buffer, 5 μ l of 0.1 M DTT and 1 μ l of RNA guard were added, and the mixture was incubated for 2 min at 42°C. The samples were divided into two aliquots of 23,5 μ l. To one of the aliquots 2 μ l of Superscript II were added. The second aliquot was kept as negative control for the reaction. RNA was reverse-transcribed by incubation for 1 h at 42°C and the enzyme was subsequently inactivated at 70°C for 15 min. cDNAs were stored at –20°C.

2.2.4 Phenol:Chloroform extraction

To DNA or RNA containing solutions one volume of phenol:chloroform (1:1) (TE pH:7.5 saturated phenol for DNA, H₂O saturated phenol pH:4,5 for RNA) in a Phase Lock Gel (PLG) light expender was added. The mixture was rotated for 10 min and centrifuged at 16000 x g for 5 min. To the aqueous upper phase, one volume of chloroform was added, and the phases were again mixed for 10 min and centrifuged for 5 min at 16000 x g. The upper phase was transferred to a new eppendorf tube and DNA or RNA was precipitated with EtOH.

2.2.5 EtOH precipitation of nucleic acids

For EtOH precipitation of nucleic acids, 2,5 volumes of 95% EtOH, 1:10 LiCl for RNA or NaAc for DNA, and 1:100 glycogen were added to the samples. The mixture was placed at –20°C for > 30min and subsequently centrifuged for 20 min at 16000 x g at 4°C. Afterwards, the pellet was washed with 200 μ l 70% EtOH and centrifuged for 10 min at 16000 x g at 4°C. The pellet was air dried and resuspended in TE buffer pH 7.5.

2.2.6 Cloning

2.2.6.1 Cloning of pEGFP constructs and mutagenesis

5'-gctaagcttcgatggaacactggagtcag-3' and 5'-tcgaattctcggcagctgctctgtgca-3' primers, containing HindIII and EcoRI sites respectively, were used to amplify MID1 cDNA from either control or patient fibroblast carrying the 388G>A (A130T) mutation RNA. 1 mM MgCl₂, Pfu Taq polymerase and 54°C annealing temperature were used. PCR products and pEGFP-C1 vector were digested with the corresponding restrictions enzymes for 1 h at 37°C, run in an agarose gel, excised and purified with the Gel Extraction Kit (Qiagen). The products were ligated overnight at 16°C with T4 DNA ligase.

For the ligation an insert-vector ratio of 3:1 was used as follows:

$$ng\ insert = \frac{ng\ vector \times Kb\ fragment}{Kb\ vector} \times 3$$

The MID1 splice variant, Ex2d.7, was generated in pEGFP-C2 from a pBUDCE4-Ex2d.7 clone available in the laboratory (Winter et al., 2004). The insert was extracted with Sall and HindIII restriction enzymes and ligated into pEGFP-C2 (which provides the correct ORF) as described above.

The constructs lacking the RING and the RING plus the Bboxes were amplified with the primers 5'-gctcaagcttgggaaagcatcagtgagcggg-3' and 5'-gctcaagcttgggccttgt-gtaaactggttgg-3' as forward primers respectively, both containing HindIII restriction site, and 5'-tcgaattcttcacggcagctgcacagt-3' as reverse primer for both, which contained EcoRI restriction site. 1 mM MgCl₂, Pfu polymerase and 57°C annealing temperature were used. PCR products were ligated into pEGFP-C1 vector as described above.

Mutagenesis experiments were performed to produce the remaining mutated constructs according to the instruction manual provided with the QuickChange® Site Directed Mutagenesis Kit. In brief, 50 ng of template were amplified in 5 µl of 10x reaction buffer with 1,25 µl (125 ng) of each primer, 1 µl of dNTP mix and 1 µl *Pfu Turbo* polymerase in a 50 µl reaction in bidest H₂O.

The following thermal profile was used for the amplification

| Step | Temperature | Time | Cycles |
|----------------------|-------------|-------------------------|---------|
| Initial denaturation | 95°C | 4 min | 1x |
| Denaturation | 95°C | 30 sec | 12-18x* |
| Annealing | 55°C | 30 sec | |
| Elongation | 68°C | 2 min/kb plasmid length | |
| Storage | 4°C | Infinite | |

Table 2.14. Thermal profile for mutagenesis reactions

*Note: 12 cycles for point mutations, 16 cycles for single amino acid changes and 18 cycles for multiple amino acids deletions or insertions.

Non-mutated plasmids DNA were restricted with *Dpn* I (10 U/µl) for 1 h at 37°C and subsequently, 1 µl of the reaction was chemically transformed into XL1-Blue supercompetent cells. Plasmid DNA from the mutated constructs was prepared as described in section 2.2.7. Controls for the transformation and for the amplification reaction were included for every reaction.

| Primer | Nucleotide | Sequence (5'→3') | Cycles |
|---------------|---------------|---|--------|
| 403-411delfor | 403_411del9bp | gacgctgtgaagacctgtgaagtatcctactgtgacgag | 18 |
| 403-411delrev | | ctcgtcacagtaggatacttcacaggtcttcacagcgtc | |
| H178Yfor | 532C>T | ggctgatgtgcttggagtatgaggatgagaaggtg | 12 |
| H178Yrev | | caccttctcatcctcatactccaagcacatcagcc | |

| | | | |
|--|------------------------------------|--|----|
| C145Sfor C145Srev | 434T>A | cctactgtgacgagagcctgaaagccactc gagtggctttcaggctctcgtcacagtagg | 12 |
| ΔBbox2for Δbbox2rev | Deletion of Bbox2 | cacatccgggggctgatgggtggcagctttgagtga cacactcaaagctgtcaccatcagcccccgatgag | 18 |
| Δbbox1for Δbbox1rev | Deletion of Bbox1 | ctccgccgagaaggctcctcgtctgattgagccaattc gaattggctcaatcagacggaggaccttctcggcggag | 18 |
| V183Tfor V183Trev | 547GT>AC | gagcatgcggatgagaagacgaatatgtactgtgtgacc ggcacacagtacatattcgtcttctcatcctcatgctc | 12 |
| C198Afor C198Arev | 592TG>GC | gttaatctgtgccttggctaaactggttgggcggc gccgccaagtttagccaaggcacagattaac | 12 |
| C195Ffor C195Frev | 584G>T | ccgatgaccagttaatctttgccttgtgtaaactgg ccagtttacacaaggcaaagattaactggtcacgg | 12 |
| C175Afor C175Arev | 523TG>GC | cacatccgggggctgatggccttggagcatgaggatgag ctccatcctcatgctccaaggccatcagcccccgatgt | 12 |
| ΔBbox2+7aafor ΔBbox2+7aarev | Deletion of Bbox2 +7aa | gcttggagcatgaggatgaggtggcagcttgacgtgagc gctcactcaaagctgccacctcatcctcatgctccaagc | 18 |
| ΔBbox2+7aa-C175Afor ΔBbox2+7aa-C175Arev | Deletion of Bbox2+ 7aa+523TG>GC | ccgggggctgatggccttggagcatgagg ctcatgctccaaggccatcagcccccg | 18 |
| ΔBbox2+7aa-H178Afor ΔBbox2+7aa-H178Arev | Deletion of Bbox2+ 7aa+532CA>GC | ctgatgtgcttggaggctgaggatgaggtggc gccacctcatcctcagcctccaagcacacag | 18 |

Table 2.15. Oligos used for mutagenesis

2.2.6.2 Preparation of the pCMVTag2C and pBMT116 constructs

The MID1 (wild-type and mutated forms) cDNA from the different constructs in the pEGFP-C1 vector was cut out with HindIII and Sall and ligated into the multiple cloning site of pCMVTag2C.

For the cloning in the pBMT116 vector, the different MID1 inserts from the pEGFP-C1 clones were amplified with the 5'-tggctggaattcgaaaacactggagtcagaactg-3' and 5'-aggtcgacggattcacggcagctgctctgtgc-3' primers, containing EcoRI and Sall restriction sites respectively. PCR products and pBMT116 vector were digested, purified and ligated as described above.

A pBMT116 clone including MID1 splice variant Ex2d.7 was already available in the laboratory (Winter et al., 2004)

2.2.6.3 α4/44aa peptide clones

pGAD10-α4, pBudCE4-α4 and pCMVTag3a-α4 were already available in our laboratory (Troockenbacher et al., 2001; Winter et al., 2004).

For the cloning of the 44aa peptide into the PET32a vector, the 44aa peptide sequence was amplified with 5'-atctgggtaccaggcctccagtgaacccc-3' and 5'-gcaagcttggt-atgctccatatttccgatgttg-3' primers, which contained restriction sites for KpnI and HindIII respectively. 1,5 mM MgCl₂, Pfu polymerase and 55°C annealing temperature were used.

PCR product was digested and cloned into the multiple cloning site pET32a vector as described above.

For cloning the 44aa peptide into the Pinpoint™-Xa vector, the primers 5'-gctgggatccggaggcctccagtgaaccc-3' and 5'-ggagatctgttatccatatttccgatgttg-3', containing BamHI and BglII restriction sites respectively, were used for amplification of the insert. 1 mM of MgCl₂, Pfu polymerase and 58°C annealing temperature were used. Both reverse primers contained a stop codon.

To incorporate the His-Tag, 1 µl (100 picomoles) of the following oligos: 5'-agtttcaagaggatcgcatcaccatcaccatcacgg-3' and 5'-gatcccgatgatggatgatggatg-gcgatcctcttga-3' containing the BamHI and HindIII restriction sites respectively were annealed in 48 µl annealing buffer. The following thermal reaction was performed:

| Step | Temperature | Time |
|----------------------|---------------|-------------|
| Initial denaturation | 95°C | 4 min |
| Annealing | 70°C | 10 min |
| Cooling | - 0.1°C / sec | down to 4°C |
| Final step | 4°C | 10 min |
| Storage | 4°C | infinite |

Table 2.16. thermal profile to anneal oligos

Annealed oligos were digested with BamHI and HindIII and ligated into the multiple cloning site of the Pinpoint vector already containing the 44aa peptide (N-terminally located with respect to the peptide).

2.2.7 Plasmid DNA isolation and transformation

2.2.7.1 Plasmid DNA isolation

Single bacterial colonies carrying the plasmid of interest were grown overnight at 37°C with vigorous shaking in 5 ml LB medium with the appropriate antibiotic (Table 2.6). Next day, plasmids were prepared using the Miniprep Kit (Qiagen) according to the manufacturer instructions.

When larger amounts of DNA were required, 5 ml of LB/antibiotic were inoculated with a single colony, and incubated during 8 hours. 0,5 ml of this culture were used to inoculate 100 ml of LB/specific antibiotic, which was incubated overnight at 37°C with vigorous shaking. Next day, plasmid DNA was prepared using either the Maxiprep Kit or the Endofree Maxiprep Kit (for plasmids required for transfection of eukaryotic cells) according to the manufacturer's instructions.

To verify whether the obtained plasmids contained the expected fragments, the constructs were digested with corresponding restriction enzymes and checked on agarose gels. Clones carrying inserts of the right size were sequenced.

2.2.7.2 Chemical transformation

Plasmid DNA (10 ng of supercoiled or 100 ng of ligation product) was incubated with 100 μ l of chemically competent cells (DH 5 α , XL-1 blue) for 30 min on ice, heat shocked at 42°C for 1 min 30 sec and chilled on ice for 2 min. Cells were incubated for 1 h in 1 ml LB with vigorous shaking at 37°C. Afterwards, cells were plated onto selective agar plates containing the appropriate antibiotic and incubated overnight at 37°C.

2.2.7.3 Electroporation

40 μ l of competent cells (BL21, JM109) were added to plasmid DNA that had been previously dialysed, and the mixture was placed in a 1 mm electroporation cuvette. Electroporation took place at 25 μ F capacity, 1,7 V voltage and 200 Ω resistance with a time constant of about 4,5 msec. Immediately, 1 ml LB was added to the transformed cells. The solution was incubated at 37°C with vigorous shaking for 1 h and afterwards, cells were plated onto selective agar plates containing the appropriate antibiotic and incubated overnight at 37°C.

2.2.8 Transfection

2.2.8.1 siRNA transfection

1x10⁶ cells in 75 cm² culture flasks were seeded the previous day to transfection. A solution “A” containing 40 μ l of siRNA oligo and 1,3 ml of OptiMEM, and a solution “B” containing 40 μ l of Oligofectamine and 375 μ l of OptiMEM were prepared. After 8 min incubation at RT, both solutions were mixed and incubated for 20 min at RT. In the meanwhile, cells were washed with PBS, and 2 ml of fresh medium without antibiotics were added to the cells. The transfection mix was slowly added onto the cells, and the cells were incubated at 37°C in a humidified incubator with 5% CO₂ v/v for 48h.

2.2.8.2 Polyfect transfection of plasmid DNA

1x10⁵ COS-7 cells in a 6 well plate with cover slips for immunofluorescence experiments (1,5x10⁶ in a 75 cm² flask or 3x10⁶ in a 150 cm² flask for immunoprecipitation experiments) were seeded the day previous to transfection. Transfection was performed according to manufacturer’s instructions. Briefly, a transfection mix containing 1,5 μ g of plasmid DNA (20 μ g, 30 μ g), 100 μ l OptiMEM, (750 μ l, 1,2 ml) and 10 μ l polyfect (75 μ l, 100 μ l) was prepared and incubated for 10 min at RT. In the meanwhile, cells were washed with PBS and 1,5 ml of fresh medium without antibiotics (12 ml, 16 ml) were added to the cells. After 10 min, 0,6 ml of fresh medium (4,8 ml, 6 ml) were added to the transfection mixture and after mixing, the

solution was slowly placed onto the cells. Cells were incubated at 37°C in a humidified incubator with 5% CO₂ v/v for 24h.

Blue indicates the amounts used for 75 cm² cell culture flasks and orange for 150 cm² cell culture flasks.

2.2.8.3 Lipofectamine transfection of plasmid DNA

3x10⁶ in a 150 cm² flask were seeded the day previous to transfection. A solution “A” containing 15 µg of plasmid DNA and 2,5 ml OptiMEM, and a solution “B” with 50 µl lipofectamine and 2,5 ml OptiMEM were prepared and kept for 5 min at RT. Subsequently, solutions were mixed and incubated at RT for 20 min. In the meanwhile, cells were washed with PBS and 18 ml of fresh medium without antibiotics were added. Transfection mixture was slowly added to the cells, which then were incubated at 37°C in a humidified incubator with 5% CO₂ v/v for 24h.

2.2.9 Sequencing

2 ng DNA per 100 bp DNA length for PCR products, or 100 ng of plasmid DNA, were mixed with 6 µl H₂O, 1 µl sequencing primer (10 pmol/µl) and 3 µl “Terminator ready reaction mix”.

Thermal profile used for amplification and labelling of probes is indicated in Table 2.17:

| Step | Temperature | Time | Cycles |
|------------------|-------------------------|----------|--------|
| Pre-denaturation | 96°C | 1 min | 1x |
| Denaturation | 96°C | 10 sec | 25x |
| Annealing | Primer specific (table) | 5 sec | |
| Elongation | 60°C | 4 min | |
| Storage | 4°C | Infinite | |

Table 2.17. Thermal cycle for sequencing reactions

Sequencing reactions were purified with EtOH. To a 10 µl reaction, 25 µl of absolute EtOH were added and thoroughly mixed by inversion of the tube. After 10 min incubation, samples were centrifuged for 45 min at 4000 rpm at RT. Supernatants were discarded and 100 µl of 70% EtOH were added to the samples. After inverting the tubes a few times, samples were centrifuged for 15 min at 4000 rpm at RT. The ethanol was removed and the samples were air-dried. The samples were analysed in an ABI377 DNA sequencer.

Primers used for sequencing are indicated in Table 2.18

| Primer | Sequence (5'→3') | T ^a | Vector |
|--------------|------------------------|----------------|----------|
| Sp6 | atctaggtgacactatag | 47 | Pinpoint |
| Pinpoint | cgtgacgcggtgcagggcg | 67 | Pinpoint |
| T7 | gtaatacgactcactatagggc | 58°C | pCMV |
| T3 | aattaaccctcactaaaggg | 56°C | pCMV |
| S*Tag | cggttctggttctggccata | 58°C | PET32a |
| T7terminator | gctagttattgctcagcggc | 58°C | PET32a |
| GFPfor | gacaaccactacctgagcac | 58°C | pEGFP |

| | | | |
|---------|----------------------|------|---------|
| GFPprev | tgtttcaggttcagggggag | 58°C | pEGFP |
| BMT116r | gttggggttattcgcaac | 52°C | PBMT116 |
| BMT116r | cataagaaattcgcccg | 52°C | PBMT116 |

Table 2.18. Sequencing primers

The following primers were used for the precise sequencing of MID1 mutations : Ex2r-1r , 2RT-8, 2RT-9, 2RT-10A, 2RT-4, Ex2f1, 3'-RACE1, Ex3-r1, 2RT-19, 2RT-11, 2RT-13, 2RT-17, 2RT-6, 2RT-18, 2RT-12. They were already available in the laboratory and have been described previously (So et al., 2005; Winter, 2003; Winter et al., 2004).

Sequences were analysed by using the databases indicated in section 2.1.9

2.3 Protein methods

2.3.1 Bradford assay

A starting 10 µg/ml BSA solution was prepared by diluting a 5 mg/ml BSA stock solution 1:500 in the working buffer (specific for each experiment), which had been previously diluted 1:1000 in bidest water (2 µl 5 mg/ml BSA + 998 µl 1:1000 buffer).

BSA standard solutions were prepared by diluting the 10 µg/ml BSA solution in 1:1000 working buffer as indicated in Table 2.19:

| BSA standard curve (Name-µg/ml) | BSA 10 µg/ml (µl) | 1:1000 buffer (µl) |
|------------------------------------|----------------------|-----------------------|
| S6-10 | ---- | ---- |
| S5-7.5 | 150 | 50 |
| S4-5 | 100 | 100 |
| S3-4 | 80 | 120 |
| S2-2 | 40 | 160 |
| S1-1 | 20 | 180 |

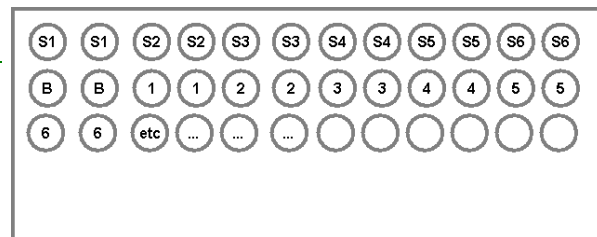


Table 2.19. Standard BSA curve preparation **Figure 2.1. Disposition of samples in Falcon plate**

2 x 80 µl of each sample, a blank (only 1:1000 buffer) and the standards (S) were placed into a Falcon microtitre plate as shown in Figure 2.1, 20 µl of Bradford reagent were added with a multichannel pipette and the samples were extensively mixed. The reaction proceeded for 1-5 min. Bubbles were carefully removed and the absorbance at 595 nm of each probe was measured in an anthos 2020 spectrophotometer (anthos), which also calculated the protein concentration by correlation with the BSA standard curve.

2.3.2 SDS-PAGE Gel

For the separation of proteins according to their molecular weights, samples were run in SDS-PAGE gels. 5 ml of separating gel and 1 ml of stacking gel were prepared per SDS-PAGE gel as showed in Table 2.20:

| Component volumes in ml per 5ml of separating gel/1ml stacking gel | | | | |
|--|-----------------------|-------|-------|----------------------|
| Components | Separating gel 10% | 12% | 15% | stacking gel |
| Bidest H ₂ O | 1,9 | 1,6 | 1,2 | 0,68 |
| Rothiphorese gel 30 | 1,7 | 2 | 2,5 | 0,17 |
| Separating gel buffer | 1,3 | 1,3 | 1,3 | 0,13 stacking buffer |
| Ammonium persulfate | 0,05 | 0,05 | 0,05 | 0,01 |
| TEMED | 0,002 | 0,002 | 0,002 | 0,001 |

Table 2.20. SDS gels composition

Separating gels were poured in between a short plate and a spacer plate using the Protean III system, covered with isopropanol and allowed to polymerise for 45 min at RT. Afterwards, the isopropanol was removed and the gels were washed with bidest H₂O. The stacking gel was then added on top of the separating gel, and a comb was incorporated in between the 2 glass plates to form the wells. They polymerised for 30 min.

2.3.3 Western blot

Protein samples were mixed with either 5x SDS-PAGE buffer or 2x magic mix and denatured for 5 min at 95°C before loading. The separation of the samples was performed in 1x Laemmli buffer at 200 V for 50-70 min using a Mini-PROTEAN 3 electrophoresis system (Bio-Rad). After running, gels were equilibrated for 15 min in 1x blotting buffer.

Different protein markers were run with the samples, according to the size of the proteins in study. Table 2.21 indicates the sizes covered by each marker and the study in which they were used:

| Protein ladders | Size | Study | Manufacturer |
|-----------------|--------------|--------------------|----------------------|
| Kaleidoscope | 10-250 KDa | MID1 complex | BioRad |
| Rainbow | 14,3-220 KDa | MID1 complex | Amershan Biosciences |
| See Blue Plus2 | 4-250 KDa | Peptide expression | Invitrogen |

Table 2.21. Protein markers

The blotting PVDF membrane was equilibrated for 3 sec in MeOH, 2 min in bidest H₂O and 15 min in 1x blotting buffer. Proteins were then blotted onto the membrane in a Trans-Blot SD Semi-dry Transfer Cell (Bio-Rad) at 15 V for 30 min. To saturate the unbound regions on the blot, it was incubated in PBST/5% milk powder for 30 min at RT or overnight at 4°C. Then, it was incubated with the primary antibody diluted in PBST/1%BSA for 1 hour at RT or overnight at 4°C followed by three wash steps of 5 min each in PBST. The corresponding HRP conjugated secondary antibody was diluted in PBST and, subsequently, added to the blot for 30 min, followed by three washing steps as before. Protein signals were detected by incubating the blots with the Western Lightning Chemiluminescence Reagent Plus

(PerkinElmer) for 1 min and subsequent exposure to Fuji Medical X-Ray films in a hypercassette. Blots were developed in a Curix 60 automatic film processor (Agfa).

2.3.4 Silver staining

Silver staining was performed using the SilverQuest Silver Staining Kit, following manufacturer's instructions. Shortly, gels were fixed for 20 min to overnight in 40 ml EtOH/10 ml HAc/50 ml H₂O, washed in 30 ml EtOH/70 ml H₂O, sensitised in 30 ml EtOH/10 ml sensitizer, 60ml H₂O again washed in 30 ml EtOH/70ml H₂O and for a second time in water, stained with 1 ml stainer solution, 100 ml H₂O, washed in water, developed in 10 ml developer solution/1 drop developer enhancer solution/90 ml H₂O and stopped with 10 ml stopper solution directly added to the developing solution when the expected signals were detected. Finally, gels were washed with H₂O. The whole procedure was performed at RT.

2.3.5 Coomassie/Colloidal coomassie staining

For colloidal Coomassie staining (CBB), gels were fixed overnight in 2% H₃PO₄/50% MeOH on a shaking platform.

Next day, the CBB stock solution was throughfully mixed and diluted with methanol 4:1 (CBB:MeOH) while stirring. Gels were allowed stain until bands were observed (12 hours to 4-5 days). Finally, gels were washed with bidest H₂O. The whole procedure was performed at RT.

For standard Coomassie staining, gels were incubated for >1 h in Coomassie staining solution and subsequently destained for 1 h in destaining solution.

2.3.6 Immunofluorescence

10⁵ cells COS-7 per well were seeded onto cover slips in six well plates. Next day, they were transfected with the corresponding endofree prepared plasmid DNA using polyfect (section 2.2.8.2) and allowed to grow for 24 or 48 hours. Afterwards, the medium was removed and cells were washed in 1.2 x PEM, fixed in 3,7% paraformaldehyde for 10 min at RT and shortly washed in 1x PBS. Next, they were permeabilized with 0,2 % Triton-100 in 1x PBS for 10 min at RT and washed 3 times in 1x PBS. To block unspecific interactions, cover slips were incubated for 20 min at RT in 1x PBS-0,5% BSA. Primary antibodies were diluted in PBS-0,5% BSA, added onto the covers slips and incubated for 1 h in a humid chamber, followed by three washings in 1x PBS for 5 min. The corresponding Cy3-labelled secondary antibodies were diluted in 1x PBS and added to the cover slips for 30 min, followed by 3 washes as before. Finally, cover slips were placed onto a 12 µl drop of 0,5 µg/ml DAPI in mounting medium previously added onto a slide, dried by pressing the slide between two pieces of Whattman paper and fixed to the slide with Fixogum.

Cells were visualised by fluorescence microscopy with a Zeiss Axioskop epifluorescence microscope equipped with single band pass filters for excitation of green, red and blue fluorescence (Chroma Technologies), and 63x or 100x plan-neofluolar lenses. Digital black and white images were recorded with a cooled CCD camera (Hamamatsu Photonics) and merged into RGB-images by the ISIS immunofluorescence image analysis system (MetaSystems).

2.3.7 Microtubule assembly experiment

Microtubules were polymerised *in vitro* from HeLa cell extracts according to previously reported protocols (Kimble et al., 1992; Vallee, 1982). 3×10^7 HeLa cells were incubated in ice cold PBS for 10 min at -20°C and for 30 min at 4°C to depolymerise the microtubules. After washing twice with ice-cold PBS, cells were disrupted with 1,8 ml of ice-cold microtubule assembly buffer (plus a complete mini tablet each 10ml of buffer) and centrifuged at 55000 rpm for 1 h at 4°C in a TL100 centrifuge. The pellet was discarded, to the supernatant 18 μl of dGTP (100 mmol) and 7,2 μl taxol (5 mg/ml) were added, and the microtubules were allowed to polymerise for 30 min at 37°C . In the meanwhile, a 50% sucrose solution (0,2 g sucrose, 1 μl Taxol, 4 μl dGTP in 280 μl microtubule assembly buffer) was prepared. Polymerised microtubules were added on top of 180 μl of the sucrose solution, and centrifuged at 25000 rpm for 30 min at 37°C in a TL100 centrifuge. The supernatant was discarded, and polymerised microtubules were washed by resuspension in microtubule assembly buffer with taxol and pelleted again at 25000 rpm for 30 min at 37°C in a TL100 centrifuge. The pellet was finally resuspended in 50 μl microtubules assembly buffer, 0,5 μl dGTP and 0,25 μl Taxol and left for some minutes in the fridge. Polymerised microtubules were stored at -80°C .

2.3.8 Immunoprecipitation

During the study of the Bboxes, for the immunoprecipitation of MID1-FLAG or $\alpha 4$ -myc polyclonal anti-FLAG or anti-myc antibodies were used as follows:

COS-7 cells overexpressing MID1-FLAG were homogenised by sonication in IP1 buffer, supplemented with proteinase inhibitors. Nuclei and cellular debris were pelleted for 15 min at $12000 \times g$ at 4°C . 1 mg of cytosolic protein extract in 1 ml IP1 buffer was placed in a new eppendorf tube. A preclearing step to avoid unspecific absorption of the agarose beads was performed by incubation the solution with 50 μl of 50% protein A agarose suspension (previously washed for 3 times in IP1) for > 2 h at 4°C with rotation. Beads were pelleted by centrifugation for 1 min at 3000 rpm in a table centrifuge at 4°C and the supernatant was transferred to a new eppendorf tube. 1,5 μg of anti-myc or 1,6 μg of anti-FLAG (Table 2.5), were added to the sample which was incubated overnight at 4°C on a rocking platform. Next day, 75 μl of 50% protein A agarose suspension were added and the mixture was incubated

for > 2h at 4°C on a rocking platform. Agarose beads were pelleted by centrifugation for 1 min at 3000 rpm in a table centrifuge, followed by 3 washings with 500 µl of IP1 buffer. Beads were boiled for 5 min at 95°C in freshly prepared SDS buffer (20 µl IP1, 3,8 µl 1M DTT, 2 µl 10x Laemmli buffer and 5 µl 5x SDS-PAGE buffer per sample). Immunoprecipitated proteins were analysed on 10 % SDS gels and Western blots with anti-FLAG or anti-myc monoclonal antibodies.

For the immunoprecipitation of MID1-FLAG for the verification of the novel members of the MID1 complex, the following protocol was used:

HeLa cells overexpressing MID1-FLAG were lysed in TKM buffer, supplemented with proteinase inhibitors and 1% NP40, incubated for 15 min on ice and passed 5 times through a 27 $\frac{3}{4}$ Gauge needle. Nuclei were pelleted for 15 min at 12000 x g at 4°C. 4 mg of cytosolic extract were precleared with 25 µl of protein-A/G agarose and 10 µg of mouse IgG for 1,5 h at 4°C on a rocking platform. Beads were pelleted by centrifugation for 1 min at 3000 rpm in a table centrifuge at 4°C and the supernatant was transferred to a new eppendorf tube. MID1-FLAG immunoprecipitation took place overnight with 75 µl of anti-FLAG M2 coated beads in 1 ml TKM buffer. Anti-FLAG M2 agarose matrix had been previously equilibrated in TKM buffer, blocked with 1 mg/ml BSA for 30 min and washed again with TKM buffer. Next day, agarose beads were pelleted by centrifugation for 1 min at 3000 rpm in a table centrifuge and washed 3 times with 500 µl TKM buffer supplemented with 0,2 % NP40 for 10 min at 4°C rotating. Bound proteins were finally eluted for 45 min with 200 µl of 3 x FLAG (400 µg/ml). 40 µl were directly analysed by Western blotting, and the remaining 160 µl of the elution fraction were concentrated in vivaspin 500 disposable with a cut-off membrane of 5 kDa for 20 min at 15000 x g at 4°C. Concentrated fractions were analysed on 10% SDS page and Western blotting with the panel of antibodies for the respective complex members. Note: Western blots shown in the result section correspond to the concentrated fractions.

2.3.9 Yeast two-hybrid experiments

2.3.9.1 Yeast transformation

Several colonies of the L40 yeast strain were inoculated in 500 µl of YPD medium, vigorously vortexed for 3 min, transferred to flasks containing 50 ml YPD medium and was incubated for 16 h at 30°C with shaking (225 rpm).

Next day, 19 ml of the overnight cultures were diluted in 300 ml of YPD medium in a 2 l flask to produce a OD₆₀₀ of 0,2 to 0,3 and incubated until OD₆₀₀ had reached 0,4-0,6 (approximately 3,5 h). Cells were then placed in 50 ml tubes and centrifuged for 5 min at 1000 x g. The supernatant was discarded and pellets were washed with 50 ml of TE buffer and centrifuged again. The supernatant was discarded and cells were resuspended in 1,5 ml of

freshly prepared 1x TE/1x LiAc. Then 0,1 µg of plasmid DNA and 0,1 mg of herring testes carrier DNA (previously denaturated for 20 min at 95°C) were mixed in an eppendorf tube and mixed by vortexing with 0,1 ml of the freshly prepared yeast competent cells. 600 µl of PEG/LiAc were added, and the solution was vortexed for 10 sec before being incubated for 30 min at 30°C. Afterwards, 70 µl of DMSO were added and the solution was mixed by inversion. Cells were heat shocked for 15 min at 42°C and consequently chilled on ice for 1-2 min. Cells were then centrifuged for 5 sec at 14000 rpm in a table centrifuge, the supernatant was discarded and the cells were resuspended in 500 µl of TE buffer. Finally, transformed yeast were placed on plates with -Leu/-Trp selections medium and incubated for 3-4 days at 30°C. For the selection of colonies presenting interaction of both plasmids, several colonies were placed on plates with -His/-Leu/-Trp selective medium and incubated again 3-4 days at 30°C.

For each construct, each experiment was repeated at least twice. As controls, empty pGAD10 was cotransformed with pBMT116-MID1, empty pBMT116 with pGAD10-α4 and both empty vectors together.

2.3.9.2 β-Galactosidase activity

β-galactosidase activity was assayed by the *o*-nitrophenyl-β-D-galactopyranoside (ONPG) method (Fields and Sternglanz, 1994). A colony from the selective medium containing plates was inoculated into 5 ml cultures containing the corresponding selective medium (-His/-Leu/-Trp or -Leu/-Trp), well mixed by vortexing and incubated for 16-18 h at 30°C with shaking (225 rpm).

Next day, ONPG was diluted in Z buffer to a concentration of 4 mg/ml by stirring for 1-2 hours. Cell clumps in the overnight culture were dissolved by vortexing and diluted in YPD-medium until the OD₆₀₀ was 0,2-0,3 (approximately 10 ml). The culture was incubated for 3-5 h at 30°C with shaking (225 rpm). After 2 h, the OD₆₀₀ was measured every 30 min until the cultures had reached the mid-log phase (OD₆₀₀ 0,5-0,8).

1,5 ml of the cultures were split into three tubes and centrifuged at 10000 x *g*. Supernatants were discarded and cell pellets were resuspended in 300 µl of Z buffer. 0,1 ml of each probe was transferred to a new eppendorf tube, hold for 1 min in N₂ and then placed for 1 more minute in a water bath at 37°C. Freezing/thawing cycles were repeated twice.

To the probes 700 µl of Z buffer+ β-mercaptoethanol (0,27 ml β-mercaptoethanol in 100 ml Z buffer) were added and subsequently 160 µl of ONPG in Z buffer. A blank probe was performed in parallel with only 100 µl of Z buffer. When the probes turned yellow, Na₂CO₃ was added to stop the reaction. Time passed between ONPG addition and stop of the reaction was measured.

The Photometer was calibrated with the blank sample at a wavelength of 420 nm and subsequently the OD₄₂₀ of the samples were measured.

For calculating the β -galactosidase units the following equation was used:

$$\beta\text{-galactosidase units} = \frac{1000 \times OD_{420}}{t \times V \times OD_{600}}$$

t = incubation time (ONPG-addition-stop)

V = 0,1 ml x concentration factor (5 in this case)

2.3.10 Cell culturing and trypsinisation

HeLa or COS-7 cells were grown in the previously described media. For seeding cells, they were trypsinised and counted with the cell counter and analysis system CASY1 (Schärffe system).

Trypsination

1 ml per each well in a six well plate (4 ml for a 75cm² flask and 8 ml for a 150cm² flask) of medium from the cells was kept. After removing the remaining medium, cells were washed with sterile PBS. Next 0,5 ml (2 ml, 4 ml) of trypsin (prewarmed at 37°C) were added to the cells and incubated for 3 min at 37°C. When cells were loosened, the trypsin was inactivated by adding medium. Cells were then centrifuged at 1200 x g for 10 min at 4°C, the supernatant was discarded, and the pellet was washed with PBS and pelleted again. When not used immediately, cell pellets were frozen with liquid N₂ and kept at –80°C.

For cell seeding, cells were counted after trypsinisation and the necessary amount indicated for each experiment was mixed with fresh medium and placed in the cell culture flasks or plates.

2.4 Preparation of the 44aa peptides

Two different 44aa peptides of $\alpha 4$ were prepared:

Biotinylated 44aa peptide: created in the PinPoint vector system. Used for the production of the column.

44aa peptide: created in the PET32 vector system, containing a Trx, His and S-Tag. After tags removal peptide was called **free 44aa peptide**. The last was used for elution of the column.

2.4.1 Growth of *E. Coli* cultures

Pinpoint vector constructs were expressed in JM109 *E. coli* cells (Promega) and PET32a constructs in BL-21Codon-Plus (DE3)-RIL (Novagen) *E. coli* cells.

20 ml of LB medium with antibiotic (PET32 vector system: 50 µg/ml ampicillin and 34 µg/ml chloramphenicol; PinPoint vector system: 50 µg/ml ampicillin, 2 µM biotin) were inoculated with a colony and grown overnight with vigorous shaking. Next day, 1 l culture with antibiotic was inoculated 1:50 with the overnight culture. The culture was grown until OD₆₀₀ was 0,5-0,7 and then induced with 0,1 mM IPTG during 2 h for the PET32 vector system and 4 h for the PinPoint vector system. An aliquot of each culture was resuspended in magic mix and directly analysed on a Coomassie stained 15 % SDS gel. Cells were harvested by centrifugation for 20 min at 4000 x g. When not directly used, cell pellets were frozen in liquid N₂ and kept at –80°C.

For the establishment of optimal conditions for protein expression 5 ml cultures were performed as described above. Different conditions tested are indicated in the result section.

2.4.2 Preparation of cleared *E. Coli* lysates

Cell pellets were resuspended in native condition lysis buffer (QiaExpressionist) at 3 ml/gram wet weight. Lysates were 2x frozen in liquid N₂/thawed on ice and sonicated 5x at 50% power for 10 sec with 10 sec cooling period between each burst. Lysates were centrifuged at 10000 x g for 20 min at 4°C. An aliquot of the pellet was kept for analysis and the rest was discarded. The supernatant was kept at –80°C.

2.4.3 Purification of 6xHis tagged proteins from *E. Coli*

1 ml of 50% Ni-NTA slurry was added to each 4 ml of cleared lysate, and it was gently mixed for 1h on a rotary platform at 4°C. The lysate Ni-NTA mixture was loaded into a propylene column with the bottom outlet capped. The bottom cap was removed and the flow through collected; afterwards, the column was washed twice with 8 ml of washing buffer (QiaExpressionist) per each ml of packed column volume. Finally, peptides were eluted with 1 ml elution buffer (QiaExpressionist) per each ml of packed column volume. For future use, protein samples were dialysed (or concentrated with a centricon) into the required buffer.

2.4.4 Thrombin digestion

For thrombin digestion the peptide was previously dialysed in HS buffer.

Optimal conditions were established after testing different enzyme concentrations and reaction times (see result section) following manufacture's instructions (Novagen). Final conditions were used as follows: 10 µg of protein were digested with 1 µl of Thrombin (0,02 U/µl) in a 50 µl reaction in bidest water from 4 h to overnight at 4°C. For bigger amounts of proteins, the reactions were scaled up with the same ratio of components. When necessary, thrombin was removed by dialysis or centricon (Millipore).

To cleave the free 44aa peptide from the tags, Ni-NTA agarose was used. 1 mg of digested peptide was incubated with 300 μ l of Ni-NTA slurry and equilibrated in HS buffer for 1 h at 4°C in a rocking platform. The flow-through was collected and free peptide was concentrated in a centricon device with a 3 kDa cut-off membrane.

2.5 Chromatography column and Mass spectrometry

For generating the column, 50 μ g of biotinylated 44aa peptide in TBS were incubated with 250 μ l of washed streptavidin coated agarose slurry (ProFound pull down kit) for 1 h at 4°C rotating in a 500 μ l final volume reaction. A control column without peptide was performed in the same way. Beads were blocked with free biotin for 5 min, washed with HS buffer and again blocked with 1 mg/ml BSA overnight at 4°C. Beads were placed in a Handee-mini spin tube to create the columns, followed by washing with 100 volumes of HS and 2 volumes of washing buffer (250 mM NaCl/0,05% Tween), and eluted with an excess of free peptide after thrombin digestion (section 2.4.4). Columns were again washed as before and equilibrated in HS buffer.

Cytoplasmic HeLa extracts from 1×10^7 cells, previously subjected to $\alpha 4$ knock down (section 2.2.8.1), were obtained by lysis in HS buffer for 15 min on ice, potter disruption for 10 times and centrifugation for 10 min at 3000 rpm at 4°C in a table centrifuge. Approximately 4 mg of cytoplasmic extracts were incubated with the columns overnight at 4°C on a rocking platform. Next day, columns were washed as before and eluted 3x 15 min with excess of free peptide. The eluted fractions were dialysed against 20 mM TRIS pH 8, run in a 10% SDS gel and stained with colloidal Coomassie. Differential bands (1-12, indicated in the results section 3.2.3) were excised, trypsinised and analysed by mass spectrometry.

Mass spectrometry was performed by the service group in the SFB 577. Briefly, the peptide mixture in the cut bands was identified by chromatographic separation on a LC Packings 75 μ m PepMap C18 column (Dionex) using a capillary liquid chromatography (CapLC) system delivering a gradient to formic acid (0.1%) and acetonitrile (80 %). The eluting peptides were ionised by electrospray ionisation on a Q-TOF hybrid mass spectrometer (Micromass). The instrument, in automated switching mode, selects precursor ions based on intensity for peptide sequencing by collision induced fragmentation tandem MS. The MS/MS analyses were conducted using collision energy profiles that were chosen based on the m/z value of the precursor. The mass spectral data were processed into peak lists containing m/z value, charge state of the parent ion, fragment ion masses and intensities, and correlated with the SwissProt database using Mascot software (Perkins et al., 1999).

2.6 Sucrose gradients

2.6.1 Discontinuous gradients

HeLa cells, with and without overexpressed MID1-FLAG, were lysed for 15 min on ice in TKM buffer supplemented with 1 mM DTT, 0.5 % NP40 and 1 U/ μ l sample of Prime RNase inhibitor and passed 10 times through a 27 $\frac{3}{4}$ Gauge needle. Cell debris and nuclei were discarded by centrifugation 10 min at 12000 x g at 4°C. Approximately 2 mg of protein dissolved in 900 μ l of buffer were added on a sucrose discontinuous gradient, formed by 500 μ l of a 50% sucrose solution in TKM and 600 μ l of a 20% sucrose solution of TKM. Centrifugation was performed in a TLA 100.2 rotor at 55000 rpm for 270 min at 4°C (for overexpressing cells) or 15 hours at 30000 at 4°C in a TLS55 rotor (for non-overexpressing cells) in a TL100 ultracentrifuge.

Ribosome studies:

0.5% DOC, 0.5 M KCl, 30mM EDTA treatment: to 2 mg of concentrated cytoplasmic extracts, the necessary amounts of 10% DOC, 1 M KCl, or 0,5 M Na₂EDTA were added to have a final concentration of protein of 2 mg/ml in TKM buffer (supplemented with 1 mM DTT, 0.5 NP40 % and Prime RNase inhibitor) with 0,5% DOC, 0,5 M KCl or 30 mM EDTA. Ribosomes were run through a TKM sucrose gradient, as previously described, for 15 hours at 30000 at 4°C in a TLS55 rotor.

RNase A/DNase I treatments: cytoplasmic extracts were obtained as previously described, except that Prime RNase inhibitor was not included. To 2 mg of cytoplasmic extracts either 500 μ g/ml of RNaseA, 50 units of DNase I or 12 μ l of RNA guard were added and the volumes of the reactions were brought up to 1 ml in TKM buffer (supplemented with 1 mM DTT, 0.5 NP40 %). Ribosomes were run through a TKM sucrose gradient, as previously described, for 15 hours at 30000 rpm at 4°C in a TLS55 rotor.

Puromycin/cycloheximide: HeLa cells in culture were treated either 0,1 mg/ml puromycin for 6 hours or with 0,35 mM cycloheximide for 20 minutes at 37°C in a humidified incubator with 5% CO₂ v/v for 48h. Cell extracts were prepared, and sucrose gradient run, as previously described.

2.6.2 Linear sucrose gradient

3x10⁷ HeLa cells were lysed for 15 min on ice in TKM buffer supplemented with 1 mM DTT, 0.5 % NP40 and 1 U/ μ l sample of Prime RNase inhibitor, passed 10 times through a 27 $\frac{3}{4}$ Gauge needle and centrifuged for 15 min at 12000 x g to eliminate the nuclei and cellular debris. The cytoplasmic homogenate was sedimented in a 15%-45% (w/v) sucrose gradient by centrifugation for 120 min at 38000 rpm at 4°C in a Beckmann SW40 rotor. 1 ml fractions were collected starting from the bottom of the centrifuge tube with a 2132 Microperpex peristaltic

pump a 2111 multirac system (LKB Bromma). The absorbance of the fractions was measured with a 2138 UVI-CORD (LKB Bromma). Fractions were analysed by Western blotting either directly, or after being precipitated overnight with trichloroacetic acid and 5 µg BSA as carrier.

15%-45% linear sucrose gradients were prepared in TKM buffer in a 14 x 95 mm Ultra-Clear centrifuge tube (Beckmann) with a gradient master (Biocom).

2.7 RNA-Protein binding experiments

2.7.1 Homopolymer binding assay

MID1-FLAG overexpressing HeLa cells were homogenised in HSMN buffer, supplemented with proteinase inhibitors and 1 U/µl Prime RNase inhibitor, in a potter-elvehjem. Binding of overexpressed MID1 to homoribopolymers was performed as previously described (Brown, 1998; Siomi et al., 1993b; kiledjian and dreyfuss, 1992; Swanson and Dreyfuss, 1988). Briefly, 100 µg of cytosolic extract were incubated with 5 µg of homoribopolymer coated beads in 500 µl of HSMN buffer during 30 min at 4°C. Beads were pelleted and washed 3 times for 5 min at 4°C with 500 µl HSMN buffer before being resuspended in magic mix. Bound proteins were eluted by boiling the sample at 95°C for 5 min and analysed by Western blotting with anti-FLAG antibody.

For the different treatments performed the standard procedure was the same, except that this time 2 µl of poly-rG agarose coated beads were used. After lysis, cytosolic extracts were modified according to each experimental condition as follows:

For the different salt treatments the concentration of NaCl in the cytosolic extracts was adjusted to 250 mM and 500 mM with 1 M NaCl. For heparin treatments, heparin from a 100 mg/ml stock solution in HSMN buffer was added to the samples in order to have a final concentration of 1 or 2 mg/ml. For the competition experiments with free homopolymer, 5 or 50 µl of a 10 mg/ml solution of the corresponding free homopolymer (poly-rU or poly-rG) was added to create a 1:1 or 1:10 bound:free homopolymer solution.

2.7.2 Ephrin mRNAs-MID1 binding experiments

2.7.2.1 Amplification of G-quartets and EFNB1 mRNA

All forward primers contained the T7 promotor sequence (5'-ccaagcttctaatacgaactcactatagggaga-3') to allow subsequent *in vitro* transcription of the PCR product. PCRs were performed with advantage polymerase. PCR conditions and primers for the different amplification reactions are given in Table 2.22. TD indicates PCRs that were performed with a touchdown thermal programm.

| Primer | Sequence (5'→3') | Annealing T ^a (°C) |
|--------|------------------------|-------------------------------|
| EFNB1a | T7cccatgctcttgtgccttcc | 65 |

| | | |
|---------------|---------------------------|----------|
| | gtcctgggaaggtggcaag3 | |
| EFNB1b | T7ggtcagccaggaagcatagg | 64 |
| | tgggacaccttgcccagtg | |
| EFNB1c | T7cttaattggctggtgcctgg | 64 |
| | gtaaggagagaacaggggtgg | |
| EFNB1d | T7cctagcacaggtgggtaac | 64 |
| | agccgtgctggcaaggaactg | |
| EFNB1bAS | T7tgggacaccttgcccagtg | 64 |
| | ggtcagccaggaagcatagg | |
| EFNB2a | T7ggtgcccttttagccagatg | 66-55 TD |
| | cctttccaactttctgtttcag | |
| EFNB2b | T7cgatgtgcaggaagaaaagcc | 64 |
| | gtaccacaacagtcctgcc | |
| EPBH1 | T7gtcagtcaccaacggcaatgg | 66-55 TD |
| | tcagctgagaagccagtcctct | |
| EPBH2a | T7ctaattggactccactacagc | 66-55 TD |
| | caaacacggttgacacactgg | |
| EPBH2b | T7gttgatcctgcatctgggtttg | 55 |
| | gtcaaagtgtcacttcattgtc | |
| EPBH3a | T7ctcatggacacaaaatgggtaac | 66-55 TD |
| | gcacattacacacctggtatg | |
| EPBH3b | T7cttcctgctctccagcag | 66-55 TD |
| | ctgctctccgcctacctg | |
| EPBH3c | T7gatttggttctgggggctgag | 65 |
| | cacatcccatctctggctctg | |
| EPBH4a | T7gatgagagcgagggtctgg | 66-55 TD |
| | ctgcttctctcccattgtctc | |
| EPBH6a | T7gcagcagcttcttaaccagc | 66-55 TD |
| | gtttctgggtcaatcttaccct | |
| EPBH6b | T7ggaagcaagcttagctgtacac | 64 |
| | tgggcagcccccttcagtag | |
| EFNB1-3'UTR | T7gaagatggctcggcctggg | 74-64 TD |
| | gtgccgggcactcagaccttg | |
| EFNB1+1Gq | T7gaagatggctcggcctggg | 74-64 TD |
| | gtcctgggaaggtggcaag | |
| EFNB1+2Gq | T7gaagatggctcggcctggg | 74-64 TD |
| | tgggacaccttgcccagtg | |
| EFNB1+3Gq | T7gaagatggctcggcctggg | 74-64 TD |
| | gtaaggagagaacaggggtgg | |
| EFNB1+4Gq | T7gaagatggctcggcctggg | 74-64 TD |
| | agccgtgctggcaaggaactg | |
| EFNB1+3Gq rev | T7agccgtgctggcaaggaactg | 74-64 TD |
| | gaagatggctcggcctggg | |
| EFNB1+4Gq rev | T7gtaaggagagaactgggtgg | 74-64 TD |
| | gaagatggctcggcctggg | |

Table 2.22. Primers for amplification of G-quartets and ephrin mRNAs

As template for the PCR reactions, the IRATp970C0237D6 clone containing EFNB1 coding sequence or cDNA from embryonic human fibroblasts were used.

PCRs were checked on agarose gels and purified by gel extraction before RNA transcription was performed. Longer PCR fragments were additionally digested with Proteinase K by incubation with 100 µg/ml proteinase K, 0.5 % SDS in 50 mM TRIS-HCl (pH 7,5) and 5 mM CaCl₂ for 30 min at 37°C. Subsequently, they were purified by phenol:chloroform extraction.

2.7.2.2 *In vitro* transcription of biotinylated RNA

Amplified transcripts were *in vitro* transcribed with the RiboMAX™ Large scale RNA production system-T7 from Promega, following the manufacture's instructions with some modifications. Briefly, 2 µg of purified PCR product were transcribed for 4 h at 37°C in the following reaction mixture:

| Reaction components | Sample reaction |
|--|-----------------|
| T7 transcription buffer | 4 µl |
| rNTPs (25 mM rATP, rGTP, rCTP, 1,6 mM biotin-rUTP, 2,5 mM UTP) | 6 µl |
| PCR template | 2 µg |
| RNA polymerase enzyme mix | 2 µl |
| DEPC-H ₂ O | Up to 20 µl |

Table 2.23. *In vitro* transcription

Transcribed RNA was purified by phenol:chloroform extraction and precipitation with ethanol. Products were kept in nuclease free TE.

RNA concentration was measured with a NanoDrop ND-1000 Spectrophotometer (PEQLAB) or with a Gene Quant RNA/DNA calculator (Pharmacia). The efficiency of the biotinylation was tested by Dot Blotting.

2.7.2.3 Biotinylation efficiency dot blot

6 x 10 µl of 6x SSC buffer were pipetted onto a piece of parafilm. To the first dot, 1 µl RNA was added, then, 1 µl of this first dot was taken and applied to the next dot, and successively like that until the sixth dot, which had a final dilution of RNA of 1:10⁶.

1 µl of each dot was transferred to a Roty-Nylon Plus membrane. The RNA was cross-linked to the membrane with a UV linker. The membrane was blocked in PBS-5% BSA for 15 min, followed by incubation with 1:1000 streptavidin-AP in PBS and 5% BSA for another 15 min. The blot was then washed and the AP activity was developed by incubation with freshly prepared NBT-BCIP in the dark until signals appeared. Membranes were finally washed with H₂O and kept in a plastic bag.

Note: NBT-BCIP was prepared by dissolving a tablet in 10 ml DEPC water.

2.7.2.4 RNA-PROTEIN binding assay

1 or 2 µg of RNA (G-quartets or longer EFNB1 fragments) were incubated with 150 µg of cytosolic protein extract from HeLa cells (cells were lysed as described in section 2.6.1) containing overexpressed MID1-FLAG in 450 µl of TKM buffer with proteinase inhibitors and 30 µl of Prime RNase Inhibitor for 1 hour at 4°C. Subsequently, the mixture was incubated for 2 h at 4°C with 40 µl of 50% slurry of M280 streptavidin coated magnetic beads. Beads were washed 3 times with TKM buffer for 10 min at 4°C and bound proteins were eluted by boiling

the beads in magic mix for 10 min at 95°C. Bound proteins were tested by Western blotting with the respective antibodies.

Note: for the experiment with the cDNA containing varying numbers of G-quartets, the concentration of KCl in TKM buffer had to be adjusted to 50 mM to observe specific binding.

2.7.3 Bioinformatics

Bioinformatic approaches were performed by the bioinformatics department at the Max Planck Institute for Molecular Genetics (Berlin). Briefly, Bioperl and Ensembl-API (both available from CVS-concurrent version systems) were used to create a programm to screen all the gene entries of the ENSEMBL database (Version v37. human) for the presence and number of G-quartets.

3 Results

3.1 Characterisation of the Bboxes of MID1

As previously described, most of the so far characterised OS patients harbour mutations in the C-terminal domain of MID1, that disrupt the association with microtubules and result in aggregation of the mutant protein in cytosolic clumps. In contrast, these mutations do not affect the interaction with $\alpha 4$, regulatory subunit of PP2A, which is then recruited to the cytoplasmic clumps, leading to accumulation of microtubule-associated PP2Ac (introduction section 1.2.2). Except for microtubule-association of the C-terminus and $\alpha 4$ -binding properties of the Bbox1 domain of MID1, functions of other MID1 regions (including Bbox2) are largely unknown.

Knowing that MID1 interacts with $\alpha 4$ through the Bbox1 domain (Trockenbacher et al., 2001), and assuming that Bbox2 might participate in the regulation of the MID1 protein function (Winter et al., 2004), a series of experiments was performed in order to elucidate and characterise the function of the two Bboxes of MID1.

3.1.1 Mutations in Bbox1 disrupt MID1- $\alpha 4$ interaction

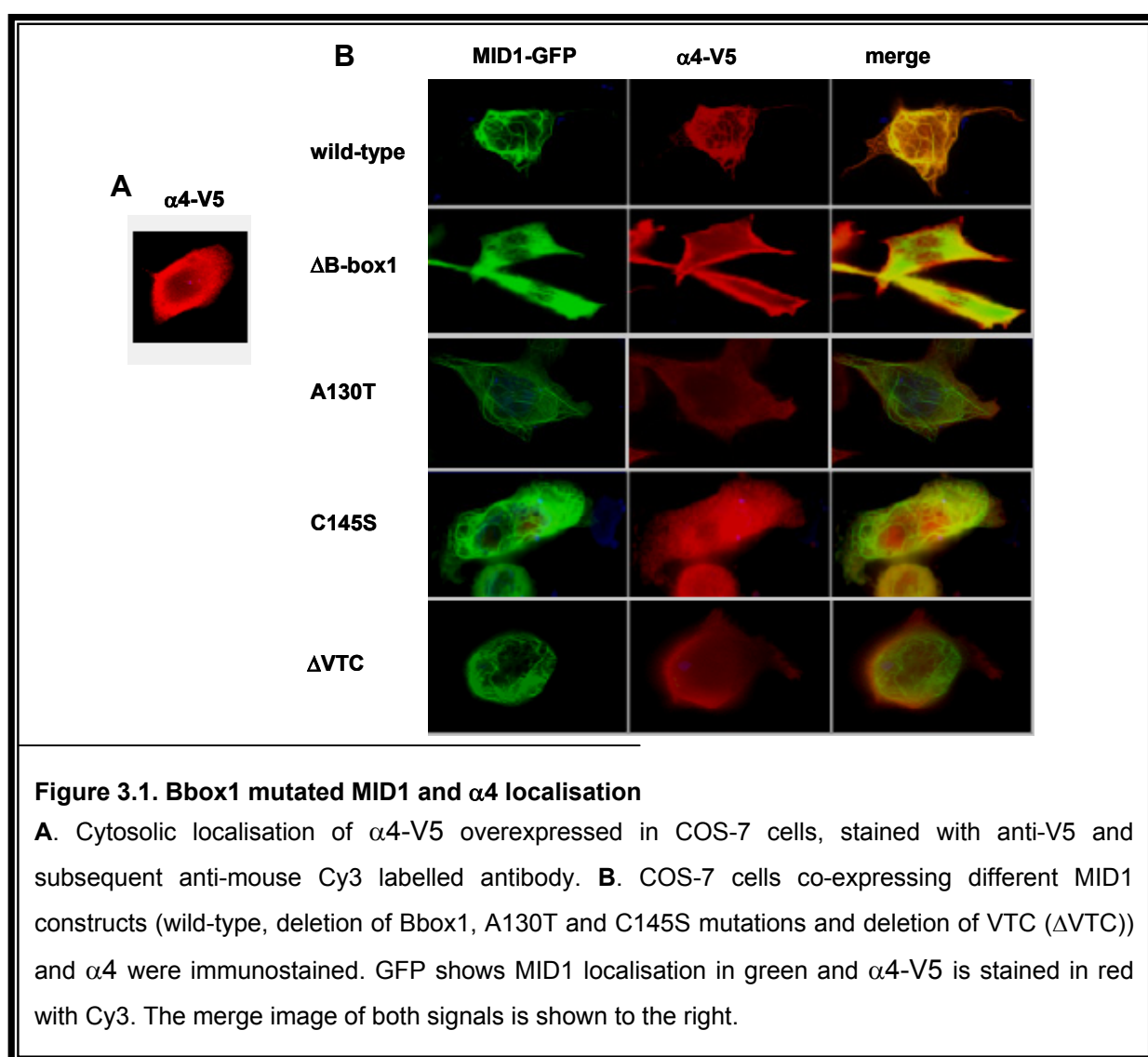
Mutation analysis on DNA from OS patients is being performed on a regular basis in our laboratory. Recently, two new mutations located in exon1 of MID1 were identified in two unrelated patients. One patient was found to have a 388G>A mutation, predicting a change of an alanine into a threonine at position 130 (A130T) in the Bbox1 domain of MID1. The second patient had a 433T>A mutation, predicting a cysteine to serine change at position 145 (C145S) also located in Bbox1. Both were *de novo* mutations.

To date, only two mutations in the Bboxes of MID1 have been described in the literature, namely deletion of a valine, threonine and cysteine at positions 135 to 138 (Δ VTC) in Bbox1 (De Falco et al., 2003; Pinson et al., 2004) and an amino acid change of a cysteine into a phenylalanine at position 195 (C195F) in Bbox2 (De Falco et al., 2003), both resulting in severe OS phenotypes. The novel mutations described in this thesis were also identified in severely affected individuals, supporting an important role of the Bboxes for the correct functioning of MID1. Since MID1 interacts with $\alpha 4$ through its Bbox1 domain, it was first tested whether mutations in this domain lead to disruption of the MID1- $\alpha 4$ interaction.

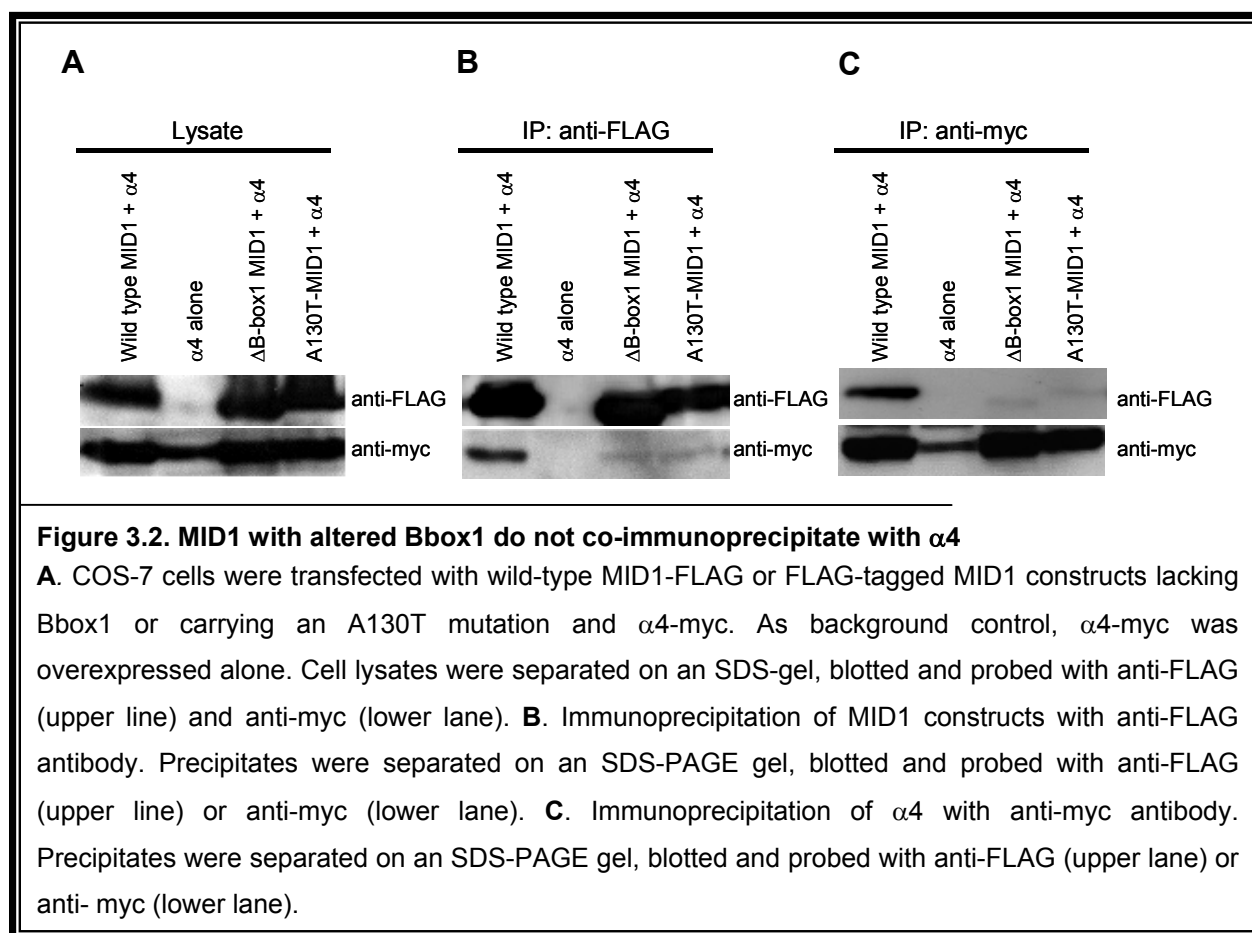
The following N-terminally green fluorescent protein (GFP)-tagged MID1 constructs carrying different mutations in the Bbox1 domain were used in this study:

- **A130T, C145S:** novel identified mutations in OS patients in our laboratory.
- **Δ VTC:** published mutation in Bbox1 (above described).
- **Δ Bbox1:** deletion of the entire Bbox1 domain.

These constructs, as well as wild-type MID1, were co-expressed in COS-7 cells together with V5-tagged $\alpha 4$, and their subcellular localisation was examined by immunostaining. While MID1 constructs were followed by the presence of the GFP-tag, anti-V5 and subsequent anti-mouse Cy3 labelled antibodies were used to assess $\alpha 4$ localisation (subsequent experiments were done in the same manner). As previously reported (Trockenbacher et al., 2001), $\alpha 4$ alone localised diffusely in the cytosol (Figure 3.1A) and in the presence of wild-type MID1, it was tethered to the microtubules (Figure 3.1B-wild-type). As expected, in contrast to the wild-type form (Figure 3.1B, wild-type), Bbox1 mutated or deleterious MID1 forms were unable to bind $\alpha 4$ *in vivo* (Figure 3.1B, Δ Bbox1, 130T, C145S and Δ VTC). While point mutated MID1 could still bind to microtubules, $\alpha 4$ remained spread all over the cell. Of note, deletion of the entire Bbox1 also seemed to slightly influence microtubule binding-properties of the protein.



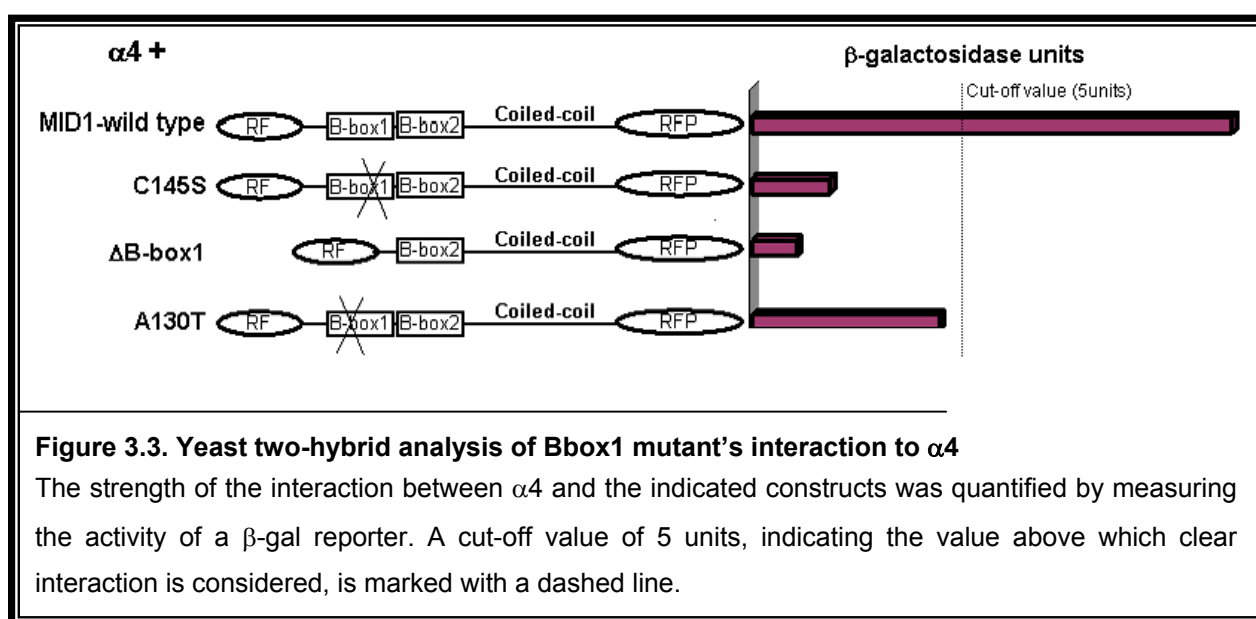
For further verification, co-immunoprecipitation experiments were performed in COS-7 cells co-expressing different N-terminally FLAG-tagged MID1 (MID1-FLAG) constructs (A130T, Δ Bbox1 and wild-type) and N-terminally myc-tagged α 4 (α 4-myc) (Figure 3.2A). Immunoprecipitation experiments were performed with anti-FLAG and anti-myc antibodies (Figures 3.2B and 3.2C respectively) and Western blots of the precipitates were developed with the corresponding antibodies, anti-myc or anti-FLAG respectively. Cells expressing α 4-myc alone were used as background control. Co-precipitation of α 4 and MID1 could only be shown with wild-type MID1 but not with either of the mutant proteins (Figure 3.2B-lower lane and 3.2C-upper lane), independently of the antibody used for the immunoprecipitation. Both blots were also incubated with the antibodies used for immunoprecipitation, proving that MID1-FLAG had been pulled down with anti-FLAG (Figure 3.2B-upper lane) and α 4-myc with anti-myc (Figure 3.2C-lower lane).



In addition, yeast two-hybrid experiments based on β -galactosidase activity measurements were performed to quantify the putative binding affinities of different Bbox1 mutants to α 4. Different MID1 constructs in pBMT116 vector, corresponding to wild-type, A130T, C145S and Δ Bbox1, were used as baits to screen for interaction with the α 4 protein cloned in pGAD10. A cut-off value of 5 β -galactosidase units was defined, and measurements above this value were

considered as clear interaction. Accordingly, measurements below 5 units were considered as no interaction.

With β -galactosidase measurements below 5 units, both mutants (C145S and A130T), as well as the construct lacking Bbox1, did not interact with $\alpha 4$ (Figure 3.3), while wild-type MID1 showed clear interaction. This data fully supported the results of the immunofluorescence and immunoprecipitation experiments, confirming that mutations in the Bbox1 domain of MID1 disrupt the interaction of the protein with $\alpha 4$ and that Bbox1 is responsible for the interaction between MID1 and $\alpha 4$.

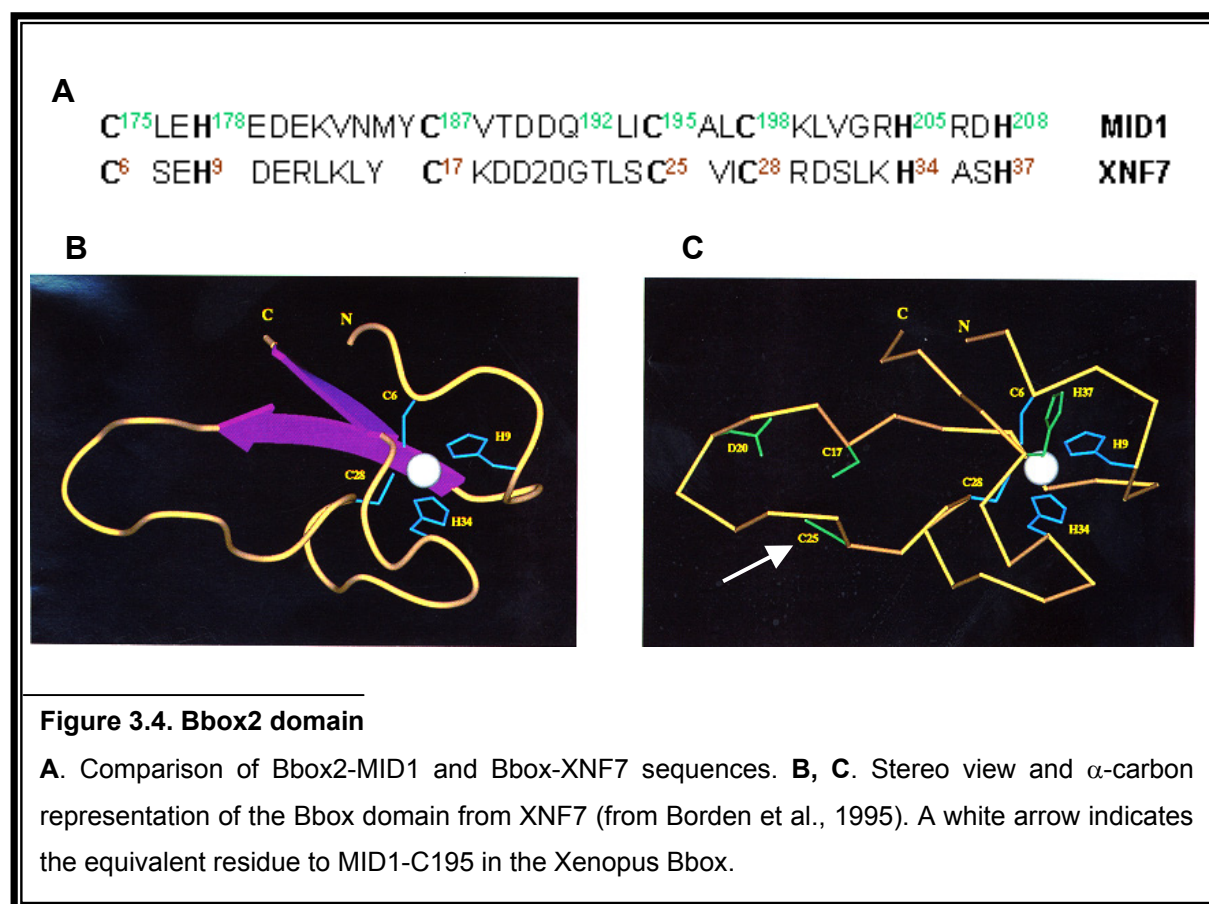


3.1.2 Analysis of the structure of the Bbox2 domain

In addition to the OS related mutations described in Bbox1, one mutation has been identified so far in the Bbox2 domain of MID1 in an OS patient (De Falco et al., 2003). However, the effects of such mutations on the MID1 protein function have not yet been studied. Additionally, previous experiments in our group have shown that a mutated form of MID1 harbouring a single amino acid change in Bbox2, glutamine to arginine at position 192 (Q192R), while binding to microtubules, is unable to co-localise with $\alpha 4$ *in vivo*. Since Bbox1 alone is sufficient for MID1 to interact with $\alpha 4$, Bbox2 was proposed to act as a regulator of this interaction (Winter, 2003).

A first theoretical impression of the importance of these residues (Q192 and C195) in Bbox2 with respect to the structure of the domain, was acquired by comparison with a model of a previously reported *Xenopus* Bbox (Borden et al., 1995b). As outlined in the introduction section, Bboxes contain seven conserved histidines or cysteines and is arranged in a particular fashion, having two perpendicular β -strands connected by a flexible loop (Figure 3.4B) and a hydrophobic core. Four of the conserved Cys/His bind one zinc atom, as indicated

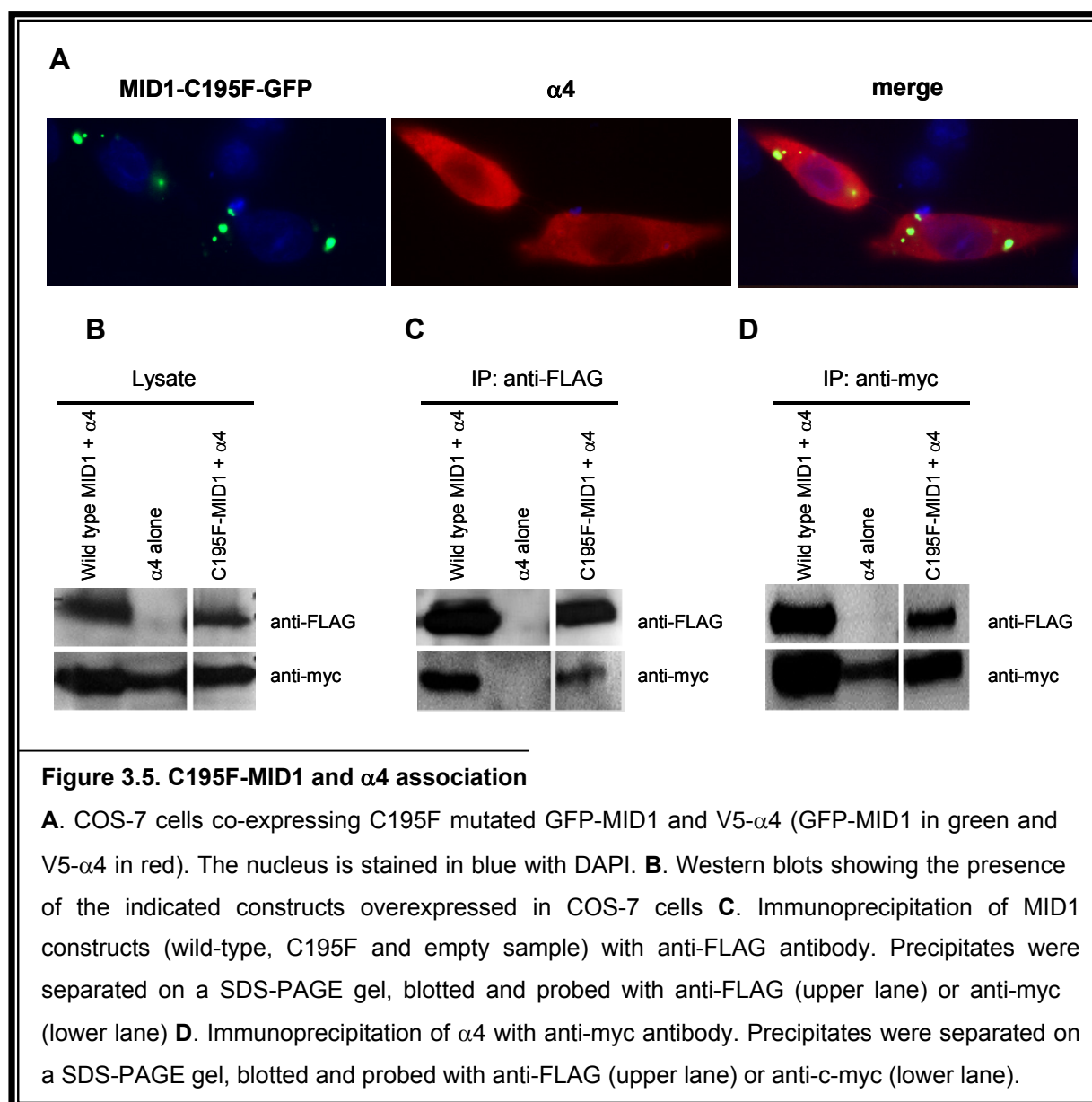
in figures 3.4B and 3.4C (sphere). According to this arrangement, it was predicted that C195 in MID1 Bbox2 (indicated with an arrow in Figure 3.4C) would form a part of the conserved core of residues, and that it is placed in the flexible loop of the domain. This structure has been proposed to probably participate in the correct positioning of the coiled-coil domain and, subsequently, the C-terminal end of MID1 (Borden et al., 1995b). Evolutionary conservation confirms the predicted important structural roles of this residue (Khuri et al., 2001; Mnayer et al., 2005). Interestingly, while also located in the above described loop, Q192 was not found to be a conserved residue.



3.1.3 C195F, mutated MID1 form found in an OS patient, disrupts MID1- α 4 interaction

In order to test for putative consequences of a mutation such as C195F in Bbox2 with respect to the association of MID1 to α 4 *in vivo*, N-terminally GFP-tagged C195F-MID1 was overexpressed in COS-7 cells together with V5-tagged α 4. Subcellular localization of both proteins was subsequently assayed by immunostaining as previously described. Confirming predictions, C195F-MID1 mutant protein not only lost α 4 binding properties, but also its microtubule-binding affinity, probably due to major structural changes of the entire protein. In immunostained cells, while α 4 appeared diffusely distributed in the cytosol, C195F mutant

protein accumulated in cytosolic aggregates (Figure 3.5A). The pictures clearly prove a loss of interaction of the two proteins, $\alpha 4$ and C195F MID1 *in vivo*.



For further research, immunoprecipitation experiments were performed with cytosolic extract from COS-7 cells co-expressing FLAG-tagged C195F-MID1 and $\alpha 4$ -myc (Figure 3.5B). Immunoprecipitation with anti-FLAG and subsequent Western blotting of the precipitates with anti-myc, showed that both wild-type and C195F mutated MID1 interact with $\alpha 4$ *in vitro* (Figure 3.5C-lower lane). Similarly, a clear MID1 band was seen in both samples wild-type and C195F-mutant after immunoprecipitation of $\alpha 4$ with anti-myc and anti-FLAG incubation of the Western blots of the precipitates (Figure 3.5D-upper lane). Both blots were also incubated with the antibodies used for immunoprecipitation, confirming the efficiency of the precipitation reactions (Figure 3.5C-upper lane, Figure 3.5D-lower lane). In other words, unexpectedly,

these data indicate that while not being strong enough to disrupt the interaction of Bbox1 with $\alpha 4$ *in vitro*, a mutation such as C195 into F leads to misplacement and missfolding of MID1 that, consequently, can no longer interact with $\alpha 4$ *in vivo*.

3.1.4 Bbox2 mutants do not interact with $\alpha 4$ *in vivo*

All observations made thus far pointed towards a relevant structural and functional role for the Bbox2 domain of MID1, which would not only play an important role in the interaction of MID1 with $\alpha 4$ but also with microtubules. To further characterise the function of this domain, site directed mutagenesis of selected amino acids was performed, and the influence of these mutations on the known functional abilities ($\alpha 4$ - and microtubule-binding) of MID1 was studied. Mutated residues were chosen according to their putative effect on the MID1 structure predicted by comparison with the 3D-structure of XNF7 Bbox and the Bbox2 consensus sequence.

The following N-terminally GFP-tagged MID1 constructs were used in this study:

C175A: Cysteine-175 is located at the N-terminal end of Bbox2 and immediately precedes a loop/turn. It is conserved and participates in zinc binding. It was mutated into alanine, a hydrophobic amino acid.

C198A: Cysteine-198 is located in the flexible turn. It is conserved and participates in zinc binding. It was also mutated into alanine.

H178Y: Histidine-178 is located in the middle of the N-terminal loop. It is conserved and participates in zinc binding. It was mutated into tyrosine, another polar amino acid that contains an aromatic ring.

V183T: Valine-183, a hydrophobic amino acid would be the first amino acid of the first β -strand. It was mutated into threonine, a polar amino acid.

Q192R: Glutamine-192, a polar hydrophilic residue would be located at the loop region. It was mutated into arginine, a basic amino acid.

Δ Bbox2: deletion of the entire Bbox2 domain.

Δ Ring: deletion of the RING finger domain.

Δ Ring-Bboxes: deletion of the RING finger domain and both Bboxes.

Splice variant-Ex2d.7: MID1 splice variant which has been shown to bind $\alpha 4$ more strongly than full-length MID1 (Winter et al., 2004).

Splice variant-Ex2d.7-C175A: splice variant with a C175A mutation in Bbox2.

Splice variant-Ex2d.7-H178Y: splice variant with a H178Y mutation in Bbox2.

Immunostaining experiments were performed in the same manner as described previously; the different GFP-MID1 constructs were co-expressed with $\alpha 4$ -V5 in COS-7 cells and analysed by immunostaining (GFP-MID1 in green and $\alpha 4$ -V5 in red). Like the OS mutant

C195F, the missense mutations C175A, C198A, H178Y and the deletion of the entire Bbox2, all of which are predicted to have drastic structural effects on the MID1 protein, produce aggregates that hardly interact with microtubules and do not interact with $\alpha 4$ (Figure 3.6A). In contrast, V183T and Q192R, non-conserved residues that are expected not to have such a significant effect on the MID1 protein structure as the previous mutations, showed a clear interaction with microtubules, but not with $\alpha 4$.

The splice variant *Ex2.d7* has been previously shown to have much higher binding affinity to $\alpha 4$ than full length MID1 in a β -galactosidase based yeast two-hybrid assay, and therefore, it was proposed to participate in the regulation of the MID1 protein function (Winter et al., 2004). This splice variant has a protein truncation stop signal after the coiled-coil domain and, in addition, exon1 is shortened, therefore losing most of the Bbox2 domain (only the seven first amino acids of the domain are kept).

Ex2d.7 does not interact with microtubules but appears diffusely distributed similar to $\alpha 4$, although they both seem to co-localise, as previously reported (Winter et al., 2004). In this case, none of the mutations, C175A or H178Y, contained in the Bbox2 part seemed to have strong effects; localisation of the protein was not modified and no clumps were formed (Figure 3.6B, middle and lower panels). However, as both proteins showed diffuse pattern in the cytosol, it was difficult to charge if they interact by immunofluorescence. For this reason, β -galactosidase based yeast two-hybrid assays were also performed (see below).

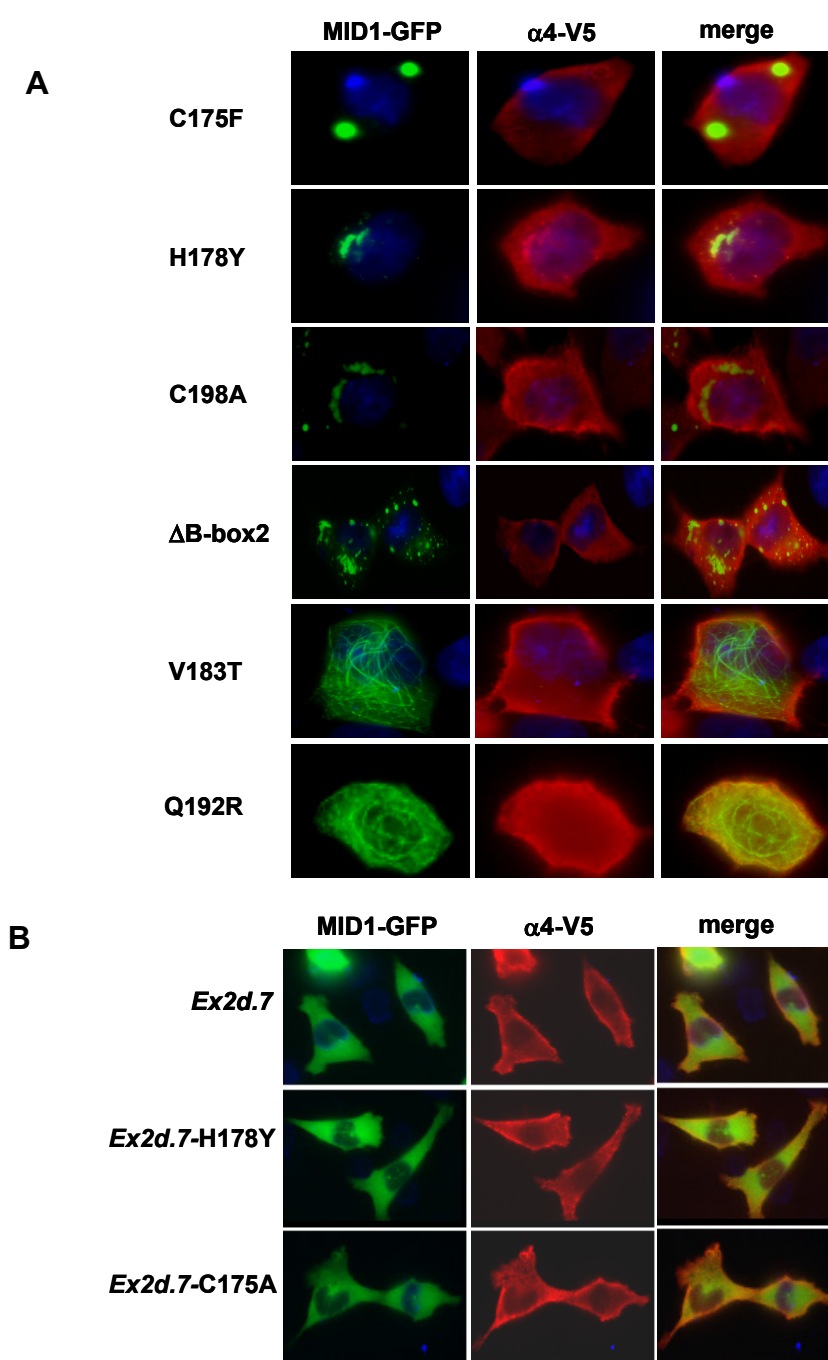
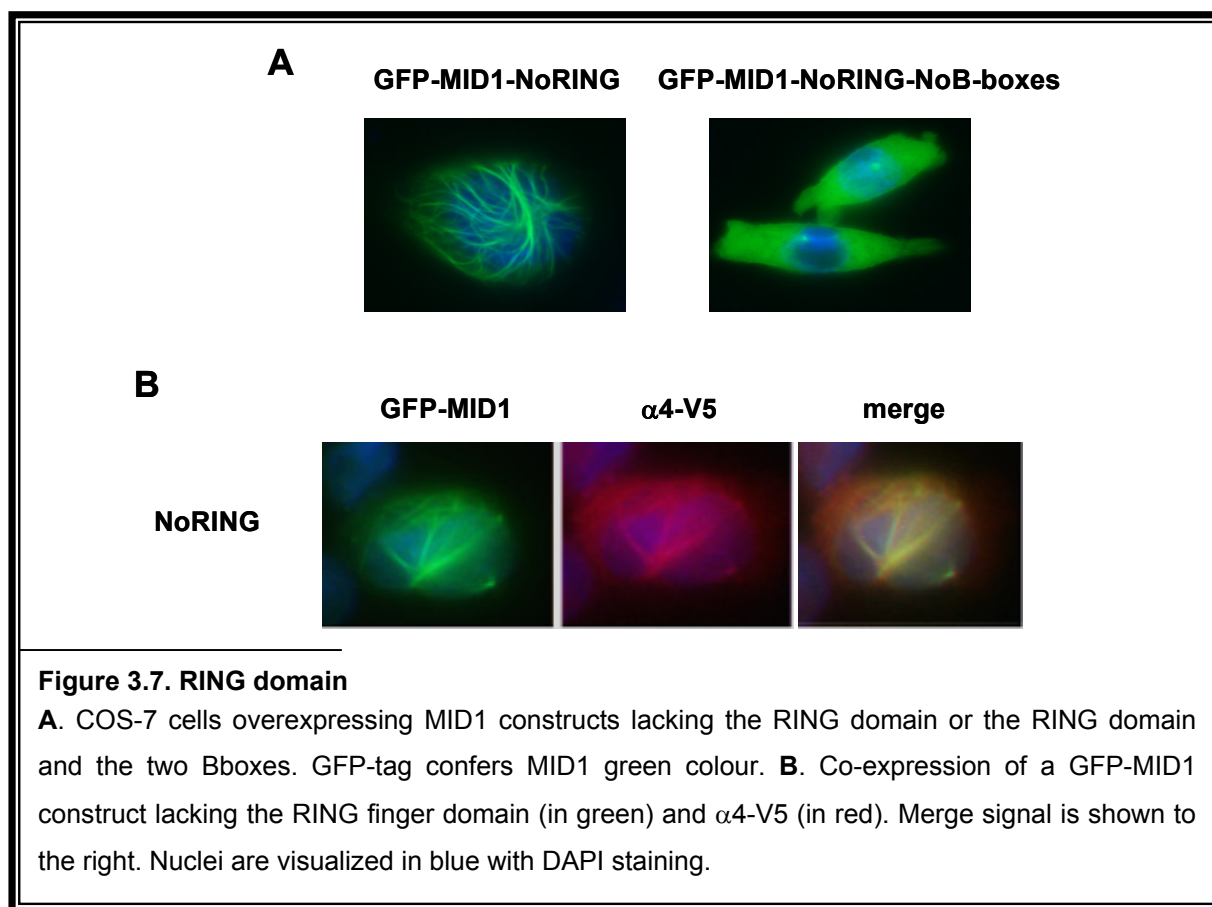


Figure 3.6. Bbox2 mutants do not interact with Bbox2 *in vivo*

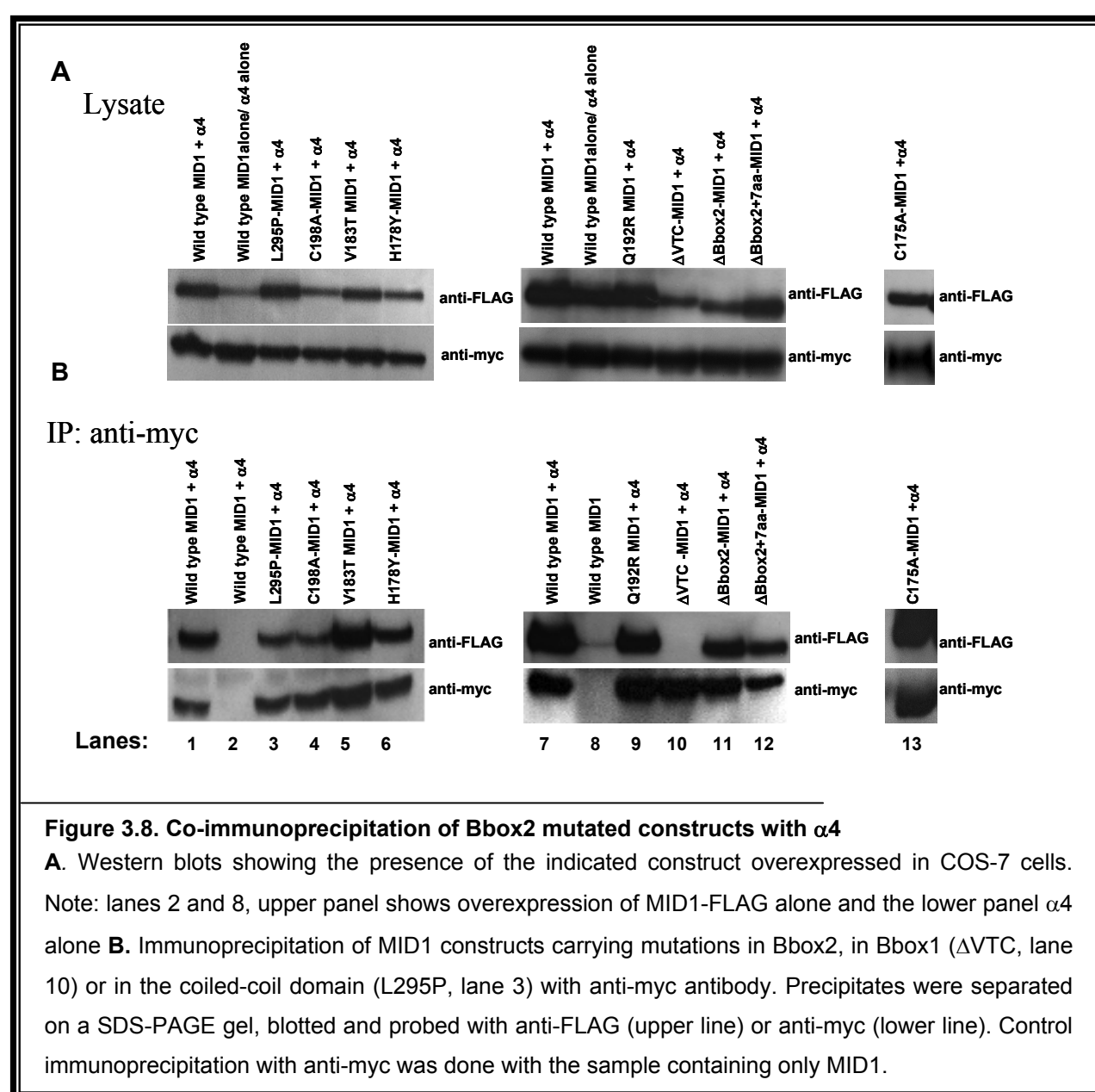
A. COS-7 cells co-expressing different MID1 constructs with mutations in the Bbox2 domain or the complete deletion of the domain and $\alpha 4$ were immunostained. GFP shows the localisation of MID1 in green, and $\alpha 4$ is labelled in red with Cy3. Merge signals are shown to the right. Nuclei are visualized in blue with DAPI staining. **B.** Constructs carrying the Ex2d.7 splice variant without or with mutations (C175A, H178Y) were examined in the same way.

Most of the Bbox2 mutants, as well as the deletions of any of the Bboxes, exhibited difficulties to interact with microtubules, suggesting that not only an intact C-terminus but also the Bboxes are essential for the correct folding and positioning of MID1 at the microtubules. It has previously been shown that mutations in the coiled-coil domain do not misplace MID1 or affect its interaction with $\alpha 4$. A mutated C-terminal domain, while abolishing microtubule-association, has also no influence on $\alpha 4$ binding (Liu et al., 2001; Schweiger et al., 1999; Trockenbacher et al., 2001). However, no data about putative effects of the RNG finger domain are available yet. Thus, a MID1 construct lacking the RING domain and a second one lacking the RING and the Bboxes domains were examined by immunostaining for microtubule-association. In addition, the $\alpha 4$ binding properties of the construct lacking exclusively the RING were studied. It was observed that, while the absence of the RING did not have any effect on the position of MID1 at the microtubules or its binding with $\alpha 4$, the additional absence of the Bboxes led to misplacement of the protein (Figure 3.7). This result confirms again that the Bboxes are necessary not only for proper $\alpha 4$ interaction (as shown in sections 3.1.1 and 3.1.4), but also for providing the correct emplacement of MID1 at the microtubules, even when the C-terminal end of the protein remains unaltered.



3.1.5 Bbox2 mutants interact with $\alpha 4$ *in vitro*

Further characterisation of a putative interaction of Bbox2 MID1 mutants with $\alpha 4$ required a study of the *in vitro* situation, which would help to clarify whether Bbox2 mutants do not interact with $\alpha 4$ *in vivo* because they are not well positioned, or because the interface of the $\alpha 4$ binding site is affected. Immunoprecipitation experiments with anti-myc antibody were performed with different N-terminally FLAG-tagged Bbox2 mutants co-expressed with myc-tagged $\alpha 4$ in COS7-cells (Figure 3.8A). Apart from a MID1 construct lacking the entire Bbox2 and the previously described constructs carrying point mutations in the Bbox2 domain, a construct including only the first seven amino acids of the domain, resembling the earlier

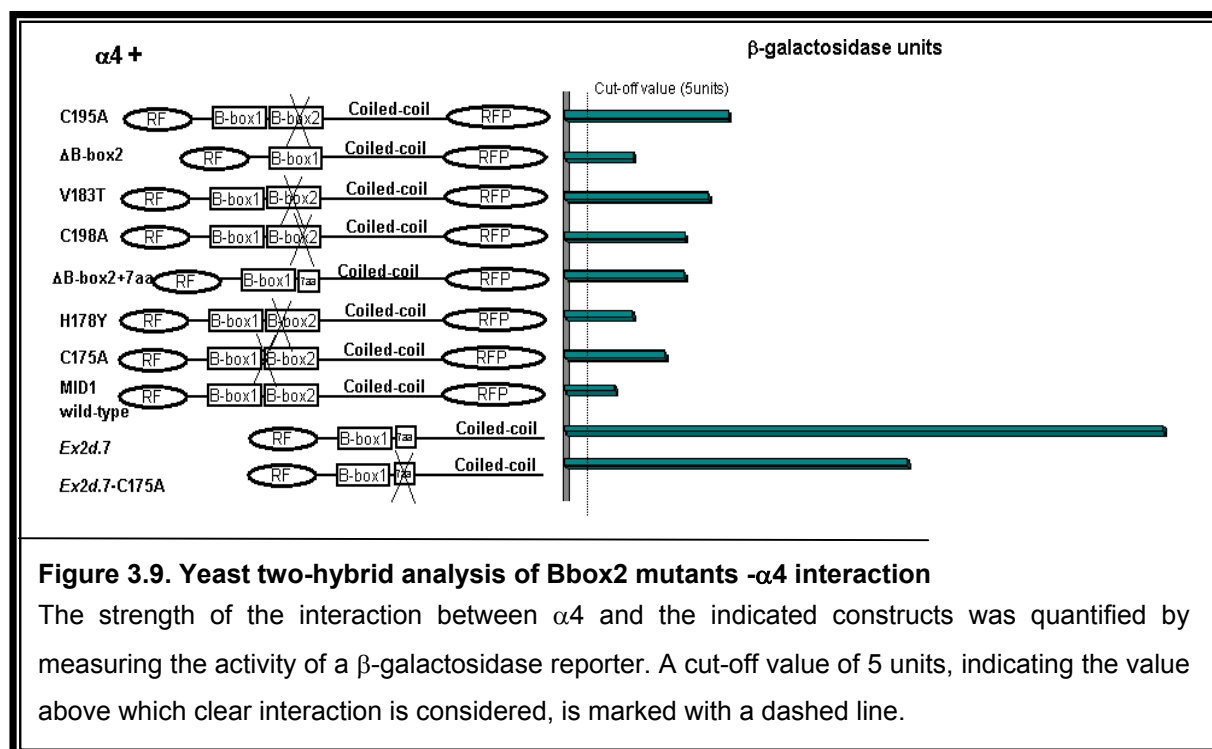


described splice variant (section 3.1.4) was included. A construct carrying the mutation Δ VTC

in Bbox1 was included as negative control for MID1- α 4 binding. As positive control, a construct carrying a mutation in the coiled-coil domain, L295P (So et al., 2005), that was previously shown not to interfere with α 4 binding (Schweiger et al, unpublished data), was used. Western blots developed with anti-FLAG antibody and with anti-myc antibody proved the efficiency of the precipitation reaction. Samples only expressing FLAG-tagged wild-type MID1 were used as background control.

As expected, the construct carrying a mutation in Bbox1 (Δ VTTC) did not interact with α 4, agreeing with the results from section 3.1.1 (Figure 3.8B-lane10), and the L295P mutation maintained unaltered its association with α 4 (Figure 3.8B-lane3). Similarly to what was observed for the C195F mutant, all the Bbox2 mutants studied (C198A, V183T, H178Y, Q192R, C175A and deletion of Bbox with and without extra seven amino acids) were able to interact with α 4 *in vitro* (Figure 3.8B-lanes 4,5,6,9,11,12,13), associating to α 4 with similar intensity as L295P.

For further characterisation, β -galactosidase activity was measured in yeast two-hybrid assays to quantify the strength of the interaction between the different constructs and α 4. Similarly to what was done for the Bbox1, a cut-off value at 5 units β -galactosidase activity was assigned. Measurements above this value were considered as interaction between the MID1 construct and α 4. In confirmation with all the *in vitro* immunoprecipitation results obtained, all constructs tested were able to interact with α 4 in the yeast system (Figure 3.9). The splice variant, *Ex2d.7* with and without C175A mutation, was also tested and showed higher binding affinity than all the other constructs (Figure 3.9). However, since unexpectedly all the Bbox2 mutated constructs interact with α 4 *in vitro* and given that both splice variant and α 4 are spread in the cytosol in immunofluorescence experiments, at this point it is not possible to make conclusions about the interaction of this splice variant with α 4 *in vivo*.



In summary, the results obtained during this thesis show that the Bbox2 domain considerably influences the interaction between $\alpha 4$ and MID1 *in vivo*. Single point mutations lead to complete disruption of this interaction *in vivo* but not *in vitro*. Furthermore, amino acid changes in the conserved core of amino acids in Bbox2 appear to affect the protein to a greater extent and lead to dissociation of the mutant protein from the microtubules, and disruption of the interaction between MID1 and $\alpha 4$.

3.2 Characterisation of the MID1 multiprotein complex

The elucidation of previously reported multiprotein complexes has allowed a much better understanding of the function of their main component proteins. Well-characterised examples are PML, FMRP or Staufen (Brendel et al., 2004; Ceman et al., 1999; Hodges et al., 1998; Sternsdorf et al., 1997). As mentioned earlier, MID1 forms part of a macromolecular complex, the composition of which was mainly unknown. Therefore, the elucidation of its components could shed light on different functions in which MID1 might be involved.

In this thesis, affinity chromatography was the method of choice to identify protein components of the macromolecular MID1 complex. For the preparation of the chromatography column, a peptide that was recombinantly produced in *E.coli* in a PinPoint vector system was used (see section 3.2.2). This peptide covered the MID1 binding region in the $\alpha 4$ protein, which had been recently narrowed down to 44 amino acids (44aa peptide) (Figure 3.10; R. Schneider and A. Köhler, unpublished data). Unfortunately, MID1 could not be used for the preparation of the column, as it contains many cysteines that impede the correct folding of the protein in *E.coli*.

237-PPVKPFILTRNMAQAKVFGAGYPSLPTMTVSDWYEQHRKY GAL-280

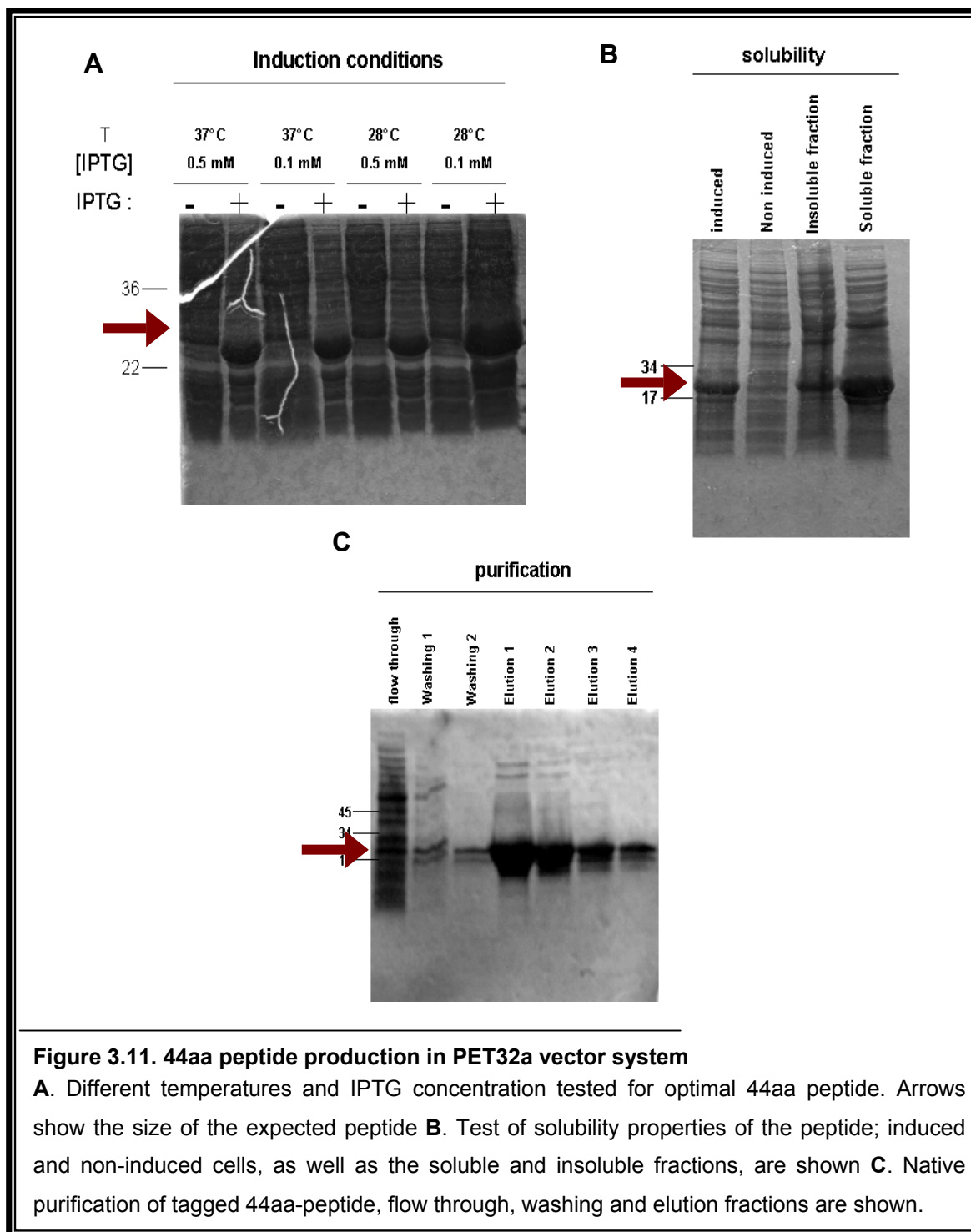
Figure 3.10. $\alpha 4$ peptide

44 amino acids peptide corresponding to the region of $\alpha 4$ that specifically interacts with MID1.

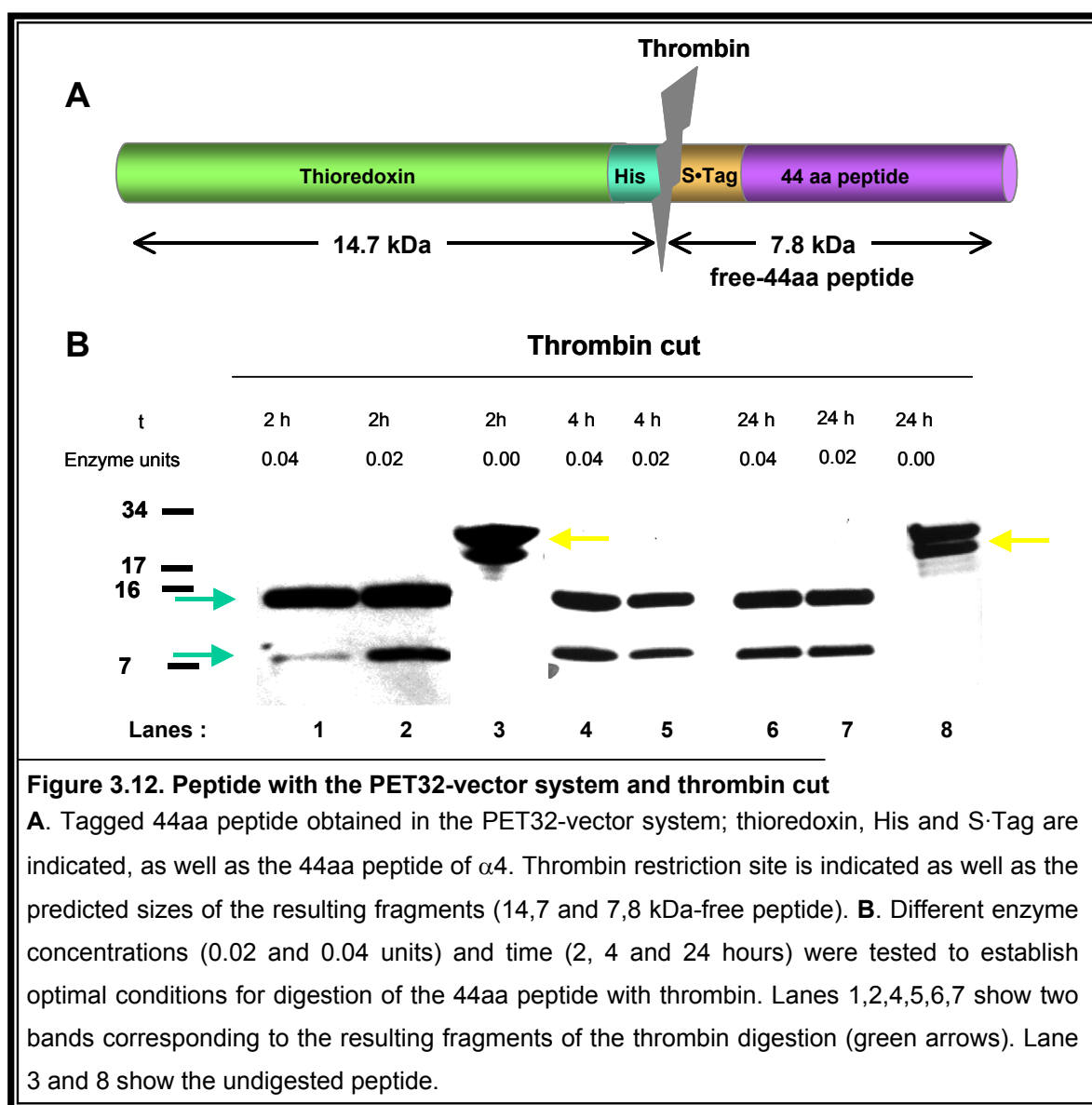
3.2.1 44aa peptide of $\alpha 4$ production in the PET32a vector system

Conditions for the expression of the 44aa peptide in *E.coli* were first established with the PET32a vector system, a very efficient protein expression system. Moreover, with this vector a His-tag suitable purification through Ni-NTA agarose and a Thioredoxin tag and a S-Tag that improve the solubility of the peptide could be incorporated to the peptide (Figure 3.12A). Several temperatures and concentrations of IPTG for induction of protein expression were tested in order to establish optimal conditions in the BL21 strain of *E.coli* (Figure 3.11, induction conditions). An aliquot of each culture was lysed under denaturing conditions with SDS-PAGE buffer or magic mix and analysed on a 15 % Coomassie stained SDS gel (Figure 3.11A). Having observed no difference in any of the tested conditions 2 h after induction, the minimum amount of IPTG (0.1 mM) at 37°C were taken as the conditions of choice. To test the solubility of the peptide produced under those conditions, cells were lysed in native conditions lysis buffer (see Methods section), and the soluble fraction was separated from

the insoluble by centrifugation at 10000 x g. Aliquots of the soluble and insoluble fractions, as well as induced and non-induced cells (lysed with SDS buffer), were analysed on a 15% Coomassie gel, and it was confirmed that the peptide was soluble under native conditions (Figure 3.11B). Subsequently, the peptide was purified through Ni-NTA and aliquots of each fraction (flow through, washes and elutions) were run on a 15% Coomassie stained SDS gel (Figure 3.11C).



Although a stop codon had been introduced after the 44aa peptide coding sequence, the purified peptide presented with more than one band in the Coomassie gel (Figure 3.11C, Elutions 1-4). Therefore, the peptide was digested with thrombin in order to find out if the additional bands were degradation products, the result of translation from a later initiation codon or gel artefacts (Figure 3.12). Upon thrombin restriction, two bands of 14,7 kDa and 7,8 kDa were expected, and variations on the sizes of the obtained bands would indicate the source of the additional bands. Different conditions, including different incubation times and enzyme concentration, were tested for optimal digestion of the purified peptide at 4°C (Figure 3.12B). Samples were run on 15% SDS gels and silver stained. While the control experiment without enzyme remained intact, after 2 hours most of the peptide had been already digested with all enzyme concentrations tested. Interestingly, thrombin digestion resulted in two well-defined bands at the expected sizes (green arrows), confirming that the additional bands



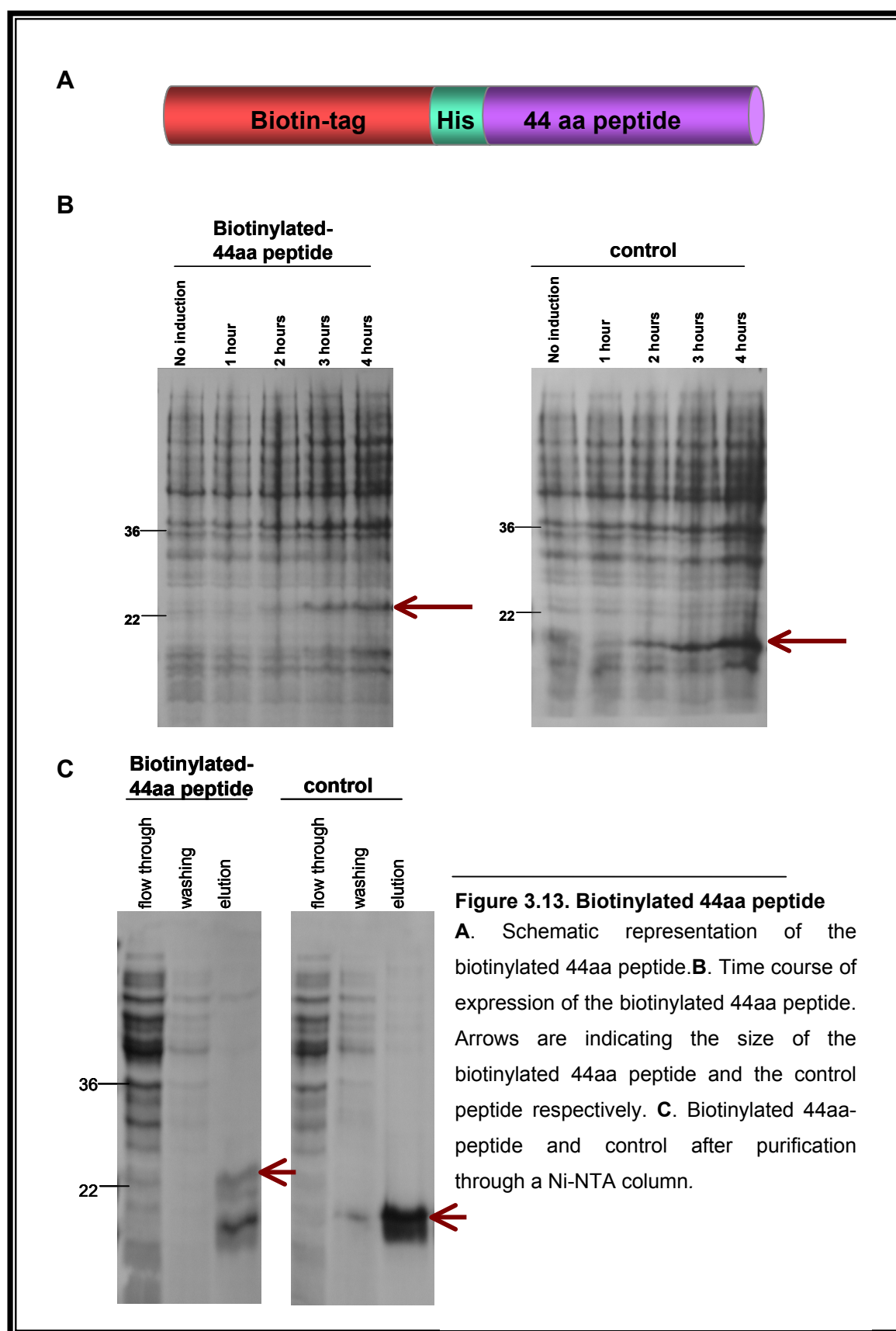
observed in the undigested peptide are probably due to gel artefacts. No degradation of the undigested peptide (yellow arrows) was observed even after 24 hours at 4°C in untreated controls.

The free 44aa peptide was subsequently used for elution of the chromatography column (see below) and for that purpose, thrombin was used to cleave the thioredoxin-tag and the His-Tag as previously described (Figure 3.12A). The free 44aa peptide, only including the S-Tag, was recovered by trapping the fragment including the tags in Hepes sucrose buffer (HS buffer) equilibrated Ni-NTA agarose and collecting the flow through containing the 44aa peptide.

3.2.2 $\alpha 4$ peptide production in the PinPoint vector system

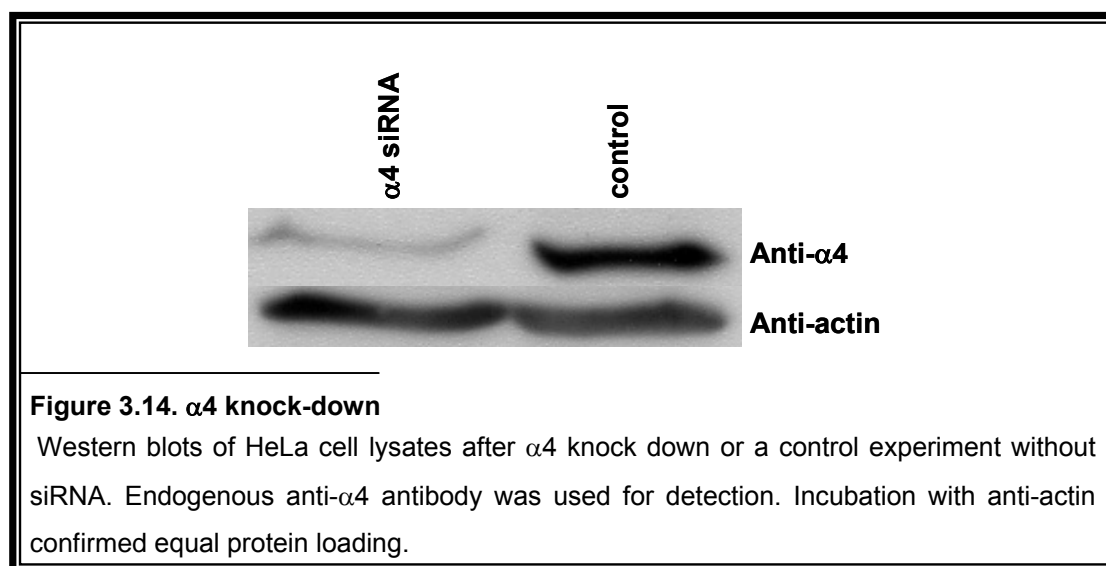
With the pinpoint vector system, a biotinylated peptide can be produced which can then be immobilized on streptavidin-coated agarose beads. Thus, the sequence corresponding to the 44aa peptide including a stop codon was cloned into the PinPoint -Xa vector, and a His-RGS tag was additionally included in order to purify the peptide through Ni-NTA agarose. To set up optimal expression time the biotinylated peptide was overexpressed in *E.coli* (strain JM109) in the presence of 2 μ M biotin upon induction with 0.1 mM IPTG for one, two, three or four hours. An aliquot from each culture was run in a 15% SDS-PAGE gel and checked by Coomassie staining (Figure 3.13A). Although the approximately 22 kDa big peptide started to be expressed 2 hours after induction, at least three to four hours were necessary to obtain the highest expression levels. As a control, the same vector without the peptide was used, showing a similar induction pattern.

Having established the expression conditions, the peptide was purified through Ni-NTA agarose and its purity was tested on a 15% Coomassie gel (Figure 3.13B). Of note, two bands corresponding to the peptide were obtained, probably due to gel artefacts.



3.2.3 Affinity chromatography column

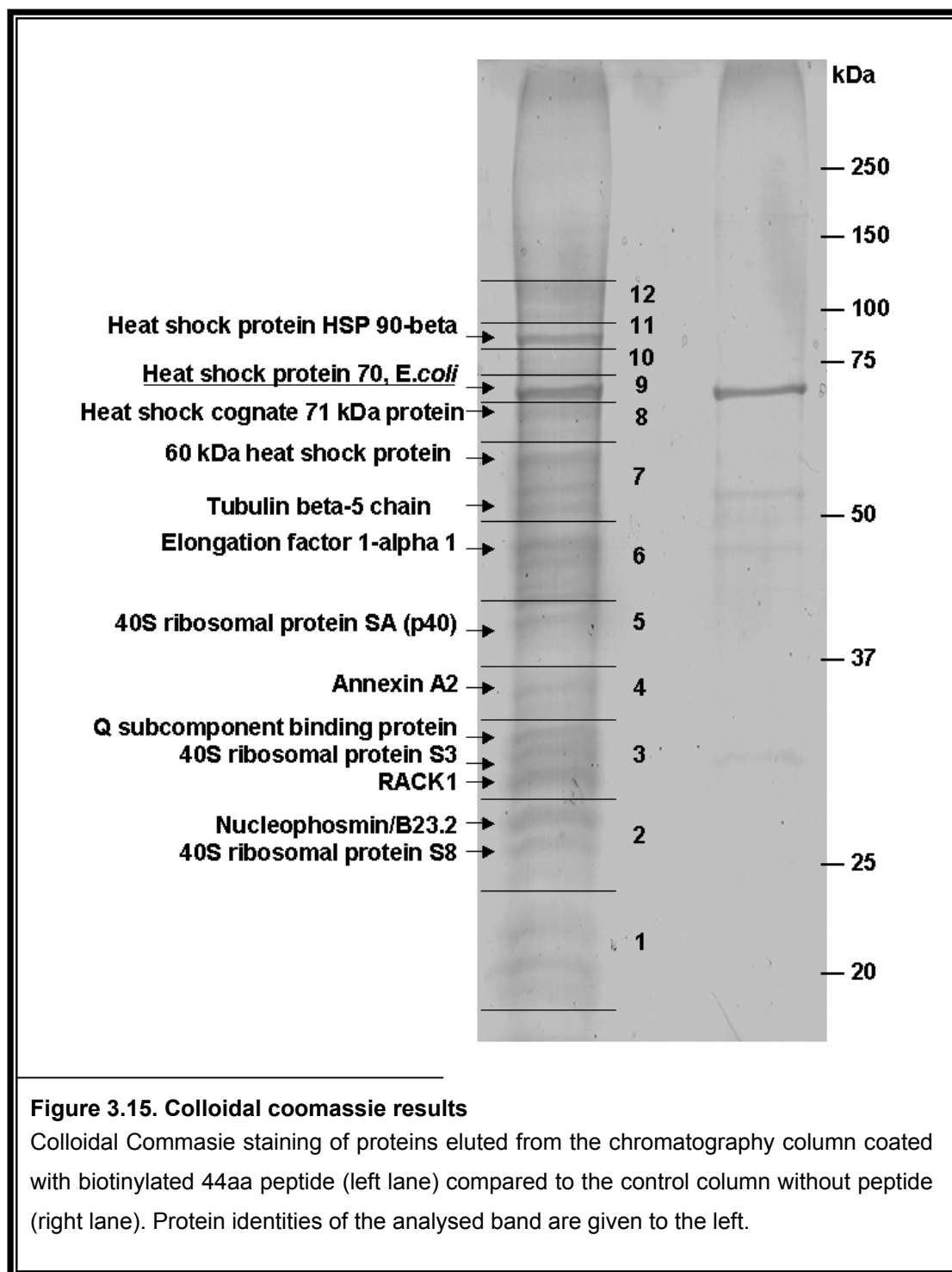
For preparing the affinity chromatography, the biotinylated 44aa peptide was bound to streptavidin coated agarose beads and subsequently blocked with BSA to reduce unspecific interactions. In parallel, a control experiment without peptide was performed. After blocking, the columns were extensively washed first with free 44aa peptide and, then, with 100 volumes of HS buffer and 2 volumes of washing buffer (250 mM NaCl/0,05% Tween), followed by equilibration in HS buffer. Afterwards, cytosolic HeLa extracts were added to both columns (with and without peptide). In order to avoid competition for MID1 between endogenous $\alpha 4$ and the biotinylated 44aa peptide bound to the column, endogenous $\alpha 4$ had been previously knocked-down by siRNA (Figure 3.14).



After extensive washing, MID1 and its interaction partners were eluted with free 44aa peptide (section 3.2.1). Eluted proteins were dialysed to remove the excess of peptide and analysed on a 10% SDS gel that was subsequently colloidal Coomassie stained. Bands absent in the control gel were cut out and analysed by electrospray ionisation mass spectrometry (ESI-MS). Figure 3.15 shows the colloidal Coomassie stained gel and the protein identities of the analysed bands, after correlation of the obtained peptides with the Swiss-Prot database.

Tubulin beta-5-chain identification (Figure 3.15) resembled microtubule binding ability of MID1 shown before in our lab (Schweiger et al., 1999) and served as a proof of specificity. In addition, several heat shock proteins, namely Heat shock protein HSP 90-beta (Hsp90), Heat shock cognate protein 71kDa protein (Hsc70) and 60 kDa heat shock protein (Hsc60), being Hsp90 the most abundant, were identified. Unfortunately, MID1 detection was hindered by a very strongly encountered *E.coli* heat shock protein (Heat shock protein 70, *E.coli*) that has the same molecular size and was also present in the control sample. In addition,

elongation factor 1- α 1 (EF-1 α), Annexin A2 (ANXA2), Q subcomponent binding protein (p32), RACK1, Nucleophosmin (NPM) and several ribosomal proteins of the small 40S subunit (S3, S8) were found. Table 1 shows a summary of already reported functions of the proteins identified after mass spectrometry.



| Protein | Short name | Accession number | Function | References |
|---|---------------|------------------|---|--|
| Heat shock protein HSP90-beta | Hsp90 | P08238 | <ul style="list-style-type: none"> •RNA binding protein •Cell cycle progression as chaperon of cell cycle regulation and Polo-like kinases •Centrosome duplication •Buffer of insulin-like growth factor and insuline signalling •Participates in the reduction of Huntingtin aggregates | (Burrows et al., 2004; de Carcer, 2004; de Carcer et al., 2001; Lange et al., 2000; Meares et al., 2004; Nakai and Ishikawa, 2001; Sittler et al., 1998) |
| 60 kDa heat shock protein | Hsc60 | P10809 | <ul style="list-style-type: none"> •Chaperon •Mitochondrial functions •Regulation of stress-induced apoptosis | (Bukau and Horwich, 1998; Gupta and Knowlton, 2005; Voos and Rottgers, 2002) |
| Heat shock cognate 71 kDa protein | Hsc70 | P11142 | <ul style="list-style-type: none"> •Chaperon •Associates with Huntingtin aggregates | (Jana et al., 2000) |
| Tubulin beta-5 chain or Tubulin beta-1 | Tubulin | P05218 | <ul style="list-style-type: none"> •Monomer of microtubules •Microtubule dynamics | (Cooper, 2000) |
| Elongation factor 1-alpha 1 | EF-1 α | P04720 | <ul style="list-style-type: none"> •Peptide chain elongation •Cytoskeleton regulation •Interaction with mitotic apparatus •Regulation of microtubules dynamics •Associates with Huntingtin aggregates | (Condeelis, 1995; Mitsui et al., 2002; Moore R.C and R.J., 2000; Moore RC et al., 1998; Negrutskii and El'skaya, 1998; Ohta et al., 1990); |
| 40S ribosomal protein SA (p40) (34/67 kDa laminin receptor) | SA | P08865 | <ul style="list-style-type: none"> •Tumor cell growth and proliferation •RNA processing and ribosome maturation | (Ford et al., 1999) |
| Annexin A2 | ANXA2 | P07355 | <ul style="list-style-type: none"> •RNA-binding protein •Mediator of Ca²⁺ regulated endocytosis and exocytosis. Regulation of ion channels •DNA binding •Inhibition of cell adhesion | (Balch and Dedman, 1997; Filipenko et al., 2004; Vedeler and Hollas, 2000) |

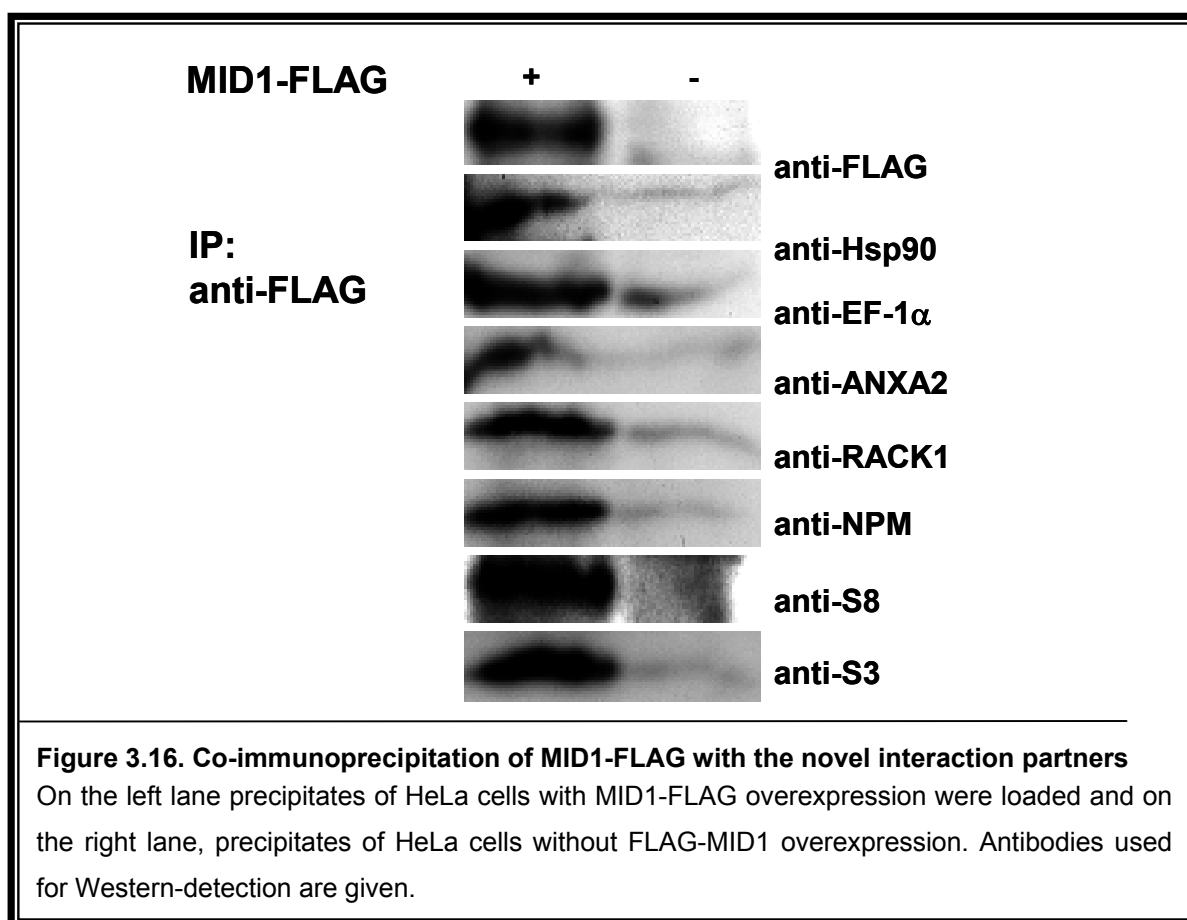
| Protein | Short name | Accession number | Function | References |
|-----------------------------------|------------|------------------|--|---|
| Receptor for activated C kinase 1 | RACK1 | P25388 | <ul style="list-style-type: none"> • RNA binding protein • Scaffold protein • Regulation of cycle progression • Constituent of the eukaryotic ribosomes. • Positioning of ribosomes where translation is required, eg. Focal adhesions • Regulation of STAT3 activation through insulin-like growth factor 1 and insuline signalling • Intracellular Ca²⁺ regulation • Regulation of integrin-mediated adhesion | (Cox et al., 2003; Mamidipudi et al., 2004a; Mamidipudi et al., 2004b; McCahill et al., 2002; Nilsson et al., 2004; Sklan et al., 2006; Zhang et al., 2006) |
| 40S ribosomal protein S3 | S3 | P23396 | <ul style="list-style-type: none"> • Constituent of the small ribosome subunit; DNA repair • Apoptosis/cell growth regulation | (Jang et al., 2004; Stahl, 2001; Wittmann-Liebold and Graack 2001) |
| Q subcomponent binding protein | p32 | Q07021 | <ul style="list-style-type: none"> • Chaperon – PKC μ regulatory protein • Mitochondrial oxidative phosphorylation • Splicing modulation | (Chattopadhyay et al., 2004; Krainer et al., 1991; Storz et al., 2000) |
| 40S ribosomal protein S8 | S8 | RS8_HUMAN | <ul style="list-style-type: none"> • Constituent of the small ribosome subunit | (Stahl, 2001; Wittmann-Liebold and Graack 2001) |
| Nucleophosmin/B2 3.2 | NPM | Q9BYG9 | <ul style="list-style-type: none"> • RNA binding protein • Ribosome biogenesis • Regulation of transcription, • DNA replication and apoptosis Centrosome duplication • Cytoplasmic nuclear trafficking • Cancer pathogenesis • Pre mRNA processing | (Fankhauser et al., 1991; Grisendi et al., 2005; Okuda, 2002; Shinmura et al., 2005; Tarapore et al., 2002; Tarapore et al., 2006; Wang et al., 1994); |

Table 3.1 Previously reported functions of novel identified MID1 interaction partners

Name, short name, accession numbers from the Swiss-Prot data base and functions of the different identified MID1 interaction partners by MS are listed. References are also given.

3.2.4 Confirmation of novel MID1 interaction partners

In order to verify the association of the proteins identified by MS with MID1, co-immunoprecipitation experiments were performed with HeLa extracts overexpressing N-terminally FLAG tagged-MID1 (MID1-FLAG). Agarose-beads coated with anti-FLAG antibody were used to immunoprecipitate MID-FLAG, and bound proteins were specifically eluted with 3 x FLAG-peptide. Precipitated proteins were analysed on Western blots incubated with endogenous antibodies for the respective proteins and anti-FLAG to detect MID1-FLAG itself. As negative control, the same immunoprecipitation experiment was performed with cytosolic HeLa extracts without MID1-FLAG expression.



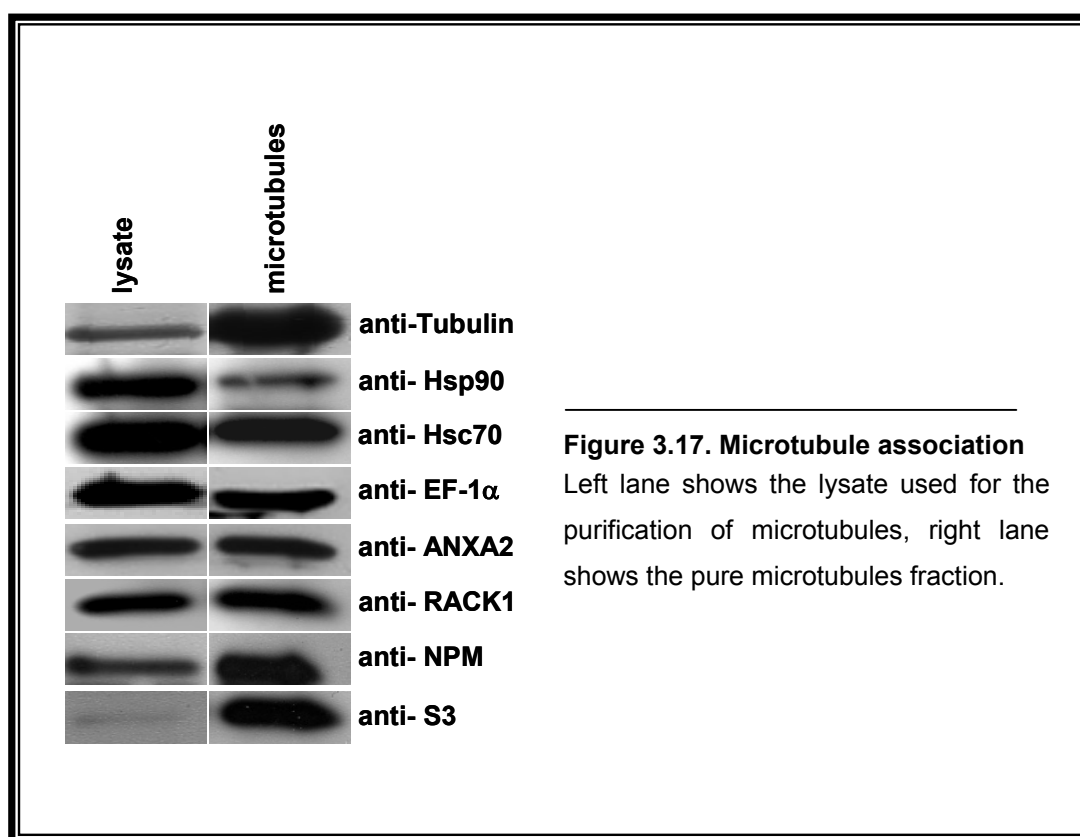
In the presence of MID1-FLAG, all the proteins studied could be pulled down with the anti-FLAG coated beads (Figure 3.16, left lane). On the contrary, in the control experiment only background binding was observed (Figure 3.16, right lane), confirming specific association of MID1 with the identified proteins.

3.2.5 The MID1 protein complex is found in purified microtubules

As mentioned previously, association of MID1 with microtubules has previously been demonstrated (Schweiger et al., 1999), which was again confirmed here by the identification

of Tubulin β -5 chain in the protein complex. In order to test whether the other components of the MID1 complex associate to microtubules as well, microtubules were purified from HeLa cells lysates through subsequent polymerisation/depolymerisation steps with taxol and carefully washed. The presence and enrichment of the different proteins in the pure microtubule fraction was tested on Western blots incubated with antibodies detecting the respective members of the complex. Bands in purified microtubules were compared to total HeLa cell lysates loaded with the same amounts of protein (Figure 3.17).

A tubulin α/β enrichment in the purified fraction compared to the lysate, indicated successful isolation of microtubules (Figure 3.17). An enrichment in S3, NPM and RACK1 was also observed, corroborating the interaction of the complex with microtubules. Moreover, considerable amounts of EF-1 α and ANXA2 were found at the microtubules, although interaction of these proteins depends on Ca^{2+} and this factor was not considered. Finally, only small amounts of Hsp90 and Hsc70 were found in the microtubules fraction, indicating a weaker interaction of those proteins with the complex.



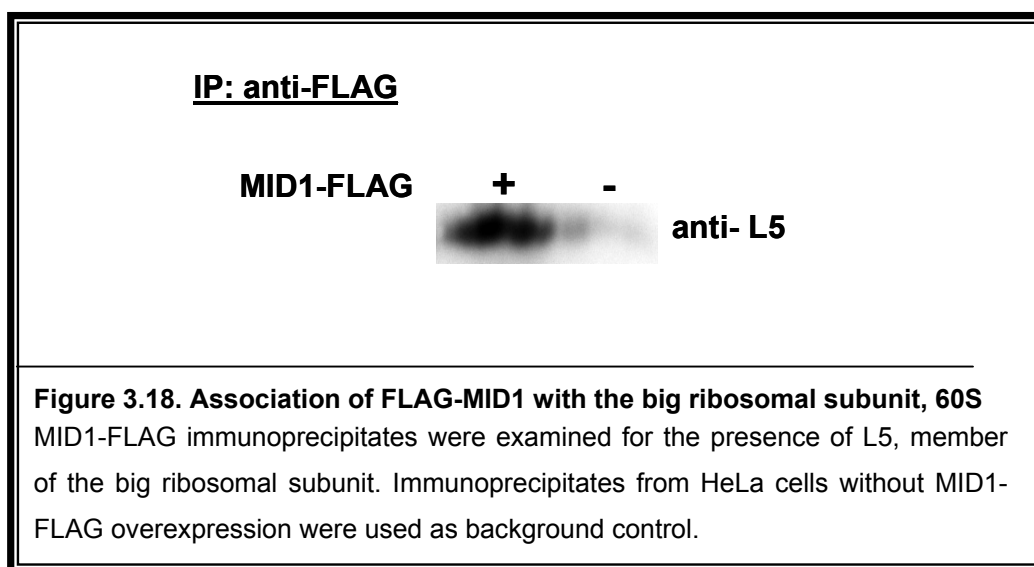
3.2.6 The MID1 complex associates with both ribosomal subunits

Among the newly identified MID1 complex members, it was remarkable the presence of ribosome related proteins such as S3, S8, p40 and RACK1, which have been found to be constituents of the small ribosomal subunit. Additionally, EF-1 α , an important member of the translation machinery, several heat shock proteins, NPM (involved in ribosome biogenesis) and

ANXA2 (another ribosome-associated protein) were found in the complex. All these data together indicated that the MID1 complex associates with ribosomes. However, interaction with the big ribosomal 60S subunit, had not been observed in the already performed experiments.

In order to test if the MID1 complex also associates with the big ribosomal subunit, MID1-FLAG overexpressed in HeLa cell lysates was immunoprecipitated with anti-FLAG antibody, following the same procedure as in section 3.2.4. Instead, this time MID1-FLAG immunoprecipitates were examined by Western blot for the presence of L5, a ribosomal protein component of the big ribosomal subunit 60S (Figure 3.18).

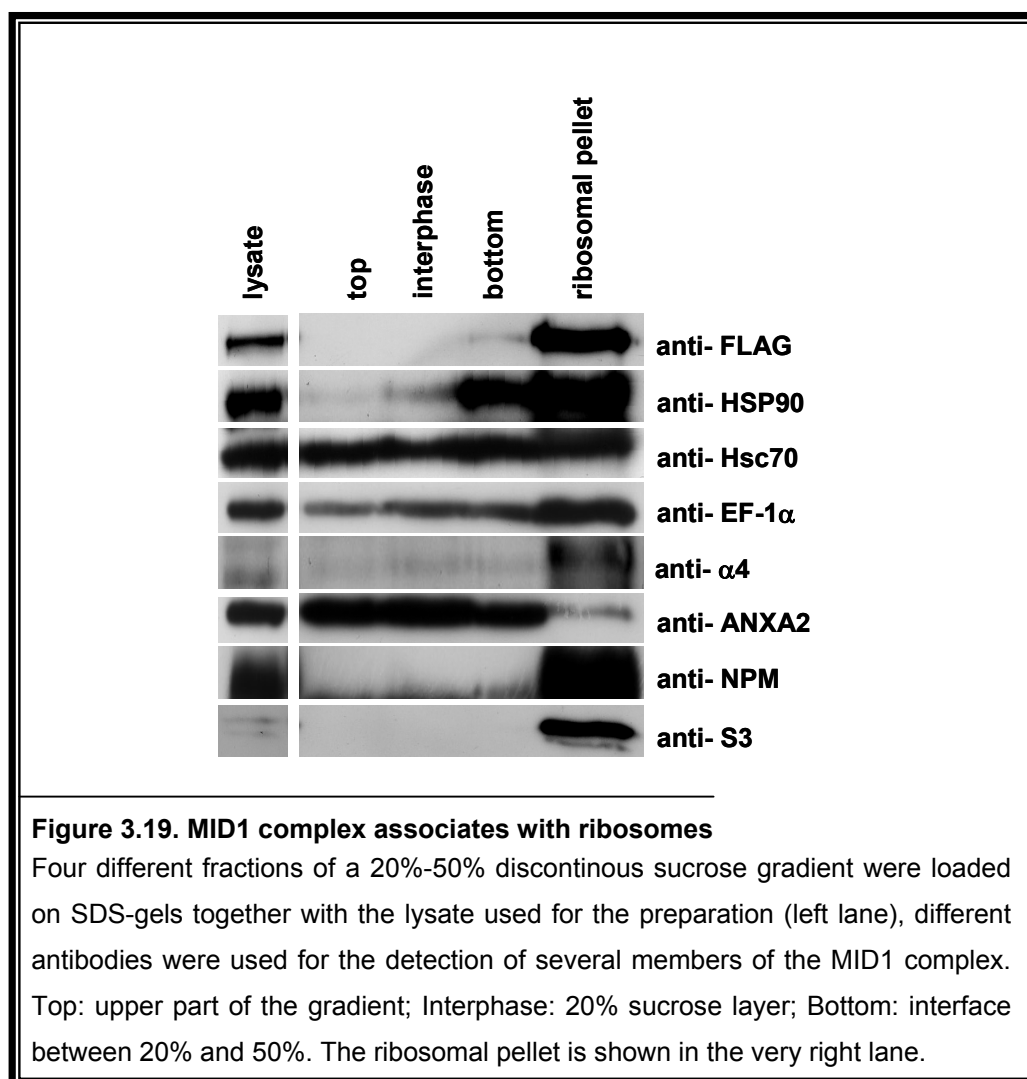
While only background binding was observed in the control sample (Figure 3.18, right



lane), clear co-immunoprecipitation of L5 and MID1-FLAG was seen in FLAG-MID1 overexpressing HeLa cells (Figure 18, left lane). This result confirms the association of the MID1 protein complex with both ribosomal subunits.

3.2.7 MID1 associates with intact ribosomes

Previous experiments strongly indicated that the MID1 complex associates with ribosomes. To further characterise this association, HeLa cytosolic extracts overexpressing MID1-FLAG were run through discontinuous sucrose gradients (20%-50%) by ultracentrifugation in a fix-angle rotor to, consequently, separate the ribosomal fraction from the rest. Four distinct fractions of the resulting gradient were studied on Western blots developed with antibodies corresponding to the different members of MID1 complex. The first fraction was the top of the gradient with no sucrose, the second was the 20% sucrose layer, the third was the interface between the 20% and the 50% layer, and the ribosomal pellet resolved in urea and SDS containing magic-mix (see Method section) was the fourth fraction. The lysate was additionally loaded on the SDS gel.



As shown in Figure 3.19, Hsp90, Hsc70, EF-1 α , NPM, ANXA2, α 4 and MID1-FLAG co-sediment in the ribosomal pellet, which is indicated by the presence of the ribosomal protein S3, another a member of the complex. However, not all the members of the complex showed the same affinity. α 4, the best-characterised MID1 interaction partner, was mainly found in the ribosomal pellet together with MID1 and NPM. Other members of the complex, such as Hsc70, Hsp90 and EF-1 α , were found in all the fractions, indicating that probably only a pool of those proteins associate with the MID1 complex and the ribosome. Interestingly, only small amounts of ANXA2 were found in the ribosomal pellet, which could be due to Ca^{2+} dependency of ANXA2 properties. All experiments described were performed under cold-shock conditions, so that microtubules remained depolymerised and could not pellet with the ribosomal fraction.

3.2.8 MID1 forms part of a ribonucleoprotein complex

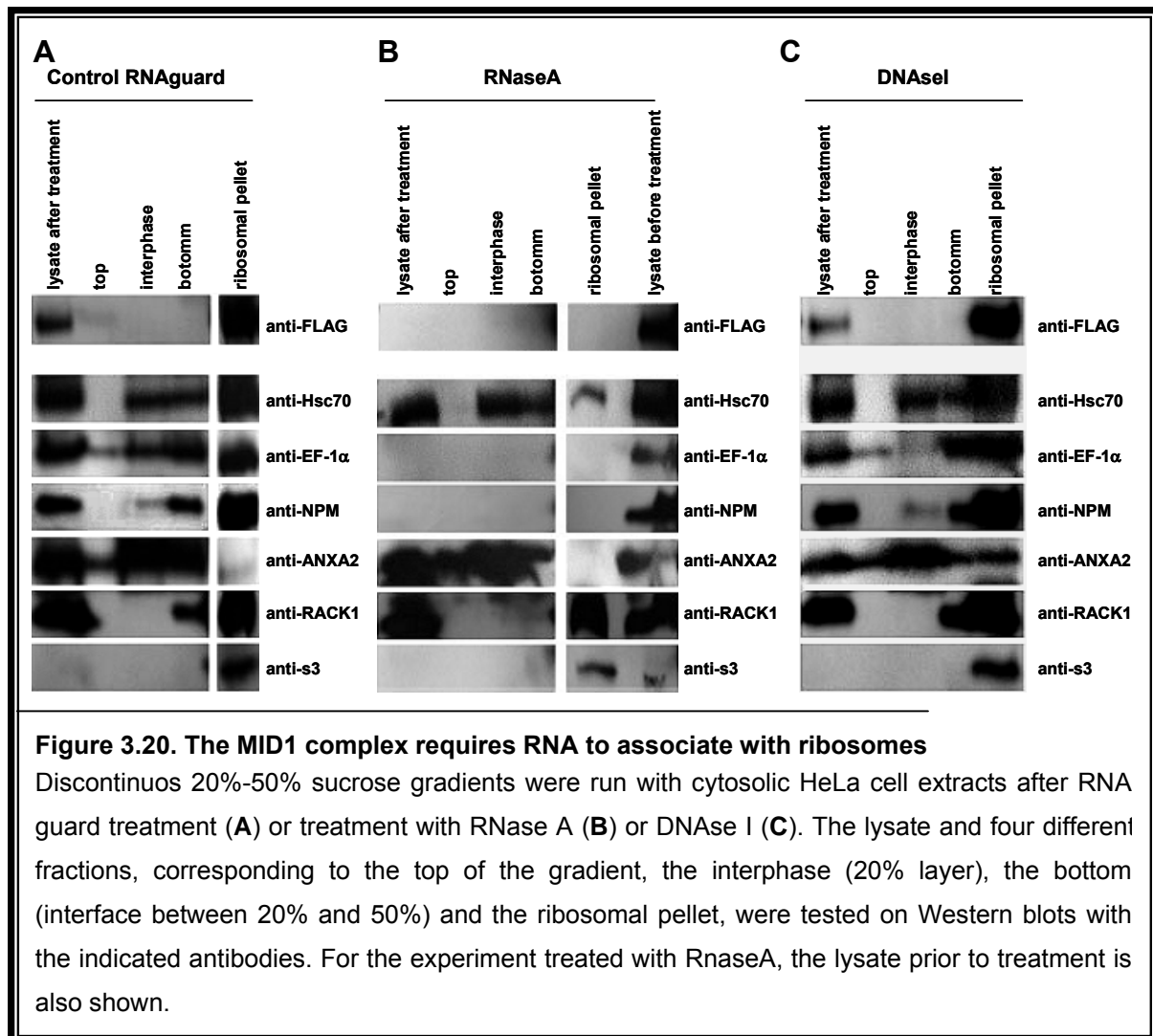
Taking together that the MID1 complex associates with ribosomes and that some of the identified proteins are RNA binding protein or closely related to RNA (namely NPM, ANXA2,

RACK1), it was reasonable to think that the MID1 complex could be the core of a ribonucleoprotein (RNP) complex, composed of proteins and RNA.

To test this possibility, the influence of RNA on the association of the MID1 complex with ribosomes was assayed by running discontinuous 20%-50% sucrose gradients in a fixed-angle rotor with MID1-FLAG overexpressing cytosolic extracts, which were pre-treated with RNaseA, DnaseI or RNaguard (RNase inhibitor). Subsequently, Western blots of the different fractions (same as before) were incubated with the panel of antibodies recognizing the respective members of the complex. S3 was used again as marker of the ribosomal fraction.

While in the presence of RNaguard MID1-FLAG associated with ribosomes (Figure 3.20A), after treatment with RNaseA, MID1-FLAG could not sediment with the ribosomal fraction anymore (Figure 3.20B). Surprisingly, in spite of the presence of a cocktail of protease inhibitors in the sample, MID1 also disappeared from the lysate. Given that it was present in the lysate before treatment, this suggests that MID1 is not stable without RNA. Probably it precipitated or was degraded by proteases that were not inhibited by the used cocktail (Complete mini, see methods section) and that only can access the protein when it is not bound to RNA. On the other hand, DNaseI treatment (Figure 3.20C) did not affect MID1 stability or ribosome association.

EF-1 α and NPM, proteins of the complex closely related to ribosomes, showed a pattern similar to MID1-FLAG. Before RNaseA treatment they were present in the lysate, and after treatment, they disappeared and, consequently, were not found in the ribosomal pellet (Figure 3.20B). Other proteins like Hsc70 and ANXA2, while being present in the lysate after RNase treatment, they lost their association to the ribosomal pellet in the absence of RNA (Figure 3.20B). As expected, neither RNaseA nor DNaseI treatment affected the sedimentation properties of integral components of the ribosomes, such as RACK1 and S3 (Figure 3.20B, lanes 6,7).

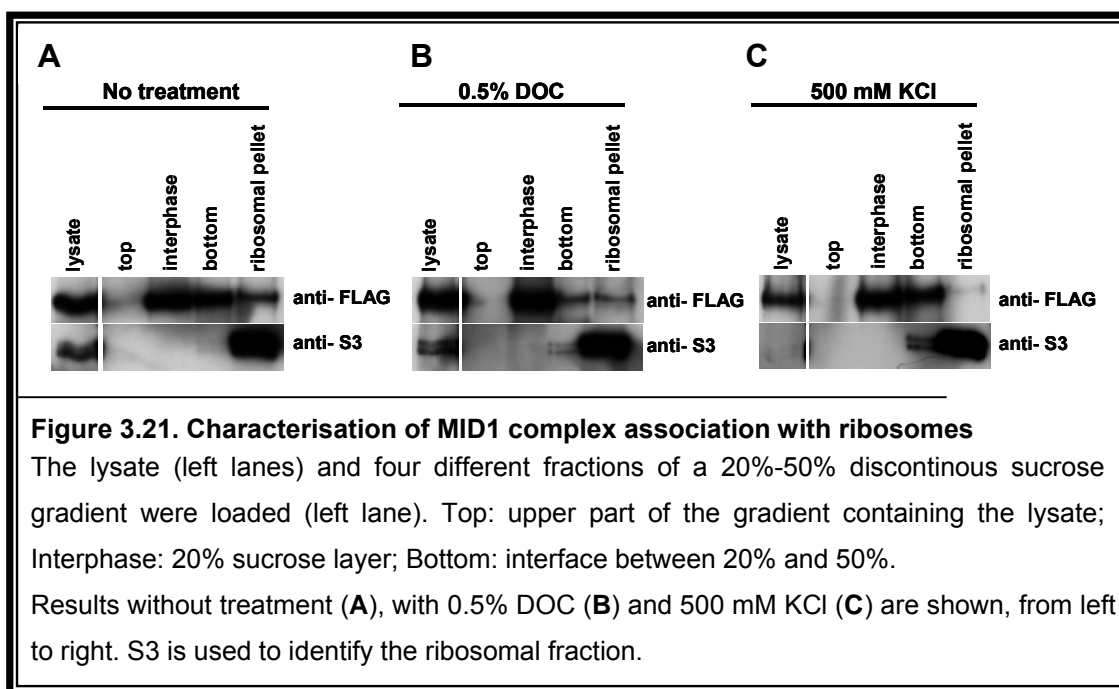


3.2.9 Characterisation of the association of MID1-FLAG with ribosomes

Having shown that the MID1 complex associates with ribosomes in an RNA-dependent manner, a battery of different conditions were tested to further characterise this association. Thus, discontinuous sucrose gradients were run, this time using a swing-out rotor in order to allow a more precise definition of the different phases.

3.2.9.1 Salt and detergent treatments

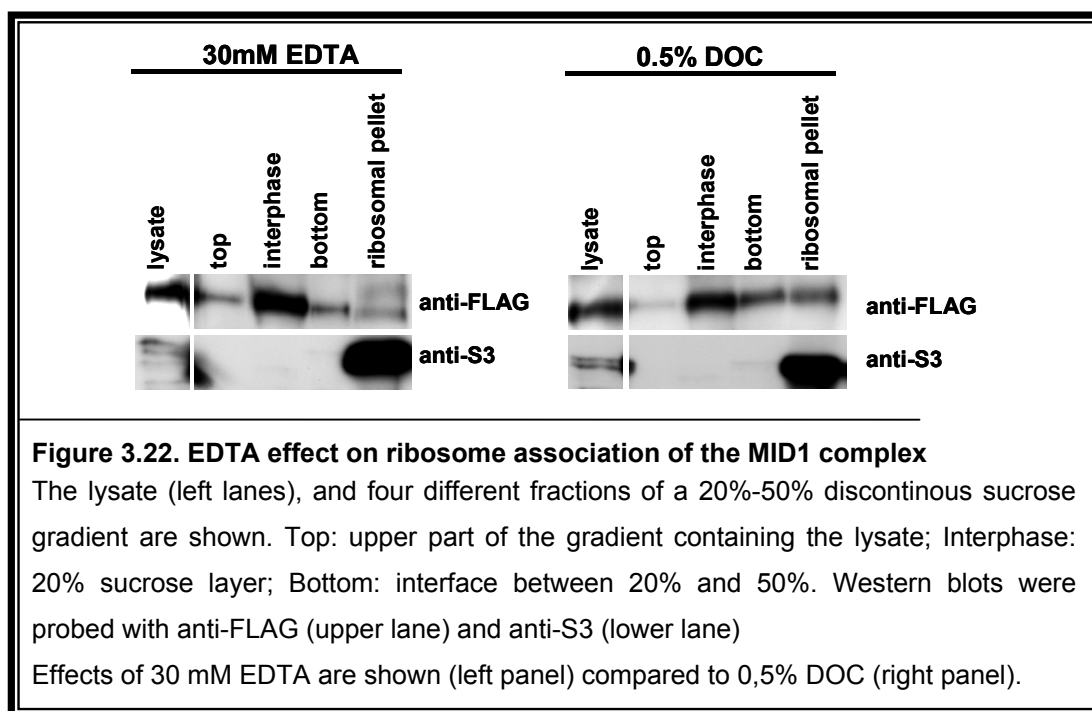
In order to analyse if the MID1 complex association to ribosomes is influenced by salt or detergent, cytoplasmic extracts of HeLa cells overexpressing MID1-FLAG were treated with 0.5 mM KCl or 0.5% deoxycholate (DOC). Same fractions were studied as previously described on Western blots developed with anti-FLAG antibody.



Again, without treatment, MID1-FLAG sediments with S3 in the ribosomal pellet (Figure 3.21A). However, the better definition of the phases, due to a slower sedimentation process in the swing-out rotor, leads to a major retention of MID1-FLAG in the different fractions. After addition of 0.5% DOC (Figure 3.21B) or 500 mM KCl (Figure 3.21C) to the cytosolic extracts, most of MID-FLAG was washed off from the ribosomal pellet. Of note, KCl had stronger consequences than DOC.

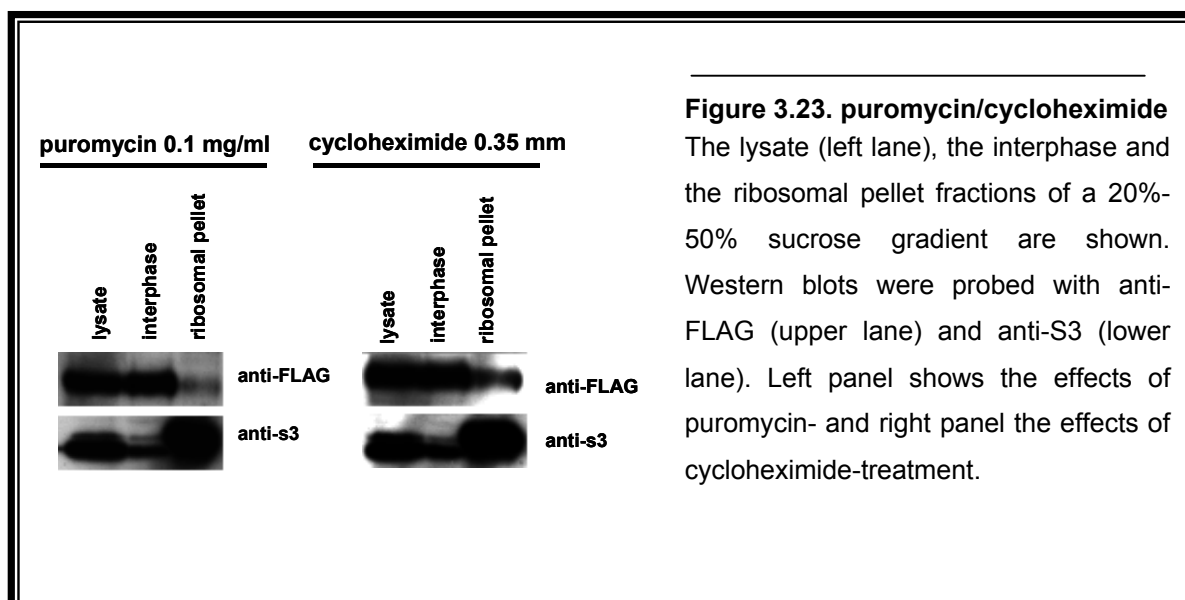
3.2.9.2 EDTA treatment

For further characterisation, HeLa cell lysates were treated with EDTA, which destroys ribosome integrity, and compared to detergent treatment. In contrast to S3, which as an integral component of the small ribosomal subunit remained in the ribosomal pellet, EDTA presence lead to dissociation of MID1-FLAG from the ribosomes (Figure 3.22). This indicates that active ribosomes are necessary for association with MID1-FLAG.



3.2.9.3 Puromycin and cycloheximide treatments

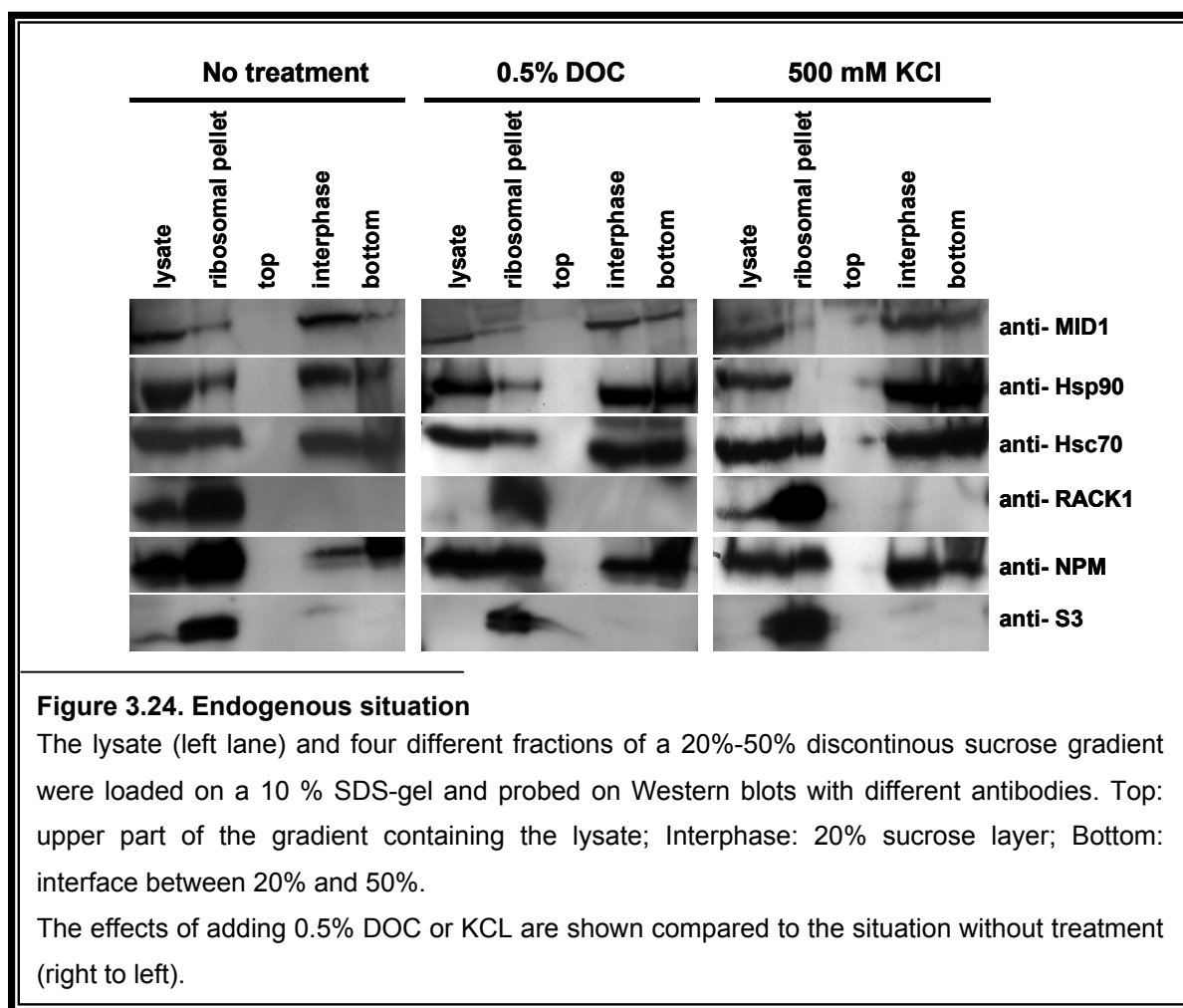
Finally, effects of puromycin compared to cycloheximide were likewise examined. While puromycin provokes the disassembly of the ribosomes from RNA leading to disruption of polyribosomes, cycloheximide stops translation by blocking polyribosome run-off. Same experiments as before were done but, in order to reduce complexity, only the interphase, the lysate and the ribosomal pellet were examined.



As predicted, cycloheximide treatment preserved the association of MID1-FLAG with the ribosomal fraction (Figure 3.23). In contrast, puromycin caused dissociation, indicating that the MID1 complex associates with active polyribosomes and that their disruption leads to MID1 dissociation from the ribosomal fraction.

3.2.10. Endogenous MID1 and other components of the complex associate with ribosomes

Having established MID1-FLAG association with ribosomes, the endogenous situation was analysed and this time, additional members of the MID1 complex were included in the study. Same procedure as before with a swing-out rotor, and KCl and DOC treatments, was followed, but this time HeLa cell extracts did not contain MID1-FLAG.



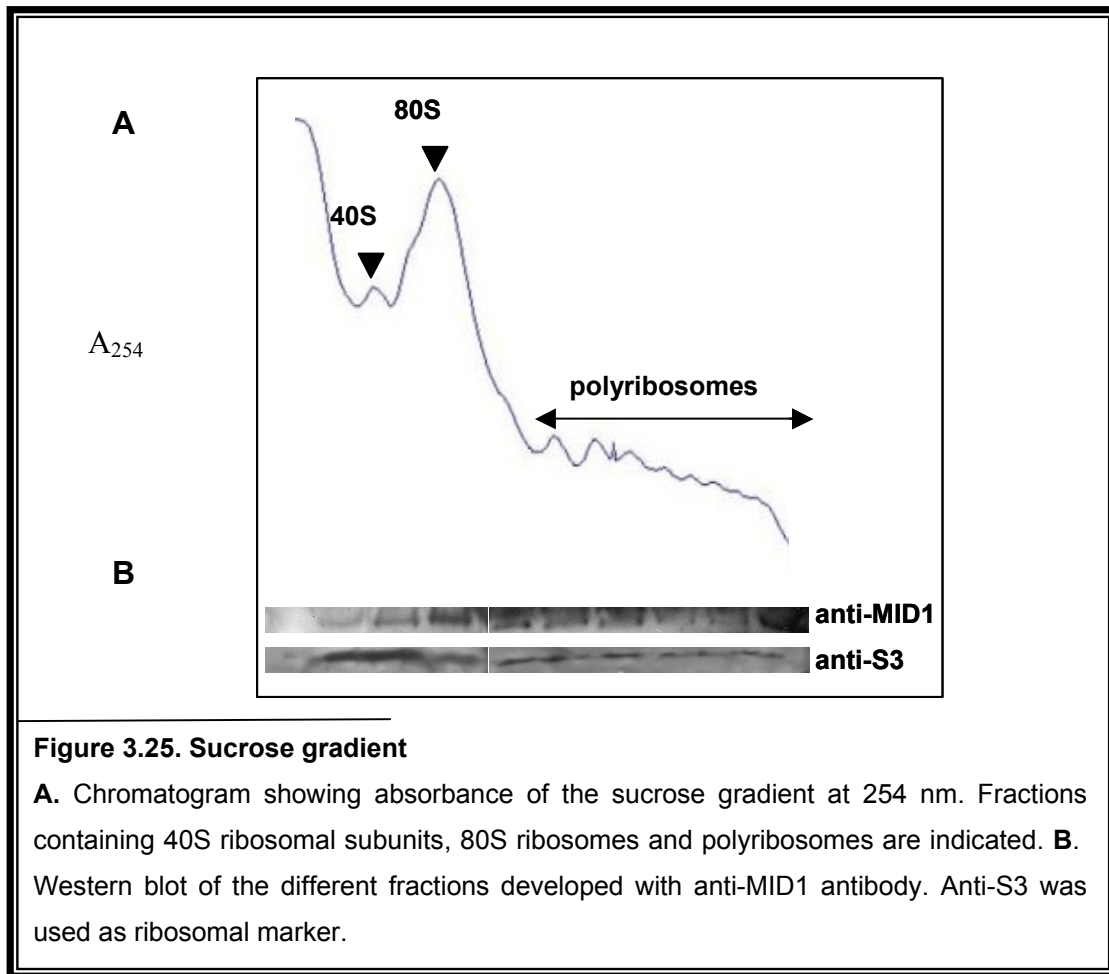
As shown in Figure 3.24, endogenous MID1 associates with ribosomes (tracked by the presence of S3) similar to overexpressed MID1-FLAG (Figure 3.24) and, accordingly, DOC and KCl (Figure 3.24, middle and right panels) washed off the protein from ribosomes, with KCl exhibiting a stronger influence. Interestingly, not all the complex components showed the same sedimentation properties in the gradient after salt and detergent treatment. While Hsp90 was washed off from the ribosomes with KCl, and partly with DOC, Hsc70 sedimentation properties were not affected under any of the experimental conditions tested. Some other members of the complex such as NPM and RACK1 are closely related to ribosomes and, as expected, their association with the ribosomal fraction was not affected with any of the treatments (Figure 3.24).

3.2.11 MID1 associates with polyribosomes

In section 3.2.9, it was shown that disruption of polyribosomes with puromycin or disassembly of ribosomal subunits with EDTA leads to dissociation of MID1 from the ribosomal fraction, suggesting that the MID1 complex associates not only with active ribosomes but also with active polyribosomes. To verify this, HeLa extracts were run through a continuous 15%-45% sucrose gradient in an SW40 swing-out rotor. Fractions were collected while measuring RNA absorbance at 254 nm, indicative of ribosomes or polyribosomes presence, precipitated, and analysed by Western blots incubated with anti-MID1 and with anti-S3, as a ribosomal marker.

The first peak of the chromatogram (Figure 3.25A) from the left corresponds to the top of the gradient, which contains the lightest ribosomal subunit, 40S. The next big peak corresponds to the entire ribosome, 80S. The big subunit, 60S, is found overlapping with 80S as a little deviation of the peak to the left. The last fractions of the gradient contain polyribosomes; at least eight peaks corresponding to different amounts of associated ribosomal monomers are observed.

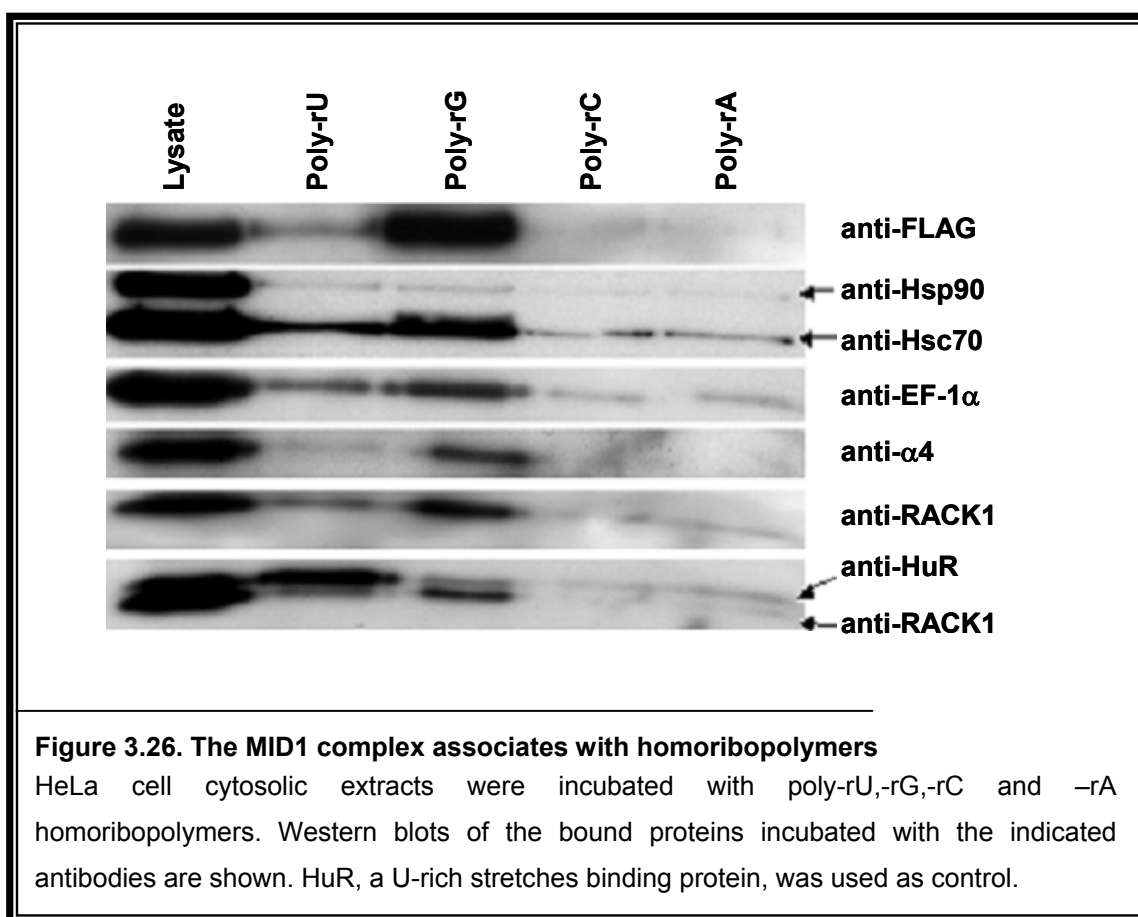
S3 was again used as a ribosomal marker. Co-sedimentation of the two proteins, MID1 and S3 throughout in all fractions of the gradient could be observed (Figure 3.25), confirming that MID1 had gone through the entire gradient (Figure 3.25). Consequently, it could be demonstrated that the MID1 complex associates with active polyribosomes and forms a big ribonucleic protein complex (RNPs).



3.2.12 MID1 associates with homoribopolymers

Knowing that the MID1 complex associates with ribosomes in an RNA dependent manner (section 3.2.8) and that some members of the complex, such as ANXA2, bind directly to RNA (Filipenko et al., 2004), a possible direct interaction between the MID1 complex and RNA was studied.

A classic way to assay RNA binding properties of a protein is to test it for interaction with homoribopolymers. Some to date well-established RNA binding proteins like Fragile mental retardation protein (FMRP), ANXA2 or poly(A)-binding protein have been thereby characterised (Brown et al., 1998; Burd et al., 1991; Filipenko et al., 2004). Likewise, the MID1 protein complex was analysed for RNA binding properties. Following standard procedures, cytosolic HeLa cell extracts overexpressing MID1-FLAG were incubated with homoribopolymers - rU, rG, rA and rC. After extensive washing, bound proteins were boiled off and analysed on Western blots with a panel of antibodies detecting the respective proteins of the complex. Incubation of the membrane with anti-HuR antibody, a protein known to interact with U-rich stretches (Lopez de Silanes et al., 2004), was used as control to confirm the specificity of the reaction.



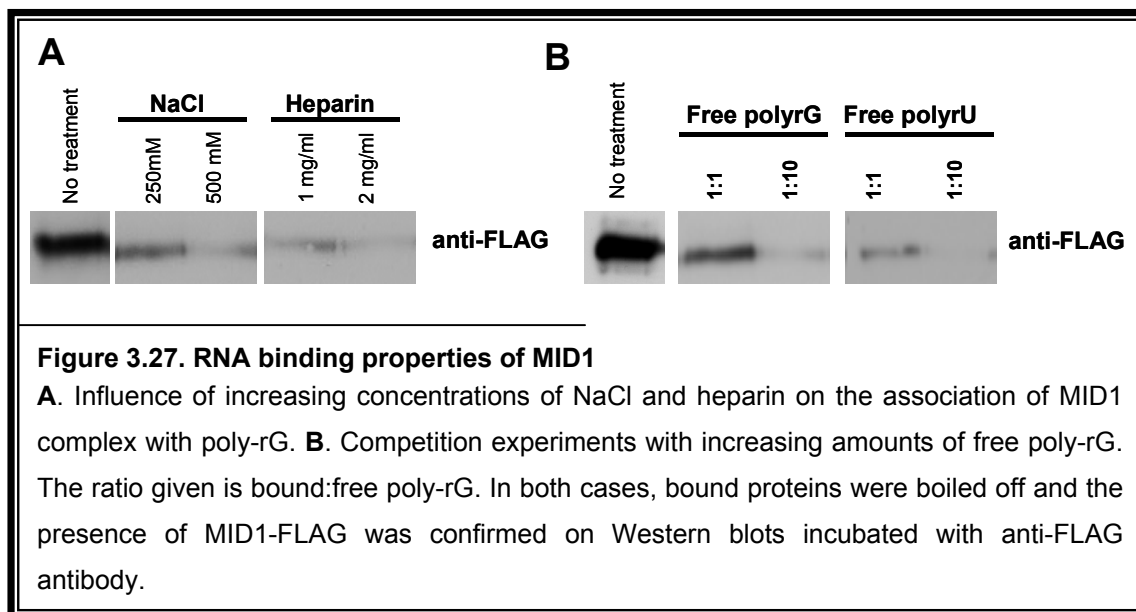
Specific bands corresponding to FLAG-MID1, Hsp90, Hsc70, EF-1 α and RACK1 were detected in the rG-homopolymer- (Figure 3.26) and, although much weaker, in the rU-homopolymer sample. As expected, HuR showed a stronger binding to poly-rU homoribopolymers, confirming the specificity of the interaction.

3.2.13 Characterisation of the Poly-rG-MID1 binding

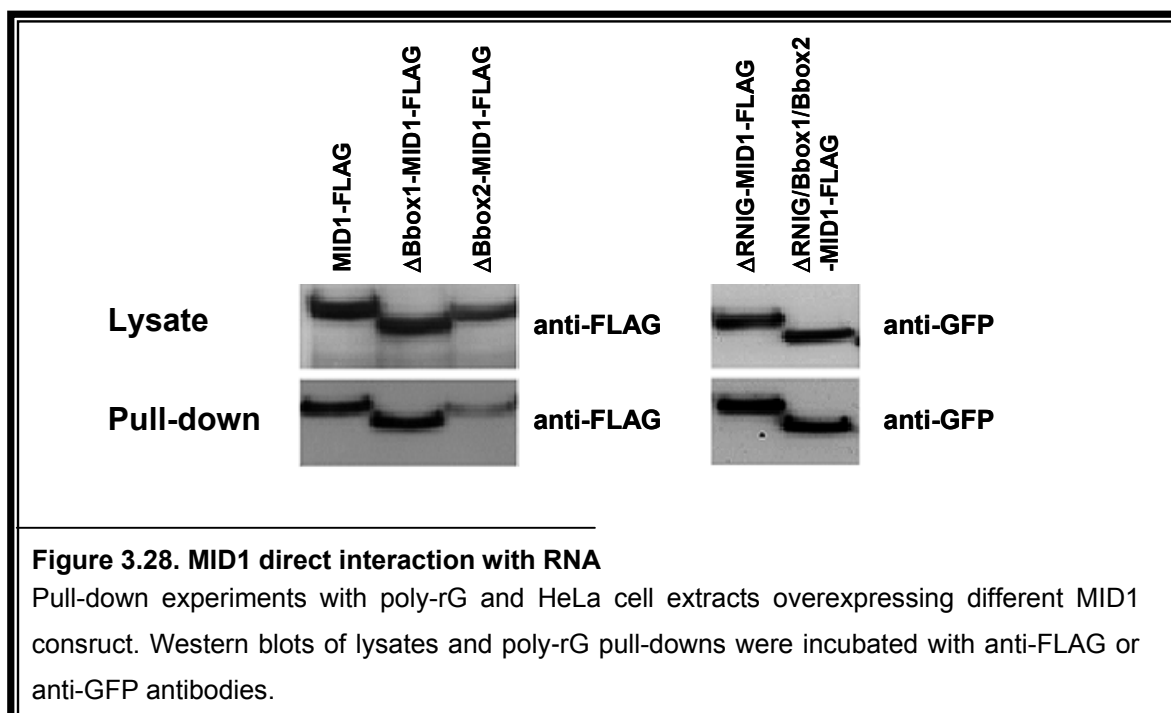
In order to characterise the interaction of the MID1 complex with poly-rG, a series of different experimental conditions was tested. Increasing amounts of NaCl and heparin were used to check the resistance of the interaction to ionic forces. Competition assays by increasing amounts of free poly-rG and free poly-rU were also performed.

Although much weaker compared to the non-treated control, MID1-FLAG could still associate to poly-rG in the presence of 250 mM NaCl and 1 mg/ml heparin (Figure 3.27A), increasing NaCl concentration up to 500 mM and heparin up to 2 mg/ml destroyed almost the entire interaction.

Competition experiments with free poly-rG and polyrU confirmed the specificity of the reaction between the MID1 complex and immobilized homopolymers. As shown in Figure 3.27B, addition of free poly-rG or free poly-rU 1:1 already produced a notable decrease of the interaction with agarose bound poly-rG. The addition of free homoribopolymers 1:10 led to almost total disruption of the association on the MID1 complex to bound poly-rG.



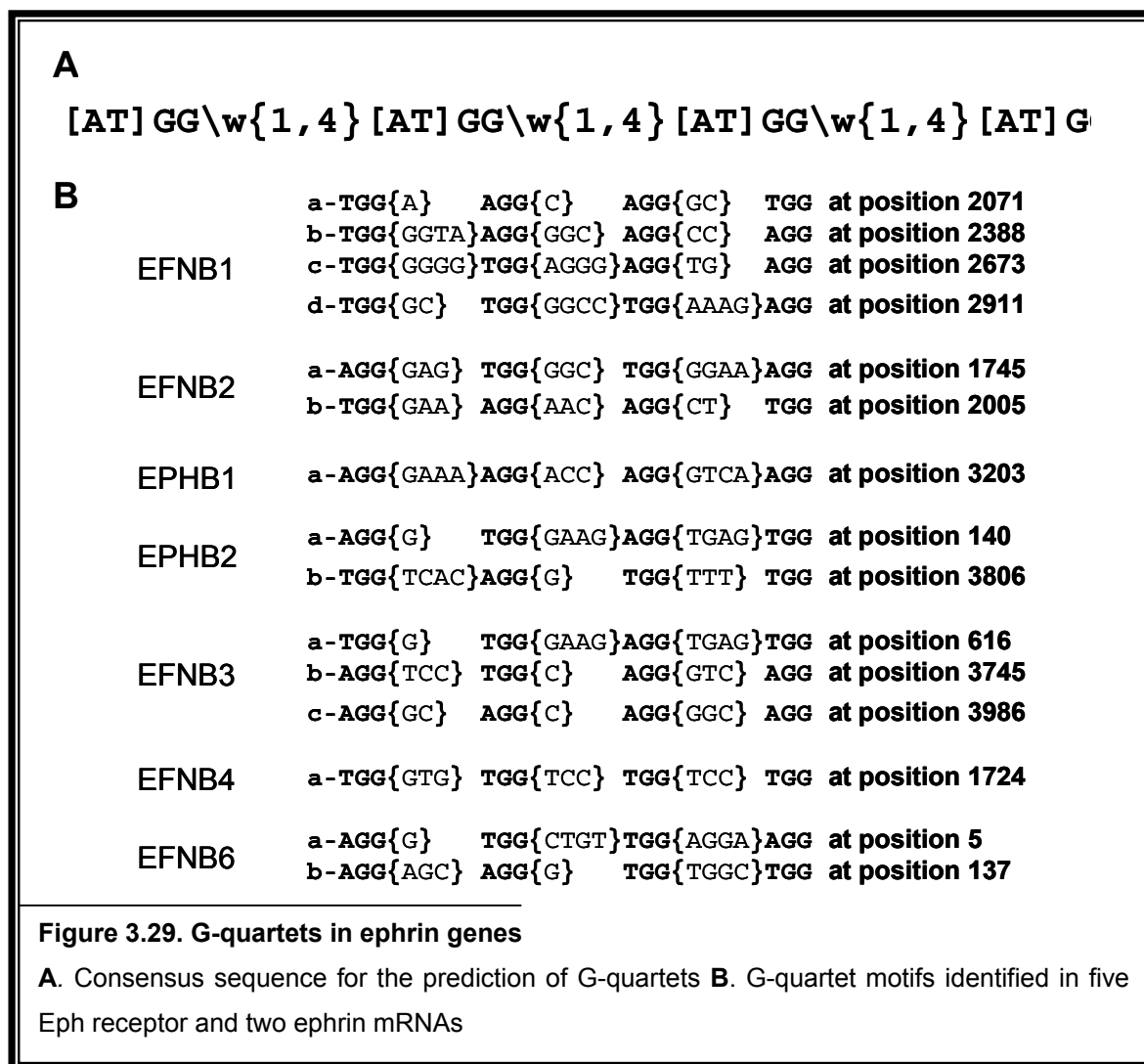
In order to test if the zinc-binding protein domains of MID1, RING and/or Bboxes, are involved in the association of the protein complex with RNA, cell extracts of HeLa cells overexpressing MID1-FLAG, FLAG-tagged constructs lacking Bbox1 or Bbox2 and GFP-tagged constructs with MID1 lacking either the RING-finger domain or the RING-finger and both Bboxes were incubated with poly-rG homoribopolymers. As described above, after extensive washing bound proteins were boiled off and analysed by Western blotting with anti-FLAG or anti-GFP antibodies.



All mutant MID1 proteins associated with poly-rG stretches, (Figure 3.28), showing that neither the RING-finger nor the Bboxes are directly involved in the association of the MID1 complex with RNA.

3.2.14 MID1 complex binds ephrin mRNA via G-quartet structures

In order to get an idea of specific mRNAs that might be associated to the MID1 complex described, a candidate strategy applying phenotype and protein function comparisons was used. As outlined earlier, patients with craniofrontonasal dysplasia present with mutations in the ephrin-B1 gene (*EFNB1*), a member of the ephrin family of proteins (Twigg et al., 2004; Wieland et al., 2004). The phenotype of this patients highly resembles facial features of patients with OS. The remarkable phenotypic overlap of the two syndromes, plus a functional overlap of ephrins and MID1 during NCC migration, makes ephrins attractive candidates to be related to the MID1/ α 4 complex. Specifically, as the MID1/ α 4 complex might play a role in localising RNAs to distinct subcompartments of the cell, it is reasonable to consider the mRNAs of Eph receptor and ligand genes as potential targets of this complex. Given that the MID1 protein complex had been shown to bind poly-rG, EphB receptor and ephrin-B mRNAs were screened for the presence of G-quartets, which are G-rich motifs that were first described in mRNA targets of the fragile X mental retardation protein (FMRP) complex and that have been shown to be responsible for RNA localisation. Based on G-quartet sequences described in the literature (Brown et al., 2001; Darnell et al., 2001; Ramos et al., 2003) combined with re-analysis of known target genes of FMRP (Brown et al., 2001; Kaytor and Orr, 2001), a consensus sequence for the prediction of G-quartet structures was extracted (Figure 3.29A). Based on Bioperl regular expressions, an algorithm for the prediction of such mRNA structures was made in collaboration with the bioinformatics department at Max Planck Institute for Molecular Genetics (<http://genereg.molgen.mpg.de/cgi-bin/regEchse/regEchse.pl>). Following this algorithm, EphB receptor and ephrin-B mRNAs, as well as the 3' and 5'UTR of all genes available in the ENSEMBL database, were scanned for the presence of putative G-quartets.



In two ephrins, six G-quartet like structures were identified, EFNB1a-d and EFNB2a, b (Figure 3.29B). To note, in *EFNB1*, the gene mutated in patients with craniofrontonasal dysplasia, four G-quartet like structures were spotted. Moreover, nine different G-quartet like structures were found in five different Eph receptors, EPBH1, EPBH2a,b, EPBH3a-c, EPBH4 and EPBH6a,b (Figure 3.29B). Interestingly, while one or more G-quartets were found in either the 5' or 3' UTR in 22% of all genes from the ENSEMBL database, only 1,33% of the analysed genes contained more than three G-quartets (Table2).

| Number of G-quartet motifs | 1 | 2 | 3 | >3 | Total found |
|--|------|------|-----|-----|-------------|
| 3' UTR | 3053 | 1128 | 443 | 357 | 4981 |
| 5' UTR | 1342 | 235 | 66 | 51 | 1694 |
| Total number of genes searched : 30686 | | | | | 6675 |

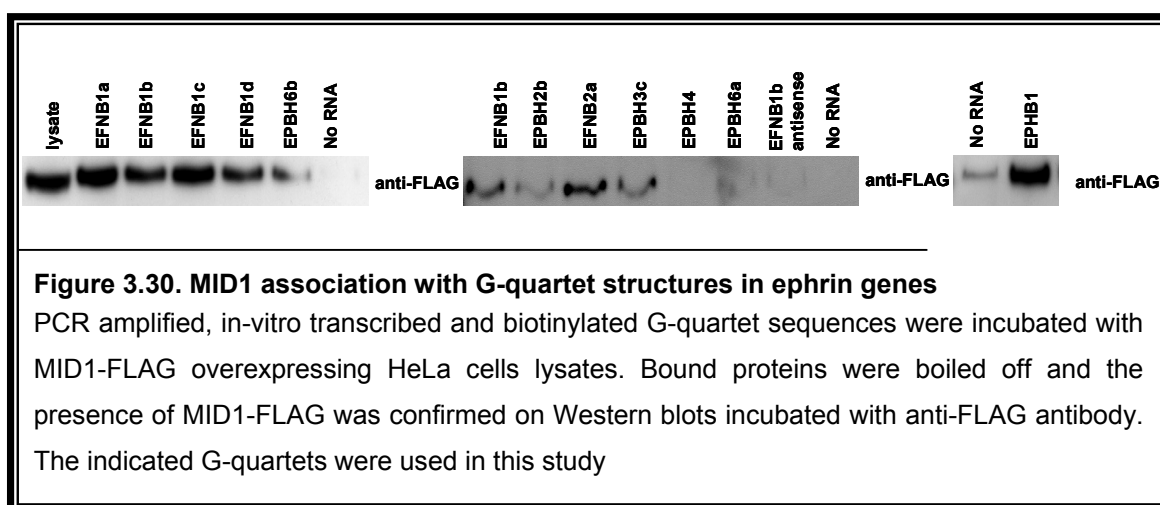
Table 3.2. G-quartet predictions

Number of 3' or 5' UTRs containing varying numbers (1, 2, 3 or >3) of G-quartet structures from a set of 30686 genes available in ENSEMBL.

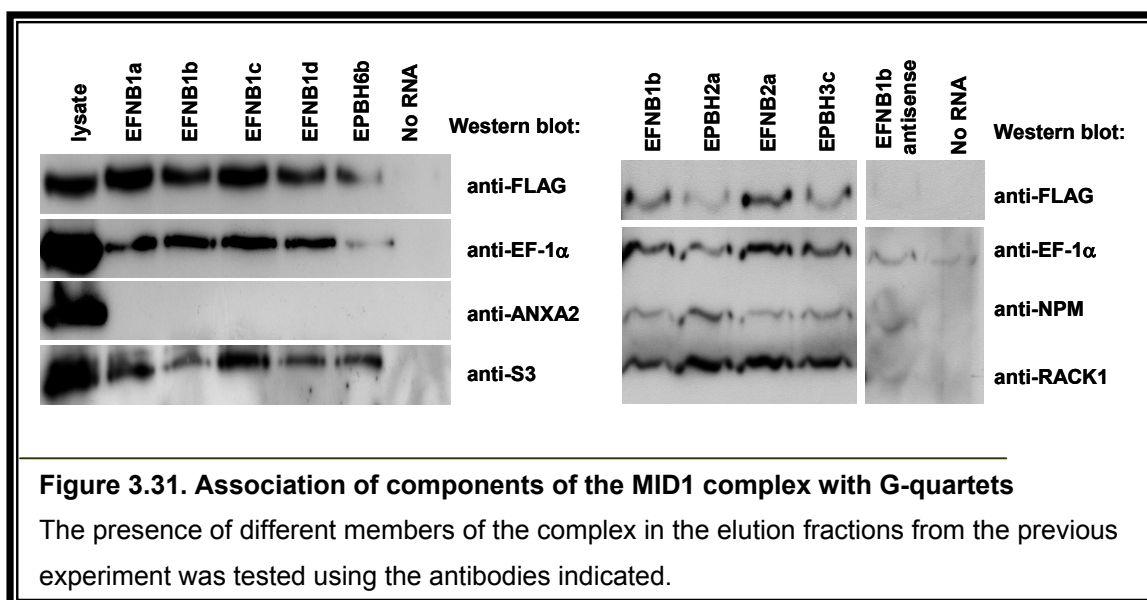
3.2.15 Binding of the G-quartets to the MID1 Complex

Subsequent to identification of G-quartet like structures in the ephrin genes, it was tested whether these structures indeed associate with the MID1 complex. Some of the identified G-quartet motifs were PCR amplified with primers including the T7 promotor sequence at the 5' end. Primer sequences were chosen such that approximately fifty base pairs were flanking both ends of the G-quartet in order to allow proper folding of the structure. Obtained PCR products were purified and *in vitro* transcribed in the presence of biotinylated-UTP. Subsequently, the transcripts were incubated with cytosolic extracts of HeLa cells overexpressing MID1-FLAG. Biotin transcripts were pulled down with streptavidin coated magnetic beads, and extensively washed. Bound proteins were finally boiled off and checked on Western blots that were probed with anti-FLAG antibody (Figure 3.30).

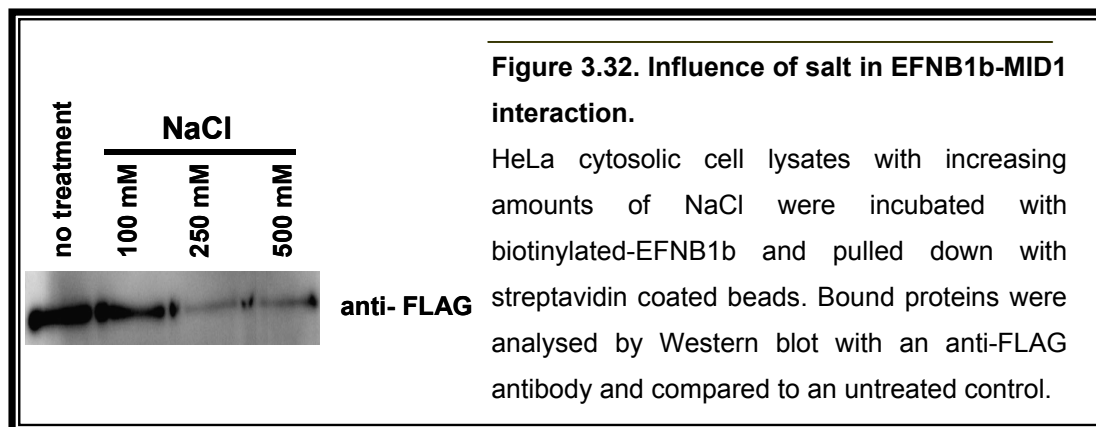
All four G-quartets of EFNB1 (EFNB1a-d), EFNB2a and motifs of several Eph receptors (EPBH6a, b, EPBH3c, EPBH2b and EPBH1) were tested for MID1 complex interaction (Figure 3.30). While most of them were confirmed to associate with MID1-FLAG (Figure 3.30), two of them, EPBH4 and EPBH6a, did not show association with MID1-FLAG. The specificity of the reaction could be further confirmed by controls done with the antisense sequence of one of the motifs, EFNB1b, or with a sample that did not contain RNA.



Posterior incubation of the blots with different antibodies allowed the study of other member of the complex. Thus, incubation with anti-EF-1 α , anti-NPM, anti-S3 and anti-RACK1 showed association of all of them to the G-quartets tested (Figure 3.31). Hsp90, a weaker interaction partner of the complex, and ANXA2, the RNA association of which has been described to be Ca²⁺ dependent, showed only background binding. Lysates were loaded to confirm the presence of all proteins.



One of the motifs, EFNB1b, was further characterised by studying the effect of salt on the interaction of G-quartets with MID1-FLAG. Same experiment as before was done but in the solution increasing amounts of salt were added (100-500 mM). A Western blot of the bound proteins probed with anti-FLAG antibody shows decrease in the EFNB1b-MID1 association with increasing amounts of salt, probing the specificity of the interaction (Figure 3.32).

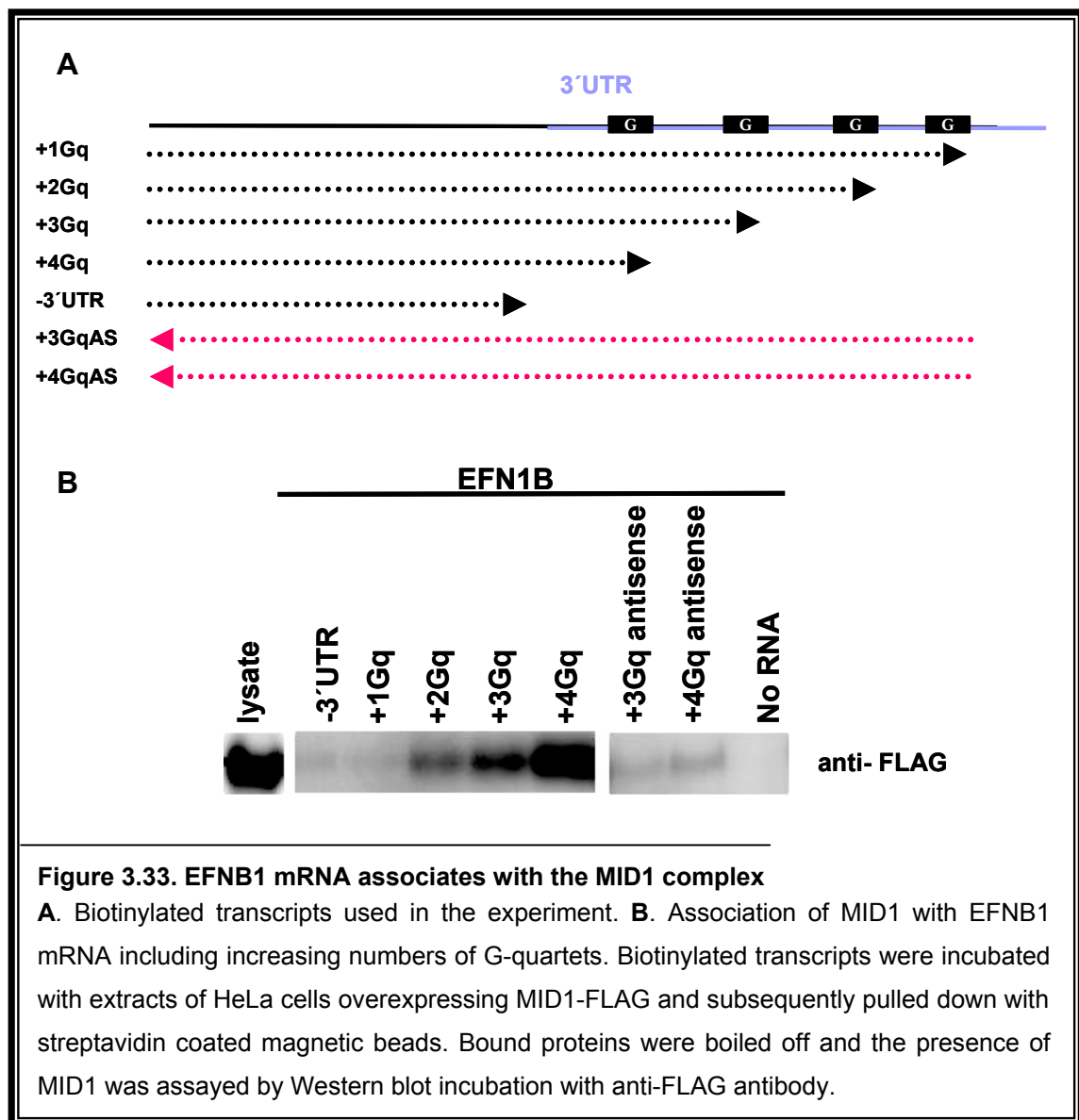


3.2.16 MID1 complex associates with EFNB1 mRNA

Finally, it was studied whether the MID1 complex associates with the entire mRNA of EFNB1, including the G-quartet containing 3'UTR. In addition, biotinylated transcripts containing none, one (+1Gq), two (+2Gq), three (+3Gq) or all four G-quartets (+4Gq) (Figure 3.33A) were analysed. Two antisense transcripts containing three (+3GqAS) and four (antisense) G-quartets (+4GqAS) and a sample without RNA were used as negative control.

Biotinylated transcripts were incubated with extracts of HeLa cells overexpressing MID1-FLAG and subsequently pulled down with streptavidin-coated beads. After washing, bound

proteins were boiled off, and the presence of MID1-FLAG was tested by Western blot analysis with anti-FLAG antibody. As shown in Figure 3.33B, MID1-FLAG associated with G-quartet containing transcripts in an additive manner; that is, the probe having a single G-quartet present almost no association to MID1, and the binding increased with increasing numbers of G-quartets. Maximal binding was obtained in the sample with four G-quartets. As expected, the probe without the 3'UTR did not bind to the MID1 complex, similarly to the sample without RNA. None of the antisense transcripts, which corresponded to the longest probes, showed any binding to the MID1 complex. This demonstrated that the reason for the additive effect is not the increasing length of the transcripts but the specific association of the MID1 complex to G-quartets.



4 Discussion

The RBCC protein MID1, which is involved in ventral midline development, has been shown to form a macromolecular cellular complex, whose components were, up to now, mainly unknown. Several domains of the MID1 protein are putative protein–protein interaction domains that potentially contribute to the formation of this complex. However, apart from their participation in protein binding, no other function could be assigned to them so far. In order to shed light on the functions exerted by some of the domains of MID1, both Bboxes were characterised during this thesis. These studies allowed the identification of a novel pathomechanism for the development of OS.

In addition, after identifying the MID1 complex partners via affinity chromatography and mass spectrometry (MS), the MID1 protein was characterised as the core of a novel translation unit that associates with microtubules. Therefore a new panel of functions for the MID1 protein was introduced.

4.1 A novel pathomechanism for OS caused by mutations in the Bboxes domains of MID1

In a broader context, Bboxes have been shown to play an important role for the correct positioning of RBCC proteins within the cell and to participate in protein-protein interactions (Cao et al., 1997; Reymond et al., 2001). Determining the solution structure of the Bbox of XNF7 in *Xenopus* revealed a novel zinc-binding fold; however, no functional clues could be deduced from this structure. In this thesis, the basic functions Bbox1 and Bbox2 of the RBCC protein MID1 were elucidated and, in addition, the dependence of Bbox1 function on an intact Bbox2 *in vivo* was described.

Recently, we showed that the microtubule-associated MID1 protein targets the pool of microtubule-associated PP2A towards ubiquitin specific modification and degradation. This can only be achieved after bringing the catalytic subunit of PP2A into close proximity to the MID1 RING finger domain via the $\alpha 4$ protein as adapter. MID1 mutations causing OS are mostly clustered in the C-terminal end of the protein and lead to disruption of microtubule-association of MID1, which then forms clumps in the cytosol and, therefore, leads to accumulation of PP2Ac at the microtubules. We could further show that the binding of $\alpha 4$ takes place through the Bbox1 of MID1 and that the cytoplasmic clumps consisting of C-terminally mutant MID1 harbour, in addition, $\alpha 4$ tightly bound to Bbox1 (Schweiger and Schneider, 2003; Trockenbacher et al., 2001).

In this thesis, two novel mutations in the Bbox1 region of MID1, namely A130T and C145S, both causing full-blown OS were described. Several lines of evidence indicate that these mutations specifically compromise the protein-protein interaction interface between MID1 and $\alpha 4$ without producing major changes in the overall structure of MID1. Mutations in the Bbox1 domain of MID1 seem not to disturb the structure of the entire protein, which can still perfectly bind to microtubules. In addition, circular dichroism (CD) spectra of intact and A130T mutated Bbox1 have shown no significant differences in their overall structure (R. Schneider, unpublished data). However, when examining the interaction with $\alpha 4$, it becomes obvious that mutations in this domain generate a MID1 form that is unable to bind $\alpha 4$. Hence, while Bbox1 mutated MID1 associates to microtubules, co-expressed $\alpha 4$ remains evenly distributed in the cell, can not be pulled down by MID1-immunoprecipitation and does not interact with MID1 in yeast two-hybrid experiments. Homology modelling of the MID1 Bbox1 structure based on the XNF7 structure shows that the respective leucine corresponding to A130 (Figure 4.1, underlined) is on the surface of Bbox1, intriguingly located at the bottom of a hydrophobic pocket (Borden et al., 1995b). This suggests that $\alpha 4$ might bind MID1 via this pocket, and that the exchange of the small hydrophobic alanine to the more bulky and slightly hydrophilic threonine could severely interfere with correct high binding affinity between $\alpha 4$ and MID1. On the other hand, using the same XNF7 model, residue C145 would participate in zinc binding. Since the ability to bind zinc is critical to maintain a native 3D structure of a protein, an exchange of the excellent metal ligand cysteine into a serine, would hinder the interaction between $\alpha 4$ and MID1. This change probably interferes with the correct folding of the domain and presentation of the hydrophobic core to $\alpha 4$, despite not having major apparent effects on the structure of the entire MID1, as it appears intact in immunofluorescence experiments.

| |
|--|
| C ¹¹⁹ QFC ¹²² DQDPAQDA <u>V</u> TK C ¹³⁷ VT C EVSY C ¹⁴² DE C ¹⁴⁵ LKAT H ¹⁵⁰ PNKKPFTG H ¹⁵⁸ MID1-Bbox1 |
| C ⁶ SEH ⁹ DERLKLY C ¹⁷ KDDGTL S ²⁵ VI C ²⁸ RDSL H ³⁴ AS H ³⁷ XN F7-Bbox |
| C ¹⁷⁵ LE H ¹⁷⁸ EDEKVNMY C ¹⁸⁷ VTDDQLI C ¹⁹⁵ AL C ¹⁹⁸ KLVGR H ²⁰⁵ RD H ²⁰⁸ MID1-Bbox2 |

Figure 4.1. Homology with XNF7 Bbox

Comparison of Bbox1- and Bbox2-MID1 sequences with Bbox-XNF7 sequence. Conserved cysteines and histidines including their positions are indicated in bold. A130 in Bbox1 is underlined. Zinc binding residues are indicated in red (Borden et al., 1995b). C139 and corresponding aspartic acid are indicated in blue.

Although yeast two-hybrid experiments with MID1 deletion constructs clearly indicated that exclusively Bbox1 is responsible for the binding to $\alpha 4$ (Trockenbacher et al., 2001), further analysis of Bbox2 mutations revealed that there is a clear regulatory influence of the Bbox2 on the interaction between $\alpha 4$ and MID1 *in vivo*. During this thesis, the study of a MID1-Bbox2 mutation (C195F), which has been found in an OS patient and affects a conserved residue (Figure 4.1), by immunofluorescence showed loss of MID1 colocalisation with microtubules and complete failure to bind $\alpha 4$ *in vivo*. However, immunoprecipitation and yeast two-hybrid experiments showed that $\alpha 4$ -binding *in vitro* remains intact, which points at specific intracellular conditions that are mediated by the Bbox2 and are disturbed by this mutation.

Interestingly, when the study was extended to different engineered mutations, it was observed that the influence of Bbox2 mutations on *in vivo* binding abilities of MID1 change with the character of the particular mutation. While mutations disturbing conserved amino acids (Figure 4.1, amino acids in bold) hamper MID1 association with microtubules and $\alpha 4$, mutations affecting non-conserved amino acids only disrupt MID1 interaction with $\alpha 4$. These differences can probably be explained by more severe effects that some amino acid exchanges have on the global structure of the protein.

Most of the conserved residues included in this study, apart from being conserved, were supposed to participate in zinc binding, as predicted by comparative analysis with the XNF7 Bbox (C175, H178 and C198, marked in red in Figure 4.1). In C175A, H178Y or C198A mutated MID1, the unfair trade of a metal ligand residue, such as cysteine or histidine, for a residue unable to bind metal atoms, such as alanine or tyrosine, is likely to affect the correct stability and folding of the domain. Consequently, the disturbance of the overall structure of MID1 due to mutations in these residues denotes that intact zinc-binding plays a highly important role in the *in vivo* function of the Bbox2, as it appears not only to regulate $\alpha 4$ -MID1 interaction, but also to influence the correct folding and positioning of the entire protein.

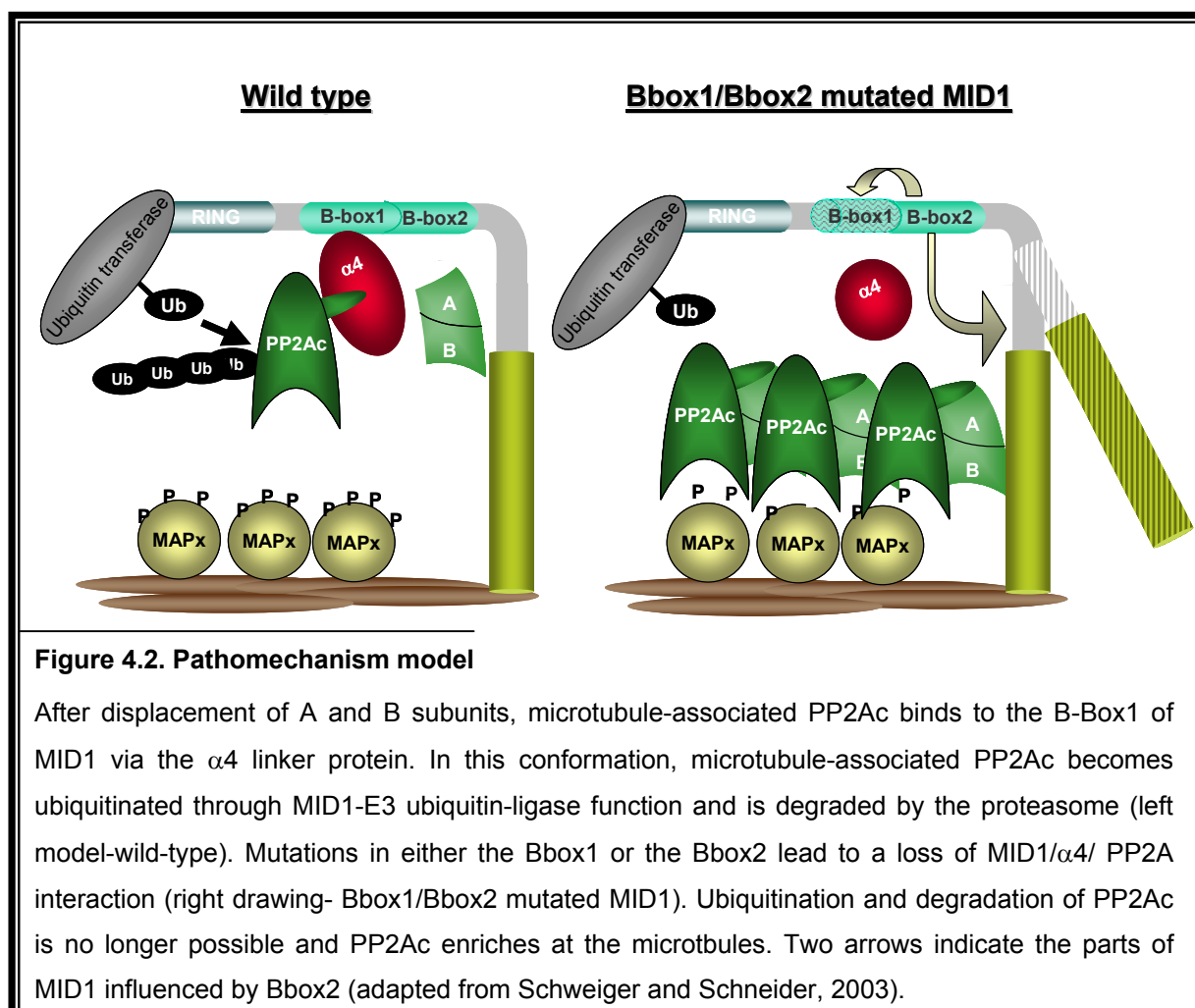
Nevertheless, the C195F mutation, despite not affecting a known zinc-binding site in Bbox2 residue, had similar drastic consequences as the above described mutations. It has been previously suggested that the conserved region between this cysteine and C187, which forms a flexible loop, composes another divalent metal binding site that involves interaction with another domain (Borden, 1998; Borden et al., 1995b). Given that the Bbox1 also contains some unligated putative metal ligands, such as C134, C139 or C142, it could well be that both domains cooperate to bind a zinc ion (Figure 4.1). Such an arrangement would also explain the strong influence that mutations in the Bbox2 domain exert on Bbox1 protein binding.

Mutations affecting non conserved residues on the other hand, such as Q192R or V183T, only affect the interaction of MID1 with $\alpha 4$ but not with the microtubules, which is another conspicuous indication of the close relation of the two Bboxes, and evidences the high

importance of an intact Bbox2 for the proper functioning of Bbox1, even when the protein is correctly folded and positioned.

Interestingly, mutations in a zinc-binding ligand in Bbox1, such as C145S, seem not to have similar drastic consequences on the global structure of the entire MID1. This might be due to an extra cysteine at position 139 of Bbox1 that has also been proposed to participate in zinc binding (Borden et al., 1995b; Reymond et al., 2001). This cysteine is commonly conserved in Bbox1 domains along RBCC proteins, while the Bbox2 and the XNF7-Bbox have a conserved aspartic acid at that position (Figure 4.1, blue residues). Therefore, this residue could further stabilise the structure of this domain, and of the entire protein (Borden et al., 1995b), and would keep effects of a C145 mutation mild.

In summary, during this thesis it could be shown that the Bbox2 domain acts as a flexible regulatory junction that provides the different domains of MID1 with their proper relative disposition, thus linking different components necessary for the MID1-ubiquitin ligase function. This would explain why *in vitro* experiments, which do not present the steric effects encountered in an *in vivo* system, allow the interaction of MID1 constructs having an intact $\alpha 4$ -binding interface in Bbox1, despite having mutations in Bbox2. Further, they describe a novel



pathomechanism for the development of Opitz BBB/G syndrome in patients with mutations in either the Bbox1 or the Bbox2 (Figure 4.2). In both cases, loss of interaction with $\alpha 4$ seems to be crucial, fact that once again underlines the importance of this protein as a linker between PP2Ac and the ubiquitin ligase MID1 (Schweiger and Schneider, 2003; Trockenbacher et al., 2001).

4.2 The MID1 multiprotein complex

4.2.1 MID1 forms part of a ribonucleoprotein complex

In addition to its previously identified association with tubulin (Schweiger et al., 1999), during this thesis it was found by affinity chromatography and MS, and subsequently verified by immunoprecipitation, that the MID1 complex includes several ribosomal proteins of the small subunit (S3, S8). Several other proteins that are also closely related to ribosome function namely EF-1 α , NPM, RACK1 and p40, were found as well (Filipenko et al., 2004; Ford et al., 1999; Nilsson et al., 2004; Okuwaki et al., 2002; Tarapore et al., 2006; Vedeler and Hollas, 2000) in the protein complex. ANXA2 was also identified within the MID1 complex, fact that further supports a role for the MID1 complex at the ribosome (Filipenko et al., 2004; Vedeler and Hollas, 2000). Moreover, several heat shock proteins, Hsp90, Hsc70 and Hsc60 were identified in the complex, together with another multifunctional chaperone protein, p32 (Storz et al., 2000). Among these heat shock proteins, special attention should be drawn to Hsp90. Besides assisting protein folding, and in contrast to other heat shock proteins, Hsp90 is known for having many different substrates or “clients” and facilitating their functions (Richter and Buchner, 2001). Interestingly, it has been shown this year that Hsp90 also regulates ribosomal function by protecting several ribosomal proteins including S3 (novel component of the MID1 complex) and S6 (a downstream factor of the TOR pathway, to which the MID1 complex is related (Schweiger and Schneider, 2003)), from ubiquitination and proteasome dependent degradation, thereby regulating their stability and activity (Kim et al., 2006).

Association of MID1 complex with the big ribosomal subunit, 60S, was confirmed by immunoprecipitation experiments. Following, MID1 complex association with the entire ribosome was confirmed and characterised by discontinuous sucrose gradients. Different experimental conditions demonstrated it to be a stable association, which was only disrupted by high concentrations of salt or by substances that cause ribosomal disruption, such as EDTA or puromycin. Some other members of the complex such as RACK1 or NPM (Nilsson et al., 2004; Okuwaki et al., 2002), which are known to be more closely related to ribosomes, remained bound under all conditions tested. However, although an interaction of the MID1 complex with ribosomes could be demonstrated, it remains unclear whether MID1 itself associates directly or through any of the previously reported ribosome-related proteins.

Similar to other well-characterised proteins forming RNPs, such as FMRP (Tamanini et al., 1996), RNase A treatment prior to gradient loading demonstrated that the association of the MID1 complex with ribosomes is RNA-dependent. In addition, association of the complex to poly-rG ribopolymers and G-quartet like RNA structures in Eph receptor and ephrin mRNAs could be proven in this thesis. Since direct association of MID1 through its zinc-binding domains with RNA could not be confirmed and MID1 does not contain any of the known RNA binding domain, MID1 most probably incorporates RNA into the complex through any of the RNA-binding proteins of the complex or through an RNA helicase that has been found previously to interact with MID1 in a yeast two-hybrid screen (R. Schneider, unpublished data).

4.2.2 The components of the MID1 complex associate with microtubules

In agreement with MID1 association with microtubules (Schweiger et al., 1999), most of the novel members of the MID1 complex could be found in microtubule fractions, pointing to an important function of the complex exerted at the microtubules. Supporting this hypothesis, the majority of the proteins identified in the MID1 complex have previously been reported to associate with microtubules. Thus, EF-1 α , one of the most abundant proteins, has been reported to participate in the compartmentalisation of protein translation at the cytoskeleton (Condeelis, 1995). In addition, it has been shown to be a microtubule-associated protein that binds, stabilises and promotes assembly of microtubules *in vitro*, independently of its role in protein translation (Moore and Cyr, 2000; Moore et al., 1998; Ohta et al., 1990; Shiina et al., 1994).

Hsp90, another abundant cytosolic protein, and several Hsc70 homologues have also been found to localise at microtubules (Czar et al., 1996; Liang and MacRae, 1997). Since some of its clients need to be transported in the cell as a prerequisite to carry out their function, Hsp90 has been proposed to participate in microtubule-based movements (Craig et al., 1994). Moreover, it has been shown to be a component of the main microtubule organizing centre (MOTC), the centrosome, ensuring its correct functioning, including microtubules nucleation and centrosome duplication (de Carcer, 2004; de Carcer et al., 2001; Doxsey, 2001; Lange et al., 2000). Similarly, NPM has been found to participate in centrosome duplication upon phosphorylation by CDK2/cyclin E on Thr¹⁹⁹ (Okuda, 2002; Tokuyama et al., 2001). In addition, it participates in a variety of mitotic processes, upon phosphorylation of Ser⁴ through polo-like kinase1 (Plk1), the major mitotic regulator kinase (de Carcer, 2004; Zhang et al., 2004).

ANXA2 and RACK1 have also been shown to exert some of their functions in collaboration with the cytoskeleton. ANXA2 is the most abundant protein in fractions containing cytoskeleton-bound polysomes (Vedeler and Hollas, 2000), and RACK1 was found to reside in cytoskeleton fractions from unstimulated fibroblasts and epithelial cells (Hermanto et al., 2002).

The fact that many of the proteins identified in the MID1 complex have previously been localized to microtubules, in addition to their ribosomal function, appears to be of outstanding significance for the putative function of the complex. This implies that the MID1 complex, including PP2A and $\alpha 4$, could well be the core of a microtubule-associated translation unit that carries active polysomes and RNA.

4.2.3 The MID1 complex and its role in translation at the microtubules

RNPs are often described as functional venues that carry pre-mRNAs and mRNAs in the cell. Proteins participating in these complexes mostly exercise functions on mRNA export, localisation, translation and stability. At the same time, contained mRNAs need to have mRNA localisation signals, which are commonly situated in the 3'UTR, where they are the least likely to interfere with any other function. In addition, RNPs are highly dynamic complexes, in which their components, usually fulfilling a large variety of functions, come and go, responding to the necessities of the complex at a given moment (reviewed in Dreyfuss et al., 2002; Mohr and Richter, 2001; St Johnston, 2005). A central function of RNPs is the active transport along the cytoskeleton in order to ensure asymmetric mRNA localisation in the cell. Some of the best-studied systems in which asymmetric RNA localisation has been reported to be fundamental are oocyte polarisation, embryonic axis formation (Bashirullah et al., 1998; Driever and Nusslein-Volhard, 1988; Lasko, 1999; Lehmann and Nusslein-Volhard, 1986), and local protein synthesis in dendrites and growth cones (Steward and Schuman, 2003; Steward and Worley, 2001).

FMRP, mutated in patients with Fragile X syndrome (FXS, one of the most frequent causes of mental retardation), is a well-established example of an RNP in charge of translation and mRNA transport along the cytoskeleton in neurons (Antar et al., 2004; Bagni and Greenough, 2005; Zalfa and Bagni, 2005). A subset of brain mRNAs, including EF-1 α (Sung et al., 2003), has been identified to associate with FMRP-containing RNPs (Brown et al., 1998; Sung et al., 2000; Zalfa et al., 2003). In addition, its association with polyribosomes and subsequent link with translation has also repeatedly been reported (Ceman et al., 1999; Feng et al., 1997; Tamanini et al., 1996; Zalfa and Bagni, 2005).

Another RNA-binding protein, Staufén, also forms an RNP complex with transport-cargo properties along the cytoskeleton. It has been in-depth studied for its role in mRNA trafficking and translation in *Drosophila*, where it plays an essential role in the localisation of *oskar* and *bicoid* mRNAs in the oocyte to the posterior and anterior poles respectively (Li et al., 1997; St Johnston, 2005). In mammals, the two homologues of Staufén, have also been shown to form RNPs, to associate with polyribosomes, and to participate in microtubule-dependent transport of RNA in neurons (Kanai et al., 2004; Kiebler et al., 1999; Tang et al., 2001b; Thomas et al., 2005). Interestingly, it has been recently reported to co-immunoprecipitate with FMRP, EF-1 α ,

nucleolin, tubulin, protein phosphatase 1, HuR and RNA helicase A (Thomas et al., 2005; Villace et al., 2004), showing that mammalian Staufen is closely related to the previously described FMRP-RNP.

After having characterised the MID1 complex, it is striking noticeable its properties resemble many of the characteristics required to be a RNP in charge of transport along microtubules, supporting a novel model for the function of the MID1 complex (Figure 4.3). Similar to FMRP and Staufen, the MID1 complex associates with polyribosomes, the translation related protein EF-1 α , several multifunctional proteins, microtubules and RNA. Moreover, PP2A and its regulatory subunit, $\alpha 4$, are also main components of the complex, which integrate the MID1 complex into the TOR pathway, one of the main translation regulatory pathways (Schweiger and Schneider, 2003). However, MID1 has never been found in the nucleus, where the target mRNAs to be transported should be recruited, which suggests that any of the other members of the complex would bring the mRNAs from the nucleus to the microtubules. An attractive candidate would be NPM, which binds RNA, is involved in ribosome biogenesis, and has been shown to shuttle between the nucleus and the cytosol.

A required motor protein, which would allow the movement of the MID1 complex along the microtubules remains to be identified.

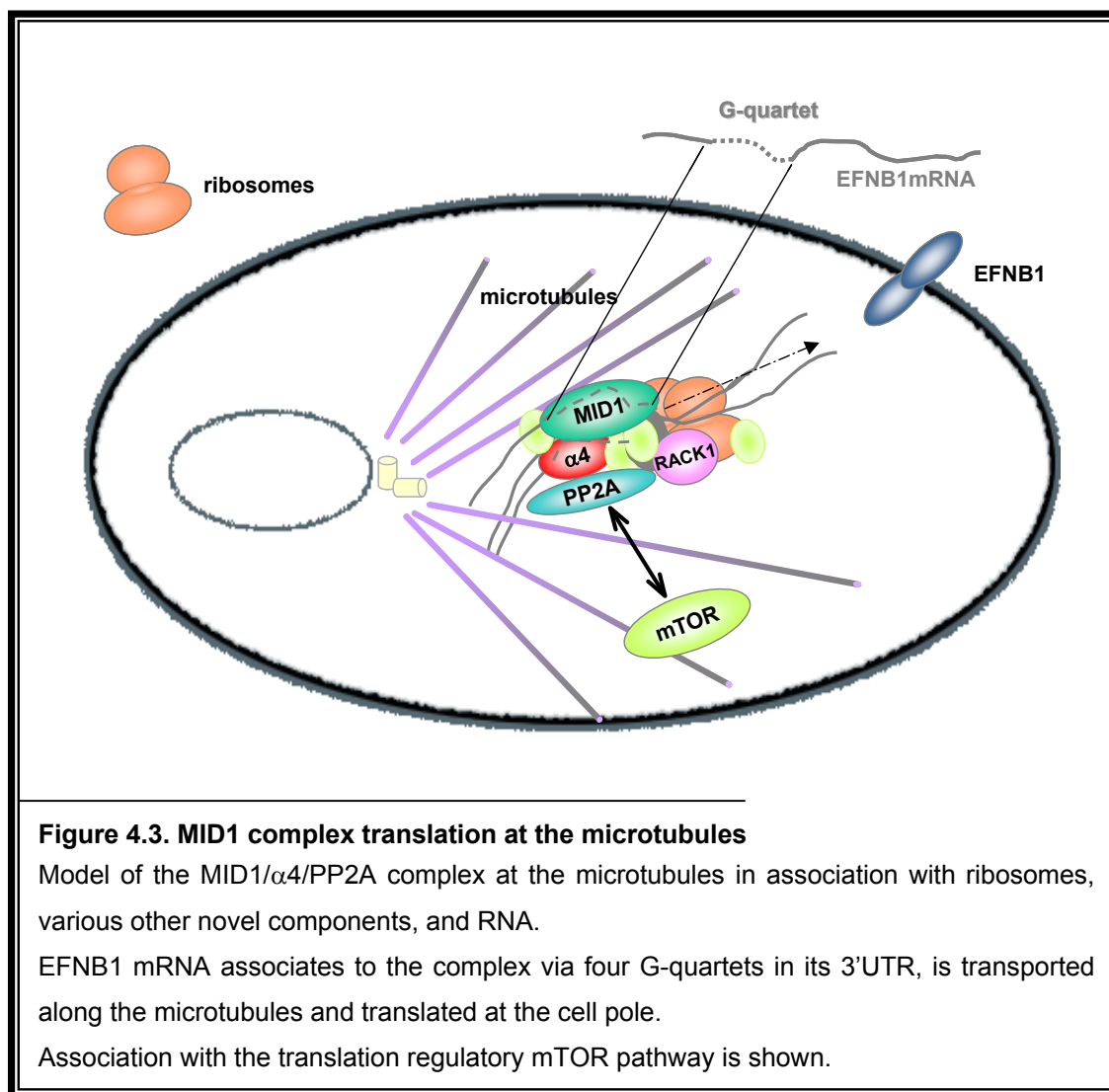
4.2.4 The MID1 complex and translational repression

For the successful completion of mRNA localisation and compartmentalisation of protein production in the cell, the translation of the transported mRNAs needs to be repressed during transport and until their protein functions are required. Although little is known about the mechanisms governing translational repression during transport, some processes have been already described (St Johnston, 2005).

For example, in *Drosophila* oocytes and early embryos, translation of the anteriorly localised *bicoid* mRNA transcripts is regulated by delayed cytoplasmic polyadenylation of the respective mRNAs, which formerly carry a very short poly(A) tail incompatible with efficient protein translation. A more complicated process that has been described for mRNAs localised to the posterior pole, such as *oskar*, involves the binding of the translation repressor Bruno to *cis*-elements in its 3'UTR while the transcript is being transported to the pole and, once there, Bruno falls off and translation is derepressed. However, in recent years, the role of RNA silencing in translational repression as a novel mechanism for translational repression has gained attention. At least two genes that encode components of the RNA silencing pathway, namely *aubergine* and *armitage* (involved in microtubule polarisation), have been implicated in the localisation of *oskar* transcripts (Kavi et al., 2005; Kloc and Etkin, 2005; Wilhelm and Smibert, 2005). Similar mechanisms for the regulation of translation have been attributed to the FMRP protein, which has been shown to associate with non-coding RNAs (ncRNA) and

microRNAs (miRNA) that contain sequences complementary to FMRP target mRNAs and thereby, represses their translation (Jin et al., 2004a; Jin et al., 2004b; Zalfa et al., 2005).

During this thesis, it was described an interaction of a microtubule-associated translation unit with PP2A and its negative regulators $\alpha 4$ and MID1, all essential players of the mTOR pathway, that regulates the translation of selected capped and 5'TOP mRNAs (Duvel and Broach, 2004; Fingar and Blenis, 2004; Peterson et al., 1999). Selective up-regulation of PP2A activity at low MID1/ $\alpha 4$ levels or activities during transport could therefore be another mechanism of translational inhibition in mRNPs (Figure 4.3). Interestingly, last year, it was reported that RACK1 mRNA contains a TOP motif and that its translation depends on a rapamycin-sensitive pathway, such as the mTOR pathway (Loreni et al., 2005). Since RACK1 is one of the complex components, this would suggest self-regulatory properties of the complex.



Nevertheless, it would also be interesting to know whether the MID1 complex carries any miRNAs or ncRNA that could assist the complex in regulating the translation of transported

mRNAs. In addition, the identification of mRNAs carried by the complex will also shed light on how the MID1 complex regulates the translation of its target mRNAs.

4.2.5 MID1 complex and development of the ventral midline development: implications in cell migration

As mentioned previously, improper function of the MID1 complex leads to X-linked OS, which is characterised by defective fusion of ventral midline structures, whose establishment heavily rely on polarised cells, including asymmetric distribution of signalling molecules and reorganization of the cytoskeleton. Two fundamental processes during midline development governed by this mechanism are NCC migration and EMT of epithelial cells (Jones and Trainor, 2005; Roessler and Muenke, 2001; Schweiger and Schneider, 2003). Dysfunctional transport of mRNA along the microtubule in defective MID1-containing RNPs would, as suggested in this thesis, inhibit asymmetric protein production in cells involved in these processes and therefore, would form the molecular basis for an attractive model for the development of OS.

Cell polarisation, adhesion and migration are fundamentally related processes that require the asymmetric concentration of cellular activities mediated by the cytoskeleton. Cell migration involves the formation of protrusions such as lamellipodia and filopodia at the leading edge of the cell, followed by nuclear translocation and retraction of the cell rear (Small and Kaverina, 2005). During migration, adhesion to the extracellular matrix, commonly mediated by integrins, needs to be carefully regulated for the cell to move properly. The family of small Rho GTPases has an essential role in the regulation of adhesion formation and cytoskeleton reorganization. Although cell migration has often been described in terms of actin cytoskeleton reorganization, already in 1970 it was shown that also the disruption of microtubules in fibroblasts leads to disruption of cell polarity and arrest of direct locomotion (Vasiliev et al., 1970). However, how actin and microtubule cytoskeletons collaborate to provide correct migration is only starting to be understood (Kole et al., 2005).

Microtubules are often discussed as cellular highways that transport signalling molecules to modulate the tension of the actin cytoskeleton and the disassembly of cell adhesions. They have been shown to meet actin at focal adhesions formed at the cell front and rear during migration and negatively regulate them by promoting their turnover or impeding their growth (Kaverina et al., 1999; Krylyshkina et al., 2003; Palazzo and Gundersen, 2002). In addition, active transport along the microtubules has been shown to be essential for cell migration; kinesin inhibition mimics the changes in cell polarisation and adhesion found during microtubule disruption with nocodazole (Kaverina et al., 1997; Krylyshkina et al., 2002). In addition, focal adhesions have microtubule-capturing and -stabilizing abilities that could help to prolong the communication of the microtubules with focal adhesions and thereby, allow the delivery of more signals (Kaverina et al., 1998).

Recently, novel adhesion structures have been defined, namely spreading initiation centres (SICs), which only appear in early stages of cell migration. Despite being highly similar to focal adhesions, they have been shown to also contain RNA, RNA-binding proteins and RACK1, one of the MID1/ α 4 interaction partners, supporting that asymmetric mRNA transport and compartmentalised protein translation of proteins is required for the formation of focal adhesions (de Hoog et al., 2004). In line, it has previously been shown that cytoskeleton dependent recruitment of mRNA and ribosomes to focal adhesions provides local synthesis of proteins in response to integrin-mediated signalling from the extracellular matrix and mechanical tension (Chicurel et al., 1998). According to these results, it has been proposed that not only molecular trafficking, but also translation, might be required in the early establishment of focal adhesions (Nilsson et al., 2004).

Knowing that the MID1 protein bundles and stabilize microtubules, a critical step for the organization of the leading edge (Schweiger et al., 1999), and that the MID1 complex, which contains RNA-binding proteins, ribosomes, RNA and RACK1, participates in mRNA localisation via microtubules, it is very appealing to think that it could also participate in the transport of mRNAs required for the formation and regulation of early focal adhesions or SICs. Moreover, the MID1 complex contains some proteins, such as RACK1 or ANXA2, that also associate with the actin cytoskeleton; therefore, the complex might as well provide a link for the cross-talk communication between actin and microtubules.

4.2.6 The MID1 complex components and their involvement in cell migration, polarisation and adhesion

Apart from associating with SICs, RACK1 has previously been shown to be a scaffolding protein that participates in cell spreading, establishment of early focal adhesions and cell-cell contacts. To fulfil these functions, it recruits Src, STATs and PKCs, among others, and links them to integrin receptors upon activation by insulin-like growth factor I receptor (IGF-IR) signalling (Cox et al., 2003; Hermanto et al., 2002; Meares et al., 2004; Miller et al., 2004; Sklan et al., 2006; Zhang et al., 2006). As mentioned before, RACK1 has also been proposed to be involved in the localisation of translation by the recruitment of RNA and ribosomes to focal adhesions (Nilsson et al., 2004). In addition to RACK1, p32, another interaction partner of the MID1/ α 4 complex, bind atypical PKC isozymes (Sklan et al., 2006; Storz et al., 2000), which respond to integrin signalling and are central players in the regulation of cell spreading and focal adhesion assembly (Disatnik et al., 2002; Henrique and Schweisguth, 2003). Independent studies have also shown that activation of p32, in collaboration with integrins, induces cell adhesion and spreading in endothelial cells (Feng et al., 2002; Ghebrehiwet et al., 2003). Interestingly, p32 (also referred as to Hyaluronan binding protein 1, HABP1) interacts with hyaluronan (HA), which is known to form a pericellular matrix concomitant to detachment during

mitosis or cell migration and, in combination with HA, p32 has been shown involved in the regulation of adhesion and de-adhesion (Sengupta et al., 2005).

Another member of the complex that has been closely related to cell adhesion is p40, a conserved receptor of laminin. Laminin is a very abundant extracellular molecule in basal laminae synthesized in very early embryos or in epithelial cells (Ford et al., 1999). Curiously, p40 has always attracted attention for its dual function in cell adhesion and ribosomal assembly and maintenance. Recently, it has been found that midkine also binds to p40 thereby competing with laminin, and that this interaction leads to enhanced protein translation (Kazmin et al., 2003). Interestingly, coming back to the mechanisms of ventral midline development, midkine is highly expressed in mouse NCC during development and plays an important role in cell migration (Mitsiadis et al., 2003; Mitsiadis et al., 1995; Qi et al., 2001).

Also ANXA2, another complex partner, has been shown to participate in cell adhesion and migration. Thus, it rapidly localises to cell-cell contacts after IGF-RI stimulation (Meares et al., 2004; Zhao et al., 2003), and has been suggested to be responsible for the initial recruitment of GTPase activity, that is essential for the formation of filopodia at the leading edge of migrating fibroblasts and epithelial cells (Balch and Dedman, 1997; Hansen et al., 2002; Nobes and Hall, 1995).

The importance of the microtubule-organizing centre, the centrosome, in cell polarisation and migration should also not be forgotten. The centrosome determines the direction of migration by placing itself in front of the nucleus, and projecting microtubules to the leading edge (Badano et al., 2005). After generation of the leading edge, and for the successful progression of migration, the nucleus must be translocated towards the front, a process that is highly governed by the centrosome. Alterations of this process have been linked to monogenic disorders. For instance, some mutations in lissencephaly gene 1 (LIS1) and doublecortin gene (DCX), the protein products of which localise to centrosomes, lead to defects in neural migration and microtubule dynamics. A connection between these proteins and the MID1 complex has been suggested previously since their phosphorylation status is regulated by microtubule-associated PP2A activity (Schweiger and Schneider, 2003; Trockenbacher et al., 2001). Interestingly, two novel members of the MID1 complex, namely NPM and Hsp90, have been shown to also play key roles in centrosome function.

In our group, we have observed that overexpression of $\alpha 4$ in HeLa or COS-7 cells results in the formation of filopodia to which $\alpha 4$ locate, indicating that it might play a role in the formation or regulation of filopodia. These protrusions are no longer observed when MID1 recruits $\alpha 4$ to microtubules in non-polarised cells (Schweiger et al, unpublished data). Given that filopodia formation in the leading edge is essential for cell migration, further studies would be necessary to investigate whether MID1 could be involved in bringing $\alpha 4$ to the locations

where protrusions need to arise in polarised cells, and whether $\alpha 4$ indeed plays a role in filopodia formation or regulation.

Last but not least, ephrin molecules (ligands and receptors), and specially ephrin-B1, the mRNAs of which were shown during this thesis to be associated to the MID1 complex, are also involved in cell migration and, in particular, in the migration of NCC. Apart from being known for having Rho family GTPases as the major downstream targets, which points at a central involvement in the formation of focal adhesions (see above), it has been shown that EphB-ephrin-B engagement is a critical determinant of integrin-mediated responses (Huynh-Do et al., 1999; Pasquale, 2005). In line, it has been shown that ephrin-B1 and EphB2 regulate the cytoarchitecture and spatial organization of kidney cells through Rho family GTPases, and that EphB activation promotes cell adhesion and induces focal adhesion enlargement (Ogawa et al., 2006).

In summary, most of the proteins that compose the MID1 complex have been reported to participate in cell adhesion, migration and local protein synthesis. Therefore, a concerted organization of their functions in the MID1 complex is an attractive model for the regulation of proper cell migration, polarisation, and adhesion, all essential processes for the correct development of the ventral midline.

4.2.7 EphB and ephrin-B mRNAs can be integrated in the MID1 complex

As earlier outlined, Eph receptors and ephrins have key roles in the regulation of cell migration, polarisation and adhesion during development. Their functions, often described in the context of NCC pathfinding, heavily rely on the establishment of asymmetric gradients of their proteins in polarised cells (Pasquale, 2005; Poliakov et al., 2004; Robinson et al., 1997). This makes them particularly attractive mRNA candidates to be positioned in the cell via a mechanism involving mRNA transport along the microtubules.

Within the frame of this study, it was demonstrated that the MID1 complex associates to G-quartet like structures mainly in the 3'UTRs of EphB receptor and ephrin-B mRNAs. G-quartets were identified in two ephrins (B1 and B2) and five Eph receptor mRNAs (B1, B2, B3, B4, B6), indicating that probably only those ephrin molecules participate in functions exerted by the MID1 complex. However, it is not possible to exclude a role for the others in the MID1 complex, which might contain another not-yet-targeted sequence in their mRNAs that also associates with the MID1 complex. Interestingly, it was possible to shown that the number of identified G-quartets varies among the ephrin molecules with up to four motifs identified in the *EFNB1* mRNA, mutations of which lead to craniofrontonasal dysplasia (Wieland et al., 2004). While G-quartets were present in 22% of all genes available from the ESEMBL database, only 1,33% of those had more than 3 G-quartets. In RNA-protein pull-down experiments, it was

further showed that increasing numbers of G-quartets in EFNB1 lead to an increase in protein binding affinity, which is not dependent on the length of the transcript. Consequently, the additive effect of the protein binding affinity seen with the *EFNB1* mRNA combined with a systematic displacement of lower affinity binding mRNAs might be an effective mechanism for a highly specific inclusion of G-quartet containing mRNAs in the described mRNPs.

As mentioned previously, the phenotypes of craniofrontonasal dysplasia syndrome and OS present striking overlaps, both of them being characterised by malformations of the facial ventral midline, such as hypertelorism/telecanthus or broad nasal bridge. This kind of malformation is most probably caused by defective cell migration and/or polarisation, and most likely affects NCC-migration and -orientation (Schweiger and Schneider, 2003; Wieland et al., 2004). Interestingly, recently, it has been reported that cardiac and cranial NCCs, but not trunk NCCs, require EFNB1 to migrate properly during development in mice (Davy et al., 2004). Moreover, these NCCs require EFNB1 autonomously and non-autonomously to properly complete craniofacial development, especially during palate elevation and fusion, an important process disrupted in many patients with OS and craniofrontonasal dysplasia. Furthermore, it has been shown that ephrin-B1, in addition to other EphB receptors and B-class ligands, participates in regulating the formation of the corpus callosum (Mendes et al., 2006), which also presents with defects in some OS patients. Given that EFNB1 is localised at chromosomal position Xq12-q13.1, it was also suggested as a candidate gene for FG syndrome, another ventral midline malformation syndrome, which has been mapped to Xq12-q21.3.

Therefore, the findings of this thesis, which involve the MID1 complex assisted transport of Eph receptor and ephrin mRNAs to the required places of the migrating cell in order to establish a protein gradient, are an attractive explanation for the conspicuous phenotypic overlap between OS and craniofrontonasal dysplasia and other midline malformation syndromes.

5 Conclusions and Outlook

During this thesis, a novel pathomechanism for OS was identified with a basis in mutations in Bbox1 or Bbox2 domains of MID1. Bbox1 was shown to be responsible for the interaction of MID1 with $\alpha 4$, a regulatory subunit of PP2A, and Bbox2 was demonstrated to act as a regulatory arm that couples the MID1 ubiquitin ligase function to the microtubules by regulating the association of MID1 with both $\alpha 4$ and microtubules. The inefficient MID1- $\alpha 4$ binding observed with mutations in any of the Bboxes causes accumulation of PP2Ac at the microtubules and hypophosphorylation of its downstream proteins, thus leading to the development of OS. A possible explanation for the striking dependence of Bbox1 function on Bbox2 could be a putative zinc atom shared by both domains. Consequently, zinc-binding stoichiometry has to be analysed in next series of experiments.

As main focus of this thesis, MID1 was demonstrated to form part of an mRNP complex, which associates to microtubules and RNA, and is likely to participate in the transport of mRNAs to the poles of the cell, providing asymmetric mRNA localisation and protein production. Compartmentalised protein translation is an important prerequisite for NCC to migrate and polarised cells to step into EMT, both essential processes during ventral midline development. Therefore, the data obtained during this thesis suggest a molecular basis for both the development of the ventral midline and the pathogenesis of OS.

However, several lines of investigation remain open. The exact pathomechanism derived from MID1 mutations in other domains rather than the C-terminus or, now, the Bboxes remains unknown. Therefore, in further experiments, the effects of diverse MID1 forms carrying mutations in different domains on RNA or ribosome binding should be studied and hopefully, regions involved in this association will be narrowed down.

In addition, direct association of MID1 with RNA could not be proven during this work. Further experiments will also have to show which members, if not MID1 itself, are involved in the incorporation of RNA into the complex. As mentioned in the discussion, attractive candidates would be the RNA helicase identified by yeast two-hybrid experiments or any of the other RNA-binding proteins contained in the complex. The study of RNA-MID1 complex association should be also extended to the identification of further mRNAs that associated with the complex, via for instance protein-RNA experiments. In theory, gene products of the identified mRNAs could collaborate with ephrins during ventral midline development.

Despite having all the characteristics of a cargo transport, no motor protein that provides movement along the microtubules was found to associate to the complex. Further experiments, such as immunoprecipitations with the different complex members or candidate specific co-immunoprecipitations with motor proteins, should allow the identification of such a protein

integrated in the complex. Furthermore, immunofluorescence experiments in living cells should be done, thus aiming to visualize movement of the whole mRNP *in vivo*.

In addition, the role of the MID1 complex in cell migration would also open a new area of study, in which the involvement of the complex in focal adhesions and cytoskeleton remodelling should be studied. Moreover, polarisation studies, including activation of integrin receptors by different effectors or by activation of EFNB1, could shed light on the functions of the MID1 complex in cell polarisation and migration. These studies could be extended to OS patient cell lines, which might show defects in migration compared to control cell lines.

While underlying genetic defects in patients with autosomally inherited OS remain totally unknown, mutations in MID1 have only been found in 68% of cases with X-linked OS. Since during this thesis it was shown that ephrin mRNAs are integrated into the MID1 complex via G-quartet structures, these structures appear as good candidates to harbour the “missing” mutations. Therefore, mutation analysis of G-quartet structures in ephrin mRNAs in OS patients not holding mutations in MID1 should be done.

Last but not least, direct influence of the MID1 complex on EFNB1 mRNA translation should be studied, and it should be checked whether it is affected in OS patients.

6 Summary

Opitz BBB/G syndrome (OS) is a congenital disorder characterised by malformations of the ventral midline, with hypertelorism and hypospadias being the two cardinal phenotypic manifestations. OS is genetically heterogeneous, with an autosomal and an X-linked locus. While the gene at the autosomal locus remains to be identified, the X-chromosomal form has been shown to be caused by mutations in the *MID1* gene, which harbours mutations in approximately 68% of patients with X-linked OS. Most of the mutations identified in OS patients are located at the 3' end of the MID1 open reading frame, thus affecting the C-terminus of the MID1 protein.

The MID1 protein belongs to the RFP subfamily of the RBCC family of proteins. At its N-terminal end it contains a RING finger, two Bboxes (Bbox1, Bbox2), and a coiled-coil domain (RBCC domain), which are followed by a FNIII domain and a B30.2 domain (RFP domain) at its C-terminal end. MID1 has been shown to form macromolecular cellular complexes, the components of which were, up to now, mainly unknown. Similar to other RBCC proteins, MID1 contains several putative protein-protein interaction domains. Recently, we have shown that the C-terminally microtubule-associated MID1 protein binds $\alpha 4$, a regulatory subunit of phosphatase 2A (PP2A), through the Bbox1 domain, thereby targeting the catalytic subunit of microtubule-associated PP2A (PP2Ac) towards ubiquitin-specific modification and degradation. MID1 mutations in the C-terminal end of the protein lead to disruption of microtubule association of MID1 and subsequent formation of clumps in the cytosol. Despite preserving its association with $\alpha 4$, C-terminally mutated MID1 can not approach the vicinity of microtubule-associated PP2Ac and, therefore, the ubiquitination and degradation of microtubule-associated PP2Ac becomes disrupted, leading to hypophosphorylation of its downstream targets.

During this thesis, basic functions of Bbox1 and Bbox2, with respect to MID1- $\alpha 4$ and MID1-microtubule interactions, were studied in detail by immunofluorescence, immunoprecipitation and yeast two-hybrid experiments. In this way, a novel pathomechanism for OS could be identified based on mutations in Bbox1 or Bbox2 domains of MID1 rather than C-terminal mutations. While the Bbox1 was shown to be responsible for the interaction of MID1 with $\alpha 4$, the Bbox2 was demonstrated to act as a regulatory arm that couples the MID1 ubiquitin ligase function to the microtubules by regulating the association of MID1 with both $\alpha 4$ and microtubules.

As the main focus of this thesis, the MID1 multiprotein complex was elucidated via affinity chromatography and mass spectrometry. Besides tubulin association, which has previously been reported, MID1 was shown to associate with several proteins of the small ribosomal subunit (S3, S8, p40) and other multifunctional proteins such as NPM, RACK1 and ANXA2,

which also associate with ribosomes and RNA. In addition, heat shock proteins, such as Hsp60, Hsc70, and the multifunctional chaperones Hsp90 and p32, were identified in the complex.

Through further characterisation of the MID1 protein complex, it could be demonstrated during this thesis that the MID1 protein, together with the mTOR target $\alpha 4$, forms a microtubule-associated mRNP that contains active polyribosomes and RNA, and thus links the translation regulatory mTOR pathway with a microtubule-associated translation unit. This complex is likely to participate in the transport of mRNAs to the poles of the cell, providing asymmetric mRNA localisation and protein production. Compartmentalised protein translation is an important prerequisite for neural crest cells to migrate and polarised cells to step into epithelial-mesenchymal transition, both essential processes during ventral midline development. Therefore, the results of this thesis suggest a molecular basis for both the development of the ventral midline and the pathogenesis of OS.

Moreover, it could be shown that the MID1/ $\alpha 4$ complex integrates mRNAs of ephrinB molecules (ligands and receptors) through G-quartet structures located in their 3'UTRs. Ephrins and Eph receptors participate in the regulation of essential processes during the development of the ventral midline, such as cell attachment, cell migration and embryonic patterning. Therefore, this thesis suggests a central role for the MID1/ $\alpha 4$ protein complex in the microtubule-associated compartmentalised translation of EphB receptors and ephrins-B. Interaction of the MID1 protein complex with the mRNA of ephrin-B1 (*EFNB1*) is of particular interest since mutated *EFNB1* leads to the development of craniofrontonasal dysplasia, a monogenic disorder with manifestations that are highly reminiscent of the OS phenotype. Consequently, the model proposed here also provides an attractive explanation for the conspicuous phenotypic overlap of the two disorders.

7 Sumario

El síndrome de Opitz BBB/G (OS) es un desorden congénito que se caracteriza por anomalías de la línea media ventral del cuerpo y que presenta como manifestaciones más prominentes hipertelorismo e hipospadias. OS es una enfermedad genéticamente heterogénea para la que existen dos loci, uno autosomal y otro ligado al cromosoma X. El gen causante de la herencia de carácter autosómico aún no ha sido identificado. Por otro lado, se ha demostrado que la herencia ligada al cromosoma X se debe a mutaciones en el gen *MID1*, que se presenta con mutaciones en aproximadamente un 68% de los pacientes con OS ligado al cromosoma X. La mayoría de las mutaciones identificadas en pacientes con OS, están situadas en el extremo 3' de la región codificante de *MID1* y por lo tanto afectan al extremo carboxilo de la proteína *MID1*.

La proteína *MID1* pertenece a la subfamilia RFP de la familia RBCC de proteínas. En la parte amino-terminal, *MID1* comprende un RING-Finger, dos Bboxes (Bbox1 y Bbox2) y un dominio "Coiled-coil" (dominio RBCC), seguidos de los dominios FNIII y B30.2 en el extremo carboxilo de la proteína. *MID1* tiene la capacidad de formar grandes complejos macromoleculares, cuyos componentes eran hasta ahora desconocidos. Como otras proteínas de la familia RBCC, *MID1* tiene varios dominios que participan en interacciones entre proteínas. Recientemente demostramos en nuestro laboratorio que *MID1*, asociada a través de su extremo carboxilo con los microtúbulos, interacciona con $\alpha 4$ ($\alpha 4$), una subunidad reguladora de la proteína fosfatasa 2A (PP2A), por medio de Bbox1. De este modo, *MID1* es capaz de ubiquitinar la subunidad catalítica de PP2A (PP2Ac), que en consecuencia, será degradada por el proteasoma. Las mutaciones en el extremo carboxilo de *MID1* hacen que ésta pierda su asociación con los microtúbulos y se formen agregados en el citoplasma de la célula. A pesar de seguir unida a $\alpha 4$, *MID1* ya no puede acercarse a PP2Ac y ubiquitinarla, por lo tanto PP2Ac se acumula en los microtúbulos, lo que provoca la hipofosforilación de proteínas que de ella dependen.

Durante esta tesis, la base experimental para el estudio de las funciones básicas de Bbox1 y Bbox2 en lo concerniente a la interacción de *MID1* con los microtúbulos y con $\alpha 4$ fueron experimentos tales como inmunofluorescencias, inmunoprecipitaciones y "yeast two-hybrid system". De esta manera y por primera vez se pudo describir un nuevo mecanismo patológico para *MID1* con mutaciones en uno de los Bboxes en lugar de en el extremo carboxilo. Concretamente, los resultados de esta tesis demostraron que sólo Bbox1 interviene directamente en la interacción de *MID1* con $\alpha 4$ y que Bbox2 tiene un papel regulador en la interacción entre *MID1* y $\alpha 4$ y la de *MID1* con los microtúbulos

El principal objetivo de esta tesis fue identificar el complejo multiproteico formado por MID1 usando técnicas como cromatografía de afinidad y espectrometría de masas. Además de la ya demostrada interacción de MID1 con tubulina, en el complejo se identificaron varias proteínas pertenecientes a la subunidad pequeña del ribosoma (S3, S8 y p40) en conjunto con diversas proteínas multifuncionales, tales como NPM, RACK1 y ANXA2, que se han visto anteriormente asociadas con ARN y ribosomas. También fueron encontradas en el complejo varias proteínas de choque térmico, tales como Hsp60, Hsc70 y las chaperonas multifuncionales Hsp90 y p32, fueron encontradas en el complejo.

El complejo multiproteico formado por MID1 se estudió en detalle y se encontró que, junto con $\alpha 4$ (una proteína diana de mTOR), MID1 forma un complejo ribonucleoproteico que se encuentra asociado con los microtúbulos y contiene polisomas y RNA y por lo tanto, sirve de vínculo entre la vía de mTOR (reguladora de la traducción de proteínas) y una nueva unidad de traducción situada en los microtúbulos. Probablemente, este complejo participa en el transporte de ARN mensajero (ARNm) a los polos de la célula y de ese modo proporciona la requerida asimetría en la distribución ARNm y en la producción de proteínas. Para que células de la cresta neural migren y células polarizadas entren en transición epitelial-mesenquimal, procesos esenciales durante el desarrollo de la línea ventral media, es necesario que la producción de proteínas se distribuya en compartimentos diferentes. Por consiguiente, los resultados de esta tesis sugieren una base molecular para el desarrollo de la línea media y para la patogénesis de OS.

Asimismo, se demostró que el complejo multiproteico de MID1/ $\alpha 4$ integra ARNm pertenecientes a efrinas y sus receptores a través de estructuras en forma de “G-quartets” que se ubican en sus 3’UTRs. Las efrinas y sus receptores participan en la regulación de procesos fundamentales durante el desarrollo de la línea ventral media, tales como adhesión y migración celular y desarrollo embrionario. Así pues, esta tesis plantea un papel central para el complejo multiproteico MID1/ $\alpha 4$ en la distribución de la traducción de efrinas y sus receptores en la célula a través del transporte de sus ARNm por los microtúbulos. Se debe hacer hincapié en la interacción que el complejo de MID1 presenta con la efrina-B1 (EFNB1), ya que mutaciones en este gen causan displasia craneofrontonasal, un desorden monogénico cuyos pacientes presentan un fenotipo altamente similar al de los pacientes con OS. Por lo tanto, el modelo que en esta tesis se propone, también proporciona una explicación muy atractiva para el llamativo solapamiento entre los fenotipos de pacientes con OS y displasia craneofrontonasal.

8 Zusammenfassung

Das Opitz BBB/G Syndrom (OS) ist eine Erbkrankheit, die durch Fehlbildungen der ventralen Mittellinie, insbesondere Hypertelorismus und Hypospadie, charakterisiert ist. OS ist mit einem autosomalen und einem X-chromosomalen Locus genetisch heterogen. Während das Gen auf dem autosomalen Genlocus noch nicht identifiziert wurde, konnte die X-chromosomale Form auf Mutationen im *MID1*-Gen zurückgeführt werden. Im offenen Leserahmen dieses Gens konnten bei etwa 68% der Patienten mit X-chromosomalem OS Mutationen gefunden werden. Die meisten Mutationen, die bei OS-Patienten identifiziert wurden, befinden sich im 3' Bereich des offenen Leserahmens des *MID1*-Gens und wirken sich somit auf den C-terminalen Bereich des MID1-Proteins aus.

Das MID1-Protein gehört zur RFP-Familie, die eine Unterfamilie der RBCC-Familie ist. Am Ende des N-Terminus befinden sich ein RING-Finger, zwei Bboxen (Bbox1, Bbox2) und eine Coiled-coil Domäne (RBCC-Domäne). Am C-terminalen Ende schließt sich eine FNIII-Domäne und eine B30.2-Domäne (RFP-Domäne) an. Es wurde gezeigt, dass MID1 makromolekulare Komplexe bildet, deren Komponenten zu Beginn dieser Arbeit weitestgehend unbekannt waren. Ähnlich wie andere Proteine der RBCC-Familie besitzt MID1 verschiedene Domänen, die an Proteininteraktionen beteiligt sind. Wir konnten vor kurzem zeigen, dass das Mikrotubulus-assoziierte MID1-Protein mit seiner Bbox1 an das $\alpha 4$ -Protein, einer regulatorischen Untereinheit der Phosphatase 2A (PP2A), bindet. Dies führt zur Übertragung von Ubiquitin auf die katalytische Untereinheit der Mikrotubulus-assoziierten PP2A (PP2Ac) und zu deren Aufbau im Proteasom. Auch MID1 mit Mutationen am C-terminalen Ende bindet an das $\alpha 4$ Protein. Es hat jedoch die Fähigkeit, an Mikrotubuli zu binden, verloren und bildet Aggregate im Zytoplasma. Eine Interaktion mit der Mikrotubulus-assoziierten PP2Ac kann somit nicht mehr stattfinden, was dazu führt, dass die Ubiquitinierung und Degradierung der Mikrotubulus-assoziierten PP2Ac verhindert wird und ihre Zielproteine hypophosphorylieren.

Im Rahmen dieser Arbeit wurden grundsätzliche Funktionen von Bbox1 und Bbox2 im Zusammenhang mit MID1- $\alpha 4$ und MID1-Mikrotubuli-Interaktionen im Detail untersucht. Durch Immunfluoreszenz-, Immunprecipitation- und Yeast-Two-Hybrid-Experimente konnte ein neuer Pathomechanismus für OS nachgewiesen werden, der eher auf Mutationen der Bbox1 oder Bbox2-Domänen von MID1 basiert als auf Mutationen des C-Terminus. Während sich die Bbox1 für die Interaktion zwischen MID1 und $\alpha 4$ verantwortlich zeigte, ist die Bbox2 an der Regulierung der Assoziation von MID1 mit $\alpha 4$ und den Mikrotubuli beteiligt.

Als Hauptanliegen dieser Arbeit wurde der MID1-Multiprotein-Komplex mit Hilfe von Affinitätschromatographie und Massenspektrometrie identifiziert und analysiert. Neben der bekannten Assoziation mit Tubulin, konnte gezeigt werden, dass MID1 auch verschiedene

Proteine der kleinen ribosomalen Untereinheit (S3, S8, p40) und andere multifunktionale Proteine wie NPM, RACK1 und ANXA2, welche ebenfalls mit Ribosomen und RNS assoziieren, bindet. Weiterhin wurden Hitzeschock-Proteine, wie Hsp60, Hsc70 und die multifunktionalen Chaperone Hsp90 und p32, im Komplex identifiziert.

Durch weitere Charakterisierung des MID1-Protein-Komplexes, konnte im Rahmen dieser Arbeit gezeigt werden, dass das MID1-Protein, zusammen mit dem mTOR-Zielprotein $\alpha 4$, ein Mikrotubulus-assoziiertes mRNP bildet, welches aktive Polyribosome und RNS enthält, und so den regulierenden Translations-mTOR-Weg mit einer Mikrotubulus-assoziierten Translations-Einheit verbindet. Dieser Komplex reguliert wahrscheinlich den Transport der mRNS zu den Polen der Zelle, was zu asymmetrischer mRNS Lokalisierung und Protein-Produktion führt. Asymmetrische Protein-Translation ist eine wichtige Voraussetzung, damit die Zellen der Neuralleiste migrieren können und polarisierte Zellen in die Epithelial-Mesenchymale-Transition treten können. Beides sind essenzielle Prozesse bei der Entwicklung der ventralen Mittellinie. Daher bereiten die Ergebnisse dieser Arbeit eine molekulare Basis sowohl der Entwicklung der ventralen Mittellinie als auch der Pathogenese von OS.

Darüber hinaus wurde in dieser Arbeit gezeigt, dass der MID1/ $\alpha 4$ -Komplex an G-Quartet-Strukturen in den 3'UTR von ephrin-B Molekülen (Liganden und Rezeptoren) bindet. Dies weist darauf hin, dass der MID1/ $\alpha 4$ -Komplex die asymmetrische Translation der ephrin-B Moleküle in Subkompartimenten der Zelle steuert. Die Regulation wichtiger Prozesse der Entwicklung der ventralen Mittellinie durch Ephrine, wie z.B. Zellhaftung und Zellmigration könnte durch diese Steuerung gewährleistet werden. Die Interaktion des MID1-Protein-Komplexes mit mRNS des Ephrin-B1 (*EFNB1*) ist besonders interessant, da mutiertes EFNB1 zu craniofrontonasaler Dysplasie führt, einer monogenen Störung, die zu einem sehr ähnlichen Phänotypen führt wie OS. Dementsprechend bietet das hier vorgeschlagene Modell auch eine attraktive Erklärung für die offensichtliche phänotypische Übereinstimmung der zwei Krankheiten.

9 References

- **Antar, L. N., Afroz, R., Dichtenberg, J. B., Carroll, R. C., and Bassell, G. J.** (2004). Metabotropic glutamate receptor activation regulates fragile x mental retardation protein and FMR1 mRNA localization differentially in dendrites and at synapses. *J Neurosci* **24**, 2648-2655.
- **Avela, K., Lipsanen-Nyman, M., Idanheimo, N., Seemanova, E., Rosengren, S., Makela, T. P., Perheentupa, J., Chapelle, A. D., and Lehesjoki, A. E.** (2000). Gene encoding a new RING-B-box-Coiled-coil protein is mutated in mulibrey nanism. *Nat Genet* **25**, 298-301.
- **Avila, J., Dominguez, J., and Diaz-Nido, J.** (1994). Regulation of microtubule dynamics by microtubule-associated protein expression and phosphorylation during neuronal development. *Int J Dev Biol* **38**, 13-25.
- **Badano, J. L., Teslovich, T. M., and Katsanis, N.** (2005). The centrosome in human genetic disease. *Nat Rev Genet* **6**, 194-205.
- **Bagni, C., and Greenough, W. T.** (2005). From mRNP trafficking to spine dysmorphogenesis: the roots of fragile X syndrome. *Nat Rev Neurosci* **6**, 376-387.
- **Balch, C., and Dedman, J. R.** (1997). Annexins II and V inhibit cell migration. *Exp Cell Res* **237**, 259-263.
- **Barembaum, M., and Bronner-Fraser, M.** (2005). Early steps in neural crest specification. *Semin Cell Dev Biol* **16**, 642-646.
- **Barrallo-Gimeno, A., and Nieto, M. A.** (2005). The Snail genes as inducers of cell movement and survival: implications in development and cancer. *Development* **132**, 3151-3161.
- **Bashirullah, A., Cooperstock, R. L., and Lipshitz, H. D.** (1998). RNA localization in development. *Annu Rev Biochem* **67**, 335-394.
- **Berti, C., Fontanella, B., Ferrentino, R., and Meroni, G.** (2004). Mig12, a novel Opitz syndrome gene product partner, is expressed in the embryonic ventral midline and co-operates with Mid1 to bundle and stabilize microtubules. *BMC Cell Biol* **5**, 9.
- **Borden, K. L.** (1998). RING fingers and B-boxes: zinc-binding protein-protein interaction domains. *Biochem Cell Biol* **76**, 351-358.
- **Borden, K. L.** (2000). RING domains: master builders of molecular scaffolds? *J Mol Biol* **295**, 1103-1112.
- **Borden, K. L., Boddy, M. N., Lally, J., O'Reilly, N. J., Martin, S., Howe, K., Solomon, E., and Freemont, P. S.** (1995a). The solution structure of the RING finger domain from the acute promyelocytic leukaemia proto-oncoprotein PML. *Embo J* **14**, 1532-1541.
- **Borden, K. L., Lally, J. M., Martin, S. R., O'Reilly, N. J., Etkin, L. D., and Freemont, P. S.** (1995b). Novel topology of a zinc-binding domain from a protein involved in regulating early *Xenopus* development. *Embo J* **14**, 5947-5956.
- **Brendel, C., Rehbein, M., Kreienkamp, H. J., Buck, F., Richter, D., and Kindler, S.** (2004). Characterization of Staufen 1 ribonucleoprotein complexes. *Biochem J* **384**, 239-246.
- **Brown, V., Jin, P., Ceman, S., Darnell, J. C., O'Donnell, W. T., et al.** (2001). Microarray identification of FMRP-associated brain mRNAs and altered mRNA translational profiles in fragile X syndrome. *Cell* **107**, 477-487.
- **Brown, V., Small, K., Lakkis, L., Feng, Y., Gunter, C., Wilkinson, K. D., and Warren, S. T.** (1998). Purified recombinant Fmrp exhibits selective RNA binding as an intrinsic property of the fragile X mental retardation protein. *J Biol Chem* **273**, 15521-15527.
- **Buchner, G., Montini, E., Andolfi, G., Quaderi, N., Cainarca, S., Messali, S., Bassi, M. T., Ballabio, A., Meroni, G., and Franco, B.** (1999). MID2, a homologue of the Opitz

syndrome gene MID1: similarities in subcellular localization and differences in expression during development. *Hum Mol Genet* **8**, 1397-1407.

- **Bukau, B., and Horwich, A. L.** (1998). The Hsp70 and Hsp60 chaperone machines. *Cell* **92**, 351-366.
- **Burd, C. G., Matunis, E. L., and Dreyfuss, G.** (1991). The multiple RNA-binding domains of the mRNA poly(A)-binding protein have different RNA-binding activities. *Mol Cell Biol* **11**, 3419-3424.
- **Burkhard, P., Stetefeld, J., and Strelkov, S. V.** (2001). Coiled coils: a highly versatile protein folding motif. *Trends Cell Biol* **11**, 82-88.
- **Burrows, F., Zhang, H., and Kamal, A.** (2004). Hsp90 activation and cell cycle regulation. *Cell Cycle* **3**, 1530-1536.
- **Cainarca, S., Messali, S., Ballabio, A., and Meroni, G.** (1999). Functional characterization of the Opitz syndrome gene product (midin): evidence for homodimerization and association with microtubules throughout the cell cycle. *Hum Mol Genet* **8**, 1387-1396.
- **Cao, T., Borden, K. L., Freemont, P. S., and Etkin, L. D.** (1997). Involvement of the rfp tripartite motif in protein-protein interactions and subcellular distribution. *J Cell Sci* **110** (Pt 14), 1563-1571.
- **Ceman, S., Brown, V., and Warren, S. T.** (1999). Isolation of an FMRP-associated messenger ribonucleoprotein particle and identification of nucleolin and the fragile X-related proteins as components of the complex. *Mol Cell Biol* **19**, 7925-7932.
- **Chattopadhyay, C., Hawke, D., Kobayashi, R., and Maity, S. N.** (2004). Human p32, interacts with B subunit of the CCAAT-binding factor, CBF/NF-Y, and inhibits CBF-mediated transcription activation in vitro. *Nucleic Acids Res* **32**, 3632-3641.
- **Chen, J., Peterson, R. T., and Schreiber, S. L.** (1998). Alpha 4 associates with protein phosphatases 2A, 4, and 6. *Biochem Biophys Res Commun* **247**, 827-832.
- **Chicurel, M. E., Singer, R. H., Meyer, C. J., and Ingber, D. E.** (1998). Integrin binding and mechanical tension induce movement of mRNA and ribosomes to focal adhesions. *Nature* **392**, 730-733.
- **Cohen, M. M., Jr.** (2002). Malformations of the craniofacial region: evolutionary, embryonic, genetic, and clinical perspectives. *Am J Med Genet* **115**, 245-268.
- **Compagni, A., Logan, M., Klein, R., and Adams, R. H.** (2003). Control of skeletal patterning by ephrinB1-EphB interactions. *Dev Cell* **5**, 217-230.
- **Condeelis, J.** (1995). Elongation factor 1 alpha, translation and the cytoskeleton. *Trends Biochem Sci* **20**, 169-170.
- **Consortium, F.** (1997). A candidate gene for familial Mediterranean fever. *Nat Genet* **17**, 25-31.
- **Cooper, G. M.** (2000). *The Cell, a Molecular Approach*.
- **Cordero, J. F., and Holmes, L. B.** (1978). Phenotypic overlap of the BBB and G syndromes. *Am J Med Genet* **2**, 145-152.
- **Cox, E. A., Bennin, D., Doan, A. T., O'Toole, T., and Huttenlocher, A.** (2003). RACK1 regulates integrin-mediated adhesion, protrusion, and chemotactic cell migration via its Src-binding site. *Mol Biol Cell* **14**, 658-669.
- **Cox, T. C.** (2004). Taking it to the max: the genetic and developmental mechanisms coordinating midfacial morphogenesis and dysmorphology. *Clin Genet* **65**, 163-176.
- **Cox, T. C., Allen, L. R., Cox, L. L., Hopwood, B., Goodwin, B., Haan, E., and Suthers, G. K.** (2000). New mutations in MID1 provide support for loss of function as the cause of X-linked Opitz syndrome. *Hum Mol Genet* **9**, 2553-2562.

- **Craig, E. A., Weissman, J. S., and Horwich, A. L.** (1994). Heat shock proteins and molecular chaperones: mediators of protein conformation and turnover in the cell. *Cell* **78**, 365-372.
- **Czar, M. J., Welsh, M. J., and Pratt, W. B.** (1996). Immunofluorescence localization of the 90-kDa heat-shock protein to cytoskeleton. *Eur J Cell Biol* **70**, 322-330.
- **Darnell, J. C., Jensen, K. B., Jin, P., Brown, V., Warren, S. T., and Darnell, R. B.** (2001). Fragile X mental retardation protein targets G quartet mRNAs important for neuronal function. *Cell* **107**, 489-499.
- **Davy, A., Aubin, J., and Soriano, P.** (2004). Ephrin-B1 forward and reverse signaling are required during mouse development. *Genes Dev* **18**, 572-583.
- **Davy, A., and Soriano, P.** (2005). Ephrin signaling in vivo: look both ways. *Dev Dyn* **232**, 1-10.
- **de Carcer, G.** (2004). Heat shock protein 90 regulates the metaphase-anaphase transition in a polo-like kinase-dependent manner. *Cancer Res* **64**, 5106-5112.
- **de Carcer, G., do Carmo Avides, M., Lallena, M. J., Glover, D. M., and Gonzalez, C.** (2001). Requirement of Hsp90 for centrosomal function reflects its regulation of Polo kinase stability. *Embo J* **20**, 2878-2884.
- **De Falco, F., Cainarca, S., Andolfi, G., Ferrentino, R., Berti, C., et al.** (2003). X-linked Opitz syndrome: novel mutations in the MID1 gene and redefinition of the clinical spectrum. *Am J Med Genet A* **120**, 222-228.
- **de Hoog, C. L., Foster, L. J., and Mann, M.** (2004). RNA and RNA binding proteins participate in early stages of cell spreading through spreading initiation centers. *Cell* **117**, 649-662.
- **Dennis, P. B., Fumagalli, S., and Thomas, G.** (1999). Target of rapamycin (TOR): balancing the opposing forces of protein synthesis and degradation. *Curr Opin Genet Dev* **9**, 49-54.
- **Di Como, C. J., and Arndt, K. T.** (1996). Nutrients, via the Tor proteins, stimulate the association of Tap42 with type 2A phosphatases. *Genes Dev* **10**, 1904-1916.
- **Disatnik, M. H., Boutet, S. C., Lee, C. H., Mochly-Rosen, D., and Rando, T. A.** (2002). Sequential activation of individual PKC isozymes in integrin-mediated muscle cell spreading: a role for MARCKS in an integrin signaling pathway. *J Cell Sci* **115**, 2151-2163.
- **Doxsey, S.** (2001). Re-evaluating centrosome function. *Nat Rev Mol Cell Biol* **2**, 688-698.
- **Dreyfuss, G., Kim, V. N., and Kataoka, N.** (2002). Messenger-RNA-binding proteins and the messages they carry. *Nat Rev Mol Cell Biol* **3**, 195-205.
- **Driever, W., and Nusslein-Volhard, C.** (1988). A gradient of bicoid protein in Drosophila embryos. *Cell* **54**, 83-93.
- **Duband, J. L., Monier, F., Delannet, M., and Newgreen, D.** (1995). Epithelium-mesenchyme transition during neural crest development. *Acta Anat (Basel)* **154**, 63-78.
- **Duvel, K., and Broach, J. R.** (2004). The role of phosphatases in TOR signaling in yeast. *Curr Top Microbiol Immunol* **279**, 19-38.
- **El-Hodiri, H. M., Shou, W., and Etkin, L. D.** (1997). xnf7 functions in dorsal-ventral patterning of the Xenopus embryo. *Dev Biol* **190**, 1-17.
- **Everett, A. D., and Brautigan, D. L.** (2002). Developmental expression of alpha4 protein phosphatase regulatory subunit in tissues affected by Opitz syndrome. *Dev Dyn* **224**, 461-464.
- **Fankhauser, C., Izaurrealde, E., Adachi, Y., Wingfield, P., and Laemmli, U. K.** (1991). Specific complex of human immunodeficiency virus type 1 rev and nucleolar B23 proteins: dissociation by the Rev response element. *Mol Cell Biol* **11**, 2567-2575.

- **Feng, X., Tonnesen, M. G., Peerschke, E. I., and Ghebrehiwet, B.** (2002). Cooperation of C1q receptors and integrins in C1q-mediated endothelial cell adhesion and spreading. *J Immunol* **168**, 2441-2448.
- **Feng, Y., Absher, D., Eberhart, D. E., Brown, V., Malter, H. E., and Warren, S. T.** (1997). FMRP associates with polyribosomes as an mRNP, and the I304N mutation of severe fragile X syndrome abolishes this association. *Mol Cell* **1**, 109-118.
- **Fields, S., and Sternglanz, R.** (1994). The two hybrid system: an assay for protein-protein interaction. *Trends Genet* **10**, 286-292.
- **Filipenko, N. R., MacLeod, T. J., Yoon, C. S., and Waisman, D. M.** (2004). Annexin A2 is a novel RNA-binding protein. *J Biol Chem* **279**, 8723-8731.
- **Fingar, D. C., and Blenis, J.** (2004). Target of rapamycin (TOR): an integrator of nutrient and growth factor signals and coordinator of cell growth and cell cycle progression. *Oncogene* **23**, 3151-3171.
- **Ford, C. L., Randal-Whitis, L., and Ellis, S. R.** (1999). Yeast proteins related to the p40/laminin receptor precursor are required for 20S ribosomal RNA processing and the maturation of 40S ribosomal subunits. *Cancer Res* **59**, 704-710.
- **Gammill, L. S., and Bronner-Fraser, M.** (2003). Neural crest specification: migrating into genomics. *Nat Rev Neurosci* **4**, 795-805.
- **Gaudenz, K., Roessler, E., Quaderi, N., Franco, B., Feldman, G., et al.** (1998). Opitz G/BBB syndrome in Xp22: mutations in the MID1 gene cluster in the carboxy-terminal domain. *Am J Hum Genet* **63**, 703-710.
- **Gauthier, L. R., and Robbins, S. M.** (2003). Ephrin signaling: One raft to rule them all? One raft to sort them? One raft to spread their call and in signaling bind them? *Life Sci* **74**, 207-216.
- **Ghebrehiwet, B., Feng, X., Kumar, R., and Peerschke, E. I.** (2003). Complement component C1q induces endothelial cell adhesion and spreading through a docking/signaling partnership of C1q receptors and integrins. *Int Immunopharmacol* **3**, 299-310.
- **Gilbert, S. F.** (2003). Developmental Biology: (Sinauer associates)).
- **Gingras, A. C., Raught, B., and Sonenberg, N.** (2001). Regulation of translation initiation by FRAP/mTOR. *Genes Dev* **15**, 807-826.
- **Gong, C. X., Wegiel, J., Lidsky, T., Zuck, L., Avila, J., Wisniewski, H. M., Grundke-Iqbal, I., and Iqbal, K.** (2000). Regulation of phosphorylation of neuronal microtubule-associated proteins MAP1b and MAP2 by protein phosphatase-2A and -2B in rat brain. *Brain Res* **853**, 299-309.
- **Granata, A., Savery, D., Hazan, J., Cheung, B. M., Lumsden, A., and Quaderi, N. A.** (2005). Evidence of functional redundancy between MID proteins: implications for the presentation of Opitz syndrome. *Dev Biol* **277**, 417-424.
- **Grignani, F., Fagioli, M., Alcalay, M., Longo, L., Pandolfi, P. P., Donti, E., Biondi, A., Lo Coco, F., and Pelicci, P. G.** (1994). Acute promyelocytic leukemia: from genetics to treatment. *Blood* **83**, 10-25.
- **Grisendi, S., Bernardi, R., Rossi, M., Cheng, K., Khandker, L., Manova, K., and Pandolfi, P. P.** (2005). Role of nucleophosmin in embryonic development and tumorigenesis. *Nature* **437**, 147-153.
- **Gupta, S., and Knowlton, A. A.** (2005). HSP60, Bax, apoptosis and the heart. *J Cell Mol Med* **9**, 51-58.
- **Hall, B. K.** (2000). The neural crest as a fourth germ layer and vertebrates as quadroblastic not triploblastic. *Evol Dev* **2**, 3-5.

- Hansen, M. D., Ehrlich, J. S., and Nelson, W. J. (2002). Molecular mechanism for orienting membrane and actin dynamics to nascent cell-cell contacts in epithelial cells. *J Biol Chem* **277**, 45371-45376.
- Hara, K., Maruki, Y., Long, X., Yoshino, K., Oshiro, N., Hidayat, S., Tokunaga, C., Avruch, J., and Yonezawa, K. (2002). Raptor, a binding partner of target of rapamycin (TOR), mediates TOR action. *Cell* **110**, 177-189.
- Hasegawa, N., Iwashita, T., Asai, N., Murakami, H., Iwata, Y., Isomura, T., Goto, H., Hayakawa, T., and Takahashi, M. (1996). A RING finger motif regulates transforming activity of the rfp/ret fusion gene. *Biochem Biophys Res Commun* **225**, 627-631.
- Hay, E. D. (2005). The mesenchymal cell, its role in the embryo, and the remarkable signaling mechanisms that create it. *Dev Dyn* **233**, 706-720.
- Hay, N., and Sonenberg, N. (2004). Upstream and downstream of mTOR. *Genes Dev* **18**, 1926-1945.
- Heitman, J., Movva, N. R., and Hall, M. N. (1991). Targets for cell cycle arrest by the immunosuppressant rapamycin in yeast. *Science* **253**, 905-909.
- Helbling, P. M., Tran, C. T., and Brandli, A. W. (1998). Requirement for EphA receptor signaling in the segregation of *Xenopus* third and fourth arch neural crest cells. *Mech Dev* **78**, 63-79.
- Helms, J. A., Cordero, D., and Tapadia, M. D. (2005). New insights into craniofacial morphogenesis. *Development* **132**, 851-861.
- Henrique, D., and Schweisguth, F. (2003). Cell polarity: the ups and downs of the Par6/aPKC complex. *Curr Opin Genet Dev* **13**, 341-350.
- Henry, J., Mather, I. H., McDermott, M. F., and Pontarotti, P. (1998). B30.2-like domain proteins: update and new insights into a rapidly expanding family of proteins. *Mol Biol Evol* **15**, 1696-1705.
- Hermanto, U., Zong, C. S., Li, W., and Wang, L. H. (2002). RACK1, an insulin-like growth factor I (IGF-I) receptor-interacting protein, modulates IGF-I-dependent integrin signaling and promotes cell spreading and contact with extracellular matrix. *Mol Cell Biol* **22**, 2345-2365.
- Hodges, M., Tissot, C., Howe, K., Grimwade, D., and Freemont, P. S. (1998). Structure, organization, and dynamics of promyelocytic leukemia protein nuclear bodies. *Am J Hum Genet* **63**, 297-304.
- Holder, N., and Klein, R. (1999). Eph receptors and ephrins: effectors of morphogenesis. *Development* **126**, 2033-2044.
- Huang, X., and Saint-Jeannet, J. P. (2004). Induction of the neural crest and the opportunities of life on the edge. *Dev Biol* **275**, 1-11.
- Huynh-Do, U., Stein, E., Lane, A. A., Liu, H., Cerretti, D. P., and Daniel, T. O. (1999). Surface densities of ephrin-B1 determine EphB1-coupled activation of cell attachment through α 5 β 1 and α 3 β 1 integrins. *Embo J* **18**, 2165-2173.
- Jacinto, E., and Hall, M. N. (2003). Tor signalling in bugs, brain and brawn. *Nat Rev Mol Cell Biol* **4**, 117-126.
- Jacinto, E., Loewith, R., Schmidt, A., Lin, S., Ruegg, M. A., Hall, A., and Hall, M. N. (2004). Mammalian TOR complex 2 controls the actin cytoskeleton and is rapamycin insensitive. *Nat Cell Biol* **6**, 1122-1128.
- Jana, N. R., Tanaka, M., Wang, G., and Nukina, N. (2000). Polyglutamine length-dependent interaction of Hsp40 and Hsp70 family chaperones with truncated N-terminal

huntingtin: their role in suppression of aggregation and cellular toxicity. *Hum Mol Genet* **9**, 2009-2018.

- **Jang, C. Y., Lee, J. Y., and Kim, J.** (2004). Rps3, a DNA repair endonuclease and ribosomal protein, is involved in apoptosis. *FEBS Lett* **560**, 81-85.
- **Jensen, K., Shiels, C., and Freemont, P. S.** (2001). PML protein isoforms and the RBCC/TRIM motif. *Oncogene* **20**, 7223-7233.
- **Jerome, L. A., and Papaioannou, V. E.** (2001). DiGeorge syndrome phenotype in mice mutant for the T-box gene, Tbx1. *Nat Genet* **27**, 286-291.
- **Jiang, Y., and Broach, J. R.** (1999). Tor proteins and protein phosphatase 2A reciprocally regulate Tap42 in controlling cell growth in yeast. *Embo J* **18**, 2782-2792.
- **Jin, P., Alisch, R. S., and Warren, S. T.** (2004a). RNA and microRNAs in fragile X mental retardation. *Nat Cell Biol* **6**, 1048-1053.
- **Jin, P., Zarnescu, D. C., Ceman, S., Nakamoto, M., Mowrey, J., Jongens, T. A., Nelson, D. L., Moses, K., and Warren, S. T.** (2004b). Biochemical and genetic interaction between the fragile X mental retardation protein and the microRNA pathway. *Nat Neurosci* **7**, 113-117.
- **Jones, N. C., and Trainor, P. A.** (2005). Role of morphogens in neural crest cell determination. *J Neurobiol* **64**, 388-404.
- **Kanai, Y., Dohmae, N., and Hirokawa, N.** (2004). Kinesin transports RNA: isolation and characterization of an RNA-transporting granule. *Neuron* **43**, 513-525.
- **Kang, P., and Svoboda, K. K.** (2005). Epithelial-Mesenchymal Transformation during Craniofacial Development. *J Dent Res* **84**, 678-690.
- **Kang, Y., and Massague, J.** (2004). Epithelial-mesenchymal transitions: twist in development and metastasis. *Cell* **118**, 277-279.
- **Kaverina, I., Krylyshkina, O., and Small, J. V.** (1999). Microtubule targeting of substrate contacts promotes their relaxation and dissociation. *J Cell Biol* **146**, 1033-1044.
- **Kaverina, I., Rottner, K., and Small, J. V.** (1998). Targeting, capture, and stabilization of microtubules at early focal adhesions. *J Cell Biol* **142**, 181-190.
- **Kaverina, I. N., Minin, A. A., Gyoeva, F. K., and Vasiliev, J. M.** (1997). Kinesin-associated transport is involved in the regulation of cell adhesion. *Cell Biol Int* **21**, 229-236.
- **Kavi, H. H., Fernandez, H. R., Xie, W., and Birchler, J. A.** (2005). RNA silencing in Drosophila. *FEBS Lett* **579**, 5940-5949.
- **Kaytor, M. D., and Orr, H. T.** (2001). RNA targets of the fragile X protein. *Cell* **107**, 555-557.
- **Kazmin, D. A., Chinenov, Y., Larson, E., and Starkey, J. R.** (2003). Comparative modeling of the N-terminal domain of the 67kDa laminin-binding protein: implications for putative ribosomal function. *Biochem Biophys Res Commun* **300**, 161-166.
- **Keyes, W. M., and Sanders, E. J.** (2002). Regulation of apoptosis in the endocardial cushions of the developing chick heart. *Am J Physiol Cell Physiol* **282**, C1348-1360.
- **Khuri, S., Bakker, F. T., and Dunwell, J. M.** (2001). Phylogeny, function, and evolution of the cupins, a structurally conserved, functionally diverse superfamily of proteins. *Mol Biol Evol* **18**, 593-605.
- **Kiebler, M. A., Hemraj, I., Verkade, P., Kohrmann, M., Fortes, P., Marion, R. M., Ortin, J., and Dotti, C. G.** (1999). The mammalian stau protein localizes to the somatodendritic domain of cultured hippocampal neurons: implications for its involvement in mRNA transport. *J Neurosci* **19**, 288-297.

- **Kim, D. H., Sarbassov, D. D., Ali, S. M., King, J. E., Latek, R. R., Erdjument-Bromage, H., Tempst, P., and Sabatini, D. M.** (2002). mTOR interacts with raptor to form a nutrient-sensitive complex that signals to the cell growth machinery. *Cell* **110**, 163-175.
- **Kim, D. H., Sarbassov, D. D., Ali, S. M., Latek, R. R., Guntur, K. V., Erdjument-Bromage, H., Tempst, P., and Sabatini, D. M.** (2003). GbetaL, a positive regulator of the rapamycin-sensitive pathway required for the nutrient-sensitive interaction between raptor and mTOR. *Mol Cell* **11**, 895-904.
- **Kim, T. S., Jang, C. Y., Kim, H. D., Lee, J. Y., Ahn, B. Y., and Kim, J.** (2006). Interaction of Hsp90 with Ribosomal Proteins Protects from Ubiquitination and Proteasome-dependent Degradation. *Mol Biol Cell* **17**, 824-833.
- **Kimble, M., Khodjakov, A. L., and Kuriyama, R.** (1992). Identification of ubiquitous high-molecular-mass, heat-stable microtubule-associated proteins (MAPs) that are related to the Drosophila 205-kDa MAP but are not related to the mammalian MAP-4. *Proc Natl Acad Sci U S A* **89**, 7693-7697.
- **Kirby, M. L., Gale, T. F., and Stewart, D. E.** (1983). Neural crest cells contribute to normal aorticopulmonary septation. *Science* **220**, 1059-1061.
- **Kloc, M., and Etkin, L. D.** (2005). RNA localization mechanisms in oocytes. *J Cell Sci* **118**, 269-282.
- **Klugbauer, S., and Rabes, H. M.** (1999). The transcription coactivator HTIF1 and a related protein are fused to the RET receptor tyrosine kinase in childhood papillary thyroid carcinomas. *Oncogene* **18**, 4388-4393.
- **Knecht, A. K., and Bronner-Fraser, M.** (2002). Induction of the neural crest: a multigene process. *Nat Rev Genet* **3**, 453-461.
- **Kole, T. P., Tseng, Y., Jiang, I., Katz, J. L., and Wirtz, D.** (2005). Intracellular mechanics of migrating fibroblasts. *Mol Biol Cell* **16**, 328-338.
- **Kontges, G., and Lumsden, A.** (1996). Rhombencephalic neural crest segmentation is preserved throughout craniofacial ontogeny. *Development* **122**, 3229-3242.
- **Krainer, A. R., Mayeda, A., Kozak, D., and Binns, G.** (1991). Functional expression of cloned human splicing factor SF2: homology to RNA-binding proteins, U1 70K, and Drosophila splicing regulators. *Cell* **66**, 383-394.
- **Krumlauf, R.** (1993). Hox genes and pattern formation in the branchial region of the vertebrate head. *Trends Genet* **9**, 106-112.
- **Krylyshkina, O., Anderson, K. I., Kaverina, I., Upmann, I., Manstein, D. J., Small, J. V., and Toomre, D. K.** (2003). Nanometer targeting of microtubules to focal adhesions. *J Cell Biol* **161**, 853-859.
- **Krylyshkina, O., Kaverina, I., Kranewitter, W., Steffen, W., Alonso, M. C., Cross, R. A., and Small, J. V.** (2002). Modulation of substrate adhesion dynamics via microtubule targeting requires kinesin-1. *J Cell Biol* **156**, 349-359.
- **Kullander, K., and Klein, R.** (2002). Mechanisms and functions of Eph and ephrin signalling. *Nat Rev Mol Cell Biol* **3**, 475-486.
- **Landry, J. R., and Mager, D. L.** (2002). Widely spaced alternative promoters, conserved between human and rodent, control expression of the Opitz syndrome gene MID1. *Genomics* **80**, 499-508.
- **Lange, B. M., Bachi, A., Wilm, M., and Gonzalez, C.** (2000). Hsp90 is a core centrosomal component and is required at different stages of the centrosome cycle in Drosophila and vertebrates. *Embo J* **19**, 1252-1262.
- **Lasko, P.** (1999). RNA sorting in Drosophila oocytes and embryos. *Faseb J* **13**, 421-433.

- **Le Douarin, B., Zechel, C., Garnier, J. M., Lutz, Y., Tora, L., Pierrat, P., Heery, D., Gronemeyer, H., Chambon, P., and Losson, R.** (1995). The N-terminal part of TIF1, a putative mediator of the ligand-dependent activation function (AF-2) of nuclear receptors, is fused to B-raf in the oncogenic protein T18. *Embo J* **14**, 2020-2033.
- **Le Douarin, N. M., Creuzet, S., Couly, G., and Dupin, E.** (2004). Neural crest cell plasticity and its limits. *Development* **131**, 4637-4650.
- **Lehmann, R., and Nusslein-Volhard, C.** (1986). Abdominal segmentation, pole cell formation, and embryonic polarity require the localized activity of oskar, a maternal gene in *Drosophila*. *Cell* **47**, 141-152.
- **Li, P., Yang, X., Wasser, M., Cai, Y., and Chia, W.** (1997). Inscuteable and Staufer mediate asymmetric localization and segregation of prospero RNA during *Drosophila* neuroblast cell divisions. *Cell* **90**, 437-447.
- **Liang, P., and MacRae, T. H.** (1997). Molecular chaperones and the cytoskeleton. *J Cell Sci* **110** (Pt 13), 1431-1440.
- **Lim, J., and Lu, K. P.** (2005). Pinning down phosphorylated tau and tauopathies. *Biochim Biophys Acta* **1739**, 311-322.
- **Liu, J., Prickett, T. D., Elliott, E., Meroni, G., and Brautigan, D. L.** (2001). Phosphorylation and microtubule association of the Opitz syndrome protein mid-1 is regulated by protein phosphatase 2A via binding to the regulatory subunit alpha 4. *Proc Natl Acad Sci U S A* **98**, 6650-6655.
- **Locascio, A., Manzanares, M., Blanco, M. J., and Nieto, M. A.** (2002). Modularity and reshuffling of Snail and Slug expression during vertebrate evolution. *Proc Natl Acad Sci U S A* **99**, 16841-16846.
- **Lopez de Silanes, I., Zhan, M., Lal, A., Yang, X., and Gorospe, M.** (2004). Identification of a target RNA motif for RNA-binding protein HuR. *Proc Natl Acad Sci U S A* **101**, 2987-2992.
- **Loreni, F., Iadevaia, V., Tino, E., Caldarola, S., and Amaldi, F.** (2005). RACK1 mRNA translation is regulated via a rapamycin-sensitive pathway and coordinated with ribosomal protein synthesis. *FEBS Lett* **579**, 5517-5520.
- **Lumsden, A., Sprawson, N., and Graham, A.** (1991). Segmental origin and migration of neural crest cells in the hindbrain region of the chick embryo. *Development* **113**, 1281-1291.
- **Lutsch, G., Stahl, J., Kargel, H. J., Noll, F., and Bielka, H.** (1990). Immunoelectron microscopic studies on the location of ribosomal proteins on the surface of the 40S ribosomal subunit from rat liver. *Eur J Cell Biol* **51**, 140-150.
- **Mamidipudi, V., Chang, B. Y., Harte, R. A., Lee, K. C., and Cartwright, C. A.** (2004a). RACK1 inhibits the serum- and anchorage-independent growth of v-Src transformed cells. *FEBS Lett* **567**, 321-326.
- **Mamidipudi, V., Zhang, J., Lee, K. C., and Cartwright, C. A.** (2004b). RACK1 regulates G1/S progression by suppressing Src kinase activity. *Mol Cell Biol* **24**, 6788-6798.
- **Mancilla, A., and Mayor, R.** (1996). Neural crest formation in *Xenopus laevis*: mechanisms of Xslug induction. *Dev Biol* **177**, 580-589.
- **McCahill, A., Warwicker, J., Bolger, G. B., Houslay, M. D., and Yarwood, S. J.** (2002). The RACK1 scaffold protein: a dynamic cog in cell response mechanisms. *Mol Pharmacol* **62**, 1261-1273.
- **Meares, G. P., Zmijewska, A. A., and Jope, R. S.** (2004). Heat shock protein-90 dampens and directs signaling stimulated by insulin-like growth factor-1 and insulin. *FEBS Lett* **574**, 181-186.

- **Mendes, S. W., Henkemeyer, M., and Liebl, D. J.** (2006). Multiple Eph receptors and B-class ephrins regulate midline crossing of corpus callosum fibers in the developing mouse forebrain. *J Neurosci* **26**, 882-892.
- **Meroni, G., and Diez-Roux, G.** (2005). TRIM/RBCC, a novel class of 'single protein RING finger' E3 ubiquitin ligases. *Bioessays* **27**, 1147-1157.
- **Merscher, S., Funke, B., Epstein, J. A., Heyer, J., Puech, A., et al.** (2001). TBX1 is responsible for cardiovascular defects in velo-cardio-facial/DiGeorge syndrome. *Cell* **104**, 619-629.
- **Miller, L. D., Lee, K. C., Mochly-Rosen, D., and Cartwright, C. A.** (2004). RACK1 regulates Src-mediated Sam68 and p190RhoGAP signaling. *Oncogene* **23**, 5682-5686.
- **Mitsiadis, T. A., Cheraud, Y., Sharpe, P., and Fontaine-Perus, J.** (2003). Development of teeth in chick embryos after mouse neural crest transplantations. *Proc Natl Acad Sci U S A* **100**, 6541-6545.
- **Mitsiadis, T. A., Salmivirta, M., Muramatsu, T., Muramatsu, H., Rauvala, H., Lehtonen, E., Jalkanen, M., and Thesleff, I.** (1995). Expression of the heparin-binding cytokines, midkine (MK) and HB-GAM (pleiotrophin) is associated with epithelial-mesenchymal interactions during fetal development and organogenesis. *Development* **121**, 37-51.
- **Mitsui, K., Nakayama, H., Akagi, T., Nekooki, M., Ohtawa, K., Takio, K., Hashikawa, T., and Nukina, N.** (2002). Purification of polyglutamine aggregates and identification of elongation factor-1alpha and heat shock protein 84 as aggregate-interacting proteins. *J Neurosci* **22**, 9267-9277.
- **Mnayer, L., Khuri, S., Al-Ali Merheby, H., Meroni, G., and Elsas, L. J.** (2005). A structure-function study of MID1 mutations associated with a mild Opitz phenotype. *Mol Genet Metab*.
- **Mohr, E., and Richter, D.** (2001). Messenger RNA on the move: implications for cell polarity. *Int J Biochem Cell Biol* **33**, 669-679.
- **Moore R.C., and R.J., C.** (2000). Association between elongation factor-1alpha and microtubules in vivo is domain dependent and conditional. *Cell Motil Cytoskeleton* **45**, 279-292.
- **Moore RC, Durso NA, and RJ, C.** (1998). Elongation factor-1alpha stabilizes microtubules in a calcium/calmodulin-dependent manner. *Cell Motil Cytoskeleton* **41**, 168-180.
- **Moore, R. C., and Cyr, R. J.** (2000). Association between elongation factor-1alpha and microtubules in vivo is domain dependent and conditional. *Cell Motil Cytoskeleton* **45**, 279-292.
- **Moore, R. C., Durso, N. A., and Cyr, R. J.** (1998). Elongation factor-1alpha stabilizes microtubules in a calcium/calmodulin-dependent manner. *Cell Motil Cytoskeleton* **41**, 168-180.
- **Moraes, F., Novoa, A., Jerome-Majewska, L. A., Papaioannou, V. E., and Mallo, M.** (2005). Tbx1 is required for proper neural crest migration and to stabilize spatial patterns during middle and inner ear development. *Mech Dev* **122**, 199-212.
- **Morales, A. V., Barbas, J. A., and Nieto, M. A.** (2005). How to become neural crest: from segregation to delamination. *Semin Cell Dev Biol* **16**, 655-662.
- **Mowat, D. R., Wilson, M. J., and Goossens, M.** (2003). Mowat-Wilson syndrome. *J Med Genet* **40**, 305-310.
- **Murai, K. K., and Pasquale, E. B.** (2004). Eph receptors, ephrins, and synaptic function. *Neuroscientist* **10**, 304-314.
- **Murata, K., Wu, J., and Brautigan, D. L.** (1997). B cell receptor-associated protein alpha4 displays rapamycin-sensitive binding directly to the catalytic subunit of protein phosphatase 2A. *Proc Natl Acad Sci U S A* **94**, 10624-10629.

- Nakai, A., and Ishikawa, T. (2001). Cell cycle transition under stress conditions controlled by vertebrate heat shock factors. *Embo J* **20**, 2885-2895.
- Nanahoshi, M., Tsujishita, Y., Tokunaga, C., Inui, S., Sakaguchi, N., Hara, K., and Yonezawa, K. (1999). Alpha4 protein as a common regulator of type 2A-related serine/threonine protein phosphatases. *FEBS Lett* **446**, 108-112.
- Negrutskii, B. S., and El'skaya, A. V. (1998). Eukaryotic translation elongation factor 1 alpha: structure, expression, functions, and possible role in aminoacyl-tRNA channeling. *Prog Nucleic Acid Res Mol Biol* **60**, 47-78.
- Nieto, M. A., Sargent, M. G., Wilkinson, D. G., and Cooke, J. (1994). Control of cell behavior during vertebrate development by Slug, a zinc finger gene. *Science* **264**, 835-839.
- Nilsson, J., Sengupta, J., Frank, J., and Nissen, P. (2004). Regulation of eukaryotic translation by the RACK1 protein: a platform for signalling molecules on the ribosome. *EMBO Rep* **5**, 1137-1141.
- Nisole, S., Stoye, J. P., and Saib, A. (2005). TRIM family proteins: retroviral restriction and antiviral defence. *Nat Rev Microbiol* **3**, 799-808.
- Nobes, C. D., and Hall, A. (1995). Rho, rac, and cdc42 GTPases regulate the assembly of multimolecular focal complexes associated with actin stress fibers, lamellipodia, and filopodia. *Cell* **81**, 53-62.
- Noden, D. M., and Trainor, P. A. (2005). Relations and interactions between cranial mesoderm and neural crest populations. *J Anat* **207**, 575-601.
- Ogawa, K., Wada, H., Okada, N., Harada, I., Nakajima, T., Pasquale, E. B., and Tsuyama, S. (2006). EphB2 and ephrin-B1 expressed in the adult kidney regulate the cytoarchitecture of medullary tubule cells through Rho family GTPases. *J Cell Sci* **119**, 559-570.
- Ohta, K., Toriyama, M., Miyazaki, M., Murofushi, H., Hosoda, S., Endo, S., and Sakai, H. (1990). The mitotic apparatus-associated 51-kDa protein from sea urchin eggs is a GTP-binding protein and is immunologically related to yeast polypeptide elongation factor 1 alpha. *J Biol Chem* **265**, 3240-3247.
- Okuda, M. (2002). The role of nucleophosmin in centrosome duplication. *Oncogene* **21**, 6170-6174.
- Okuwaki, M., Tsujimoto, M., and Nagata, K. (2002). The RNA binding activity of a ribosome biogenesis factor, nucleophosmin/B23, is modulated by phosphorylation with a cell cycle-dependent kinase and by association with its subtype. *Mol Biol Cell* **13**, 2016-2030.
- Opitz, J. M., Frias J.L. , Guttenberger, J.E, Pellet J.R.. (1969a). The G syndrome of multiple congenital anomalies. *Birth Defects Orig Artic Ser (V)* **2**, 95-102.
- Opitz, J. M., Summitt, R.L., Smith, D.W. (1969b). The BBB syndrome. Familial telecanthus with associated congenital anomalies. *Birth Defects Orig Artic Ser (V)* **2**, 86-94.
- Palazzo, A. F., and Gundersen, G. G. (2002). Microtubule-actin cross-talk at focal adhesions. *Sci STKE* **2002**, PE31.
- Palmer, A., and Klein, R. (2003). Multiple roles of ephrins in morphogenesis, neuronal networking, and brain function. *Genes Dev* **17**, 1429-1450.
- Pasquale, E. B. (2005). Eph receptor signalling casts a wide net on cell behaviour. *Nat Rev Mol Cell Biol* **6**, 462-475.
- Pende, M., Um, S. H., Mieulet, V., Sticker, M., Goss, V. L., Mestan, J., Mueller, M., Fumagalli, S., Kozma, S. C., and Thomas, G. (2004). S6K1(-/-)/S6K2(-/-) mice exhibit perinatal lethality and rapamycin-sensitive 5'-terminal oligopyrimidine mRNA translation and reveal a mitogen-activated protein kinase-dependent S6 kinase pathway. *Mol Cell Biol* **24**, 3112-3124.

- **Perkins, D. N., Pappin, D. J., Creasy, D. M., and Cottrell, J. S.** (1999). Probability-based protein identification by searching sequence databases using mass spectrometry data. *Electrophoresis* **20**, 3551-3567.
- **Peterson, R. T., Desai, B. N., Hardwick, J. S., and Schreiber, S. L.** (1999). Protein phosphatase 2A interacts with the 70-kDa S6 kinase and is activated by inhibition of FKBP12-rapamycin-associated protein. *Proc Natl Acad Sci U S A* **96**, 4438-4442.
- **Pinson, L., Auge, J., Audollent, S., Mattei, G., Etchevers, H., et al.** (2004). Embryonic expression of the human MID1 gene and its mutations in Opitz syndrome. *J Med Genet* **41**, 381-386.
- **Pla, P., Moore, R., Morali, O. G., Grille, S., Martinuzzi, S., Delmas, V., and Larue, L.** (2001). Cadherins in neural crest cell development and transformation. *J Cell Physiol* **189**, 121-132.
- **Poliakov, A., Cotrina, M., and Wilkinson, D. G.** (2004). Diverse roles of eph receptors and ephrins in the regulation of cell migration and tissue assembly. *Dev Cell* **7**, 465-480.
- **Prescott, N. J., Winter, R. M., and Malcolm, S.** (2001). Nonsyndromic cleft lip and palate: complex genetics and environmental effects. *Ann Hum Genet* **65**, 505-515.
- **Qi, M., Ikematsu, S., Maeda, N., Ichihara-Tanaka, K., Sakuma, S., Noda, M., Muramatsu, T., and Kadomatsu, K.** (2001). Haptotactic migration induced by midline. Involvement of protein-tyrosine phosphatase zeta. Mitogen-activated protein kinase, and phosphatidylinositol 3-kinase. *J Biol Chem* **276**, 15868-15875.
- **Quaderi, N. A., Schweiger, S., Gaudenz, K., Franco, B., Rugarli, E. I., et al.** (1997). Opitz G/BBB syndrome, a defect of midline development, is due to mutations in a new RING finger gene on Xp22. *Nat Genet* **17**, 285-291.
- **Ramos, A., Hollingworth, D., and Pastore, A.** (2003). G-quartet-dependent recognition between the FMRP RGG box and RNA. *Rna* **9**, 1198-1207.
- **Raught, B., Gingras, A. C., and Sonenberg, N.** (2001). The target of rapamycin (TOR) proteins. *Proc Natl Acad Sci U S A* **98**, 7037-7044.
- **Reymond, A., Meroni, G., Fantozzi, A., Merla, G., Cairo, S., et al.** (2001). The tripartite motif family identifies cell compartments. *Embo J* **20**, 2140-2151.
- **Richman, J. M., Fu, K. K., Cox, L. L., Sibbons, J. P., and Cox, T. C.** (2002). Isolation and characterisation of the chick orthologue of the Opitz syndrome gene, Mid1, supports a conserved role in vertebrate development. *Int J Dev Biol* **46**, 441-448.
- **Richter, K., and Buchner, J.** (2001). Hsp90: chaperoning signal transduction. *J Cell Physiol* **188**, 281-290.
- **Robin, N. H., Feldman, G. J., Aronson, A. L., Mitchell, H. F., Weksberg, R., et al.** (1995). Opitz syndrome is genetically heterogeneous, with one locus on Xp22, and a second locus on 22q11.2. *Nat Genet* **11**, 459-461.
- **Robin, N. H., Opitz, J. M., and Muenke, M.** (1996). Opitz G/BBB syndrome: clinical comparisons of families linked to Xp22 and 22q, and a review of the literature. *Am J Med Genet* **62**, 305-317.
- **Robinson, V., Smith, A., Flenniken, A. M., and Wilkinson, D. G.** (1997). Roles of Eph receptors and ephrins in neural crest pathfinding. *Cell Tissue Res* **290**, 265-274.
- **Roessler, E., and Muenke, M.** (2001). Midline and laterality defects: left and right meet in the middle. *Bioessays* **23**, 888-900.
- **Roessler, E., and Muenke, M.** (2003). How a Hedgehog might see holoprosencephaly. *Hum Mol Genet* **12 Spec No 1**, R15-25.

- **Runyan, R. B., and Markwald, R. R.** (1983). Invasion of mesenchyme into three-dimensional collagen gels: a regional and temporal analysis of interaction in embryonic heart tissue. *Dev Biol* **95**, 108-114.
- **Santagati, F., and Rijli, F. M.** (2003). Cranial neural crest and the building of the vertebrate head. *Nat Rev Neurosci* **4**, 806-818.
- **Santiago, A., and Erickson, C. A.** (2002). Ephrin-B ligands play a dual role in the control of neural crest cell migration. *Development* **129**, 3621-3632.
- **Sarbassov, D. D., Ali, S. M., Kim, D. H., Guertin, D. A., Latek, R. R., Erdjument-Bromage, H., Tempst, P., and Sabatini, D. M.** (2004). Rictor, a novel binding partner of mTOR, defines a rapamycin-insensitive and raptor-independent pathway that regulates the cytoskeleton. *Curr Biol* **14**, 1296-1302.
- **Saurin, A. J., Borden, K. L., Boddy, M. N., and Freemont, P. S.** (1996). Does this have a familiar RING? *Trends Biochem Sci* **21**, 208-214.
- **Savagner, P.** (2001). Leaving the neighborhood: molecular mechanisms involved during epithelial-mesenchymal transition. *Bioessays* **23**, 912-923.
- **Schutte, B. C., and Murray, J. C.** (1999). The many faces and factors of orofacial clefts. *Hum Mol Genet* **8**, 1853-1859.
- **Schweiger, S., Foerster, J., Lehmann, T., Suckow, V., Muller, Y. A., et al.** (1999). The Opitz syndrome gene product, MID1, associates with microtubules. *Proc Natl Acad Sci U S A* **96**, 2794-2799.
- **Schweiger, S., and Schneider, R.** (2003). The MID1/PP2A complex: a key to the pathogenesis of Opitz BBB/G syndrome. *Bioessays* **25**, 356-366.
- **Sela-Donenfeld, D., and Kalcheim, C.** (1999). Regulation of the onset of neural crest migration by coordinated activity of BMP4 and Noggin in the dorsal neural tube. *Development* **126**, 4749-4762.
- **Selleck, M. A., and Bronner-Fraser, M.** (1995). Origins of the avian neural crest: the role of neural plate-epidermal interactions. *Development* **121**, 525-538.
- **Sengupta, B., Banerjee, A., and Sengupta, P. K.** (2005). Interactions of the plant flavonoid fisetin with macromolecular targets: insights from fluorescence spectroscopic studies. *J Photochem Photobiol B* **80**, 79-86.
- **Shiina, N., Gotoh, Y., Kubomura, N., Iwamatsu, A., and Nishida, E.** (1994). Microtubule severing by elongation factor 1 alpha. *Science* **266**, 282-285.
- **Shinmura, K., Tarapore, P., Tokuyama, Y., George, K. R., and Fukasawa, K.** (2005). Characterization of centrosomal association of nucleophosmin/B23 linked to Crm1 activity. *FEBS Lett* **579**, 6621-6634.
- **Short, K. M., and Cox, T. C.** (2006). Sub-classification of the rbcc/trim superfamily reveals a novel motif necessary for microtubule binding. *J Biol Chem*.
- **Short, K. M., Hopwood, B., Yi, Z., and Cox, T. C.** (2002). MID1 and MID2 homo- and heterodimerise to tether the rapamycin-sensitive PP2A regulatory subunit, alpha 4, to microtubules: implications for the clinical variability of X-linked Opitz GBBB syndrome and other developmental disorders. *BMC Cell Biol* **3**, 1.
- **Sittler, A., Walter, S., Wedemeyer, N., Hasenbank, R., Scherzinger, E., Eickhoff, H., Bates, G. P., Lehrach, H., and Wanker, E. E.** (1998). SH3GL3 associates with the Huntingtin exon 1 protein and promotes the formation of polyglutamine-containing protein aggregates. *Mol Cell* **2**, 427-436.
- **Sklan, E. H., Podoly, E., and Soreq, H.** (2006). RACK1 has the nerve to act: Structure meets function in the nervous system. *Prog Neurobiol*.

- Small, J. V., and Kaverina, I. (2005). Polarized cell motility: microtubules show the way, In Cell migration, D. Wedlich, ed. (WILEY-VCH verlag), pp. 15-31.
- **Smith, A., Robinson, V., Patel, K., and Wilkinson, D. G.** (1997). The EphA4 and EphB1 receptor tyrosine kinases and ephrin-B2 ligand regulate targeted migration of branchial neural crest cells. *Curr Biol* **7**, 561-570.
- **So, J., Suckow, V., Kijas, Z., Kalscheuer, V., Moser, B., et al.** (2005). Mild phenotypes in a series of patients with Opitz GBBB syndrome with MID1 mutations. *Am J Med Genet A* **132**, 1-7.
- **St Johnston, D.** (2005). Moving messages: the intracellular localization of mRNAs. *Nat Rev Mol Cell Biol* **6**, 363-375.
- **Stahl, J.** (2001). Ribosomal Proteins in Eukaryotes. *encyclopedia of life sciences*, 1-11.
- **Sternsdorf, T., Grotzinger, T., Jensen, K., and Will, H.** (1997). Nuclear dots: actors on many stages. *Immunobiology* **198**, 307-331.
- **Steventon, B., Carmona-Fontaine, C., and Mayor, R.** (2005). Genetic network during neural crest induction: from cell specification to cell survival. *Semin Cell Dev Biol* **16**, 647-654.
- **Steward, O., and Schuman, E. M.** (2003). Compartmentalized synthesis and degradation of proteins in neurons. *Neuron* **40**, 347-359.
- **Steward, O., and Worley, P.** (2001). Localization of mRNAs at synaptic sites on dendrites. *Results Probl Cell Differ* **34**, 1-26.
- **Storz, P., Hausser, A., Link, G., Dedio, J., Ghebrehiwet, B., Pfizenmaier, K., and Johannes, F. J.** (2000). Protein kinase C [micro] is regulated by the multifunctional chaperon protein p32. *J Biol Chem* **275**, 24601-24607.
- **Sung, Y. J., Conti, J., Currie, J. R., Brown, W. T., and Denman, R. B.** (2000). RNAs that interact with the fragile X syndrome RNA binding protein FMRP. *Biochem Biophys Res Commun* **275**, 973-980.
- **Sung, Y. J., Dolzhanskaya, N., Nolin, S. L., Brown, T., Currie, J. R., and Denman, R. B.** (2003). The fragile X mental retardation protein FMRP binds elongation factor 1A mRNA and negatively regulates its translation in vivo. *J Biol Chem* **278**, 15669-15678.
- **Tamanini, F., Meijer, N., Verheij, C., Willems, P. J., Galjaard, H., Oostra, B. A., and Hoogeveen, A. T.** (1996). FMRP is associated to the ribosomes via RNA. *Hum Mol Genet* **5**, 809-813.
- **Tang, H., Hornstein, E., Stolovich, M., Levy, G., Livingstone, M., Templeton, D., Avruch, J., and Meyuhas, O.** (2001a). Amino acid-induced translation of TOP mRNAs is fully dependent on phosphatidylinositol 3-kinase-mediated signaling, is partially inhibited by rapamycin, and is independent of S6K1 and rpS6 phosphorylation. *Mol Cell Biol* **21**, 8671-8683.
- **Tang, S. J., Meulemans, D., Vazquez, L., Colaco, N., and Schuman, E.** (2001b). A role for a rat homolog of staufen in the transport of RNA to neuronal dendrites. *Neuron* **32**, 463-475.
- **Tapadia, M. D., Cordero, D. R., and Helms, J. A.** (2005). It's all in your head: new insights into craniofacial development and deformation. *J Anat* **207**, 461-477.
- **Tarapore, P., Okuda, M., and Fukasawa, K.** (2002). A mammalian in vitro centriole duplication system: evidence for involvement of CDK2/cyclin E and nucleophosmin/B23 in centrosome duplication. *Cell Cycle* **1**, 75-81.
- **Tarapore, P., Shinmura, K., Suzuki, H., Tokuyama, Y., Kim, S. H., Mayeda, A., and Fukasawa, K.** (2006). Thr199 phosphorylation targets nucleophosmin to nuclear speckles and represses pre-mRNA processing. *FEBS Lett* **580**, 399-409.
- **Thiery, J. P.** (2003). Epithelial-mesenchymal transitions in development and pathologies. *Curr Opin Cell Biol* **15**, 740-746.

- **Thomas, M. G., Martinez Tosar, L. J., Loschi, M., Pasquini, J. M., Correale, J., Kindler, S., and Boccaccio, G. L.** (2005). Staufen recruitment into stress granules does not affect early mRNA transport in oligodendrocytes. *Mol Biol Cell* **16**, 405-420.
- **Thorogood, P.** (1989). Developmental and Evolutionary Aspects of the Neural Crest. *Trends Neuroscience* **12**, 38-39.
- **Tokuyama, Y., Horn, H. F., Kawamura, K., Tarapore, P., and Fukasawa, K.** (2001). Specific phosphorylation of nucleophosmin on Thr(199) by cyclin-dependent kinase 2-cyclin E and its role in centrosome duplication. *J Biol Chem* **276**, 21529-21537.
- **Torok, M., and Etkin, L. D.** (2001). Two B or not two B? Overview of the rapidly expanding B-box family of proteins. *Differentiation* **67**, 63-71.
- **Trainor, P. A., and Krumlauf, R.** (2001). Hox genes, neural crest cells and branchial arch patterning. *Curr Opin Cell Biol* **13**, 698-705.
- **Trockenbacher, A., Suckow, V., Foerster, J., Winter, J., Krauss, S., Ropers, H. H., Schneider, R., and Schweiger, S.** (2001). MID1, mutated in Opitz syndrome, encodes an ubiquitin ligase that targets phosphatase 2A for degradation. *Nat Genet* **29**, 287-294.
- **Trojanowski, J. Q., and Lee, V. M.** (1995). Phosphorylation of paired helical filament tau in Alzheimer's disease neurofibrillary lesions: focusing on phosphatases. *Faseb J* **9**, 1570-1576.
- **Twigg, S. R., Kan, R., Babbs, C., Bochukova, E. G., Robertson, S. P., Wall, S. A., Morriss-Kay, G. M., and Wilkie, A. O.** (2004). Mutations of ephrin-B1 (EFNB1), a marker of tissue boundary formation, cause craniofrontonasal syndrome. *Proc Natl Acad Sci U S A* **101**, 8652-8657.
- **Vallee, R. B.** (1982). A taxol-dependent procedure for the isolation of microtubules and microtubule-associated proteins (MAPs). *J Cell Biol* **92**, 435-442.
- **Vasiliev, J. M., Gelfand, I. M., Domnina, L. V., Ivanova, O. Y., Komm, S. G., and Olshevskaja, L. V.** (1970). Effect of colcemid on the locomotory behaviour of fibroblasts. *J Embryol Exp Morphol* **24**, 625-640.
- **Vedeler, A., and Hollas, H.** (2000). Annexin II is associated with mRNAs which may constitute a distinct subpopulation. *Biochem J* **348 Pt 3**, 565-572.
- **Villace, P., Marion, R. M., and Ortin, J.** (2004). The composition of Staufen-containing RNA granules from human cells indicates their role in the regulated transport and translation of messenger RNAs. *Nucleic Acids Res* **32**, 2411-2420.
- **Vitelli, F., Morishima, M., Taddei, I., Lindsay, E. A., and Baldini, A.** (2002). Tbx1 mutation causes multiple cardiovascular defects and disrupts neural crest and cranial nerve migratory pathways. *Hum Mol Genet* **11**, 915-922.
- **Voos, W., and Rottgers, K.** (2002). Molecular chaperones as essential mediators of mitochondrial biogenesis. *Biochim Biophys Acta* **1592**, 51-62.
- **Waldo, K., Miyagawa-Tomita, S., Kumiski, D., and Kirby, M. L.** (1998). Cardiac neural crest cells provide new insight into septation of the cardiac outflow tract: aortic sac to ventricular septal closure. *Dev Biol* **196**, 129-144.
- **Wang, D., Baumann, A., Szebeni, A., and Olson, M. O.** (1994). The nucleic acid binding activity of nucleolar protein B23.1 resides in its carboxyl-terminal end. *J Biol Chem* **269**, 30994-30998.
- **Wieland, I., Jakubiczka, S., Muschke, P., Cohen, M., Thiele, H., Gerlach, K. L., Adams, R. H., and Wieacker, P.** (2004). Mutations of the ephrin-B1 gene cause craniofrontonasal syndrome. *Am J Hum Genet* **74**, 1209-1215.
- **Wilhelm, J. E., and Smibert, C. A.** (2005). Mechanisms of translational regulation in Drosophila. *Biol Cell* **97**, 235-252.

- **Wilkie, A. O., and Morriss-Kay, G. M.** (2001). Genetics of craniofacial development and malformation. *Nat Rev Genet* **2**, 458-468.
- **Winter, J.** (2003) Molekulare Charakterisierung des *MID1*-Gens, thesis, Freien Universität Berlin, Berlin.
- **Winter, J., Lehmann, T., Krauss, S., Trockenbacher, A., Kijas, Z., et al.** (2004). Regulation of the MID1 protein function is fine-tuned by a complex pattern of alternative splicing. *Hum Genet* **114**, 541-552.
- **Wittmann-Liebold, B., and Graack, H.-R.** (2001). Ribosomal Proteins: Structure and Evolution. *encyclopedia of life sciences*, 1-10.
- **Zalfa, F., Adinolfi, S., Napoli, I., Kuhn-Holsken, E., Urlaub, H., Achsel, T., Pastore, A., and Bagni, C.** (2005). Fragile X mental retardation protein (FMRP) binds specifically to the brain cytoplasmic RNAs BC1/BC200 via a novel RNA-binding motif. *J Biol Chem* **280**, 33403-33410.
- **Zalfa, F., and Bagni, C.** (2005). Another view of the role of FMRP in translational regulation. *Cell Mol Life Sci* **62**, 251-252.
- **Zalfa, F., Giorgi, M., Primerano, B., Moro, A., Di Penta, A., Reis, S., Oostra, B., and Bagni, C.** (2003). The fragile X syndrome protein FMRP associates with BC1 RNA and regulates the translation of specific mRNAs at synapses. *Cell* **112**, 317-327.
- **Zhang, H., Shi, X., Paddon, H., Hampong, M., Dai, W., and Pelech, S.** (2004). B23/nucleophosmin serine 4 phosphorylation mediates mitotic functions of polo-like kinase 1. *J Biol Chem* **279**, 35726-35734.
- **Zhang, W., Zong, C. S., Hermanto, U., Lopez-Bergami, P., Ronai, Z., and Wang, L. H.** (2006). RACK1 recruits STAT3 specifically to insulin and insulin-like growth factor 1 receptors for activation, which is important for regulating anchorage-independent growth. *Mol Cell Biol* **26**, 413-424.
- **Zhao, W. Q., Chen, G. H., Chen, H., Pascale, A., Ravindranath, L., Quon, M. J., and Alkon, D. L.** (2003). Secretion of Annexin II via activation of insulin receptor and insulin-like growth factor receptor. *J Biol Chem* **278**, 4205-4215.

10 Abbreviations

| | |
|-------------------------------------|--|
| °C | grad celsius |
| µg | microgram |
| µl | microliter |
| 3D | three dimensional |
| 5'-TOP | 5'-terminal oligopyrimidine |
| A ₂₆₀ / A ₂₈₀ | absorbance at 260nm/280nm |
| aa | amino acid |
| Ala (A) | alanine |
| Amp | ampicillin |
| AP | alkaline phosphatase |
| APS | ammonium persulfate |
| Arg (R) | arginine |
| Asp (N) | asparagine |
| ATP | adenosine 5-triphosphate |
| bp | base pair |
| BSA | bovine serum albumin |
| Ca ²⁺ | calcium |
| CBB | Comassie Brilliant Blue G-250 |
| CC | coiled coil |
| cDNA | complementary DNA |
| Cys (C) | cysteine |
| DABCO | 1,4-diazobicyclo-2,2,2-octan |
| DAPI | 4,6-diamino-2-phenylindole |
| dATP | deoxyadenosine 5-triphosphate |
| dCTP | deoxycytidine 5-triphosphate |
| DEPC | diethylpirocarbonate |
| dGTP | deoxyguanosine 5-triphosphate |
| dHPLC | Denaturing High Perfomance Liquid Chromatography |
| DMEM | Dulbecco's modified eagle medium |
| DMSO | dimethyl sulfoxide |
| DNA | deoxyribonucleic acid |
| dNTP | 2'-Deoxynucleotide-5' - triphosphate |
| DOC | deoxycholate |
| DTT | dithiothreitol |
| dTTP | deoxythymidine triphosphate |
| <i>E.coli</i> | <i>Escherichia coli</i> |
| EDTA | ethylene diamine tetraacetic acid |
| EFNB1 | ephrin-B1 gene |
| GFP | green fluorescent protein |
| EMT | Epithelial Mesenchymal Transition |
| Eph receptor | ephrin receptor |
| ESI-MS | electrospray ionisation mass spectrometry |
| EtBr | ethidium bromide |
| EtOH | ethanol |

| | |
|-------------------|--|
| FITC | fluorescein isothiocyanate |
| FMRP | Fragile Mental Retardation Protein |
| FNIII | Fibronectin type III |
| FXS | Fragile X Syndrome |
| <i>g</i> | acceleration of gravity |
| g | gram |
| HEPES | 4-(2-hydroxyethyl)-1-piperazineethanesulfonic acid |
| Gln (Q) | glutamine |
| Glu (E) | glutamic acid |
| Gly (G) | glycine |
| GTP | guanosine triphosphate |
| h | hour |
| HCl | hydrogen chloride |
| His (H) | histidine |
| HRP | horse radish peroxidase |
| IgG | immunoglobulin G |
| IPTG | isopropylthio- β -D-thiogalactopyranoside |
| kb | kilobase |
| KCl | potassium chloride |
| kDa | kilodalton |
| l | liter |
| Ile (I) | isoleucine |
| LB | Luria Bertani |
| Leu (L) | leucine |
| Lys (K) | lysine |
| M | molar |
| mA | milliampere |
| MAP | microtubule associated protein |
| MeOH | methanol |
| Met (M) | methionine |
| Mg | milligram |
| MgCl ₂ | magnesium chloride |
| MOTC | microtubules organising centre |
| min | minute |
| ml | milliliter |
| mM | millimolar |
| mmol | millimol |
| MOPS | 3-(N-morpholino) propane sulfonic acid |
| mRNA | messenger RNA |
| MS | mass spectrometry |
| MT | microtubule |
| NaCl | sodium chloride |
| NCC | Neural Crest Cell |
| ng | nanogram |
| OD | optical density |
| OMIM | Online Mendelian Inheritance In Man |
| ONPG | o-nitrophenyl- β -D-galactopyranoside |

| | |
|--------------------|---|
| ORF | open reading frame |
| OS | Opitz BBB/G syndrome |
| PAGE | polyacrylamide electrophoresis |
| PBS | phosphate-buffered saline |
| PBST | phosphate-buffered saline with Tween 20 |
| PCR | polymerase chain reaction |
| Pfu | <i>Pyrococcus furiosus</i> |
| pH | negative logarithm of hydrogen ions concentration |
| Phe (F) | phenylalanine |
| Pro (P) | proline |
| PP2A | Protein Phosphatase 2A |
| PP2Ac | Catalytic subunit of PP2A |
| PVDF | polyvinylidenefluorid |
| RBCC | Ring-Bbox-Coiled-coil |
| <i>RING</i> | Really Interesting Gene |
| RNA | ribonucleic acid |
| RNase | ribonuclease |
| RNP | ribonucleic protein |
| rpm | revolutions per minute |
| RT | room temperature |
| <i>S.cerevisae</i> | <i>Saccharomyces cerevisiae</i> |
| SDS | sodium dodecyl sulphate |
| sec | second |
| Ser (S) | serine |
| SSC | standard saline citrate |
| T ^a | annealing temperature |
| TAE | Tris-acetate EDTA |
| Taq | <i>Thermus aquaticus</i> |
| TBS | Tris-buffered saline |
| TE | Tris-EDTA |
| TEMED | N,N,N',N'-tetramethyl-ethylendiamine |
| Thr (T) | threonine |
| mTOR | mammalian Target of Rapamycin |
| TRIM | Tripartite Motif |
| Tris | tris (hydroxymethyl)-aminomethane |
| Trp (W) | tryptophan |
| Tyr (Y) | tyrosine |
| U | unit |
| UCSC | University of California, Santa Cruz |
| UTP | uridin-5-triphosphate |
| UTR | untranslated region |
| UV | ultraviolet |
| V | volt |
| v/v | volume/volume |
| Val (V) | valine |
| w/v | weight/volume |
| X-gal | 5-bromo-4-chloro-3-indolyl—D-galactopyranoside |
| XNF7 | Xenopus nuclear factor 7 |

11 Curriculum Vitae

Beatriz Aranda Orgillés

Born 7th November 1976 in Zaragoza, Spain

Nationality: Spanish

e-mail aranda@molgen.mpg.de

Education

| | |
|--------------|---|
| 2001-present | PhD Max Planck Institute for Molecular Genetics, Berlin (Germany) Department of human molecular genetics (Prof Dr. H.-H Ropers) Biochemistry of inherited disorders group (Prof. Dr. S. Schweiger) Theme: Characterisation of the MID1/ α 4 multiprotein complex |
| 2000-2001 | Research project Cambridge University, England Department of Chemistry (Prof. J.K.M. Sanders) Scholarship by the Erasmus of the European Union Theme: Toward the generation of DCLs in DMSO |
| 1998-2000 | Biochemistry studies University of Zaragoza, Spain Degree: Graduated in Biochemistry (BSc, Licenciatura) |
| 1994-2001 | Chemistry studies University of Zaragoza, Spain Degree: Graduated in Chemistry (BSc, Licenciatura) |
| 1993-1994 | C.O.U (Spanish pre-university course) Colegio Sagrada Familia, Zaragoza (Spain) |
| 1990-1993 | B.U.P (Spanish secondary school) Colegio Sagrada Familia, Zaragoza (Spain) |
| 1982-1990 | E.G.B (Spanish primary school) Colegio Sagrada Familia, Zaragoza (Spain) |

12 Publications

- **Beatriz Aranda Orgillés**; Sven Krause; Stefan Roepcke; Ewa Jastrzebska; Andrea Köhler; Joachim Stahl; Eva-Christina Müller; Albrecht Otto; Erich Wanker; Rainer Schneider; Susann Schweiger (2006).

The Opitz BBB/G syndrome gene product MID1 and the mTOR target $\alpha 4$ assemble in an active polyribosome- and microtubule-associated mRNP with ephrin mRNAs recruited via G-quartet motifs.

EMBO J, Under review

- **Beatriz Aranda Orgillés**, Philipp Wechner, Sari Panjaita, Andrea Köhler, Joyce So, Vanessa Suckow, Jennifer Winter, Susann Schweiger, Rainer Schneider (2006).

A novel pathomechanism for Opitz BBB/G syndrome tracked down to the Bbox functions of the MID1 ubiquitin ligase.

In preparation

- Vera M. Kalscheuer, Kristine Freude,, **Beatriz Aranda**,....., Susann Schweiger, Hans-Hilger Ropers (2003).

Mutations in the polyglutamine binding protein 1 gene cause X-linked mental retardation.

Nat Genet Dec:35(4):313-5.

Invited speaker

The MID1 complex: compartmentalisation of protein translation in the polarising cell. 'Day of Science' at Max-Planck-Institute for Molecular Genetics, February 2004, Berlin (Germany)

Conferences and courses

- Should I bind or should I go?

30th FEBS congress and 9th IUBM conference, 2-7 July 2005, Budapest (Hungary)

- Bbox2 protein domain: novel regulator for protein-protein interaction.

European Human Genetics Conference. 12.-15.Juni 2004, Munich (Germany)

- 15th Course in Medical Genetics

European School of Genetic Medicine, Bertinoro (Italy)

13 Acknowledgements

I would like to thank Prof. Dr. Hans Hilger Ropers for his support and for giving me the opportunity to carry out my thesis in his department. I am very grateful to Prof. Dr. Volker A. Erdmann for supporting this project and accepting to be my second reviewer. I am indebted to Prof. Jeremy K.M Sanders for helping me to get access to the University.

My special thanks go to Prof. Dr. Susann Schweiger for her guidance, for all the invested time in the supervision of my thesis and for her readiness for scientific discussion. In addition, I acknowledge the very interesting theme she proposed for my thesis and the critical comments on this written work. I would additionally like to thank Prof. Dr. Rainer Schneider for his good scientific advice and input to this thesis.

I owe many thanks to Prof. Dr. Manfred Schweiger for his helpful and critical comments on this written work.

Much gratitude for Dr. Joachim Stahl, I do not only treasure the antibodies he kindly gave me and for all the knowledge he shared with me, but also for his encouragement, his contagious enthusiasm for science and friendship.

I am very grateful to Vanessa Suckow for her excellent and patient technical assistance, for believing in my potential and for the nice moments we had working together. I extend my thanks to Susanne Freier and Hannelore Madle for their experienced and valuable technical assistance with cell culture, and Dietmar Vogt for his help with the scary ultracentrifuges. I would like to express my sincere gratitude to Dr. Eva Christina Müller and Dr. Albrecht Otto for great assistance with mass spectrometry. I am also very thankful to Sven Krause and Stefan Roepcke for their help with the bioinformatics stuff, and the Ribosome group at the Max Planck Institute for their technical assistance with ribosomal work and all the people in the department that any time offered their help.

Millions of thanks go to Joyce So for the good moments we had working together, for her continuous support and for all our helpful discussions. I also thank her for the endless English corrections (thank you very much for reading this manuscript), which taught me a lot and helped improve all my writings. I thank Sven again for his help with the mysterious world of computers. Apart from these two, I want to thank the rest of my colleagues and ex-colleagues, Zosia Kijas, Jennifer Winter, Sybille Krauß, Ewa Jastrzebska, Sari Panjaita and Melanie Kunath, for their readiness to help in the lab and for the nice working atmosphere. I would also like to thank Kirsten Vormbrock for showing so much enthusiasm while working under my supervision.

A special mention goes to the “Mensa Consortium” (Joyce, Sven, Olivier, Christelle, Barbara, Mahdi, Dejan and all those that sporadically joined us) for all the funny and great

moments we had at lunchtime, for all our fruitful scientific discussions and for bringing me up in more difficult situations. I really enjoyed having lunch with you guys!

I also thank Ana, Eva and Jennifer for their help in the multiple versions of my summary.

In these lines, I would like to thank very special persons of my personal life that contributed to making this work possible. I am very grateful to Dirk, for his constant motivation, patience, encouragement, and for his love during these years. I also thank him for reading this written work and helping me with the latest set ups. Many thanks go to my parents and sister (Gabriel, Maria Jesús and Ana) for their motivation, trust, love, and for feeling so close despite being so far (muchas gracias por vuestro continuo apoyo y cariño!!!!). Of course, I do not forget the rest of my family, who supported me so much during all this time. Last, but not least, I send big thanks to all my friends, who always support me, give me good advice and make my life colourful!

I thank the Max Planck society, the Charité, the SFB577 and the “Fritz-Thyssen Stiftung” for the financial support of this project.

Finally, I thank the reader for reading my thesis.